ORFV VIRUS MANIPULATION OF TYPE I INTERFERON EXPRESSION

BASHEER AL DAIF (M.Sc.)

APRIL 30, 2020

A THESIS SUBMITTED FOR THE DEGREE OF DOCTOR OF PHILOSOPHY
AT THE UNIVERSITY OF OTAGO

DUNEDIN, NEW ZEALAND

ABSTRACT

Orf virus (ORFV) is the type species of the Parapoxvirus genus that belongs to the *Poxviridae* family. ORFV is an epitheliotropic virus inducing cutaneous pustular skin lesions in sheep and goats and is transmissible to humans. Type I interferons (IFN) are critical in the host defence against viruses. They induce hundreds of interferon stimulated genes (ISGs) many of which have an antiviral role. The aim of this study was to investigate whether ORFV modulates the type I IFN response. Previous studies suggested a role for the ORFV gene ORF116 in modulating the ISG response using a recombinant ORF116 deletion mutant. These preliminary findings were validated in this study by constructing an ORF116 revertant recombinant virus. The approach taken was to generate a revertant virus in which the ORF116 gene was re-inserted at the same locus as the deleted ORF116 gene in the knockout virus by homologous recombination and then infecting HeLa cells with the two recombinant viruses and the *wt* strain and studying specific changes in ISG expression by qRT-PCR. The data suggested that ORFV was either directly modulating the expression of about 10 ISGs involved in the anti-viral response or indirectly modulating ISG expression by inhibiting IFN production or both. The ability of ORFV to modulate type I IFN production in several cell types was undertaken to investigate whether ORFV could inhibit IFN-β via dsRNA and dsDNA dependant signalling pathways. HEK293 cells were utilized to model an RNA sensing system. It has been shown that these cells respond to poly(dA:dT), that is converted to dsRNA *via* RNA polymerase III and poly(I:C) and produce high fold IFN-β expression of RIG-I-dependent signalling as confirmed by siRNA knock-down of RIG-I and RNA polymerase III. HEK293 cells are permissive for ORFV replication and ORFV caused a potent inhibition of IFN-β mRNA when stimulated with poly(dA:dT) or poly(I:C) in a dose-dependent manner. THP-1 cells and human dermal fibroblasts (hNDF) were used to investigate the effects of ORFV on a cytoplasmic DNA sensing system. These cells respond to transfected poly(dA:dT) or poly(I:C) by producing high levels of IFN-β expression in a dose-dependent manner. Both cells are permissive for ORFV early gene synthesis and only hNDFs are permissive for ORFV replication. ORFV infection resulted in strong inhibition of IFN-β in hNDFs treated with either poly(I:C) or poly(dA:dT). The IFN signalling pathway in hNDFs was characterized by RNA interference. siRNA knock-down of STING, a critical adaptor for cytosolic DNA sensing, resulted in a reduction in IFN-β expression in cells stimulated with poly(dA:dT) and this inhibition was further enhanced when both STING and RIG-I were knocked

down. Although it was clearly shown that IFN induction was *via* DNA sensing, cytosolic DNA sensing has yet to be confirmed. Preliminary findings suggest that the two early genes ORF116 and ORF020 expressed from plasmid vectors are potentially involved in antagonising IFN expression. Overall, this study has shown for first time the ability of ORFV to counteract type I IFN expression by antagonising dsRNA and dsDNA activated IFN signalling pathways. This study suggests that ORFV early genes are involved in ISG modulation and IFN-β inhibition.

ACKNOWLEDGMENTS

I would like to express my very great appreciation to my supervisor Dr. Stephen Fleming for all the critical advice, guidance, support, enthusiastic encouragement and most importantly his patience over the period of my PhD. His valuable and constructive suggestions are highly appreciated. His willingness to give his time, especially the time for lunch or home, so generously has been much appreciated. His sustainable supervision and guidance during the COVID-19 lockdown are undeniable.

My grateful thanks are also extended to my co-supervisor Prof. Andy Mercer for his advice, support and any useful critiques of this work. His usual support and assistance are much appreciated. A grateful thanks to the department heads Prof. Frank Griffin, Prof. Vernon Ward, Prof. Clive Ronson and Prof. Greg Cook for all the support provided, and Prof. Miguel Quiñones-Mateu for his kindness and patience.

I am still indebted to the aunts Ellena Whelan, Cathy McCaughan, Gabriella Stuart, Nicky Real and Zabeen Lateef for the valuable technical support provided in my early days in the VRU prior my PhD study and techniques that I have learnt. I also thank every member of staff in the VRU and Department of Microbiology and Immunology who have contributed towards the successful completion of this work. I wish to thank also Sonya Mros for enabling me run assays in their laboratory and for the use their reagents. I would like to thank Chris Harry for assisting with lab consumables and Megan Colemen for always reminding us about lab safety and to keep us safe and sound. I thank all the students in the VRU and virology group on the 7th floor who made my time in the lab so enjoyable.

There are no words that I can say to convey my appreciation for my parents for their continuous support and encouragement throughout my study overseas. I know that they have missed me a lot during the long time I have been away studying. I am grateful to have parents like them who love and let me find my own way, their love and support have helped me not only through university but also through life. All these successes would have been impossible without them and I could not have become the person I am today without them in my life.

I would also like to express my gratitude to my parents-in-law who gave me wonderful support and stood beside me during critical period of my time in New Zealand. They have always inspired me in every decision I have made and I am extremely fortunate for have been blessed with such incredible persons.

Lastly, a very special thank you to my lovely wife Halah from the bottom of my heart for her patience, understanding and words of encouragement during the crucial stages of this work. I feel much gratitude and respect towards her for taking care of my family and thank you for helping me with everything, being with me in every situation and all the love and passion you bring, thank God for giving me you. This really proves the saying "there is a women behind the success of every man". I also thank my two girls Nawraa and Zahraa and little son Siraj for their part in bringing such joy and happiness to my life.

TABLE OF CONTENTS

LIST OF FIGURES

LIST OF TABLES

LIST OF ABBREVIATIONS

A

aa	Amino acid
AIM2	Absent in melanoma 2
Amp R	Ampicillin resistance
ANK	Ankyrin
ANO	Adenosine N1-oxide
AP-1	Activator protein 1
AraC	Cytosine arabinoside
ASC	Apoptosis-associated speck-like protein containing CARD Bcl-2 B-cell lymphoma 2

B

bp	Base pair

C

°C	Degree Celsius
CARD	Caspase recruitment domain
cDNA	Complementary DNA
cGAMP	Cyclic GMP-AMP
cGAS	Cyclic GMP-AMP synthase
CHX	Cycloheximide
CMV	Cytomegalovirus
CPE	Cytopathic effect
CpG	Cytidine-phosphate-Guanosine
CPXV	Cowpox virus
CSPD	Chemiluminescent phenyl phosphate-substituted dioxetane

D

DAI	DNA-dependent activator of IFN-regulatory factor
DNA-PK	DNA-dependent protein kinase
DDX3	DEAD-box protein 3
DENV	Dengue virus
DC	Dendritic cells
DMSO	Dimethyl Sulfoxide
dsDNA	Double-stranded DNA
dsRNA	Double-stranded RNA

E

E. coli	*Escherichia coli*
eIF2α	α subunit of eukaryotic initiation factor 2
EBV	Epstein-Barr virus
EMCV	Encephalomyocarditis virus
ER	Endoplasmic reticulum

Continued next page

F

FADD	Fas-associated death domain-containing protein
FCS	Fetal calf serum

G

GAPDH	Glyceraldehyde 3-phosphate dehydrogenase
GIF	Granulocyte-macrophage colony-stimulating factor and Interleukin-2
GM-CSF	Granulocyte-macrophage colony-stimulating factor
GUS	beta-Glucuronidase gene

H

HAV	Hepatitis A virus
HaCaT	Human keratinocytes cell line
HCMV	Human cytomegalovirus
HIV-1	Human immunodeficiency virus type 1 (HIV-1)
hNDF	Human neonatal dermal fibroblast
HPV	Human papillomavirus
HSP	Heat-shock protein
HSV-1	Herpes simplex virus type 1
HSV-2	Herpes simplex virus type 2
HTLV-1	Human T-cell leukaemia virus type 1
h.p.i.	Hour Post Infection

I

IFI	Interferon inducible
IFITM	IFN-inducible transmembrane
IFI16	Interferon-inducible protein 16
IFN	Interferon
IFN-β	Interferon-beta
IFNAR	IFN-α/β and receptor
IκB	I kappa B
IKK	IκB kinase
IKKα	IκB kinase alpha
IKKβ	IκB kinase beta
IKKε	IκB kinase epsilon
IKKλ	IκB kinase lambda
IL-2	Interleukin-2
IL-18	Interleukin 18
IL-1R	Interleukin-1 Receptor
IL-1β	Interleukin 1β
IPS-1	IFN-β promoter stimulator 1
IRAK	Interleukin-1 receptor-associated kinase
IRF	Interferon Regulatory Factor
IRF3	Interferon regulatory factor 3
ISG	Interferon-stimulated gene

Continued next page

ISGF3	Interferon-stimulated gene factor 3
ISRE	Interferon-Stimulated Response Element

J

JAK	Janus Tyrosine Kinase
JEV	Japanese encephalitis virus
JNK	c-jun N-terminal kinase

K

Kb	Kilobase
KSHV	Kaposi's sarcoma-associated herpesvirus

L

LacZ	beta-Galactosidase gene
LGP2	Laboratory of genetic and physiology 2
LRR	Leucine-rich repeat
LT cells	Lamb Testis cells

M

MAPK	Mitogen-activated protein kinase
MAVS	Mitochondrial antiviral signalling
MDA5	Melanoma Differentiation Associated Gene 5
MDDC	Monocyte-derived dendritic cells
MHV68	Murine gammaherpesvirus 68
Mito	Mitochondria
MOI	Multiplicity of infection
MPXV	Monkeypox virus
MV	Measles virus
MVA	Modified Vaccinia virus Ankara
MyD88	Myeloid differentiation primary-response gene 88

N

NF-κB	Nuclear factor kappa-light-chain-enhancer of activated B cells
NLR	NOD-like Receptor
NOD	Nucleotide-binding oligomerization domain
NYVAC	Highly attenuated Vaccinia virus strain

O

OAS	2′-5′-oligoadenylate synthetase
OASL	2′-5′-oligoadenylate synthetase-Like
OPV	Orthopoxvirus
ORFV	Orf virus
OVIFNR	Interferon resistance factor
OV-NZ2	ORFV virus strain NZ2 wild type
OV-NZ2Δ116	ORFV virus strain NZ2 ORF116 deletion mutant

Continued next page

OV-NZ2-Rev116	ORFV virus strain NZ2 ORF116 re-inserted revertant
OVIFNR	Orf virus Interferon inhibitor

P

PAMP	Pathogen-associated molecular pattern
PBMC	Peripheral blood mononuclear cell
pDCs	Plasmacytoid dendritic cells
PKR	Double-stranded RNA-activated protein kinase
Poly(dA:dT)	Poly(deoxyadenylic:deoxythymidlic) acid
Poly(I:C)	Poly(inosinic:polycytidylic) acid
PRR	Pattern-recognition receptor
PSK	Penicillin, Streptomycin. Kanamycin
PYD	Pyrin domain

Q

qRT-PCR	Quantitative Real Time-Polymerase Chain Reaction

R

RIG-I	Retinoic Acid-inducible Gene I
RIP	Receptor-interacting protein
RLR	RIG-I-like Receptor
RNA Pol III	RNA Polymerase III
RPV	Rabbitpox virus
RRV	Ross River Virus
RT-PCR	Reverse Transcription-Polymerase Chain Reaction

S

SARM	Sterile-α-and armadillo-motif-containing protein
STAT	Signal Transducers and Activators of Transcription
STING	Stimulator of interferon genes

T

TAK	TGF beta-activated kinase
TANK	TRAF family member-associated NF-kappa-B activator
TBK1	TANK binding kinase 1
THP-1	Human leukemia monocytic cell line
TIR	Toll/Interleukin-1 receptor/Resistance
TIRAP	Toll-interleukin 1 receptor (TIR) domain-containing adapter protein
TLR	Toll-like Receptor
TLR3	Toll-like Receptor 3
TLR4	Toll-like Receptor 4
TLR7	Toll-like Receptor 7
TLR8	Toll-like Receptor 8
TLR9	Toll-like Receptor 9
TRAF	TNF receptor-associated factor

Continued next page

TRAM	TRIF-related adaptor molecule
TRIF	TIR-domain-containing adapter-inducing interferon-β

V

VACV	Vaccinia virus
VARV	Variola virus
VEGF-E	Vascular endothelial growth factor-E
vIL-10	Viral Homologue of interleukin-10
VSV	Vesicular Stomatitis virus

W

WNV	West Nile virus
Wt	Wild type

X

X-Gal	5-bromo-4-chloro-3-indolyl-β-D-galactopyranoside
X-Gluc	5-bromo-4-chloro-3-indolyl-glucuronide

INTRODUCTION

1 INTRODUCTION

1.1 Overview

Poxviruses are members of the *Poxviridae* family that can infect human, animals and insects. They are large complex enveloped viruses. Unlike most other families of viruses, poxviruses have large DNA genomes which enable them to encode almost all the factors required for replication in the cytoplasm (Buller, R. M. *et al.*, 1991; Moss, B., 2007). A number of poxviruses cause lethal disease that include myxomatosis and smallpox. Smallpox was one of the most devastating diseases of humans until its eradication by the World Health Organization in 1977 in which vaccinia virus (VACV) was used as a vaccine against smallpox. Orf virus (ORFV) is a parapoxvirus that causes benign skin lesions, or severe disease in the immunocompromised, in sheep and goats and can be transmitted to humans. All poxviruses encode a range of factors that counteract the host immune response. These factors are considered accessory factors since they are not essential for replication in cell culture but often critical for replication in the host. Many such factors have been discovered in orthopoxviruses whereas only a small number have been described in parapoxviruses. Most of the accessory genes of parapoxviruses cluster at the termini of the genome.

This thesis investigates the effect of ORFV strain NZ2 (OV-NZ2) infection on the induction of type I IFN. A cell-based assay was designed to examine the effect of OV-NZ2 infection on the expression of IFN-β in cells stimulated with either poly(dA:dT) or poly(I:C). In addition, in attempts to identify virus genes involved in modulating the interferon (IFN) response, the function of ORF116 and ORF020 genes were investigated. These genes are found within the cluster of accessory genes at the termini. ORF116 knockout and revertant viruses were made to examine the differences in mRNA levels of selected interferon-stimulated genes (ISGs) between HeLa cells infected with OV-NZ2 wild type, OV-NZ2Δ116 knockout and OV-NZ2-Rev116 revertant viruses. The ORF116 and ORF020 genes were cloned in an expression vector and their effects on IFN signalling examined in HEK293 cells.

1.1.1 Classification Pathogenesis and Structure of ORFV

There are two subfamilies of the *Poxviridae* family: Entomopoxvirinae that infect insects and Chordopoxvirinae that infect vertebrates. The latter subfamily consists of ten genera with the

members of a given genus displaying similar morphology except the Parapoxvirus genus as shown in Table 1.1. Poxviruses are classified according to their phenotypic characteristics such as nucleic acid type, morphology, mode of replication, host they infect and disease they cause. In addition, the classification is based on serum cross-reactivity and cross-protection between species.

The orthopoxviruses have a broad host range affecting several vertebrates while other genera have a restricted host range and infect only birds such as avipoxvirus (Jarmin, S. *et al.*, 2006) or sheep such as capripoxvirus. There is serologic cross reactivity among viruses within a given genus but very limited reactivity across genera.

ORFV is the type species of the Parapoxvirus genus of the *Poxviridae* family. It has a unique ovoid morphology among chordopoxviruses (Figure 1.1 D) and is the causative agent of Orf disease, a contagious debilitating skin condition of sheep and goats (Figure 1.1 A and B) and can cause zoonotic infection to human and induces localized skin lesions (Figure 1.1 C) (Fleming, S. B. *et al.*, 2007; Mercer, A. *et al.*, 2011).

Poxviruses have a linear dsDNA genome (Moss, B., 2007). VACV referred to as the prototype of the poxvirus family, has been shown to have a genome linked by hairpin loops into one continuous molecule. Adjacent to the hairpin loops is a conserved sequence motif, followed by a set of tandem repeats referred to as the inverted terminal region (ITR) (Boyle, K. *et al.*, 2009; Moss, B., 2007; Moss, B. *et al.*, 2011; Smith, G. L., 2007). Unusually the parapoxvirus DNA genome is composed of 64 % G+C content (Fleming, S. B. *et al.*, 2007). They have an ovoid structure with smaller dimensions compared with other poxviruses of approximately 260 nm in length and 160 nm in width (Figure 1.1 D) (Peters, D. *et al.*, 1964). The outer membrane consists of a tubule-like structure arranged in a criss-cross pattern (Figure 1.1 D) (Mitchiner, M. B., 1969; Nagington, J. *et al.*, 1962; Nagington, J. *et al.*, 1964).

Table 1.1. Classification of *Poxviridae* family and their characteristics.

Subfamily	Genus	Species of Interest	Host Range	Host Species	Disease / Pathology	Mortality	Transmission	Morphology	dsDNA Genome Size
Chordopoxvirinae	Avipoxvirus	Fowlpox virus	Medium	Birds	Skin lesion	Medium – High	Arthropods	Brick-shaped	~260 kb
	Capripoxvirus	Sheeppox virus	Narrow	Sheep	Varied, skin lesion, generalize infection	Medium	Arthropods	Brick-shaped	~150 kb
	Cervidpoxvirus	Mule deerpox virus		Mule deers					
	Crocodylidpoxvirus	Nile crocodilepox virus		Reptiles					
	Leporipoxvirus	Myxoma virus	Medium	European and American rabbit	Myxomatosis skin lesion	High - low	Arthropods	Brick-shaped	~140 kb
	Molluscipoxvirus	Molluscum contagiosum virus	Medium	Primates, Humans	Localized tumors	Low	Contact	Brick-shaped	~180 kb
	Orthopoxvirus	Variola virus	Narrow	Humans	Smallpox	High	Inhalation	Brick-shaped	~200 kb
		Cowpox virus	Broad	>30 species	Localized skin lesions	Low	Contact		
		Vaccinia virus	Broad	Man, mouse, cow	Localized skin lesions	Low	contact		
		Monkeypox virus	Broad	Man, monkey, squirrel	Monkeypox	High	Inhalation / contact		
		Ectromelia virus		Rodents					
	Parapoxvirus	Orf virus	Medium	Sheep, goats, ruminants, humans	Localized skin lesions	Low	Contact	Ovoid	~140 kb
		Red deer poxvirus		Red deer					
		Pseudocowpox virus		Cattle, Humans					
		Bovine popular stomatitis virus		Cattle, Humans					
	Suipoxvirus	Swinepox virus	Narrow	Pigs	Localized skin lesions	Low	Arthropods	Brick-shaped	~146 kb

Continued next page

Subfamily	Genus	Species of Interest	Host Range	Host Species	Disease / Pathology	Mortality	Transmission	Morphology	dsDNA Genome Size
	Yatapoxvirus	Yaba monkey tumor virus	Medium	Primates, humans	Benign tumors, localized skin lesions	Low	Arthropods	Brick-shaped	~145 kb
Entomopoxvirinae	Alphaentomopoxvirus	Melontha melontha		Coleoptera				Ovoid	~260-370 kb
	Betaentomopoxvirus	Amsacta moorei		Lepidoptera, Orthoptera				Ovoid	~232 kb
	Gammaentomopoxvirus	Chrionimus luridus		Diptera				Brick-shaped	~250-380 kb

Table compiled from (Damon, I. K., 2007; Moss, B., 2007) and ICTV 2019 https://talk.ictvonline.org/taxonomy/.

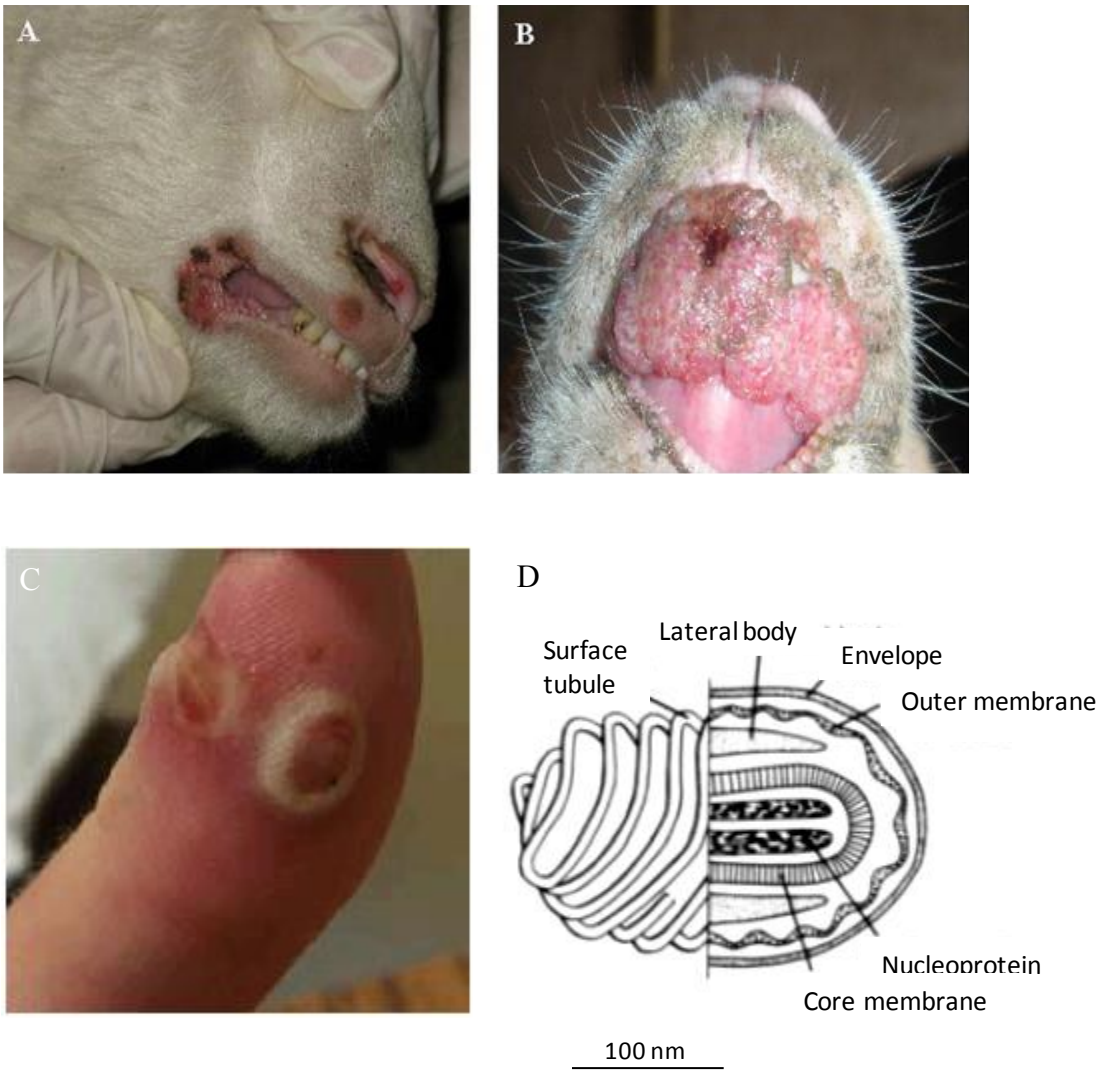

Figure 1.1. Orf disease manifestation and schematic ultrastructure of parapoxvirus virion. (**A**). Orf disease manifested by multiple nodular lesions in sheep on the upper and lower labia of lips. (**B**). Severe proliferative orf disease in the lips of sheep. Obtained from (Zhao, K. *et al.*, 2010). (**C**). A thumb with lesion caused by Orf virus. Obtain from https://www.cdc.gov. **(D).** Schematic diagram of ORFV particle section. The outer membrane consists primarily of a single long tubule that appears to wrap around the virus creating a criss-cross pattern. Adopted from Fenner, F. *et al.* (1988).

1.1.2 Replication and Morphogenesis of Poxviruses

Poxviruses replicate in the cytoplasm and encode their own machinery for DNA transcription and replication. After the virion core is released into the cytoplasm and before complete uncoating, the encapsidated early transcription machinery is activated and early gene expression is initiated within the core. Early mRNAs are extruded from the core into the cytoplasm and then translated using cellular machinery. Some of the early translated proteins are used for subversion of the host innate immune responses, while other proteins are used for DNA replication and for the transcription of intermediate mRNAs. Early gene expression ceases when the core is completely uncoated and the viral genome is released into the cytoplasm in which the replication of the genome is initiated. DNA replication enables the virus to initiate intermediate gene expression that provides proteins for transcription of late genes. Late gene expression produces structural proteins, enzymes and essential proteins required for subsequent infection. Through a process of viral morphogenesis, late gene products are packaged into newly synthesized viral particles that either egress out the cell or are released upon cell lysis as illustrated in Figure 1.2 (Boyle, K. *et al.*, 2009; Moss, B., 2007).

1.1.3 Genetic Structure of ORFV

VACV was the first poxvirus sequenced by Paoletti, E. *et al.* (1977). This illustrated the basic genetic structure of the poxvirus genome. All other poxviruses are essentially similar but the genetic differences mainly lie within the termini of the genome. The genes that are located within the central core encode factors involved in virion structure, polymerases involved in DNA replication and transcriptional factors involved in gene expression. Factors that determine host range, pathogenesis and virulence are encoded within termini of the genome. These genes are non-essential for growth in cell culture.

The genome of several ORFV strains has now been fully sequenced (Delhon, G. *et al.*, 2004; Mercer, A. A. *et al.*, 2006). It was predicted that the OV-NZ2 strain contains 132 genes and the distribution of these genes is typical of poxviruses with the central region containing genes essential for its life cycle and the host range restriction or virulence genes located within terminal regions (Fleming, S. B. *et al.*, 2007; Mercer, A. *et al.*, 2011).

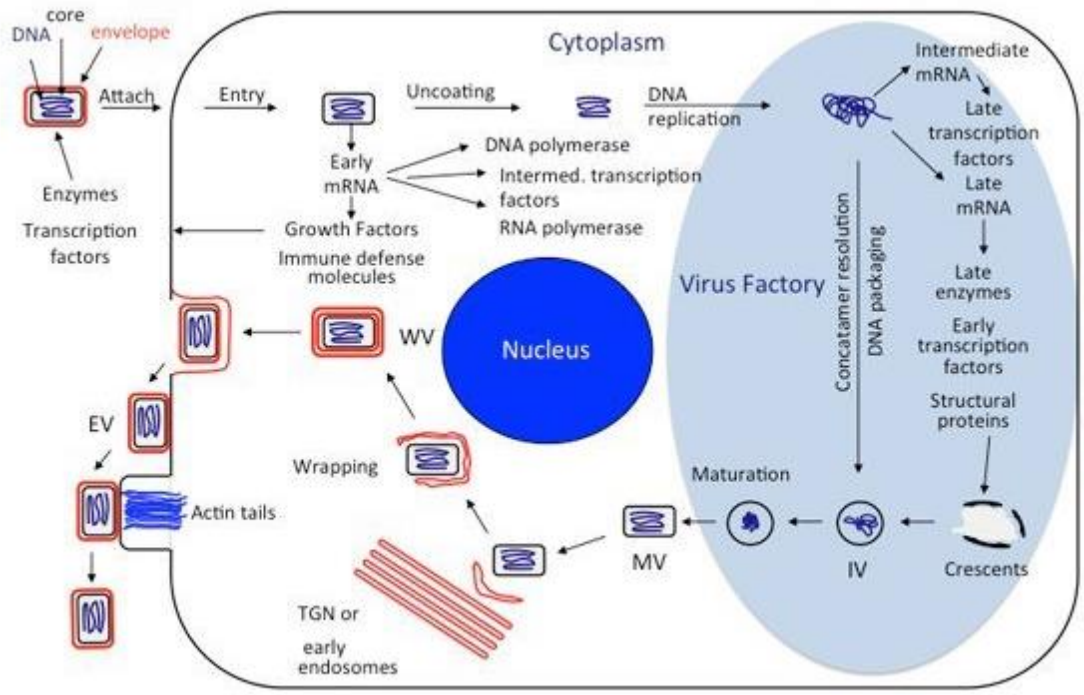

Figure 1.2. Diagrammatic representation of poxvirus replication and morphogenesis. Virus replication occurs in the cytoplasm. Upon virion attachment, virion fuses with the cell membrane and the core is released into the cytoplasm. The core encode the early genes that are translated into proteins involved in host cell modulation, factors for DNA replication and intermediate gene transcription. The core is uncoated and DNA is replicated then the intermediate genes are transcribed to produce factors for late gene transcription. The assembly of virion is formed and maturation of virion is completed and egress from the infected cell. Adopted from https://www.niaid.nih.gov/research/bernard-moss-md-phd.

Like other poxviruses, OV-NZ2 virus has several virulence and immunomodulation genes that act either intracellularly or extracellularly. Bioinformatics analysis has indicated that most genes within the termini of OV-NZ2 seem to be unique and are not found in other poxviruses or have homologues in other organisms. They are predicted to be non-essential and involved in manipulation of host physiology and immunomodulation.

1.2 Interferon System

The interferons (IFNs) are a large group of multifunctional secreted cytokines that contribute in a first line of antiviral defence and immunomodulatory activity. They are divided into three classes according to their sequence homology, receptors and functional activities: type I, type II and type III. Type I IFNs are the key cytokines that mediate antiviral responses, an innate immune response and subsequent development of adaptive immunity to viruses.

Type I IFNs were the first type of interferon discovered by Isaacs, A. *et al.* (1957) on the basis of their antiviral activity. They are a large family of IFN members that are produced in direct response to virus infection: IFN-α consists multiple subtypes which are predominantly produced by immune cells, IFN-β is one type and produced by most cell types particularly fibroblasts, and other members such as IFN-κ, IFN-ε, IFN-ω, IFN-τ and IFN-δ. Although these types are all recognized by a single shared receptor (IFNAR1 and IFNAR2 expressed on almost all cell types), they have pleiotropic activities. It is unclear yet whether these diverse types are expressed differentially in different cell types and induced in response to different types of viruses or each type has a specific function. Type III interferons (IFNs) were discovered many years after the discovery of type I IFN by two groups (Kotenko, S. V. *et al.*, 2003; Sheppard, P. *et al.*, 2003) and shown to have antiviral activity. This type comprises four subtypes of IFN-λ (λ1, λ2, λ3, λ4) and have been found to be induced in direct response to viral infection (Ank, N. *et al.*, 2006; Onoguchi, K. *et al.*, 2007; Uzé, G. *et al.*, 2007; Zhou, J. *et al.*, 2018). A comprehensive review was recently published highlighting shared and distinct features between type I and type III IFNs (Lazear, H. M. *et al.*, 2019). Importantly, they explained the reasons why the host maintains two types of IFN and they attributed that to not only provide supplementary antiviral protection but also to provide an IFN response with less collateral damage than the more potent type I IFN response, as type III IFN functions broadly at epithelia barriers where their receptor (IFNLR1 and IL-10Rβ) is expressed predominantly. Lastly, type II interferons (IFNs) consists of one member called IFN-γ and largely induced by activated T cells and natural killer (NK) cells in response to the recognition of infected cells, not direct viral infection (Alspach, E. *et al.*, 2019).

The IFN system is regulated by two signalling pathways. First, signalling is initiated by detection of viral pathogen associate molecular patterns (PAMPs) by host pattern-recognition receptors

(PRRs) which activate a series of transcription factors (IRFs, NF-κB and ATF2/c-Jun). The activated factors translocate to the nucleus where they bind to the promoter regions of IFNs and pro-inflammatory cytokines forming an enhanceosome and then activate the transcription by RNA polymerase. Upon IFN induction, a second line of signalling is initiated in which the induced IFNs interact with IFN receptors (IFNRs), in an autocrine or paracrine manner, leading to transcription of a diverse set of genes called IFN-stimulated genes (ISGs) via the Janus kinase (JAK)-signal transducer activator of transcription (STAT) pathway. These ISGs are involved in eliminating viral infection from infected cells and also conferring resistance to neighbouring cells. The established antiviral state will inhibit viral replication at various stages. Some ISGs can also be induced directly by viral infection, but less effectively than the IFN response itself, and this induction is amplified significantly by IFN (Wathelet, M. G. *et al.*, 1992).

1.3 Innate Immunity to Virus Infection and Type I Interferon Induction

Host cells adopt multiple defence mechanisms in order to respond to invading viruses. Innate immunity is a first line of defence and an immediate response against viral infection. The key step in this response is detection of the virus infection. Sensing of pathogens by innate immunity is mediated by host PRRs, also called innate immune sensors that recognize PAMPs such as viral nucleic acids that are distinct from host-derived.

These receptors (or sensors) can be classified based on their subcellular localization and distinct virus-derived molecules they recognize. C-type lectin receptors (CLR) and Toll-like receptors (TLR) are endosomal or membrane-bound receptors whereas nucleotide-binding oligomerization domain (NOD)-like receptors (NLR), AIM2-like receptors (ALR) and retinoic acid inducible gene (RIG-I)-like receptors are cytosolic receptors. Each class of these receptors activates specific signalling cascades which in turn activate specific transcription factors to induce expression of target genes namely type I IFNs and proinflammatory cytokines.

Activation of innate immunity is achieved by the recognition of virus infection in order to trigger the signalling pathways and initiate an innate immune response to eliminate the virus. The major PAMPs generated during viral infection are nucleic acids and are the most important molecules that are recognized by the host (Yoneyama, M. *et al.*, 2010). The innate immune system is capable of distinguishing self from non-self of structurally similar nucleic acids to the host's.

Upon recognition of nucleic acids derived from virus, the activation of signalling cascades is triggered leading to induction of type I IFN and proinflammatory cytokines. The secreted IFN binds its receptor and acts as an autocrine or paracrine factor activating the JAK/STAT pathway which in turn induces a number of IFN-inducible genes involved in anti-viral immunity (Kawai, T. *et al.*, 2006; Kawai, T. *et al.*, 2008).

1.3.1 Toll-like Receptors (TLRs) sensing of nucleic acids in endosomes

The importance of TLRs' role in sensing viruses was demonstrated (Bowie, A. *et al.*, 2000; Kurt-Jones, E. A. *et al.*, 2000). TLR receptors are of the best characterized PRRs and have a critical role in detecting invading pathogens outside the cell and in intracellular endosomes. There are 13 mammalian members and their cytoplasmic domains show high similarity to that of the interleukin-1 receptor (IL-1R) family. They sense a wide range of pathogens and trigger distinct signalling pathways that lead to induction of specific responses. They are defined by the presence of N-terminal leucine-rich repeats (LRRs) and a transmembrane domain, then, a cytoplasmic Toll/Interleukin-1 receptor (TIR) domain (Akira, S., 2003; Medzhitov, R., 2001; Takeda, K. *et al.*, 2005; Yoneyama, M. *et al.*, 2010).

Among all TLRs characterized to date, only TLR3, -7, -8, and -9 are the known receptors that interact with viruses (Table 1.2) and mediate the production of type I IFNs. TLR3, TLR7, TLR8, and TLR9 are mainly expressed in endosomes of some cell types. They are involved in the detection of nucleic acids derived from viruses by means of LRR domain to transmit intracellular responses through the recruitment TIR-containing adaptor (Boehme, K. W. *et al.*, 2004; Bowie, A. G. *et al.*, 2005; Kawai, T. *et al.*, 2010; Vaidya, S. A. *et al.*, 2003). Three mechanisms of delivering viral nucleic acid to the endosomal compartment have been described. The first one is dependent on the endocytosis pathway and protease-mediated degradation of invading viruses. The second one operates through autophagy in which the viral nucleic acid is transferred to endolysosomes. The last mechanism is dependent on cell-to-cell contact and transfer of viral nucleic acid-containing exosomes (Dreux, M. *et al.*, 2012).

1.3.1.1 TLR9-dependent DNA Sensing

TLR9 was the first DNA sensor identified and the only known sensor so far responsible for DNA sensing in endosome (Gilliet, M. *et al.*, 2008; Kadowaki, N. *et al.*, 2001). It is mainly expressed in B cells and plasmacytoid DCs (pDCs), a cell type that produces large amounts of type I IFNs in response to virus infection. It is well-established that TLR9 senses unmethylated cytosine-guanine dinucleotide (CpG) motif of pathogen DNA, which is frequently observed in bacteria and viruses, unlike host genomic DNA (Haas, T. *et al.*, 2008). TLR9 is mainly present on the membrane of the endoplasmic reticulum (ER) when it is inactive, however, when stimulated by its ligand, it traffics to the endosome under the control of protein unc93 homolog B (UNC93B) (Kim, Y.-M. *et al.*, 2008; Tabeta, K. *et al.*, 2006).

The antiviral role of TLR9 was identified in which the production of type I IFN was examined in response to several infections of circular or linear dsDNA viruses: herpes simplex virus 1 (HSV-1) and murine cytomegalovirus (MCMV) (Hochrein, H. *et al.*, 2004; Krug, A. *et al.*, 2004), adenovirus (ADV) (Zhu, J. *et al.*, 2007), poxviruses (Samuelsson, C. *et al.*, 2008), murine gammaherpesvirus 68 (MHV-68) (Guggemoos, S. *et al.*, 2008), Epstein-barr virus (EBV) (Fiola, S. *et al.*, 2010) kaposi's sarcoma-associated herpesvirus (KSAH) (West, J. A. *et al.*, 2011), human papillomavirus (HPV) (Hasan, U. A. *et al.*, 2007) and Merkel cell polyomavirus (MCV) (Shahzad, N. *et al.*, 2013).

Although the pivotal role of TLR9 in the antiviral response was shown in some cell types, it seems that TLR9 might only have a minor role and it is not the critical sensor for viruses in cell types that are most often infected. Therefore, the TLR9-independent mechanism is much more important in controlling virus infection. pDCs, which express TLR9 and a potent inducer of IFN, are not usually the first cells that come in contact with invading viruses. It has also been shown that DCs and monocytes deficient in TLR9 can still respond to transfected viral DNA or DNA virus infection (Hochrein, H. *et al.*, 2004; Ishii, K. J. *et al.*, 2006). Many cell types such as fibroblasts and epithelial cells do not express TLR9, but they still respond to exogenous DNA and produce type I IFN (Ishii, K. J. *et al.*, 2006; Stetson, D. B. *et al.*, 2006).

1.3.1.2 TLR3, 7, 8-dependent RNA Sensing

TLR3 recognizes a synthetic analogue of viral dsRNA, polyinosinic acid-cytidylic acid (poly(I:C)), widely used to mimic viral infection and viral dsRNA generated during virus replication (Schröder, M. *et al.*, 2005). It was identified from a study on mice deficient in IFN-inducible dsRNA-dependent protein kinase (PKR) in which it was found that they still responded to poly(I:C). Moreover, the induction of proinflammatory cytokines and type I IFNs were abolished in response to poly(I:C) in $TLR3^{-/-}$-deficient macrophages and splenocytes (Alexopoulou, L. *et al.*, 2001; Weber, F. *et al.*, 2006). It has been widely known that TLR3 is expressed in the endosome, however TLR3 expression was also found on the cell surface in some fibroblasts (Matsumoto, M. *et al.*, 2002). The location of TLR3 expression appears to be cell type-dependent, as discussed in (Randall, R. E. *et al.*, 2008). The role of TLR3 in the antiviral response upon dsRNA or virus infection detection and the induction of type I IFN mediated via TLR3 have been reviewed previously (Bowie, A. G. *et al.*, 2008; Goffic, R. L. *et al.*, 2006; Rudd, B. D. *et al.*, 2006; Schröder, M. *et al.*, 2005; Vercammen, E. *et al.*, 2008; Wang, T. *et al.*, 2004; Yoneyama, M. *et al.*, 2010).

TLR7 and TLR8 are structurally homologous and closely related to TLR9 in terms of sequence similarity and known to recognize ssRNA. TLR7 is mostly found in pDCs whereas TLR8 is mainly expressed in myeloid dendritic cells (DC) and monocytes and both are expressed exclusively in endosomes. Their role in antiviral immunity were identified from the initial observation that imidazoquinolines such as imiquimod (R-837) and resiquimod (R-848), a known antiviral compound, can activate innate immunity in a human TLR7- and TLR8-dependent and mouse TLR7-dependent manner but not in mouse TLR8 in TLR-transfected HEK293 cells (Hemmi, H. *et al.*, 2002; Jurk, M. *et al.*, 2002). Initially, it was thought that TLR8 is non-functional in mice as it failed to initiate immunity upon stimulation with natural ssRNA or R-848, however, a subsequent study showed that mouse TLR8 expressed in HEK293 cells can be activated when cells are stimulated with a combination of polyT oligodeoxynucleotides (ODNs) and imidazoquinolines (Gorden, K. K. B. *et al.*, 2006). Paradoxically, type I IFN was also induced in mouse TLR8-expressing HEK293 cells when stimulated with VACV dsDNA (Martinez, J. *et al.*, 2010). Subsequent studies have shown that guanosine- and uridine-rich ssRNA from the human immunodeficiency virus (HIV-1) genome was identified as a ligand for

murine TLR7 and human TLR8 (Heil, F. *et al.*, 2004); in addition, either synthetic ssRNA or RNA derived from influenza and vesicular stomatitis virus (VSV) were also ligands for TLR7 (Diebold, S. S. *et al.*, 2004; Lund, J. M. *et al.*, 2004). The minimal sequence content required for a TLR7 ligand was investigated for ssRNA recognition in which it was found that ssRNA must at least contain several uridines in close proximity for TLR7 stimulation (Diebold, S. S. *et al.*, 2006).

Table 1.2. The interaction of viruses with mouse and human Toll-like receptors (TLRs) in different model systems.

	TLR	Virus	Family	Macromolecules detected	Model System used	Genome Structure	Reference
Human	TLR3	Vaccinia virus (VACV)	Poxviridae	Unknown	Human keratinocytes	dsDNA	(Howell, M. D. *et al.*, 2006)
		Herpes simplex virus (HSV)	Herpesviridae	Unknown	Human polymorphisms	dsDNA	(Zhang, S.-Y. *et al.*, 2007)
		Epstein–Barr virus (EBV)	Herpesviridae	dsRNA	Human PBMCs and lymphocytes	dsDNA	(Iwakiri, D. *et al.*, 2009)
	TLR7	Human immunodeficiency virus (HIV)	Retroviridae	Unknown	Patient study	ssRNA (RT)	(Meier, A. *et al.*, 2009)
		Human immunodeficiency virus (HIV)	Retroviridae	Unknown	Human polymorphisms	ssRNA (RT)	(Oh, D. *et al.*, 2009)
		Kaposi's sarcoma-associated herpesvirus (KSHV)	Herpesviridae	Unknown	Latent infected primary effusion lymphoma cell lines	dsDNA	(Gregory, S. M. *et al.*, 2009)
	TLR8	Human immunodeficiency virus (HIV)	Retroviridae	ssRNA	HEK 293 cells	ssRNA (RT)	(Heil, F. *et al.*, 2004)
		Kaposi's sarcoma-associated herpesvirus (KSHV)	Herpesviridae	Unknown	Latent infected primary effusion lymphoma cell lines	dsDNA	(Gregory, S. M. *et al.*, 2009)
	TLR9	Human immunodeficiency virus (HIV)	Retroviridae	Unknown	Human B cells	ssRNA (RT)	(Jiang, W. *et al.*, 2008)
		Human immunodeficiency virus (HIV)	Retroviridae	CpG	Human B cells	ssRNA (RT)	(Malaspina, A. *et al.*, 2008)
		Human immunodeficiency virus (HIV)	Retroviridae	gp120	Human pDCs	ssRNA (RT)	(Martinelli, E. *et al.*, 2007)
		Human immunodeficiency virus (HIV)	Retroviridae	Unknown	Human polymorphisms	ssRNA (RT)	(Bochud, P.-Y. *et al.*, 2007)
		Hepatitis B virus (HBV)	Hepadnaviridae	Unknown	Human pDCs	dsDNA-RT	(Xie, Q. *et al.*, 2009)
		Hepatitis C virus (HCV)	Flaviviridae	Unknown	Patient liver samples	ssRNA (+)	(Huang, X. X. *et al.*, 2007)
		Respiratory syncytial virus (RSV)	Paramyxoviridae	Unknown	Human pDCs	ssRNA (−)	(Schröder, M. *et al.*, 2005)
Murine	TLR3	Vaccinia virus (VACV)	Poxviridae	Unknown	Knock-out mice	dsDNA	(Hutchens, M. *et al.*, 2008)
		Punta Toro virus (PTV)	Bunyaviridae	Unknown	Knock-out mice	ssRNA (−)	(Gowen, B. B. *et al.*, 2006)

Continued next page

TLR	Virus	Family	Macromolecules detected	Model System used	Genome Structure	Reference
	Influenza A virus (IAV)	Orthomyxoviridae	Unknown	Knock-out mice	ssRNA (−)	(Goffic, R. L. *et al.*, 2006)
	West Nile virus (WNV)	Flaviviridae	Unknown	Knock-out mice	ssRNA (+)	(Daffis, S. *et al.*, 2008; Wang, T. *et al.*, 2004; Welte, T. *et al.*, 2009)
TLR7	Influenza A virus (IAV)	Orthomyxoviridae	ssRNA	Knock-out mice	ssRNA (−)	(Diebold, S. S. *et al.*, 2004)
	Human immunodeficiency virus (HIV)	Retroviridae	ssRNA	Knock-out mice	ssRNA (RT)	(Heil, F. *et al.*, 2004)
	Vesicular stomatitis virus (VSV)	Rhabdoviridae	ssRNA	Knock-out mice	ssRNA (−)	(Lund, J. M. *et al.*, 2004)
	West Nile virus (WNV)	Flaviviridae	Unknown	Knock-out mice	ssRNA (+)	(Daffis, S. *et al.*, 2008; Wang, T. *et al.*, 2004; Welte, T. *et al.*, 2009)
TLR9	Herpes simplex virus (HSV-1)	Herpesviridae	Unknown	Knock-out mice	dsDNA	(Hochrein, H. *et al.*, 2004)
	Murine cytomegalovirus (MCMV)	Herpesviridae	Unknown	Knock-out mice	dsDNA	(Krug, A. *et al.*, 2004)
	Adenovirus (ADV)	Adenoviridae	Unknown	Knock-out mice	dsDNA	(Zhu, J. *et al.*, 2007)
	Poxviruses	Poxviridae	Unknown	Knock-out mice	dsDNA	(Samuelsson, C. *et al.*, 2008)
	Murine gammaherpesvirus 68 (MHV-68)	Herpesviridae	Unknown	Knock-out mice	dsDNA	(Guggemoos, S. *et al.*, 2008)
	Human immunodeficiency virus (HIV)	Retroviridae	CpG	Transgenic mice	ssRNA (RT)	(Equils, O. *et al.*, 2003)

Table obtained and modified from (Carty, M. *et al.*, 2010).

1.3.1.3 Toll-Like Receptor Signalling Pathways

Recognition of PAMPs by different TLRs results in activation of distinct signalling cascades that is also dependent on cell type. These differences are caused mainly by different TIR-domain adaptor proteins recruited to TLRs. Five TIR-domain adaptor proteins that control signalling from activated TLRs have been identified: myeloid differentiation primary-response gene 88 (MyD88), Toll-interleukin 1 receptor (TIR) domain-containing adapter protein (TIRAP), TIR-domain-containing adaptor protein inducing IFNβ (TRIF), TRIF-related adaptor molecule (TRAM) and sterile-α-and armadillo-motif-containing protein (SARM) which mediate cellular signalling that leads to the induction of type I IFN and proinflammatory cytokines (Kawai, T. *et al.*, 2010; O'Neill, L. A. J. *et al.*, 2007). Each TLR mediates distinctive responses in association with a different TIR-containing adaptor. TLR7, 8 and 9 recruit MyD88 to transmit cellular signalling whereas TLR3 recruits TRIF (or TICAM-1) to mediate signalling leading to interferon regulatory factor 3 (IRF3) and interferon regulatory factor 7 (IRF7) activation and type I IFN induction (Figure 1.3) (Oshiumi, H. *et al.*, 2003; Yamamoto, M. *et al.*, 2003; Yamamoto, M. *et al.*, 2002). In TLR-dependent nucleic acid sensing, two distinct TLR signalling pathways are defined that depend on the usage of MyD88 and TRIF adaptor proteins.

The MyD88-dependent Signalling Pathway

Unlike TLR3; TLR7, 8 and 9 utilize the MyD88-dependent signalling pathway in which MyD88 is the adaptor molecule for triggering the downstream signalling cascades. Upon engagement with their ligand, the receptors transmit their signal via MyD88 which then recruits the downstream signalling molecules interleukin-1 receptor- associated kinase 4 (IRAK4), a serine/threonine kinase with an N-terminal death domain. IRAK4 activates interleukin-1 receptor-associated kinase 1 and 2 (IRAK1/2) (Kawagoe, T. *et al.*, 2008). The IRAKs then dissociate from MyD88 and interact with TNFR-associated factor 6 (TRAF6), that acts as an E3 ubiquitin protein ligase to catalyses the formation of a lysine 63 (K63)-linked polyubiquitin chain on TRAF6 (Kawai, T. *et al.*, 2004). Subsequently, the IKKα/IKKβ/IKKγ complex phosphorylates IκB leading to activation of three transcription IRF7, nuclear factor kappa-light-chain-enhancer of activated B cells (NF-κB) and activator protein 1 (AP-1). In contrast to the activation of IRF3 observed in TLR3 stimulation, IRF7 is constitutively expressed in pDCs and

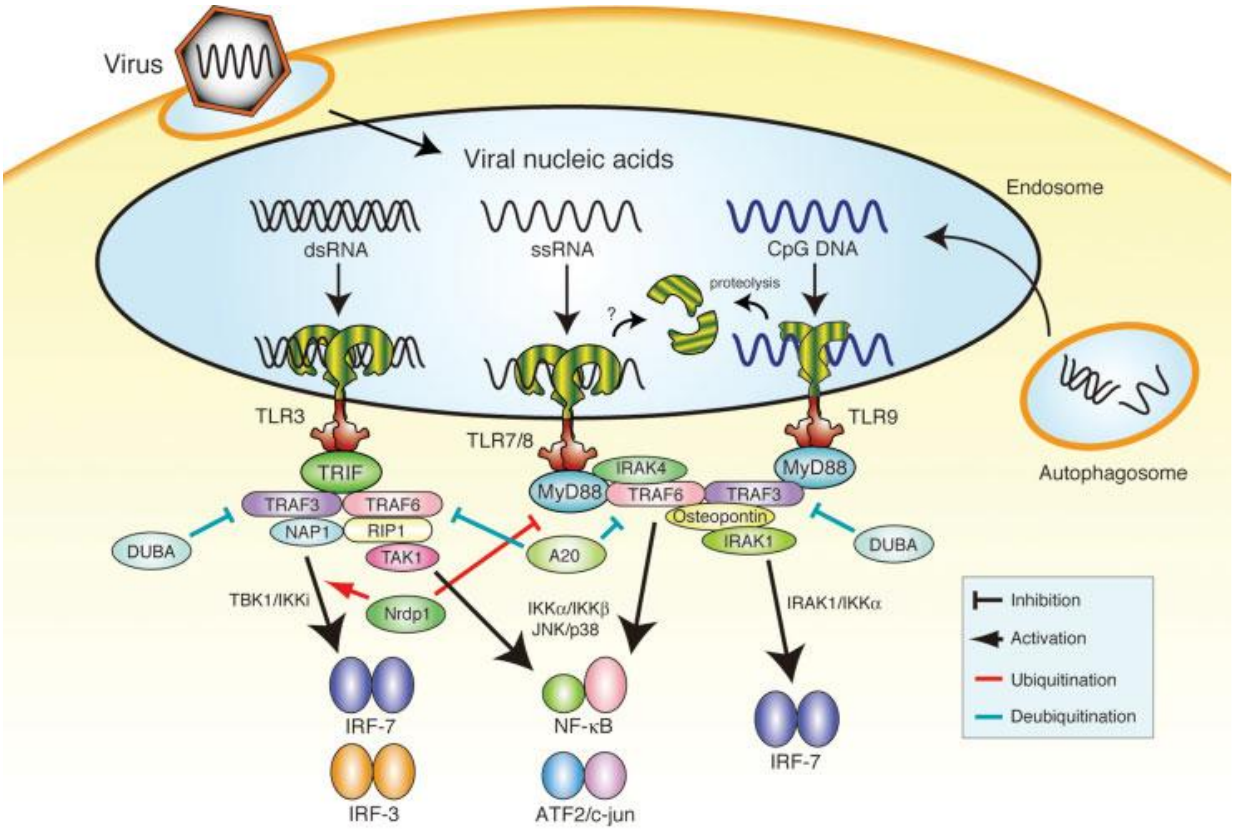

Figure 1.3. Recognition of viral nucleic acids by TLRs. TLR3/ TLR7/8 and TLR9 detect viral dsRNA, ssRNA and CpG DNA respectively in endosome. TLR3 interacts with adaptor molecule TRIF to activate the downstream signalling indicated, whereas TLR7/8 and TLR9 interact with adaptor molecule MyD88 to activate the downstream signalling indicated. See the text for detail. Obtained from (Yoneyama, M. *et al.*, 2010).

works alternatively for IFN induction. It is important to note that the action of IRF7 is different from the feedback activation of IRF7 in TLR3 stimulation (Marié, I. *et al.*, 1998). IRF7 is recruited to the signalling complex formed by signalling intermediates and activated by IRAK1 and IKK-α via phosphorylation (Hoshino, K. *et al.*, 2006; Uematsu, S. *et al.*, 2005). NF-κB and AP-1 are both activated by IRAK4 and TRAF6 then TAK1, but differ in their IκB kinases-α-β-γ (IKKα/IKKβ/IKKγ) and mitogen-activated protein kinase (MAPK) respectively (Koyama, S. *et al.*, 2008).

The TRIF-dependent Signalling Pathway

Only the TLR3 receptor, with the exception of TLR4 that triggers both MyD88-dependent and TRIF-dependent signalling, depend on the TRIF domain to initiate the signalling pathway. It is initiated upon engagement of TLR3 with dsRNA that leads to recruitment of TRIF. Then TRIF recruits and interacts with a set of signalling intermediates including TRAF6, TRAF3 and receptor-interacting protein 1 (RIP1). The interaction of TLR3 and TRIF can activate two transcription factors NF-κB and IRF3 (Jiang, Z. *et al.*, 2004). During the activation of NF-κB, TRAF6 and RIP1 co-operatively activate TGF beta-activated kinase 1 (TAK1) leading to the activation of IKKα/IKKβ/IKKγ whereas IRF3 is activated via TRAF3, then activating TANK binding kinase 1/ IκB kinase-ε (TBK1/IKK-ε) which then phosphorylates IRF3 (Fitzgerald, K. A. *et al.*, 2003; Sharma, S. *et al.*, 2003; Vercammen, E. *et al.*, 2008). It has been demonstrated that TBK1/IKKε are responsible kinases for TRIF-mediated IFN-β induction (Hemmi, H. *et al.*, 2004; Perry, A. K. *et al.*, 2004).

1.3.2 Intracellular Nucleic Acid Sensing

Intracellular PRRs are localized in the cytoplasm or nucleus including retinoic acid inducible gene (RIG-I)-like Receptors (RLRs), AIM2-like receptors (ALRs) and nucleotide-binding oligomerization domain (NOD)-like Receptors (NLRs). These intracellular sensors are widely expressed to detect virus infection in the cytoplasm and nucleus in almost all cell types and are the key intracellular sensors of viral RNA or viral DNA.

1.3.2.1 Intracellular Detection of DNA

Non-self DNA is usually detected when it is within the cells (Watson, R. O. *et al.*, 2012). Therefore, the host expresses several DNA sensors located at various intracellular sites, endosomes, cytosol and nucleus. The non-self DNAs that are detected by intracellular sensing usually originate from viruses and intracellular bacteria. DNA viruses, the focus of this study, include those replicating in the cytoplasm such as poxviruses and those replicating in the nucleus such as herpesviruses. Observations by Hochrein, H. *et al.* (2004) and his colleagues provided evidence that viral DNA can also be sensed in the cytoplasm and lead to induction of type I IFN and proinflammatory cytokines. They found that viral genomic DNA, such as VACV, can elicit

an IFN response in a TLR-independent manner which strongly suggested that there is another DNA sensing mechanism that can recognize cytoplasmic DNA.

Upon infection, viral genomic DNA is uncoated and released into the cytosol, rendering its exposure to cytosolic DNA sensors. This was demonstrated from the observation that viral genomic DNA from HSV-1 or CMV associated with the DNA sensor IFI16 (Horan, K. A. *et al.*, 2013; Li, T. *et al.*, 2013; Orzalli, M. H. *et al.*, 2012), suggesting that the viral genome could trigger cytosolic DNA sensing. Others believe that virus infection could cause cellular stress leading to the release of mitochondrial DNA into the cytosol which then results in activation of cytosolic DNA sensing as observed in herpesvirus infection (West, A. P. *et al.*, 2015).

Cytosolic sensing of DNA and the signalling pathways involved have only been identified over the last 15 years. There is growing evidence that cytosolic PRRs are important in detecting cytosolic viral DNA in the cytoplasm, despite that the underlying mechanisms are still to be elucidated. A number of proteins have been proposed so far, reviewed previously, to be important for cytosolic DNA recognition that lead to induction of type I IFN as discussed below (Table 1.3 and Figure 4.1 A). Only three (AIM2, DNAPK and cGAS) among about 13 cytosolic DNA sensors were clearly shown to have a role in DNA-dependent IFN production. It is worth noting that due to the complexity of the DNA sensing system and lack of clear understanding, the importance of the sensors and signalling components involved during virus infection were identified by the evasion strategies used by viruses to inhibit these molecules.

DNA-dependent activator of IRFs (DAI) (also known as ZBP1 or DLM1) was the first reported cytosolic DNA sensor (Takaoka, A. *et al.*, 2007). DAI was shown to have binding activity with DNA. Its role in the antiviral response was investigated in L929 cells in which the expression of the IFN response was enhanced in cells transiently expressing DAI when stimulated with poly(deoxyadenylic:deoxythymidylic) acid (poly(dA:dT)) and this response decreased in DAI-depleted L929 cells in response to HSV-1. However, its role in macrophages was not observed (Unterholzner, L. *et al.*, 2010) as $DAI^{-/-}$ mice responded normally to DNA (Ishii, K. J. *et al.*, 2008) and its role is not important in many human cell types (Lippmann, J. *et al.*, 2008). These observations suggested the existence of other cytosolic DNA sensors and DAI was either largely redundant or has a cell-type specific role.

Table 1.3. Known cytosolic DNA sensors triggering type I IFN induction and pro-inflammatory cytokines.

Receptor	Cell type	Ligand	Pathogen	Response	Signalling molecules involved	Evidence for DNA binding	Reference
DAI	Mouse L929	Poly(dA:dT), VACV DNA, E.coli DNA, CT DNA	HCMV, HSV-1, Streptococcus pneumonia	IFN-β	TBK1, IRF3, RIP1, RIP3, NF-κB	FRET between B-DNA and DAI, pull-down of DAI B-DNA ± competition	(Parker, D. *et al.*, 2011; Takaoka, A. *et al.*, 2007; Upton, Jason W. *et al.*, 2012; Wang, Z. *et al.*, 2008)
RNA Pol III	HEK293, HeLa, BMDM, BMDC, MEF, human MDDC, PBMC, L929, Mutu III, RAW264.7	Poly(dA:dT)	EBV, *Leg. pneumophila*, adenovirus, HSV-1?	IFN-β	RIG-I, MAVS,TBK1, DDX3, IRF3	Production of IFN-inducing RNA transcripts sensitive to Pol III inhibition, purified core RNA Pol III complex producing IFN-inducing RNA	(Ablasser, A. *et al*., 2009; Chiu, Y.-H. *et al.*, 2009)
IFI16/p204	RAW264.7, THP-1, HFF, corneal epithelial cells, neutrophils, human MDM, human MDDC, HeLa, BMDM	dsDNA (60, 70 bp) oligonucleotides, poly(dA:dT), poly(dG:dC), plasmid, HSV-1 DNA, VACV DNA	HSV-1	IFN-β, CXCL10, IL-6, IL-1β	STING, TBK1, IRF3, NF-κB	Co-precipitation of cytosolic IFI16 with dsDNA-coupled beads, interaction between rIFI16 and dsDNA in α-screen	(Duan, X. *et al*., 2011; Horan, K. A. *et al.*, 2013; Kerur, N. *et al.*, 2011; Orzalli, M. H. *et al.*, 2012; Søby, S. *et al.*, 2012; Unterholzner, L. *et al.*, 2010)
AIM2	Macrophages, DCs			IL-1β, IL-18		Affinity purification of Myc-tagged AIM2 with dsDNA-coupled beads, interaction between rAIM2 and dsDNA in α-screen	(Bürckstümmer, T. *et al.*, 2009; Fernandes-Alnemri, T. *et al.*, 2009; Hornung, V. *et al.*, 2009; Roberts, T. L. *et al.*, 2009)
MRE11	BMDC, human ATLD, MEF, DCs	Poly(dA:dT), ISD, *E.coli* DNA		IFN-β, CXCL10, IL-6		Precipitation of MRE11 by streptavidin beads in lysates from cells transfected with biotin-dsDNA	(Kondo, T. *et al.*, 2013)
DNA-PKcs /Ku70/Ku80	MEF, mouse ears *in vivo*, *293T*	Poly(dA:dT), ISD, plasmid, *E.coli* DNA, VACV DNA	MVA, HSV-1	IFN-λ1, IFN-β, IL-6	IRF1, IRF7	Co-precipitation of cytosolic Ku70, Ku80 and DNA-PKcs with dsDNA-coupled beads	(Ferguson, B. J. *et al.*, 2012; Zhang, X. *et al.*, 2011)
cGAS	L929, THP-1, HEK293	Poly(dA:dT), poly(dG-dC), ISD, HT DNA	HSV-1	IFN-β	STING	Precipitation of GST-cGAS with biotinylated DNA	(Ablasser, A. *et al*., 2013; Civril, F. *et al.*, 2013; Diner, Elie J. *et al.*, 2013; Sun, L. *et al.*, 2013; Zhang, X. *et al.*, 2013)

Continued next page

Receptor	Cell type	Ligand	Pathogen	Response	Signalling molecules involved	Evidence for DNA binding	Reference
HMGBs	MEF	Poly(dA:dT), ISD, plasmid, *E.coli* DNA, VACV DNA, HSV DNA, poly(I:C), 5'ppp RNA	HSV-1, VSV				(Yanai, H. *et al*., 2009)
LRRFIP1	RAW264.7, mouse PM,	Poly(dA:dT), poly(dG:dC), *Listeria* DNA, poly(I:C)	*L. monocytogenes*, VSV		β-catenin, p300, IRF3		(Yang, P. *et al*., 2010)
LSm14A	HEK293, THP-1	Poly(dA:dT), poly(I:C), 5'ppp RNA	HSV-1, SeV				(Li, Y. *et al*., 2012)
DHX9	Human pDCs	CpG-A	HSV	TNF-α	MyD88, NF-κB (p50)	Co-precipitation of DHX9 with biotin-CpG-B	(Kim, T. *et al.*, 2010)
DHX36	Human pDCs	CpG-B	HSV	IFN-α	MyD88, IRF7	Co-precipitation of DHX36 with biotin-CpG-A	(Kim, T. *et al.*, 2010)
DDX41	D2SC, BMDC, THP-1	Poly(dA:dT), poly(dG:dC), HSV DNA, VACV DNA	HSV-1, *L. monocytogenes*, adenovirus	IFN-α, IFN-β		Co-precipitation of dsDNA with HA-tagged DDX41	(Parvatiyar, K. *et al.*, 2012; Zhang, Z., Yuan, B., Bao, M., *et al*., 2011)
DDX60							(Miyashita, M. *et al.*, 2011)
Rad50-CARD9							(Roth, S. *et al.*, 2014)
Sox2							(Xia, P. *et al*., 2015)
BAF							(Kobayashi, S. *et al.*, 2015)
DHX29							(Sugimoto, N. *et al*., 2014)

Table compiled from (Keating, S. E. *et al.*, 2011; Paludan, Søren R. *et al.*, 2013; Unterholzner, L., 2013).

A further DNA sensor was soon identified following the discovery of DAI which is RNA Polymerase III/RIG-I (RNA Pol III) (Ablasser, A. *et al.*, 2009; Chiu, Y.-H. *et al.*, 2009). Surprisingly this sensor acts through an RNA sensing pathway in response to DNA. RNA Polymerase III has a role in transcribing cellular RNA such as transfer RNAs (tRNAs), 5S ribosomal RNAs and synthetic poly(dA:dT) AT-rich dsDNA, when transfected into cells, but not GC- rich dsDNA. RNA Pol III transcribes poly(dA:dT) into 5' triphosphate dsRNA which is then recognized by the cytosolic RNA sensor RIG-I, but not MDA5, which induces the expression of IFN-β (Nie, Y. *et al.*, 2013; Rathinam, V. A. K. *et al.*, 2011). However, the role of RNA Pol III in detection of virus DNA remains to be elucidated as cells that have RNA Pol III such as HEK293 do not respond to DNA species originating from viruses, bacteria or mammals, with the exception of Epstein Barr virus encoded small RNAs (EBERs) (Unterholzner, L. *et al.*, 2010). In addition, the RNA Pol III-dependent pathway seems to be redundant where the DNA-dependent sensing pathway is functional.

The PYHIN family proteins (IFI16/p204 and AIM2) harbour an N-terminal signalling PYRIN domain and one or two C-terminal DNA binding HIN200 domains. This structure proposes their role as cytosolic DNA sensors. Besides, they are strongly induced by interferon and bind DNA in a sequence-independent manner by interacting with the phosphate-sugar DNA backbone (Burdette, D. L. *et al.*, 2012; Jin, T. *et al.*, 2012). Cytosolic DNA can also activate not only IFN signalling but also inflammasome signalling in an NLRP3-independent manner. Absent in melanoma 2 (AIM2) was identified as a sensor detecting DNA in the cytoplasm and facilitates the recruitment of ASC and subsequently caspase 1 activation resulting in secretion of IL-1β (Figure 4.1 B). Furthermore, its role was demonstrated in AIM2$^{-/-}$ mice (Bürckstümmer, T. *et al.*, 2009; Fernandes-Alnemri, T. *et al.*, 2009; Hornung, V. *et al.*, 2009; Roberts, T. L. *et al.*, 2009). Another member of the PYHIN family, IFN-γ-inducible protein 16 (IFI16) or mouse ortholog p204, has been identified to have a role in cytosolic DNA sensing. IFI16 activation leads to IRF-3 and NF-κB-dependent signalling cascades that result in production of type I IFN. IFI16 role in the antiviral response was demonstrated in studies that have shown an impairment of IFN induction in IFI16-depleted cells when stimulated with DNA or infected with HSV-1 (Orzalli, M. H. *et al.*, 2012; Unterholzner, L. *et al.*, 2010), inhibition of HCMV replication (Gariano, G. R. *et al.*, 2012) or detection of HIV DNA (Jakobsen, M. R. *et al.*, 2013). Unlike AIM2, IFI16

was found to shuttle between the nucleus and cytoplasm in a cell-type specific manner (Veeranki, S. *et al.*, 2012).

DExD/H-Box Helicases (DDX) protein family comprises RNA and DNA helicases. Although many are involved in gene regulation, several helicases have been identified to be involved in innate immunity. Using a proteomic screen for proteins binding CpG-containing DNA, DHX9 and DHX36 were the first helicases identified in pDCs to act as putative cytosolic DNA sensors (Kim, T. *et al.*, 2010). These two proteins have shown differential activity. DHX9-depleted cells have shown a decrease in TNF-α production in response to HSV-1 whereas DHX-36-depleted cells have shown a decrease in IFN-α production in response to the same virus. In addition, it was found that production of IFN-α and IRF-7 activation in these cells in response to CpG-A DNA was DHX36-dependent, whereas production of TNF-α and IL-6 and NF-κB in response to CpG-B DNA was DHX9-dependent. Both proteins were found to associate with MyD88, a TLR adaptor, and TLR9-depleted cells were severely impaired in their response upon stimulation with CpG DNA. These observations could suggest that DHX9 and DHX36 might be required in a TLR9-dependent pathway in pDCs rather that DNA sensors per se. This has prompted further investigation to identify other DExD/H-box helicases involved in cytosolic DNA sensing. Zhang, Z., Yuan, B., Bao, M., *et al.* (2011) and his colleagues have identified DDX41 as a putative DNA sensor after screening 59 members of the DExD/H-box helicases using an siRNA screen approach. DDX41 was shown to bind with DNA, bacterial cyclic dinucleotides (CDN), cyclic-di-GMP and cyclic di-AMP and also interact with stimulator of interferon genes (STING), a critical adaptor for cytosolic DNA sensing, and TBK1 (Parvatiyar, K. *et al.*, 2012; Zhang, Z., Yuan, B., Bao, M., *et al.*, 2011). The role of DDX41 in the IFN response was demonstrated in DCs and THP-1 cells when transfected with DNA or infected with HSV-1 or adenovirus.

Since viruses interact with the host DNA damage machinery, possibly for the reason that any damage caused to DNA could lead to production of IFN-β, it is assumed that the DNA damage factors involved in this response act as cytosolic DNA sensors (Brzostek-Racine, S. *et al.*, 2011; Karpova, A. Y. *et al.*, 2002; Kim, T. *et al.*, 1999; Weitzman, M. D. *et al.*, 2010). DNA-dependent protein kinase (DNA-PK) is a heterotrimeric complex that consists of Ku70, Ku80 and the catalytic subunit DNA-PKcs and has a role in DNA damage repair through the two repair pathways: homology-directed repair (HDR) and non-homologous end joining (NHE). Ku70 was

first described to have a role in cytosolic DNA sensing and DNA-induced production of IFN-λ (Zhang, X. *et al.*, 2011). One year later the DNA-PK complex was also identified as a DNA sensor and it was required for the production of IFN-β. Fibroblast cells deficient in DNA-PK has shown a reduction in IRF3-dependent signalling, not NF-κB, in response to transfected DNA or MVA infection (Ferguson, B. J. *et al.*, 2012). The activity of DNA-PK was not dependent on its kinase activity. Meiotic recombination 11 homology A (MER11) is another DNA damage sensor that have a role in cytosolic DNA sensing and shown to mediate a STING-dependent response to transfected DNA but not HSV-1 infection (Kondo, T. *et al.*, 2013). Rad50-CARD9, discovered in 2014, was implicated in DNA sensing besides its role in DNA damage repair. It resides in the nucleus but translocates to the cytosol during virus infection where it detects viral DNA then initiates inflammasome activation instead of IFN induction (Roth, S. *et al.*, 2014).

Cyclic GMP-AMP (2'3'-cGAMP) was described as a second messenger, a type of bacterial-derived cyclic dinucleotide (CDN) with a 2'3' phosphodiester linkage, produced following stimulation with DNA and mediates STING-dependent signalling that result in IRF3 activation (Ablasser, A. *et al.*, 2013; Wu, J. *et al.*, 2013). Sun, L. *et al.* (2013) have subsequently identified the enzyme, called Cyclic GMP-AMP Synthase (cGAS), that catalyzes the synthesis of cGAMP following binding to DNA. Cytosolic DNA sensing by cGAS-cCAMP-STING-dependent and the signalling pathway involved are reviewed in (Cai, X. *et al.*, 2014; Chen, Q. *et al.*, 2016; Xiao, T. S. *et al.*, 2013). cGAS binding to DNA was further confirmed by structural studies (Civril, F. *et al.*, 2013; Kranzusch, Philip J. *et al.*, 2013). All the DNA receptors identified at this time were putative; however, cGAS appeared to be an essential STING-dependent cytosolic DNA receptor as the induction of type I IFNs were severely impaired in several cell types (fibroblasts, macrophages and DC) lacking cGAS (Li, X.-D. *et al.*, 2013). It was required in response to DNA viruses for the induction of IFN-β and was shown to be the most potent inducer of IFN-β expression in comparison with the other cytosolic receptors such as DAI, IFI16 and DDX41 (Sun, L. *et al.*, 2013). The role of cGAS in the antiviral response upon DNA stimulation and virus infection was also determined *in vitro* and *in vivo* in mice deficient in cGAS (Li, X.-D. *et al.*, 2013; Schoggins, J. W. *et al.*, 2014). Cells from mice deficient in cGAS showed a reduction in antiviral responses and the $cGAS^{-/-}$ mice were susceptible not only to the infection of DNA virus but also to RNA virus. It was shown that cGAS also has a role in HIV-1 infection in which HIV-

induced IFN was cGAS-dependent (Gao, D. *et al.*, 2013). HIV harbours a ssRNA genome that gets reverse transcribed to ssDNA forming an RNA:DNA hybrid molecules, which can trigger the production of cGAMP (Mankan, A. K. *et al.*, 2014). It is thought that cGAS can have an indirect effect on other DNA sensors especially those induced by IFN such as IFI16. From these observations, cGAS has been implicated as having a pan-antiviral activity in response to viral infection.

It is well established that STING acts as a critical adaptor for DNA-dependent signalling pathways, but it can also function as a direct sensor for DNA in which it directly binds DNA and activates IFN signalling. This was further supported by studies that have shown a direct binding of STING with CDNs but the binding was impaired with mutated STING (T596A, critical for CDNs binding) (Abe, T. *et al.*, 2013; Burdette, D. L. *et al.*, 2011; Sauer, J.-D. *et al.*, 2011). However, the underlying mechanism has yet to be defined as it is not clear whether this binding happens independently of other DNA sensors.

Adaptor protein STING and its regulation in cytosolic DNA sensing and signalling

STING (also known as MITA, MPYS, ERIS and TMEM173) was identified as a critical adaptor protein for induction of type I IFN (Ishikawa, H. *et al.*, 2008; Sun, W. *et al.*, 2009; Zhong, B. *et al.*, 2008). It is a 379 amino acid protein and localized in the endoplasmic reticulum (ER). It consists of an N-terminal 129 amino acid region with multiple transmembrane domains and a C-terminal 250 amino acid cytosolic domain. It shows a broad expression distribution in various tissues (Burdette, D. L. *et al.*, 2012; Chen, Q. *et al.*, 2016). STING plays a critical role in the cytosolic DNA-mediated innate response. The role of STING in the IFN response to cytosolic DNA was clearly shown in studies with $STING^{-/-}$ mice and different cells types. The induction of IFN-β was robustly induced in HEK293T cells expressing STING from a plasmid in an IRF3- and NF-κB-dependent manner: The HEK293T cell type does not express detectable levels of endogenous STING protein. Furthermore cells such as MEF, macrophages and dendritic cells lacking STING have shown a severe reduction in the induction of IFN-β in response to dsDNA transfection or even DNA virus infection. *In vivo* studies also confirmed the role of STING in the IFN response in which mice deficient in STING were susceptible to HSV-1 infection (Ishikawa, H. *et al.*, 2009).

It is well established that the STING-TBK1-IRF3 axis is the signalling pathway leading to type I IFN induction upon stimulation with cytosolic DNA. Upon DNA sensing, STING acts as platform through the C-terminal tail (CTT) to recruit TBK1 and assemble IRF3 in close proximity to TBK1 for TBK1-dependent IRF3 phosphorylation (Tanaka, Y. *et al.*, 2012). TBK1 was found to be required for IFN-β induction in response to poly(dA:dT) (Ishii, K. J. *et al.*, 2006) through IRF3 in most cell types. Moreover, the induction of type I IFN in response to DNA viruses such as HSV-1 and MHV-68 was TBK1-dependent (Ishii, K. J. *et al.*, 2008; Miyahira, A. K. *et al.*, 2009), indicating the essential role of the TBK1-IRF3 axis in the antiviral response to DNA viruses. Upon DNA recognition, STING dimerizes and undergoes Lys63-linked ubiquitylation mediated by TRIM32 and TRIM56, crucial steps for STING activation (Tsuchida, T. *et al.*, 2010; Zhang, J. *et al.*, 2012). Following STING activation, STING re-localizes to distinct intracellular compartments in which it traffics from the endoplasmic-reticulum, where it originally resides, to an ER-Golgi intermediate compartment and then to the Golgi apparatus and eventually to the perinuclear region, although the mechanism is not fully understood (Ishikawa, H. *et al.*, 2009; Konno, H. *et al.*, 2013). Once STING-dependent signalling is accomplished, STING is subjected to degradation through the autophagy pathway, which is required for the regulation of STING-dependent signalling in order to maintain cellular homeostasis and immune responsivness (Konno, H. *et al.*, 2013). Upon IRF3 activation, it dimerizes and translocates to the nucleus and binds to the IFN-stimulated regulatory elements (ISRE) in the promoters of IFR3-responsive genes including type I IFN (Figure 1.4 A). It is known that STING can activate IRF3 leading to type I IFN induction and activates STAT6 leading to chemokine induction (Chen, H. *et al.*, 2011) but it is not known whether it activates NF-κB (Paludan, Søren R. *et al.*, 2013). It has been shown that a number of IFN-stimulated genes (ISGs) can be induced via IRF3 in an IFN-independent manner (Andersen, J. *et al.*, 2008; Grandvaux, N. *et al.*, 2002; Wathelet, M. G. *et al.*, 1992).

1.3.2.2 Recognition of Cytosolic RNA

The importance of TLRs in the production of type I IFN in pDCs have been shown (Liu, Y.-J., 2005) however TLRs are not important in other cell types for the production of type I IFN in response to viral infection, instead cytosolic RNA sensors are essential (Kato, H. *et al.*, 2005). Almost all cell types respond to viral infection in the cytosol and produce type I IFN (Yoneyama,

A.

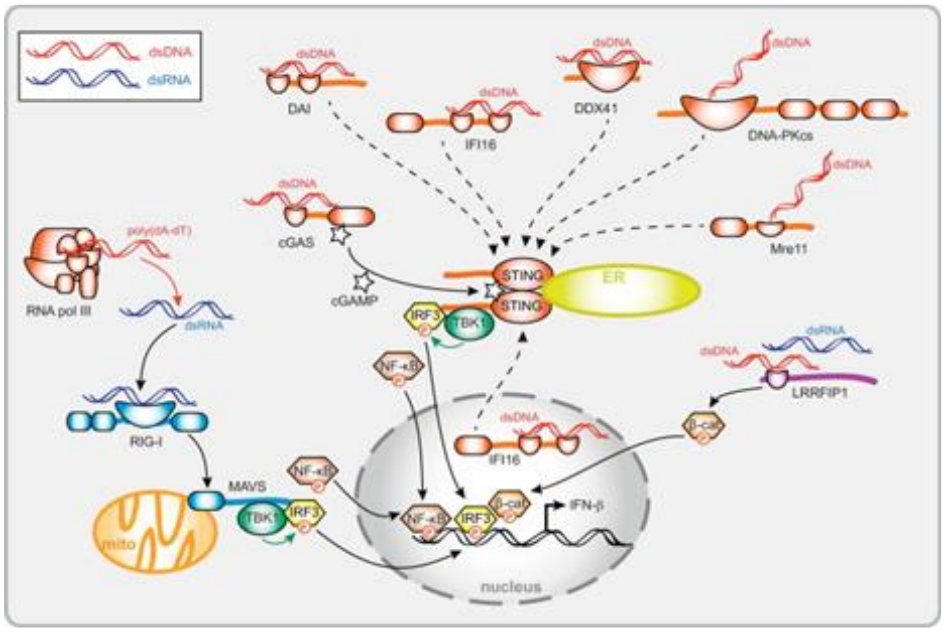

B.

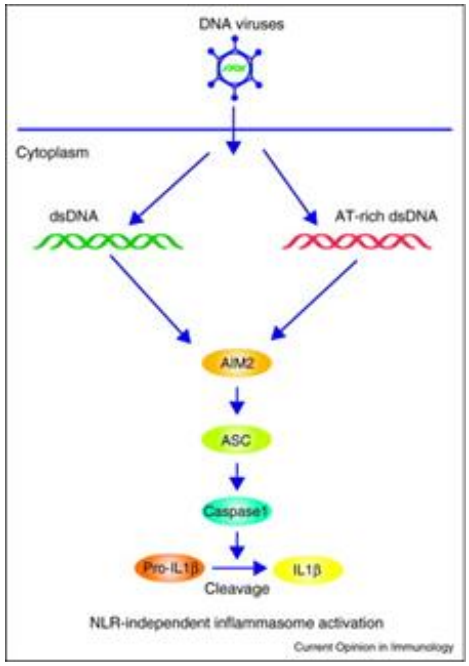

Figure 1.4. Recognition of viral nucleic acids by cytosolic receptors. (A). Intracellular DNA and RNA receptors are involved in detecting DNA or RNA in cytosol. Cytosolic DNA and RNA receptors trigger STING-dependent signalling and MAVS-dependent signalling respectively resulting in induction of IFN-β. Obtained from (Unterholzner, L., 2013). **(B).** Inflammasome signalling can also be activated upon cytosolic DNA recognition. AIM2 is a cytosolic dsDNA sensor that activates ASC/caspase1-dependent pathway leading to secretion of IL-1β. Obtained

M. *et al.*, 2010). A number of years ago the identification and characterization of RIG-I-like

receptors (RLR) as cytosolic dsRNA sensors identified a novel antiviral signalling pathway that links detection of dsRNA in the cytosol to induction of type I IFN (Yoneyama, M. *et al.*, 2004). The expression of these RLRs was found at low levels in most cell types until virus infection or interferon stimulation at which their expression rapidly increased (Kang, D. *et al.*, 2004; Yoneyama, M. *et al.*, 2005; Yoneyama, M. *et al.*, 2004)

The RLR family consist of three groups of molecules: retinoic acid-inducible gene 1 (RIG-I or DDX58), melanoma differentiation associated gene 5 (MDA5 or IFIH1) and laboratory of genetic and physiology 2 (LGP2) (Table 1.4) (Takeuchi, O. *et al.*, 2009; Yoneyama, M. *et al.*, 2008). They are DExD / H-box-containing RNA helicases with similar structures (Zhang, X. *et al.*, 2000). RIG-I and MDA5 are the most closely related receptors and share a similar structure in which they have two N-terminal caspase recruitment domains (CARDs), a central DEAD box helicase/ATPase domain and C-terminal regulatory domain (CTD). LGP2 also has a similar structure with the exception of N-terminal CARDs. They are localized in the cytoplasm and their expression is enhanced in response to IFN stimulation.

Viral PAMPs mainly consist of nucleic acids originating from the uncoating of the infectious unit resulting in exposure of virus genomes to the host receptors, from dsRNA intermediates as by products generated from transcription of viral genomes or from transcription of transcripts (Kawai, T. *et al.*, 2008; Kawai, T. *et al.*, 2010). It has been previously shown that DNA viruses can produce appreciable amounts of dsRNA because of the convergent transcription which occurs when two adjacent open reading frames are transcribed oppositely producing dsRNA with a partial 3' overlap between their transcripts (Weber, F. *et al.*, 2006).

It is well established that RIG-I and MDA5 sensors recognize dsRNA molecules either natural-derived such as genomic RNA of dsRNA viruses and dsRNA generated as replication intermediates of ssRNA viruses or synthetically-derived such as *in vitro* transcribed RNA or poly(I:C). RIG-I and MDA5 appears to have a differential role in induction of type I IFN in response to different virus infections. Over the last decade, numerous investigations have been conducted to determine the precise function and ligand of each sensor and whether they act independently and/or cooperatively in response to virus infection or have differential roles in different cell types or whether they sense different dsRNA species.

Table 1.4. RNA species and viruses and their known RLRs.

Sensors	RNA Species	Viruses	Features	RNA source	Virus Family	Virus Genome Structure	References
RIG-I	5′ppp copy-back RNA	-	In vitro transcribed RNA	Synthetic	-	-	(Schlee, M. *et al.*, 2009; Schmidt, A. *et al.*, 2009)
	5′ppp AU-rich RNA	-	Pol III product from poly(dA:dT)	Synthetic	-	-	(Ablasser, A. *et al.*, 2009; Chiu, Y.-H. *et al.*, 2009)
	Poly(I:C) short	-	Short dsRNA (<1 kb)	Synthetic	-	-	(Kato, H. *et al.*, 2008)
	Genomic RNA	IAV	5′ppp with panhandle structure	Virus-origin	-	-	(Rehwinkel, J. *et al.*, 2010)
	3′UTR U/UC rich RNA	HCV	5′ppp dependent	Virus-origin	-	-	(Saito, T. *et al.*, 2008)
	3′UTR U/A rich RNA	IAV	5′ppp independent	Virus-origin	-	-	(Davis, W. G. *et al.*, 2012)
	DI RNA	SeV, VSV	5′ppp copy-back dsRNA	Virus-origin	-	-	(Panda, D. *et al.*, 2010; Patel, J. R. *et al.*, 2013; Strahle, L. *et al.*, 2006)
	-	NDV	-	Infection	Paramyxoviridae	(−) ssRNA, non-segmented	(Kato, H. *et al.*, 2006; Yoneyama, M. *et al.*, 2004)
	-	SeV	-	Infection	Paramyxoviridae	(−) ssRNA, non-segmented	(Kato, H. *et al.*, 2006)
	-	RSV	-	Infection	Paramyxoviridae	(−) ssRNA, non-segmented	(Loo, Y.-M. *et al.*, 2008)
	-	VSV	-	Infection	Rhabdoviridae	(−) ssRNA, non-segmented	(Kato, H. *et al.*, 2006; Yoneyama, M. *et al.*, 2005)
	-	Rabies virus	-	Infection	Rhabdoviridae	(−) ssRNA, non-segmented	(Hornung, V. *et al.*, 2006)
	-	IAV	-	Infection	Orthomyxoviridae	(−) ssRNA, segmented	(Kato, H. *et al.*, 2006)
	-	Influenza B virus	-	Infection	Orthomyxoviridae	(−) ssRNA, segmented	(Loo, Y.-M. *et al.*, 2008)
	-	Rift Valley fever virus	-	Infection	Bunyaviridae	(−) ssRNA, segmented	(Weber, M. *et al.*, 2013)
	-	La Crosse virus	-	Infection	Bunyaviridae	(−) ssRNA, segmented	(Weber, M. *et al.*, 2013)
	-	HCV	-	Infection	Flaviviridae	(+) ssRNA, non-segmented	(Saito, T. *et al.*, 2008)
	-	JEV	-	Infection	Flaviviridae	(+) ssRNA, non-segmented	(Kato, H. *et al.*, 2006)
	-	EBV	-	Infection	Gammaherpesviridae	dsDNA	(Samanta, M. *et al.*, 2008)
MDA5	Poly(I:C) long	-	Long dsRNA (>7 kb)	Synthetic	-	-	(Kato, H. *et al.*, 2008)

Continued next page

Sensors	RNA Species	Viruses	Features	RNA source	Virus Family	Virus Genome Structure	References
	-	VV, EMCV	High molecular weight RNA	Virus-origin	-	-	(Pichlmair, A. *et al.*, 2009)
	-	CVB3, Mengo	Replication intermediates	Virus-origin	-	-	(Feng, Q. *et al.*, 2012)
	L mRNA	PIV5	RNase L product	Virus-origin	-	-	(Luthra, P. *et al.*, 2011)
	-	EMCV	-	Infection	Picornaviridae	(+) ssRNA, non-segmented	(Kato, H. *et al.*, 2006)
	-	Theiler's murine encephalitis virus	-	Infection	Picornaviridae	(+) ssRNA, non-segmented	(Kato, H. *et al.*, 2006)
	-	Mengovirus	-	Infection	Picornaviridae	(+) ssRNA, non-segmented	(Kato, H. *et al.*, 2006)
	-	Coxackie virus	-	Infection	Picornaviridae	(+) ssRNA, non-segmented	(Feng, Q. *et al.*, 2012)
	-	Entero virus	-	Infection	Picornaviridae	(+) ssRNA, non-segmented	(Feng, Q. *et al.*, 2012)
	-	Human parechovirus	-	Infection	Picornaviridae	(+) ssRNA, non-segmented	(Feng, Q. *et al.*, 2012)
	-	Equine rhinitis A virus	-	Infection	Picornaviridae	(+) ssRNA, non-segmented	(Feng, Q. *et al.*, 2012)
	-	Saffold virus	-	Infection	Picornaviridae	(+) ssRNA, non-segmented	(Feng, Q. *et al.*, 2012)
	-	Norovirus	-	Infection	Caliciviridae	(+) ssRNA, non-segmented	(McCartney, S. A. *et al.*, 2008)
	-	Vaccinia virus	-	Infection	Poxviridae	dsDNA	(Pichlmair, A. *et al.*, 2009)
RIG-I/MDA5	5′OH-3′p short RNA	-	RNase L product	Host-origin	-	-	(Malathi, K. *et al.*, 2007)
	-	West Nile virus	-	Infection	Flaviviridae	(+) ssRNA, non-segmented	(Loo, Y.-M. *et al.*, 2008)
	-	Dengue viurs	-	Infection	Flaviviridae	(+) ssRNA, non-segmented	(Loo, Y.-M. *et al.*, 2008)
	-	Measles virus	-	Infection	Paramyxoviridae	(−) ssRNA, non-segmented	(Ikegame, S. *et al.*, 2010)
	-	Semliki forest virus	-	Infection	Togaviridae	(+) ssRNA, non-segmented	(Schulz, O. *et al.*, 2010)
LGP2/MDA5	L antisense	EMCV	LGP2-interacting RNA	Virus-origin	Picornaviridae	(+) ssRNA, non-segmented	(Deddouche, S. *et al.*, 2014)

Table obtained and modified from (Yoo, J.-S. *et al.*, 2014).

Independent groups have determined the signature of dsRNA and found the triphosphate moiety at the 5' end is an essential determinant of RIG-I recognition (Hornung, V. *et al.*, 2006; Pichlmair, A. *et al.*, 2006; Rehwinkel, J. *et al.*, 2010). Another study reported that the 5'-diphosphate dsRNA can also be recognized by RIG-I (Goubau, D. *et al.*, 2014). Other groups, however, found that the 5'triphosphate was not sufficient (Schlee, M. *et al.*, 2009; Schmidt, A. *et al.*, 2009). Chemically synthesized dsRNA with a 5' monophosphate or without 5' phosphate can still induce the activation of RIG-I (Kato, H. *et al.*, 2008; Takahasi, K. *et al.*, 2008). Single stranded RNA with 5' triphosphate was found to bind RIG-I, however, it could not activate RIG-I (Marq, J.-B. *et al.*, 2010; Schmidt, A. *et al.*, 2009; Takahasi, K. *et al.*, 2008).

Two independent groups have identified a new class of non-self RNA that selectively activate RIG-I ligands generated from AT-rich dsDNA (Ablasser, A. *et al.*, 2009; Chiu, Y.-H. *et al.*, 2009). This AT-rich dsDNA serves as a template for RNA polymerase III which transcribes it into AU-rich dsRNA with a 5' triphosphate making it a ligand for RIG-I. Both strands of AT-rich dsDNA will be transcribed and the RNA transcripts from both strands will anneal producing 5' triphosphate dsRNA. RNA polymerase III is expressed naturally in cells and functions to transcribe 5S rRNA, tRNA or other small noncoding RNA.

A chemically synthetic analogue of viral dsRNA poly(I:C), that does not bear 5'ppp, shows RIG-I-dependent activation (Marques, J. T. *et al.*, 2006; Takahasi, K. *et al.*, 2008). In addition, poly(I:C) was found to enhance RIG-I-dependent signalling in cells transfected with a RIG-I expression vector (Yoneyama, M. *et al.*, 2005; Yoneyama, M. *et al.*, 2004) and its binding with RIG-I has been shown (Rothenfusser, S. *et al.*, 2005). Similarly, the functional role of MDA5 in dsRNA detection was studied *in vivo.* In contrast to RIG-I, the nature of MDA5 ligand is poorly understood, however, MDA5 was shown to recognize a synthetic dsRNA such as poly(I:C) (Gitlin, L. *et al.*, 2006; Kato, H. *et al.*, 2006). Kato and his colleagues have provided an interesting observation on the differential role of RIG-I and MDA5 sensors. They found that the activation of either RIG-I or MDA5 was dsRNA size-dependent in which short dsRNA (~ 300 bp) activated RIG-I-dependent signalling while long dsRNA (> 3 kb) activated MDA5-dependent signalling and this observation was further confirmed from RNA virus infection in which short dsRNA-producing viruses such as IAV and VSV activate RIG-I whereas long dsRNA-producing viruses such as EMCV trigger MDA5 (Kato, H. *et al.*, 2008; Kato, H. *et al.*, 2006; Yoneyama, M. *et al.*,

2008). EMCV is positive-sense ssRNA that belongs to the family of picornavirus and produces long dsRNA during replication which makes it consistent with the observation of MDA5 sensing dsRNA whereas IAV is negative-sense ssRNA and generates short dsRNA. MDA5 was also shown to bind with some sequence specificity such as measles virus mRNA containing an AU-rich region and the L region of the EMCV antisense RNA (Deddouche, S. *et al.*, 2014; Runge, S. *et al.*, 2014). Nevertheless, the precise underlying mechanism of MDA5 activation and ligand specificity remains to be elucidated. RIG-I and MDA5 are not only important in sensing RNA viruses but also DNA viruses such as HSV-1 and KSHV (Rasmussen, S. B. *et al.*, 2009; West, J. A. *et al.*, 2014).

LGP2 does not have CARDs, but can still bind dsRNA. This may suggest that it has no role in antiviral signalling. However, some reports have indicated that its probable role as a positive or negative regulator in which it controls the extent and/or duration of antiviral signalling mediated by RIG-I or MDA5 (Saito, T. *et al.*, 2007; Satoh, T. *et al.*, 2010; Venkataraman, T. *et al.*, 2007). The functional role of LGP2 in the antiviral response is still poorly understood.

From these observations, it seems that there are other features that could determine the specificity of sensor recognition such as dsRNA composition and structure and whether this specificity differs for different viral infections. A secondary structure like a panhandle structure was found to be necessary along with 5'ppp for RIG-I activation. This observation was seen in infection of Sendai virus (SeV) and vesicular stomatitis virus (VSV) in which they produce RIG-I agonist RNA that contains a panhandle structure (also called copy-back structure generated when the sequence is duplicated in reverse complement) with 5' triphosphates (Baum, A. *et al.*, 2010; Panda, D. *et al.*, 2010; Vignuzzi, M. *et al.*, 2019). In addition, hepatitis C virus (HCV) RNA with 5' triphosphate containing uridine-rich or adenine-rich region activates RIG-I-dependent signalling, indicating that this sequence is important for recognition of HCV by RIG-I (Saito, T. *et al.*, 2008).

It is now clear that the activation of RIG-I or MDA5 requires RNA species with distinct features that differ from cellular RNAs (or self RNA). RIG-I and MDA5 are not normally activated by host RNA as cellular RNAs are generally single stranded and have 5' ends with a methylguanosine cap such as mRNA and small nuclear RNAs or are monophosphates such as

ribosomal RNAs, tRNAs and microRNAs. In addition, these populations of cellular RNAs are subjected to modification to prevent recognition by RIG-I or MDA5.

The role of RIG-I and MDA5 in inducing IFNs to a wide range of viruses has now been proven *in vitro* and *in vivo*. RIG-I has been shown to be essential for IFN production in response to negative stranded RNA viruses such as influenza viruses (Kato, H. *et al.*, 2006; Weber-Gerlach, M. *et al.*, 2016), bunyaviruses (Spengler, J. R. *et al.*, 2015; Yamada, S. *et al.*, 2018), filoviruses (Spiropoulou, C. F. *et al.*, 2009) and rhabdoviruses (Furr, S. R. *et al.*, 2010) as well as positive stranded viruses such as Japanese encephalitis virus (Kato, H. *et al.*, 2006). On the other hand, MDA5 was found to have a role in IFN induction upon detection of positive stranded RNA viruses such as picornaviruses (Deddouche, S. *et al.*, 2014; Loo, Y.-M. *et al.*, 2008) and arteriviruses (Luo, R. *et al.*, 2008; van Kasteren, P. B. *et al.*, 2012) as well as hepatitis D virus (Zhang, Z. *et al.*, 2018) and positive stranded viruses such as Kaposi's sarcoma-associated herpesvirus (KSHV) (Zhao, Y. *et al.*, 2018).

A number of DExD/H-box helicases other than the RLRs have been shown to bind RNA and mediate antiviral signalling (Table 1.5). Some may function as RNA sensors, while others regulate RLR signalling. Nevertheless, further investigations are required to elucidate the signalling mechanisms involved (Chow, K. T. *et al.*, 2018; Sparrer, K. M. J. *et al.*, 2015). In addition, several proteins have been identified that have a role in RNA binding and antiviral signalling during virus infection (Table 1.6).

Several studies have shown the importance of cell-type specificity for RLR versus TLR pathway for the induction of type I IFN in response to different viruses. It has been shown that RIG-I was indispensable for the production of type I IFN in mouse embryonic fibroblasts (MEFs) following exposure to Newcastle disease virus (NDV) in which RIG-I$^{-/-}$ fibroblasts did not significantly produce type I IFN when infected with the virus. Similarly, conventional DC (cDCs) lacking the RIG-I gene were also defective in their ability to produce type I IFN. However, RIG-I was not essential for virus-induced IFN production by pDCs. Cells lacking RIG-I were able to produce type I IFN upon NDV infection, however, induction was severely impaired in cells deficient in both MyD88 and TRIF (MyD88$^{-/-}$TRIF$^{-/-}$), indicating that these cells use a TLR system rather than RLR for virus detection (Kato, H. *et al.*, 2005; Kato, H. *et al.*, 2006). In addition, cDCs and

Table 1.5. Non-RLR DExD/H-box Helicases involved in the detection of cytosolic non-self RNA.

DExD/H-box Helicases	Ligand	Reference
DDX1 (together with DDX21 and DHX36	Poly(I:C)	(Mitoma, H. *et al.*, 2013)
DDX3	Poly(I:C)	(Gringhuis, S. I. *et al.*, 2017; Oshiumi, H. *et al.*, 2010)
	HIV mRNA	(Gringhuis, S. I. *et al.*, 2017)
	Abortive HIV RNA	(Gringhuis, S. I. *et al.*, 2017)
	Cellular RNA lacking poly(A) tail	(Gringhuis, S. I. *et al.*, 2017)
DHX9	Poly(I:C)	(Zhang, Z., Yuan, B., Lu, N., *et al.*, 2011)
DHX15	Poly(I:C)	(Lu, H. *et al.*, 2014; Mosallanejad, K. *et al.*, 2014)
	dsRNA	(Lu, H. *et al.*, 2014; Wang, P. *et al.*, 2015)
DHX33	Poly(I:C)	(Chakrabarti, A. *et al.*, 2015; Liu, Y. *et al.*, 2014; Mitoma, H. *et al.*, 2013)
	Reovirus genomic dsRNA	(Mitoma, H. *et al.*, 2013)
	RNase L-cleaved RNA	(Chakrabarti, A. *et al.*, 2015)
DDX60	VSV ss- and ds-RNA	(Miyashita, M. *et al.*, 2011)
	Poly(I:C)	(Miyashita, M. *et al.*, 2011; Oshiumi, H. *et al.*, 2015)
	Biotinylated dsRNA	(Oshiumi, H. *et al.*, 2015)
SNRNP200	Biotinylated poly(I:C)	(Tremblay, N. *et al.*, 2016)
	SeV genomic RNA	(Tremblay, N. *et al.*, 2016)

Table obtained and modified from (Chow, K. T. *et al.*, 2018)

Table 1.6. RNA-binding proteins with roles in antiviral response.

RNA-binding Proteins	Known functions in antiviral response	Reference
OAS/RNase L	Generates RNA ligands for RLR activation	(Malathi, K. *et al.*, 2007; Malathi, K. *et al.*, 2010)
PKR	Inhibits translation in virus-infected cells	(Hull, C. M. *et al.*, 2016)
	Enhances MDA5-mediated IFN induction	(Pham, A. M. *et al.*, 2016)
IFITs	Inhibit viral translation, sequester viral RNA	(Pham, A. M. *et al.*, 2016)
LRRFIP1	Activates β-catenin to enhance transcriptional activation of Ifnb1	(Yang, P. *et al.*, 2010)
DAI	Activates RIPK1/3/MLKL	(Thapa, R. J. *et al.*, 2016)
	Activates NLRP3 inflammasome	(Kuriakose, T. *et al.*, 2016)
HMGBs	Mediates immunogenic nucleic acid signalling, in soluble form act as cytokines	(Ugrinova, I. *et al.*, 2017)

Table obtained and modified from (Chow, K. T. *et al.*, 2018)

fibroblasts lacking the MDA5 gene were defective in their ability to produce IFN upon infection with encephalomyocarditis virus (EMCV), whereas pDCs lacking the MDA5 gene (but not MyD88$^{-/-}$) produced type I IFN when infected with the same virus (Gitlin, L. *et al.*, 2006; Kato, H. *et al.*, 2006). These observations indicate that type I IFN is induced either by TLR or RLR systems in a cell type-dependent manner.

RLR Signalling Pathway (MAVS-IRF3-IFN-β axis)

The mechanism of RIG-I activation was proposed previously using high-resolution crystal structure analysis (Kolakofsky, D. *et al.*, 2012). In resting cells, RIG-I remains inactive in the cytosol by auto-repression in which the second CARD domain interacts with Hel-2i domain, whereas MDA5 remains in an open conformation state. Once the ligand is recognized by the CTD domain, RIG-I and MDA5 undergo ATP-dependent conformational change mediated by RNA-activated protein kinase R (PKR) activator (PACT) (Kok, K.-H. *et al.*, 2011), resulting in releasing the auto-repression and making the CARD domains available to interact with MAVS adaptor protein (Kowalinski, E. *et al.*, 2011). Then both receptors undergo Lys63-linked ubiquitylation onto CARDs and C-terminal domain, mediated by tripartite motif protein 25 (TRIM25) and Riplet respectively (Gack, M. U. *et al.*, 2007; Oshiumi, H. *et al.*, 2013). It seems that MDA5 has a different repression mechanism than RIG-I because the C-terminal region of MDA5 has shown no role in auto-repression (Saito, T. *et al.*, 2007). Once RIG-I and MDA5 are activated, they interact with a CARD-containing adaptor localized on the outer membrane of mitochondria called mitochondrial antiviral signalling protein (MAVS) (also known as IPS-1, CARDIF or VISA) which serves as a platform for protein complex assembly at the mitochondria. Then MAVS multimerizes into prion-like filament structures (Hou, F. *et al.*, 2011) and recruits the IKK-related serine/threonine kinases TBK1/IKKε which phosphorylate and activate IRF3 and IRF7 (Kawai, T. *et al.*, 2008; Kawai, T. *et al.*, 2010). NF-κB is activated by the IKKα/IKKβ/IKKγ complex on MAVS through this pathway. IRFs and NF-κB translocate to the nucleus and induce the expression of type I IFN and inflammatory cytokines (Figure 1.4 A) (Takeuchi, O. *et al.*, 2008; Yoneyama, M. *et al.*, 2007).

1.3.3 JAK/STAT Signalling Pathway

Type I IFN induction results in the activation of the JAK/STAT signalling pathway. The interaction between IFN-α/β and the receptor (IFNAR) recruits JAK1 and TYK2. Activation of the receptor-associated JAK1 leads to phosphorylation of STAT 1 and 2. Upon phosphorylation, STAT1 and STAT2 form a heterodimer that translocates to the nucleus forming the heterotrimeric transcription factor complex IFN-stimulated genes factor 3 (ISGF3) with interferon regulatory factor (IRF-9). This trimeric complex binds to the ISRE sequence in the promoters of interferon-stimulated genes (ISGs), inducing their upregulation. The ISGs act to promote viral clearance and establish an antiviral state in uninfected cells (Samuel, C. E., 1991; Samuel, C. E., 2001). However, the JAK/STAT pathway is not the only pathway involved in IFN signalling. The p38 mitogen activated protein (MAP) kinase pathway also mediates IFN signalling. In addition, viral infection can directly induce some ISGs in the absence of IFN production (Halfmann, P. *et al.*, 2011; Sen, G. C. *et al.*, 2007).

1.3.4 Interferon Effector Response

Upregulation of ISGs establishes the antiviral state that prevents viral replication at various stages of the viral life cycle. Initially, our knowledge of the effector function of ISGs was limited to a few proteins such as PKR, OAS and MX1. However, a large-scale screening study was recently conducted to assess the inhibitory capacity of high numbers of ISGs on viral replication. The study has revealed a large number of ISGs that exploit different strategies to inhibit viral replication and their broad effect on different RNA viruses (Schoggins, J. W., 2019; Schoggins, J. W., Wilson, S. J., *et al.*, 2011).

More than 1600 genes regulated by type I IFN have been identified (Hertzog, P. *et al.*, 2011). They are different in their molecular characteristics and targets but they are involved in protection against invading microbes and eliminating infection (Schoggins, J. W., 2019; Schoggins, J. W. & Rice, C. M., 2011; Schoggins, J. W., Wilson, S. J., *et al.*, 2011). These effectors are not only generated from the signals that originated from IFN induction, but also generated from TNF, IL-1 and TLR families. Nevertheless, IFN is the main mediator of ISGs (MacMicking, J. D., 2012). ISG-mediated antiviral activities target multiple cell types and several stages of the viral life cycle such as entry, uncoating, genome replication, virion assembly and egress. For instance,

IFN-inducible transmembrane (IFITM) effectors target viral entry and uncoating. PKR and 2'-5' oligoadenylate synthase 1 (OAS1), (OAS2), (OAS3) and OASL target viral replication. If the virus is able to replicate, the host can still counteract the virus through ISGs that target assembly and release such as tetherin (MacMicking, J. D., 2012). IFN-induced proteins function not only as antiviral effectors but also mediate apoptosis in the cell in which IFNs induce death inducing ligands. Microarray analysis has revealed a number of ISGs with apoptotic function such as TRAIL/Apo2L, Fas/Apo-1, Fas/FasL, OAS and PML-2 (Chawla-Sarkar, M. *et al.*, 2003; de Veer, M. J. *et al.*, 2001; Der, S. D. *et al.*, 1998).

1.4 Virus Manipulation of the Type I IFN Response

A successful virus infection requires the virus to enter the cell, replicate and produce infectious particles in the presence of the innate immune system. This cannot be achieved without overcoming the innate immune response or at least delay the development of the response. Interferon restricts virus replication and spread, so viruses have evolved several strategies to evade or inhibit the activation of intracellular PRRs leading to the IFN. VACV, the prototypic and most studied poxvirus, has been shown to encode a considerable number of proteins that are involved in the inhibition of the IFN signalling pathway leading to its production. Poxviruses replicate in the cytoplasm making their genomes or dsRNA intermediates accessible for detection by PRRs and leading to activation of IFN signalling. Poxviruses have evolved strategies to hide their nucleic acid PAMPs from detection or interfering with the signalling molecules that lead to IFN expression as discussed below.

1.4.1 Inhibition of Interferon Production

1.4.1.1 Viral Evasion of RNA Sensing

Detection of viral nucleic acids is a critical step for the host to initiate the innate immune response. Therefore, many viruses encode proteins to evade immune sensing. Several viruses including VACV produce dsRNA intermediates as a byproduct from encoding transcripts from both strands of the genome in opposite directions which can potentially hybridize to form dsRNA, a critical PAMP sensed by RIG-I or MDA5 and also by PKR and OAS leading to induction of IFN. Accordingly, some viruses utilize mechanisms to limit the production of

dsRNA in infected cells. The open reading frames (ORFs) of the VACV genome are organized in such a way that the formation of dsRNA intermediates are minimized (Goebel, S. J. *et al.*, 1990). The genes located at both termini are usually transcribed towards the end of the genome from one strand, resulting in the production of transcripts that lack complementarity. The genes located in the central region are encoded from both strands but they are arranged in blocks in which each block of genes are transcribed in one direction either from left to right or vice versa. Those transcribed in opposite directions from both strands are usually minimized by multiple transcriptional terminators. Such genome organization helps to minimize the production of dsRNA intermediates and is a means of evading immune detection (Smith, G. L. *et al.*, 1998; Smith, G. L. *et al.*, 2018).

Some viruses have mechanisms to evade cytosolic RNA sensing even when dsRNA is formed. These viruses have the ability to modify their RNA molecules to mimic cellular RNAs and prevent detection or hinder RLRs activation. Since the 5'-triphosphate end of RNA is a critical moiety for RIG-I recognition, some viruses produce a phosphatase that converts the 5'-triphosphate RNA into 5'-monophosphate RNA (Habjan, M. *et al.*, 2008). Arenaviruses have a genome with a 5' triphosphate but with overhang and this structure does not activate RIG-I although RIG-I binds to it (Marq, J.-B. *et al.*, 2011). Alternatively, many viruses protect their 5'end mRNA from recognition by RIG-I by capping the end of their newly synthesized mRNA. That could be by using the cellular machinery such as by paramyxoviruses or viruses that encode their own capping enzymes such as by poxviruses and rotaviruses or by cap-snatching from cellular mRNA such as by influenza viruses (Plotch, S. J. *et al.*, 1981).

As it has been shown that RIG-I and MDA5-dependent signalling is controlled by post-translational modification, namely ubiquitylation and serine/threonine phosphorylation, it is not unexpected that many viruses have evolved to encode proteins that interfere with host post-translational modification. For instance, NS1 from IAV interact with TRIM25 and NS3-NS4A protease from HCV that cleave Riplet (Gack, M. U. *et al.*, 2009; Oshiumi, H. *et al.*, 2013). Alternatively, other viruses encode de-ubiquitins (DUBs) to remove the Lys63-linked ubiquitylation of RIG-I such as ORF64 from KSHV (Inn, K.-S. *et al.*, 2011). Dephosphorylation of RLRs is a critical step to activate RLR-dependent signalling upon viral infection. The V

protein of measles virus (MeV) was found to bind to PP1α and PP1γ phosphatases and sequester their activity from MDA5 (Davis, Meredith E. *et al.*, 2014).

Another strategy used by viruses is not to modify their RNA structure, instead, they produce RNA-binding proteins that sequester RNA from being recognized. It is believed that this strategy is more advantageous than the strategies mentioned above. It will not only minimize the activation of dsRNA-dependent RIG-I/MDA5 but also inhibit the activation of PKR or OAS. Examples of these proteins are VACV E3L and EBOV VP35 (Chang, H. W. *et al.*, 1992; Haasnoot, J. *et al.*, 2007). VACV E3L protein is an early protein encoded before dsRNA is formed. Its essential role was demonstrated when the mutant virus lacking E3L was sensitive to IFN (Beattie, E *et al.*, 1995). It has been shown that VACV E3L can counteract the effects of RNA sensing not only triggered by viral dsRNA, but also by polymerase III-produced dsRNA from poly(dA:dT) (Marq, J.-B. *et al.*, 2009; Valentine, R. *et al.*, 2010). VACV also encodes a PKR inhibitor, K3L. It has homology to the N-terminal region of eIF2α and acts as a pseudosubstrate for PKR in lieu of eIF2α. E3L also competes with PKR and OAS for binding to dsRNA (Langland, J. O. *et al.*, 2002). Degradation of dsRNAs is also a way of evasion by RNA sensing. Bovine viral diarrhea virus (BVDV) secrets a protein with dsRNA binding and RNase activity that degrades dsRNA in the extracellular environment released from apoptotic bodies in order to prevent TLR3 activation (Iqbal, M. *et al.*, 2004).

Several viruses use a proteolytic mechanism to degrade RLRs and thus inhibit downstream signalling. The $3C^{pro}$ protease of poliovirus cleaves RIG-I, and $3C^{pro}$ and $2A^{pro}$ of enterovirus 71 cleave RIG-I and MDA5 respectively (Barral, P. M. *et al.*, 2009; Feng, Q. *et al.*, 2014). In addition, RLRs might be sequestered instead of degraded. Influenza A virus NS1 was identified to inhibit RIG-I activation and thus block downstream signalling (Mibayashi, M. *et al.*, 2007) and also V proteins of several paramyxoviruses were found to bind to the helicase domain of MDA5 resulting in inhibition of its ATPase activity (Andrejeva, J. *et al.*, 2004).

1.4.1.2 Viral Evasion of DNA Sensing

DNA virus replication in the cytoplasm results in the accumulation of dsDNA making the virus genome accessible to host DNA sensors such as cGAS, IFI16 and DNA-PK. Because cytosolic DNA sensing is an emerging field, there is only limited knowledge of how DNA viruses evade

cytosolic DNA sensing and a clearer understanding remains to be elucidated. Nevertheless, there is some evidence that describe viral evasion mechanisms of DNA sensing in the cytosol. Several DNA virus antagonists have been identified that interfere with DNA sensing signalling pathways as shown in Table 1.7.

VACV E3L has such antagonistic activity. It contains a Z-DNA-binding domain that can prevent the interaction of DAI with DNA, resulting in inhibition of DNA-induced IFN-β (Wang, Z. *et al.*, 2008). It has been reported that myxoma virus encodes a PYD-containing protein, M13L, which can disrupt NALP-ASC interaction and caspase 1 activation (Johnston, J. B., Barrett, J. W., *et al.*, 2005). DNA-PK was identified to be targeted by the VACV C16 protein in which it binds to the Ku subunit and prevents it from binding to DNA (Fahy, A. S. *et al.*, 2008; Peters, N. E. *et al.*, 2013). Some DNA viruses that replicate in the nucleus have also been reported to encode proteins that target DNA-dependent STING-dependent sensing such as HSV-1. HSV-1 encodes a protein called ICP0 that triggers the proteasomal degradation of IFI16 in the nucleus. The ICP0 knockout virus or catalytically inactive ICP0 mutant virus failed to induce degradation of IFI16. However, the expression of ICP0 alone did not induce IFI16 degradation which may suggest either the ICP0 directly targets IFI16 or another viral product is needed to cause the degradation of IFI16 (Cuchet-Lourenço, D. *et al.*, 2013; Diner, B. A. *et al.*, 2015; Orzalli, M. H. *et al.*, 2012). Another tegument protein encoded by HCMV targets IFI16 but through a different mechanism to HSV-1. HCMV pUL83 binds to the pyrin domain of IFI16 preventing its oligomerization rather than degradation (Li, T. *et al.*, 2013). Furthermore, HCMV encodes pUL97 that has a role in translocating IFI16 from the nucleus to the cytoplasm which prevents the sensing the virus DNA in the nucleus, but interestingly when expressed alone in cells did not show any function (Dell'Oste, V. *et al.*, 2014).

At this time most of our understanding of virus DNA sensing mechanisms comes from studies on herpesvirus. Whether this knowledge is relevant to other DNA viruses has yet to be determined since they have different routes of infection, sites of replication and pattern of genome replication.

Table 1.7. Viral regulators of DNA-dependent sensing.

Molecule	Target	Virus	Viral Protein	Proposed mechanism	Reference
DNA sensors	cGAS	KSHV	ORF52 (KicGAS)	cGAS interaction; DNA binding; disrupts cGAS binding to DNA	(Wu, J.-j. *et al.*, 2015)
		KSHV	LANA	An N-terminally truncated cytoplasmic isoform of LANA interacts with cGAS	(Zhang, G. *et al.*, 2016)
		MHV68	ORF52	cGAS interaction; DNA binding; disrupts cGAS binding to DNA	(Wu, J.-j. *et al.*, 2015)
		RRV	ORF52	cGAS interaction; DNA binding; disrupts cGAS binding to DNA	(Wu, J.-j. *et al.*, 2015)
		EBV	ORF52	cGAS interaction; DNA binding; disrupts cGAS binding to DNA	(Wu, J.-j. *et al.*, 2015)
	IFI16	HSV-1	ICP0	Promotes the degradation (?) of IFI16 in a proteasome-dependent manner, in normal human fibroblasts cells but not tumour cells	(Cuchet-Lourenço, D. *et al.*, 2013; Diner, B. A. *et al.*, 2015; Orzalli, M. H. *et al.*, 2012)
		HCMV	pUL83	Interacts with IFI16 and blocks IFI16 oligomerization; redirects IFI16 to the major HCMV immediate early promoter	(Biolatti, M. *et al.*, 2016; Cristea, I. M. *et al.*, 2010; Li, T. *et al.*, 2013)
		HCMV	pUL97	Binds to IFI16 and relocalizes IFI16 to the cytoplasm	(Dell'Oste, V. *et al.*, 2014)
	DNA-PK	VACV	C16	Binds to the Ku70-Ku80 complex and blocks DNA sensing by DNA-PK in fibroblasts	(Peters, N. E. *et al.*, 2013)
Adaptors	STING	HSV-1	ICP0, ICP4, US3-PK	Stabilizes STING in HEp-2 cells, which is required for optimal HSV-1 replication	(Kalamvoki, M. *et al.*, 2014)
		KSHV	vIRF1	STING interaction; disrupts STING phosphorylation; disrupts STING binding to TBK1	(Ma, Z. *et al.*, 2015)
		HPV	E7	STING interaction	(Lau, L. *et al.*, 2015)
		Adenovirus	E1A	STING interaction	(Lau, L. *et al.*, 2015)
		Hepatitis B virus	Pol	STING interaction; disrupts lysine 63–linked polyubiquitination of STING	(Liu, Y. *et al.*, 2015)
	MyD88	VACV	A46R	Binds to MyD88 and inhibits TLR signalling	(Stack, J. *et al.*, 2005)
	ASC1	Myxoma virus	M13L	Binds to ASC1 and disrupts appropriate formation of the host inflammasome complex	(Johnston, J. B., Barrett, J. W., *et al.*, 2005)

Table obtained and modified from (Ma, Z. *et al.*, 2018)

1.4.1.3 Viral Evasion of Nucleic Acid-Stimulated Signalling Pathways leading to Type I IFN Expression

Viral Manipulation of TRIF and MyD88 Adaptor Proteins for TLR Signalling

At this time the only two proteins that VACV encodes, known to counteract TLR-mediated signalling, are A46R and A52R (Hurst, T. *et al.*, 2008). They have distinct modes of action and target different cellular proteins involved in TLR signalling. A46R is a TIR domain-containing protein which enables it to associate with several TIR-domain-containing adaptors: MyD88, TIRAP, TRIF and TRAM that associate with the cytoplasmic domain of TLRs, leading to inhibition of TLR-induced NF-κB and IRF3 activation (Stack, J. *et al.*, 2005). A52R has the ability to inhibit TLR-induced NF-κB activation, but not IRF activation, by interacting with IRAK2 and TRAF6 (Bowie, A. *et al.*, 2000; Harte, M. T. *et al.*, 2003).

Other viruses, other than DNA viruses, also interfere with TLR signalling. Hepatitis C virus (HCV) NS3/4A protein, a non-TIR-domain containing viral protein, has the ability to not only cleave precursor polypeptides of structural proteins but also cleaves TRIF that would otherwise activate TLR3-mediated antiviral signalling (Li, K. *et al.*, 2005). TLR4-dependent signalling is also a target by viruses such as human T-cell leukaemia virus type 1 (HTLV-1) in which its protein p30 binds to and inhibits the transcriptional activity of transcription factor PU.1, mainly expressed in immune cells such as B cells and macrophages (Datta, A. *et al.*, 2006). West Nile virus (WNV) NS1 prevents the translocation of NF-κB and IRF3 causing the inhibition of IFN-β expression (Wilson, J. R. *et al.*, 2008).

Viral manipulation of MAVS, STING and ASC adaptor proteins For Cytosolic Signalling

A signalling complex is assembled on innate immune adaptor proteins upon RNA or DNA detection in order to trigger innate immunity. Therefore, disrupting the adaptors interaction with other molecules or even targeting the adaptors themselves is one such virus strategy to inhibit downstream signalling.

STING is the key adaptor of the cytosolic DNA sensing system and studies have shown that this adaptor is targeted by many DNA viruses as shown in Table 1.7. HSV-1 encodes ICP27 that interacts with STING and TBK1 that results in blocking the phosphorylation of IRF3 by TBK1

(Christensen, M. H. *et al.*, 2016). Furthermore, adenovirus E1A and HPV E7 oncoproteins were identified to bind with STING through their LXCXE motif resulting in inhibition of STING signalling (Lau, L. *et al.*, 2015). It has become apparent that STING also has a role in sensing RNA viruses and that is because some RNA virus members of the *Flaviviridae* and *Coronaviridae* families encode proteins targeting STING (Ma, Z. *et al.*, 2016). STING regulation is controlled by post-translational modification such as ubiquitylation and phosphorylation and it is not surprising that these processes can be targeted by viruses. HBV polymerase has been shown to disrupt the Lys63-linked ubiquitylation of STING through its reverse transcriptase and ribonuclease H domains resulting in inhibition of IFN-β induction (Liu, Y. *et al.*, 2015). KSHV vIRF1 has been shown to block phosphorylation and activation of STING by preventing TBK1 binding and thus TBK1-mediated phosphorylation (Ma, Z. *et al.*, 2015).

MAVS is another crucial adaptor protein for RIG-I- and MDA5-mediated signalling leading to expression of IFN-β which make it a target for many viruses. IAV PB1-F2 protein translocates into the space of the mitochondrial inner membrane leading to the fragmentation of mitochondria and also binds to the transmembrane domain of MAVS thereby inhibiting MAVS signalling and IFN induction (Varga, Z. T. *et al.*, 2012; Yoshizumi, T. *et al.*, 2014). In contrast, other viruses encode viral proteases that cleave MAVS and block RLR signalling such as HCV NS3-NS4A and HAV $3C^{pro}$ (Li, X.-D. *et al.*, 2005; Yang, Y. *et al.*, 2007).

Innate immune signalling from the inflammasome complex is also a viral target. For instance, myxoma virus encodes M13L that contains a PYRIN domain and interacts with ASC, a critical adaptor protein for inflammasome signalling (Johnston, J. B., Barrett, J. W., *et al.*, 2005).

Inhibition of TBK1/IKKε and IKKα/IKKβ/IKKγ Kinases Activation

The PRR-mediated signalling pathways described above converge at the level of the IKK family of proteins. The complex of TBK1/IKKε and associated subunits is important for the induction of type I IFN expression upon phosphorylation and activation of IRF3 and IRF7, whereas the complex of IKKα/IKKβ/IKKγ is important for the activation of NF-κB. Furthermore, these signalling cascades can also activate MAPK, leading to AP1. Inhibition of these kinases leads to

inhibition of downstream transcription factor activation. Thus, they are an important target of viruses to antagonize the induction of IFN.

VACV C6 is an early gene and has a role in IFN antagonism. C6 interacts with subunits of TBK1/IKKε: NAK-associated protein 1 (NAP1), TRAF family member-associated NF-κB activator (TANK) and similar to NAP1 TBK1 adaptor (SINTBAD) and inhibits IRF3 activation (Unterholzner, L. *et al.*, 2011). In addition, TBK1 is also inhibited by VACV N1L and other proteins from RNA viruses such as HCV NS3 protein (DiPerna, G. *et al.*, 2004; Otsuka, M. *et al.*, 2005). Furthermore, the induction of IFN-β is inhibited by VACV K7R by binding with DEAD-box protein 3 (DDX3), resulting in inhibition of TBK1/IKKε-mediated IRF3 activation (Schröder, M. *et al.*, 2008). DDX3 is believed to be part of TBK1/IKKε complex and involved in IRF3 activation (Soulat, D. *et al.*, 2008). G1 protein from hantavirus, negative ssRNA virus, was found to disrupt the interaction between TRAF3 and TBK1 leading to inhibition of IRF3 activation (Alff, P. J. *et al.*, 2008). As a strategy employed by viruses to target NF-κB signalling, viruses could encode proteins that interfere with NF-κB kinases. VACV B14R interacts with IKKβ and inhibits its phosphorylation whereas KSHC K13 interacts with the IKKα/IKKβ complex and both result in inhibition of NF-κB activation (Chen, R. A. J. *et al.*, 2008; Matta, H. *et al.*, 2007).

Inhibition of Transcription Factor Activation (IRF3 and NF-κB)

The transcription factors driving the transcription of antiviral genes are crucial molecules. IRF3, NF-κB and AP-1 are transcription factors that form an active complex and bind the IFN-β gene promoter to initiate its expression (Maniatis, T. *et al.*, 1998; Thanos, D. *et al.*, 1995). Whereas, IFN-α expression is dependent on IRF7 through IKKα kinase. So interfering with transcription factor activation or their transcription activity is an attractive target for many viruses.

Encoding viral IRF mimics by viruses is one strategy to directly target cellular IRFs. IRF homologues of human herpes virus 8 inhibit cellular IRF3 activation by preventing the interaction of cellular IRF3 with CBP/p300 co-activators. In much the same way adenovirus E1A (Juang, Y.-T. *et al.*, 1998; Lin, R. *et al.*, 2001; Zimring, J. C. *et al.*, 1998) and V proteins of paramyxoviruses act as IRF3 mimics and compete with cellular IRF3 phosphorylation by

TBK1/IKKε (Lu, L. L. *et al.*, 2008). Furthermore, human papilloma virus (HPV) E6 also inhibits IRF3's activity (Ronco, L. V. *et al.*, 1998). Other mechanisms viruses use to target IRF3 is degradation instead of sequestration as shown by bovine herpesvirus ICP0 (Saira, K. *et al.*, 2007). VACV N2 protein has a role in inhibition of IRF3 activation further downstream after IRF3 phosphorylation and translocation into the nucleus (Ferguson, B. J. *et al.*, 2013).

As mentioned previously, NF-κB has a role in the antiviral response and induction of IFN-β. African swine fever virus A283L is an early expressed IκB homologue that represses the activation of NF-κB pathway and sequesters NF-κB in the cytoplasm (Powell, P. P. *et al.*, 1996; Tait, S. W. G. *et al.*, 2000). Myxoma virus M150R co-localizes with NF-κB in the nucleus of infected cells and inhibits the response of proinflammatory cytokines (Camus-Bouclainville, C. *et al.*, 2004; Johnston, J. B. & McFadden, G., 2005; Kalvakolanu, D. V., 1999). VACV encodes a number of proteins that interfere with NF-κB activation and none are redundant as reviewed in (Smith, G. L. *et al.*, 2013; Smith, G. L. *et al.*, 2018). They include A46, A49, A52, B14, C4, E3, K1, K7, M2 and N1. They are early genes and act at different stages in the signalling pathway to inhibit NF-κB activation. It is likely that there are more NF-κB inhibitors encoded as the virus was still able to inhibit NF-κB activation even when all known inhibitors were deleted from the genome (Sumner, R. P. *et al.*, 2014).

1.4.2 Inhibition of Interferon-Induced Signalling

1.4.2.1 Inhibition of Interferon Binding to Receptors

Poxviruses not only modulate the host response intracellularly, but also extracellularly. Poxvirus proteins that are secreted from the infected cells or presented on the cell surface, in general, manipulate the immune response by intercepting IFNs and cytokines and preventing them from binding to their receptors. The VACV IFN-α/β binding proteins encoded by the *B18R* gene in Western Reserve strain and the *B19L* gene in the Copenhagen strain have similarity to the IFN-α/βRs (Colamonici, O. R. *et al.*, 1995). VACV *B15R* has been shown to encode a secretory protein that functions as a soluble IL-1βR. It binds to cellular IL-1β and prevents it from interacting with its natural receptor as does the IFN-γ receptor homologue VACV B8R which binds IFN-γ (Alcami, A. *et al.*, 1992; Alcamí, A. *et al.*, 2000).

1.4.2.2 Inhibition of JAK/STAT Pathway

IFN activates the innate immune response to counteract viral infection preventing its spread. Many poxviruses inhibit the action of interferon induction through blocking the IFN-signalling cascade. The major components of type I IFN signalling (IFN-α/β receptor, JAK1, Tyk2, STAT1 and STAT2) are targeted by viruses to inhibit IFN signalling. VACV VH1, encoded late by the *H1L* gene, has been shown to bind and dephosphorylate STAT1, resulting in blockage of IFN signalling (Najarro, P. *et al.*, 2001).

1.4.2.3 Inhibition of Interferon-induced Antiviral Effectors

As described above, IFNs are antiviral factors which induce their inhibitory activity by the induction hundreds of effector proteins (Honda, K. *et al.*, 2005; Katze, M. G. *et al.*, 2002; MacMicking, J. D., 2012; Schoggins, J. W., 2019; Schoggins, J. W., Wilson, S. J., *et al.*, 2011), however, viruses have evolved to encode molecules that interfere with their actions (Smith, G. L. *et al.*, 1998). PKR and OAS are involved in the inhibition of protein synthesis and RNA degradation respectively and induction of IFN (Der, S. D. *et al.*, 1995; Samuel, C. E., 2001). VACV E3 and K3 proteins have overlapping roles in blocking the action of PKR and OAS. VACV E3L binds dsRNA and prevents it from activating PKR and OAS. In addition to that, E3 can bind directly to PKR and prevent its activity for the required phosphorylation of eIF2α subunit (Chang, H. W. *et al.*, 1992; Davies, M. V. *et al.*, 1993). An orthologue of VACV E3L, is encoded by OV-NZ2 and binds to dsRNA to inhibit the activation of PKR (Haig, D. M. *et al.*, 1998; McInnes, C. J. *et al.*, 1998). VACV K3L, which is a homologue of eIF2α, acts as a competitive element for PKR, resulting in inhibition of eIF2α phosphorylation (Davies, M. V. *et al.*, 1992). PKR is also targeted by other viruses, for example, influenza virus NS1 prevents the activation of PKR by binding to dsRNA (Hatada, E. *et al.*, 1999). Furthermore, the VACV C7L and K1L, host range genes, were also reported to be involved in inhibition of eIF2 phosphorylation (Meng, X. *et al.*, 2009; Meng, X. *et al.*, 2012). In addition KIL and C7L also inhibit the IFN effector mechanism by targeting SAMD9 (Meng, X. *et al.*, 2009; Meng, X. *et al.*, 2012). ISG15 is an ubiquitin-like protein and is targeted by different viruses such as Crimean Congo hemorrhagic virus and influenza B virus (Speer, S. D. *et al.*, 2016). It has been also shown that VACV E3 inhibits the function of ISG15 (Guerra, S. *et al.*, 2008).

1.5 ORFV Virus: Modulation of the Immune Response

Functional analyses have identified a number of ORFV genes that modulate the immune response. Vascular endothelial growth factor-E (VEGF-E, ORF132) is a factor that stimulates the proliferation and permeability of blood vessels beneath infected lesions (Lyttle, D. J. *et al.*, 1994). A homologue of interleukin-10 (vIL-10, ORF127) binds to the ovine IL-10 receptor and inhibits production of pro-inflammatory cytokines (Fleming, S. B. *et al.*, 1997). Interferon inhibitor (OVIFNR, ORF020) is dsRNA-binding protein that inhibits the activation of PKR (McInnes, C. J. *et al.*, 1998). Inhibitor of granulocyte-macrophage colony-stimulating factor (GM-CSF) and IL-2 (GIF, ORF117) is a factor that can block the signalling transmission of ovine GM-CSF and IL-2 whereas chemokine binding protein (ORF112) binds to several chemokines and prevents their action (Deane, D. *et al.*, 2000; Seet, B. T. *et al.*, 2003). A Bcl-2-like inhibitor of apoptosis (ORF125) can regulate and inhibit the apoptotic process (Westphal, D. *et al.*, 2007). A number of NF-κB inhibitors have been identified in ORFV (ORF121, ORF002 and ORF024) (Diel, D. G. *et al.*, 2010; Diel, D. G. *et al.*, 2011a; Diel, D. G. *et al.*, 2011b). ORFV also encodes a number of ankyrin (ANK) repeats that are involved in modulating cell cycle (Mercer, A. A. *et al.*, 2005). It has recently been shown that ORFV modulates the JAK/STAT pathway and IFN effector response (Harvey, R. *et al.*, 2015). Nevertheless, no genes have been shown to interfere with IFN expression.

The functional analysis of OV-NZ2 ORF116 gene has been investigated previously (AlDaif, B., 2013). The transcriptome of HeLa cells infected with either OV-NZ2 wild type or OV-NZ2Δ116 knockout has been analyzed using microarray. The microarray data revealed a major effect on the expression pattern of a number of cellular genes by ORFV infection. Analysis of differential gene expression found that the expression level of a number of ISGs had been up-regulated in the mutant virus-infected cells to higher levels than in wild type-infected cells. Infection with OV-NZ2Δ116 led to higher induction of ISGs IFI44, RIG-I, IFIT2, IFIT1, ISG20, OASL, IL-8, MDA5, OAS1 and DDX60 compared to OV-NZ2. Quantitative RT-PCR results have concurred the data obtained by microarray for the selected genes. These observations may suggest that ORF116 is likely to be involved in modulating the antiviral effectors of the type I IFN response and targeting a number of cellular ISGs by blocking the production of type I IFN from infected cells or blocking the expression of ISGs. These observations are supported by growth and

phenotype characterization of the ORF116 deletion virus in which the growth of the mutant virus was clearly affected which may suggest that these ISGs are the targets of ORF116. It is worthwhile to mention that microarray data have shown no differential expression in IFN. In addition, data have shown that OV-NZ2 downregulated IFI16 > 3-fold. IFI16 is a cytosolic dsDNA sensor that leads to IFN-β production. It is also thought that IFI16 is involved in the inflammasome activation in response to DNA viruses. The inflammasome controls downstream processing and maturation of the IL-1β and IL-18. These two cytokines are likely to play a role in host defence against ORFV infection.

1.6 Hypothesis

It is hypothesized that ORFV encodes factors that inhibit the expression of ISGs and type I IFNs and that the ORF116 gene plays a role in this process.

1.7 Aims of the Study

As described above preliminary data was obtained from a previous study that suggests that the ORF116 gene encoded by ORFV plays a role in IFN modulation by possibly inhibiting type I IFN expression or directly targeting ISG expression. This study set out to investigate whether ORFV has the ability to inhibit type I IFN expression and whether the ORF116 gene plays a role in this process as described below.

- Carry out functional analysis of the ORFV ORF116 gene by constructing an OV-NZ2-Rev116 revertant virus.
- Examine the expression levels of specific ISGs using qRT-PCR in HeLa cells infected with the ORFV viruses: OV-NZ2 *wt*, OV-NZ2Δ116 and OV-NZ2-Rev116.
- Examine the induction of type I IFN in various cell types, e.g., THP-1, hNDF and HEK293 cells upon stimulation with the synthetic polymers poly(dA:dT) or poly(I:C).
- Establish assays that require either RNA or DNA sensing signalling pathways for IFN-β induction using poly(I:C) and poly(dA:dT).
- Investigate the effect of ORFV on IFN-β expression induced through either RNA or DNA sensing signalling pathways.
- Examine the effect of ORF116 gene on IFN-β expression using ORFV recombinant virus.
- Examine the effect of stably expressing ORF116 on the induction of IFN-β upon stimulation with poly(dA:dT) or poly(I:C).
- Examine the effect of ORFV infection on IL-1β induced with poly(dA:dT) (inflammasome activation).

MATERIALS AND METHODS

2 MATERIALS AND METHODS

2.1 DNA Cloning

2.1.1 Plasmids

The cloning was carried out under GMO approval number GMD000522. Production and maintenance of DNA plasmids were conducted according to the molecular cloning protocol (Sambrook, J. *et al.*, 2012). Detail of the plasmids used in this study either produced or obtained from other sources is shown in Figure 2.1. The ampicillin-containing plasmids were propagated in DH5α competent cells and harvested and prepared as detailed below. All solutions used in plasmid manipulation are given in Appendices: section 9.1, 9.2 and 9.3.

Whenever required, the plasmid was ethanol precipitated by adding 0.1 vol of 3M sodium acetate and 2.5 vol of ice-cooled 100% ethanol and precipitated at -20 °C overnight. Then they were centrifuged in benchtop centrifuge for 10 min at 13,000 rpm and washed with 0.3 ml with 70% ethanol twice then let it air dry. The plasmid composition was verified by the characteristic band patterns after digestion with respective restriction enzyme and separation on gel by electrophoresis and also further confirmed by sequencing. For a short-term storage, the plasmids were stored in -20 °C, and they were stored as a glycerol stock in -80 °C when long-term storage needed.

A.

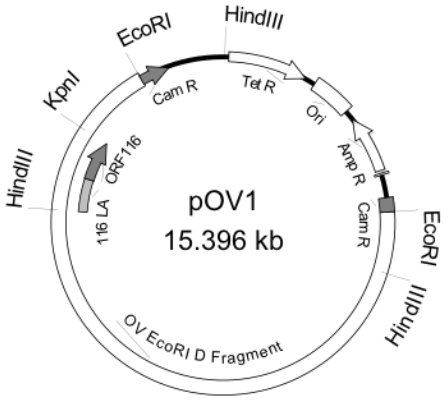

B.

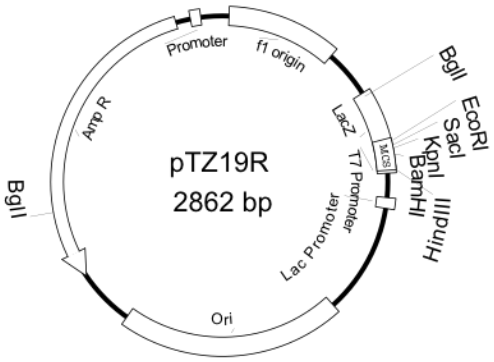

C.

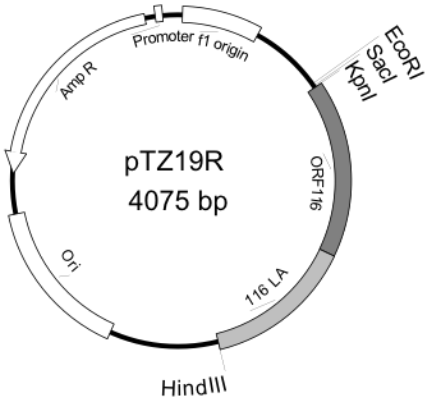

Continued next page

D.

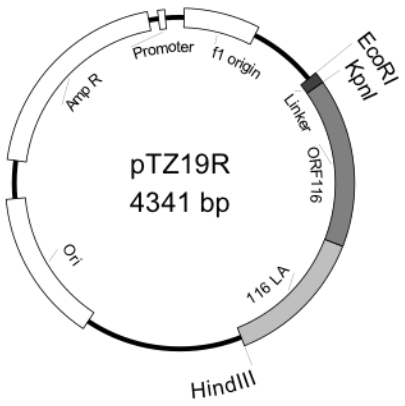

E.

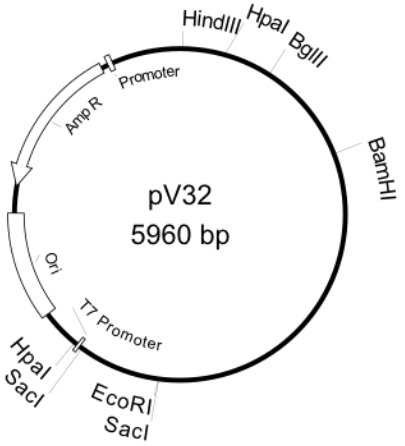

F.

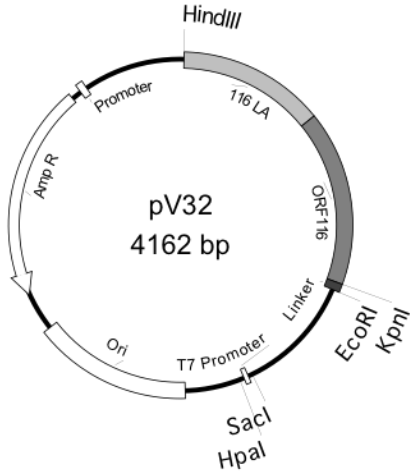

Continued next page

G.

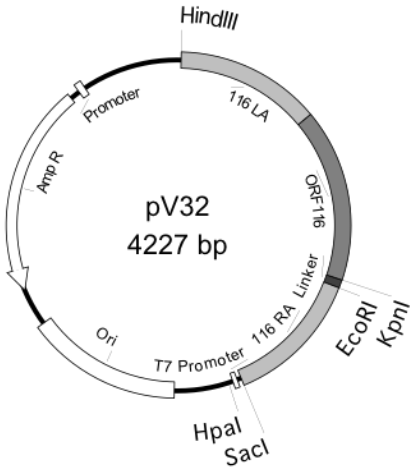

H.

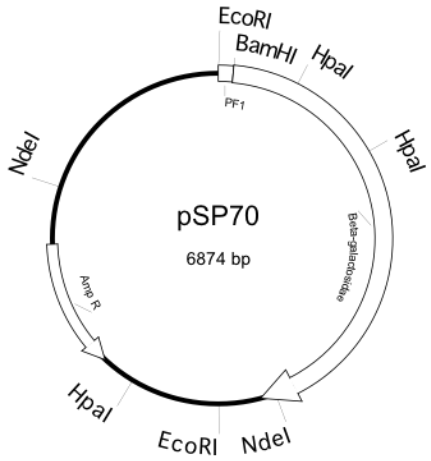

I.

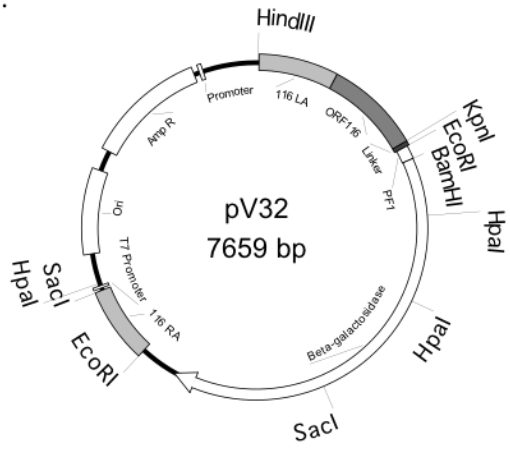

Continued next page

J.

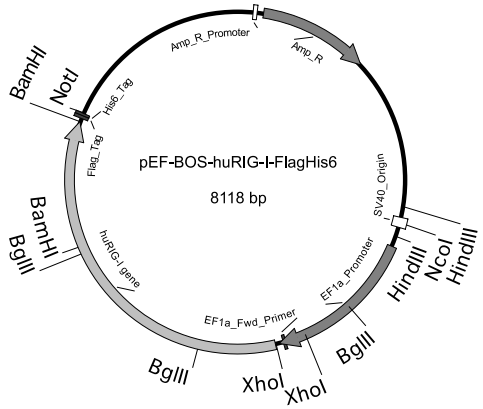

K.

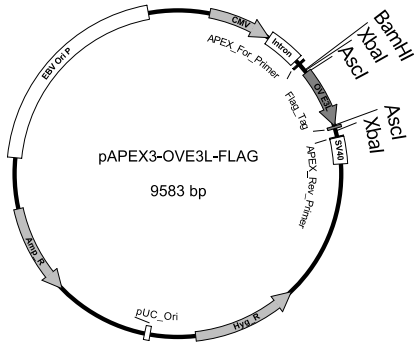

L.

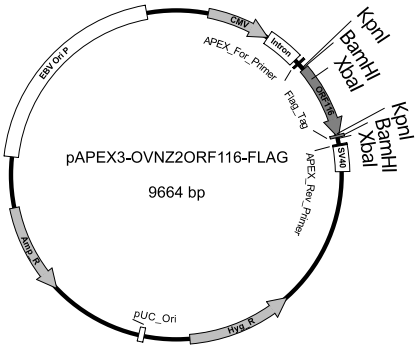

Caption is in the next page

Figure 2.1. Diagrams depicting plasmids used in this study with essential features shown. **A.** pOV1 is a vector originally derived from pBR328 that has been constructed by Soberon, X. *et al.* (1980). Orf virus NZ2 *Eco*RI-D fragment has been cloned at *Eco*RI restriction site in the chloramphenicol resistance gene by Mercer, A. A. *et al.* (1987). pBR328 confers resistance to chloramphenicol, tetracycline and ampicillin, however the cells carrying *Eco*RI-D fragment DNA was identified by their ampicillin resistance phenotype. **B.** pTZ19R confers ampicillin resistance and multiple cloning sites are located within *LacZ* gene which will provide a selection method for the presence of interested fragment DNA. Ori, ColE origin of replication, fi Ori, origin of replication and morphogenetic signal from phage f1 intergenic region. It contains sequences for forward and reverse universal sequencing primers M13. **C.** A fragment of *Hin*dIII/*Kpn*I from pOV1 was double digested with the same restriction enzymes and cloned into the same restriction sites in pTZ19R. **D.** pTZ19R containing *Hin*dIII/*Kpn*I fragment was digested with *Kpn*I and *Eco*RI restriction enzymes and a synthesised linker harbouring *Kpn*I and *Eco*RI restriction sites, stop codon and poxvirus early gene termination signal TTTTTCT was inserted at *Kpn*I and *Eco*RI restriction sites. **E.** pV32 vector was utilized to construct a transfer vector to be used for generating orf virus revertant-116. **F.** pV32 vector was digested with *Hin*dIII and *Eco*RI restriction enzymes and *Hin*dIII/*Eco*RI fragment from pTZ19R was cloned at the same restriction sites. **G.** PCR amplified *Eco*RI/*Sac*I right arm was cloned at *Eco*RI/*Sac*I restriction sites. **H.** pSP70 was obtained from Promega and it confers ampicillin resistance. *LacZ* gene under control of PF1 orf virus late promoter previously cloned was digested with *Eco*RI restriction enzyme and *LacZ* gene excised from this construct to provide a means of selection method. **I.** pV32 was digested with *Eco*RI restriction enzyme and *LacZ* gene was cloned into it at the same restriction site. This vector contains all the genetic elements required to generate the revertant-116 virus. **J.** pEF-Bos-HuRIG-Flag. pEF-BOS was constructed by (Mizushima, S. *et al.*, 1990). It is a powerful mammalian expression vector using the promoter of human EF-1α chromosomal gene. The human RIG-I gene was discovered by Takashi Fujita as detailed in (Yoneyama, M. *et al.*, 2004). The full length gene with flag tag was cloned at 5' *Xho*I and 3' *Bam*HI into pEF-BOS plasmid by Brian G. Monks as detailed in (Goutagny, N. *et al.*, 2010) and the complete construct was kindly provided by the Fitzgerald laboratory. The main features of the construct are shown in the diagram. **K**. pAPEX3-OV-E3L-Flag was constructed in this study. pAPEX3 is a mammalian expression vector constructed by Steven Squinto (Evans, M. J. *et al.*, 1995). OV-NZ2 ORF020 (vaccinia E3L homologue) was PCR amplified from pVU215 and cloned at *Asc*I restriction site, downstream of kozak sequence and upstream flag tag of pAPEX3. The plasmid contains ampicillin and also hygromycin resistance markers for selection. **L.** pAPEX3-ORF116-Flag is a mammalian expression vector in which OV-NZ2 ORF116 was cloned at the *Bam*HI restriction site. This plasmid was constructed by Fleming and McCaughan (VRU, University of Otago).

2.1.2 Preparation and Transformation of Calcium-Competent *Escherichia coli* by Heat Shock

Escherichia coli strain DH5α competent cells were prepared in a solution of 80 mM calcium chloride to be used for transformation by the heat shock method. *E. coli* DH5α from frozen stock was streaked on a 2-YT agar plate to obtain a single colony. A single colony was picked and transferred into 10 ml of 2-YT broth and incubated at 37 °C overnight with shaking at 200 rpm. The culture was diluted with 250 ml of SOB medium (Appendix: section 9.1) and incubated at 37 °C on a shaker for about 2 hours until growth reached exponential phase at an optical density (OD_{600}) of 0.4. The culture was placed on ice to cool down, then transferred to a flat-bottom centrifuge bottle and centrifuged at 3000 rpm (1350 x *g*) for 10 min at 4 °C using an F250 rotor. The supernatant was discarded and the cell pellets were resuspended in 80 ml of ice-cold transformation buffer (Appendix: section 9.1) then incubated on ice for 20 min. The cell pellets were centrifuged at 3000 rpm (1350 x *g*) for 10 min at 4 °C and the supernatant discarded. The cell pellets were resuspended in 10 ml of ice-cold transformation buffer. The cells were aliquoted in 100 µl in 1.5-ml tubes then stored at -80 °C. The cells were checked for high transformation efficiency. The competent cells were transformed with known amount of plasmid by heat shock, then plates incubated at 37 °C overnight. The colonies formed were counted and a formula was applied to determine the transformation efficiency (TE) of DH5α competent cells. TE=colonies counted/µg plasmid/dilution.

The transformation technique is described in (Hanahan, D., 1983; Sambrook, J. *et al.*, 2012). Briefly, about 10 ng of plasmid DNA was added into 50 µl of competent cells after been thawed on ice. The content was mixed by swirling gently then stored on ice for 30 min. The tube was transferred into a heat block and incubated at 42 °C for 90 seconds then rapidly transferred onto ice and incubated for 2 min. Eight hundred µl of 2-YT (Appendix: section 9.1) was added into the tube then incubated at 37 °C for 45 min on a shaker at 200 rpm to allow the bacteria to recover and to express the antibiotic resistance gene encoded by the plasmid. An appropriate volume of transformed competent cells was transferred onto LB agar plate containing ampicillin (50 µg/ml). Using a sterile plastic spreader, the transformed competent cells were gently spread over the surface of the agar then the plates were incubated at 37 °C overnight.

2.1.3 Extraction and Purification of Plasmid DNA

Small-Scale Preparation and Purification of Plasmid DNA

Five ml of Luria broth (LB) containing ampicillin at 100 µg/ml was inoculated with a single bacteria colony harbouring the plasmid of interest then incubated at 37 °C with shaking at 200 rpm for overnight. The bacterial pellets were centrifuged and the supernatant discarded then the pellets harvested, then plasmid DNA prepared and purified using QIA Prep Spin Mini Prep Kit 50 (QIAGEN). The concentration was measured by UV spectroscopy using a NanoDrop Spectrophotometer (Thermo Scientific).

Alkaline Lysis Plasmid Purification

For recombinant clone screening, plasmid DNA was prepared by alkali lysis. Five ml of Luria Broth (LB) containing ampicillin at 100 µg/ml was inoculated with a single bacterial colony and incubated overnight at 37 °C with shaking at 200 rpm. One and half ml of bacterial cells were harvested in a 1.5-ml microcentrifuge tube by benchtop microcentrifugation at 13000 rpm (14000*g*) for 1 min. The supernatant was discarded and pellets were re-suspended in 100 µl of 25 mM Tris/ 10 mM EDTA/ 50 mM Glucose solution. Two hundred µl of 0.2M NaOH/1%SDS was added then mixed by inversion to release the DNA. One hundred and fifty µl of 5M potassium acetate pH 5.0 was added and mixed by inversion to precipitate the chromosomal DNA. The sample was centrifuged for 10 min at 13000 rpm (14000*g*), then 375 µl of supernatant was transferred to a clean tube. To recover the plasmid DNA, 750 µl of pre-cooled 100% ethanol was added then mixed and spun for 5 min at 13000 rpm (14000*g*). The DNA pellet was washed twice with 100 µl of 70 % ethanol, and air dried at 37 °C for 15 min. The DNA was re-suspended in 50 µl of 10 mM Tris. RNA was degraded by adding 10 µl RNase (1 µg/ml) and incubated for 30 min at room temperature.

Large-Scale Preparation of Plasmid DNA

A single bacterial colony from a freshly selective plate was picked and inoculated in 5 ml of LB medium containing ampicillin at 100 µg/ml then incubated at 37 °C for 8 hours with shaking. Twenty five ml of LB medium was inoculated with 50 µl of starter culture then incubated at 37

°C for 16 hours with shaking. After incubation, the bacterial cells were harvested by centrifugation 6000*g* for 15 min at 4 °C using on F250 rotor in a Beckman Avarti J-26 XPI centrifuge. The supernatant was discarded and cell pellets were stored at -20 °C until DNA preparation using a Plasmid Midi Kit 100 (QIAGEN). The cell pellets were resuspended in 4 ml of buffer P1 then transferred to 50-ml polycarbonate cap-screw tubes. Four ml of buffer P2 was added and mixed thoroughly by vigorously inverting the tube 4-6 times then incubated at RT for 5 min. Four ml of chilled buffer P3 was added then mixed immediately and thoroughly by inverting 4-6 times then incubated on ice for 15 min. The lysate was cleared by filtration using a cartridge filter. The QIAGEN-tip 100 column was equilibrated by applying 4 ml of buffer QBT and allowed to empty by gravity flow. The lysate obtained was applied to the column and allowed to enter the resin by gravity flow. The column was washed with 2X 10 ml of buffer QC. Plasmid DNA was eluted with 5 ml of buffer QF. DNA plasmid was precipitated by adding 3.5 ml (0.7 volume) at room temperature of isopropanol to the eluted DNA, mixed then kept at -20 °C for overnight. Plasmid DNA was centrifuged at 15,000*g* for 30 min at 4 °C using a JA20 rotor in a Beckman Avarti J-26 XPI centrifuge, then the supernatant discarded. The DNA pellets were washed with 5 ml of 70% ethanol at RT followed by centrifugation at 15,000*g* for 10 min using an JA20 rotor then the supernatant discarded. The DNA pellets were air dried then resuspended in 100 µl of Milli-Q water.

2.1.4 Dephosphorylation of Linearized Plasmids

Linearized vector was dephosphorylated at 5'-end using Shrimp Alkaline Phosphatase rSAP (NEB) to prevent self-ligation. After digestion of 1 µg of plasmid vector, the reaction containing 1 µl of alkaline phosphatase and 2 µl of 10X buffer in a 20 µl final volume was set up. The reaction was incubated at 37 °C for 30 min then enzyme inactivated at 65 °C for 5 min. The dephosphorylation reaction was directly used in the ligation reaction.

2.1.5 Ligation

Approximately 7 µl of insert and 1 µl of linearized plasmid vector were incubated in a 10 µl ligation reaction containing 1 µl of T4 DNA ligase (Roche) and 2 µl of 10X ligation buffer (Roche) and incubated at 4 °C overnight. The ligation reaction was directly used in transformation of competent cells.

2.1.6 Polymerase Chain Reaction (PCR)

The primers used for PCR amplification were supplied by Invitrogen. The primers were shipped as lyophilized powder. They were reconstituted in Tris-EDTA (TE) buffer (pH 8.0) to obtain a final concentration of 100 µM and stored in 2-ml screw-capped tubes at -20 °C.

A PCR reaction was performed with 40 cycles in a final volume of 50 µl containing 0.5 µl of *Taq* DNA Polymerase, 5 U/µl (Roche), 5 µl of 10X buffer, 1 µl of 10 mM dNTPs (Roche), 1 µl of each 10 pmol forward and reverse primer. The cycling conditions were conducted in a PCR thermal cycler as follows: 15 sec at 94 °C (denaturation), 30 sec at 60 °C (annealing) and 45 sec at 72 °C (elongation). Initial denaturation was 2 min at 94 °C for one cycle and final elongation was 7 min at 72 °C for one cycle then cooled to 4 °C. The amount of DNA used in PCR reactions varied. Virus genomic DNA was 5 µl (5 ng), screening of *LacZ* gene correct orientation was half a colony of transformed bacteria, RT-PCR was 1 µl of cDNA and plasmid DNA was 1 ng.

2.1.7 Restriction Endonuclease Digestion

Restriction enzyme digestion was conducted in a final volume of 50 µl at 37 °C for 2 hours then the restriction enzyme inactivated at 65 °C for 15 min. One µl of restriction enzyme 10 U/µl (Roche) was used for digestion of 1 µg DNA. Bovine serum albumin (BSA) was added whenever needed at a concentration of 200 µg/ml. Where DNA digestion required more than one enzyme, double digestion was performed simultaneously, if one digestion buffer can provide high digestion activity for both enzymes, otherwise the DNA was digested sequentially starting with the enzyme that has the lowest salt concentration.

2.1.8 Separation of DNA Fragments by Gel Electrophoresis

The DNA fragments were resolved by gel electrophoresis. One percent agarose gel containing 0.5 µg/ml ethidium bromide was cast in a tray. About 10-20 µl of DNA was mixed with 5 µl of bromophenol blue tracking dye (Appendix: section 9.3) and loaded onto the gel in an electrophoresis tank filled with 1X Tris Acetate EDTA (TAE) electrophoresis buffer (Appendix: section 9.3). DNA was electrophoresed at the appropriate voltage and time. The bands of DNA were visualized under ultraviolet illumination (UV) at 365 nm.

2.1.9 Gel Extraction of DNA Fragments

The gel was placed on a UV plate and the relevant bands were excised from the gel with a clean scalpel blade, then transferred to 1.5 ml microfuge tubes. The DNA was extracted from the gel using PureLink Quick Gel Extraction Kit (Invitrogen) following the manufacturer's instructions.

2.1.10 DNA Sequencing and Analysis

DNA sequencing was conducted in the Allan Wilson Centre, Massey University, Palmerston North, New Zealand. Following their recommendations, the sequencing reaction was set up in 20 µl volumes containing 4 pmol of primer and about 50 ng of PCR product or 300 ng of DNA plasmid. Sequencing data was analysed using SeqMan (DNAStar Inc).

2.2 Cells

Primary Lamb Testis cells (LT) were cultured in minimal essential medium (MEM) (GIBCO, Invitrogen). Human embryonic kidney HEK293 cells, human neonatal dermal fibroblasts (hNDF), HaCaT and HeLa cells were cultured in Dulbecco's Modified Eagle Medium (DMEM) (GIBCO, Invitrogen). THP-1 cells were cultured in RPMI1640 (GIBCO, Invitrogen). All cell types were supplemented with 10 % heat-inactivated fetal calf serum (FCS) with penicillin (500 units/ml), streptomycin (0.5 mg/ml), and kanamycin (0.1 mg/ml) and maintained at 37 °C in a 5% CO_2 humidified incubator. Cells were counted by haemocytometer using trypan blue and seeded at the number required. THP-1 cells were differentiated to macrophages in 300 ng/ml phorbol myristate acetate (PMA) (Sigma) for 3 hours and rested for 2 to 3 days without PMA before experiments were performed. PMA was resuspended in 1 ml of DMSO making the concentration 1 µg/µl then aliquoted and stored at -20 °C (Table 9.1). An HEK293 cell line stably expressing OV-NZ2 ORF116, was generated as detailed in material and methods. Cells were stored in liquid nitrogen and revived when needed.

2.3 Viruses

ORFV strain NZ2 wild type (OV-NZ2) (Robinson, A. J. *et al.*, 1982) was used in this study. A deletion mutant-116 virus (OV-NZ2Δ116) was constructed previously in which ORF116 was deleted from the virus genome and replaced with a *GUS* gene as a reporter under a VACV late

promoter PH5. A revertant-116 virus (OV-NZ2-Rev116) was constructed in this study in which ORF116 was re-inserted at the same locus along with *LacZ* gene as a reporter under an ORFV late promoter PF1. All viruses were propagated in LT cells and titred by plaque assay on LT cells. To produce heat-inactivated virus, the virus inoculum was heated at 56 °C for 1 hour in a water bath.

2.3.1 Preparation of Virus Stock

Six 175-cm^2 flasks containing LT cells were maintained in complete MEM supplemented with 1% PSK. The flasks were infected with virus and incubated at 37 °C for 1 hour rocking at 15 min intervals. After 1 hour of adsorption, the infected cells were incubated in 25 ml of MEM 2% FCS and 1% PSK for five days or until a complete cytopathic effect (CPE) was observed. The content was harvested using a cell scraper and transferred into a 50-ml Falcon tube and stored at -80 °C. To promote cell lysis and release of virus remaining in cells, the contents were subjected to three freeze-thaw cycles. The tubes were centrifuged at 1500 rpm (512*g*) for 10 min at 4 °C to separate cell debris from the supernatant. The supernatants were transferred to a 500-ml flask on ice. The pellets were transferred into a 15-ml tube and sonicated for 1 min. The sonication was repeated if lumps of debris were visible. The contents were spun again at 1500 rpm (512*g*) for 10 min at 4 °C and the supernatant was transferred to the 500-ml flask of the supernatants. The collected supernatants were transferred into 8 Oakridge Ti70 tubes (25 ml each) and ultra-centrifuged at 20,000 rpm (41,000*g*) for 1 hour at 4 °C in a Beckman Coulter Optima L-80 XP Ultracentrifuge using Ti70 rotor. Under a laminar flow hood, the supernatants were aspirated and the pellets were re-suspended in 5 ml of PBS. The virus suspension was sonicated for 1 min and aliquoted in 1 ml volume vials and stored at -80 °C.

2.3.2 Sucrose Purification of Virus Stock

All viruses used in this study were sucrose-purified to eliminate any confounding effect from cellular cytokines in particular IFNs that might be present in the virus preparation. The protocol has been described previously (Joklik, W. K., 1962; Nagington, J. *et al.*, 1964; Zwartouw, H. T. *et al.*, 1962). Briefly, 1 ml of 40 % sucrose made up in ET buffer (0.25 M Tris, pH 7.5 and 0.01 M EDTA) was added in a Beckman Coulter Ultra-Clear Centrifuge tube (13x51 mm) then overlaid with 4 ml of virus. Using SW55Ti swing rotor, the virus was centrifuged at 23,500 rpm

(64,000*g*) for 45 min at 4 °C in a Beckman Coulter Optima L-90K Ultracentrifuge. The supernatant was discarded and the virus pellet was resuspended in 5 ml of PBS.

2.3.3 Titration of Viral Stock and Plaque Assay

Two 6-well plates were seeded with LT cells containing 2 ml of MEM medium with 10% FCS and then incubated at 37 °C with 5% CO_2. When the cells had formed an 80% confluent monolayer, they were infected with virus. Ten-fold dilutions of sonicated virus were made in PBS (10^{-1} – 10^{-8}). The medium was removed from cells then washed with PBS and 200 µl of each viral dilution was added to the cells. The infection was carried out in duplicate from 10^{-3} to 10^{-8} dilutions. The infected cells were incubated at 37 °C and 5% CO_2 for 1 hour to allow virus to adsorb, with tipping every 15 min to ensure cells did not dry out and viruses were evenly distributed. During adsorption, MEM-agarose overlay was prepared by mixing equal volumes of 2X MEM 4% FCS and 2% agarose and cooled at 37 °C. After 1 hour of incubation, the inocula were removed from the wells, and cells washed with PBS then 2.5 ml of agarose overlay at 37 °C was added to each well. The agarose was left to set at room temperature then the infected cells incubated at 37 °C 5% CO_2 for 5 days. Virus plaques were visualized by staining with neutral red (0.015%), X-Gluc (200 µg/ml) or X-Gal (200 µg/ml) in which 2% of low melting point agarose overlay was prepared and mixed with the stain. One and half ml of agarose overlay was added to each well and left to set at room temperature. The plates were incubated at 37 °C 5% CO_2 for 4 hours or until plaques were visible. The plaques were counted and plaque-forming units per ml (pfu/ml) were estimated.

2.4 Generation of ORFV Virus ORF116 Revertant

The generation of an ORFV ORF116 revertant was made according to the method adapted from standard procedures used in the generation of VACV recombinants (Broder, C. C. *et al.*, 1999; Lorenzo, M. M. *et al.*, 2004; Mackett, M. *et al.*, 1984; Rziha, H. *et al.*, 2016; Wyatt, L. S. *et al.*, 2017) and the protocol has been described previously in (Fleming, S. B. *et al.*, 2017; Savory, L. J. *et al.*, 2000).

2.4.1 Construction of Transfer Vector Containing ORF116, *LacZ* Gene and Flanking Arms

The sequence of cloning steps to make the construct for the revertant-116 virus is shown in Figure 2.2. ORFV116 of OV-NZ2 is located within the restriction fragment *Eco*RI-D which was cloned into pOV1 plasmid. The gene encoding ORF116 is mostly located within a 1.255 kb *Hin*dIII-*Kpn*I subfragment of *Eco*RI-D in which this fragment contains ORF116 except the last 13 nucleotides at the C-terminus. The 1.255 kb fragment was isolated by endonuclease digestion. One µg of pOV1- *Eco*RI-D plasmid and pTZ19R plasmid were double digested with *Hin*dIII and *Kpn*I restriction enzymes, then fragments separated by electrophoresis on 1% agarose gel. The digested *Hin*dIII-*Kpn*I subfragment and pTZ19R vector were excised and purified using PureLink Quick Gel Extraction Kit (Invitrogen). The 1.255 kb *Hin*dIII-*Kpn*I subfragment was cloned into the pTZ19R vector at the same restriction sites. This step was followed by incorporation of a linker containing *Kpn*I and *Eco*RI restriction sites, the 13 nucleotides of ORF116 at C-treminus, a stop codon and a poxvirus early transcription termination signal T_5NT (CAGCACCTCC**TAA**GTGAGTACGTAA**TTTTTTCT**G, (bolded stop codon and T5NT signal) resulting in a DNA fragment containing the full length sequence of ORF116 gene with *Hin*dIII and *Eco*RI restriction sites. The linker was produced by self-annealing of two chemically synthesized oligonucleotides (Invitrogen) (ORF116 linker F Phos-CAGCACCTCCTAAGTGAGTACGTAATTTTTCTG and ORF116 linker R Phos-AATTCAGAAAAATTACGTACTCACTTAGGAGGTGCTGGTAC, underlined *Eco*RI and *Kpn*I sites) in which 5 µl of each oligo (10 pmol) was annealed in a 50 µl final volume of annealing buffer (10 mM Tris, pH8.0, 50 mM NaCl, 1 mM EDTA) at 95 °C for 5 min then cooled at RT. The linker was first confirmed on a 2% agarose gel then incorporated into pTZ19 plasmid at the *Eco*RI and *Kpn*I restriction sites after the plasmid was double digested with the same restriction enzymes. The *Hin*dIII/*Eco*RI fragment was removed from pTZ19 by sequential

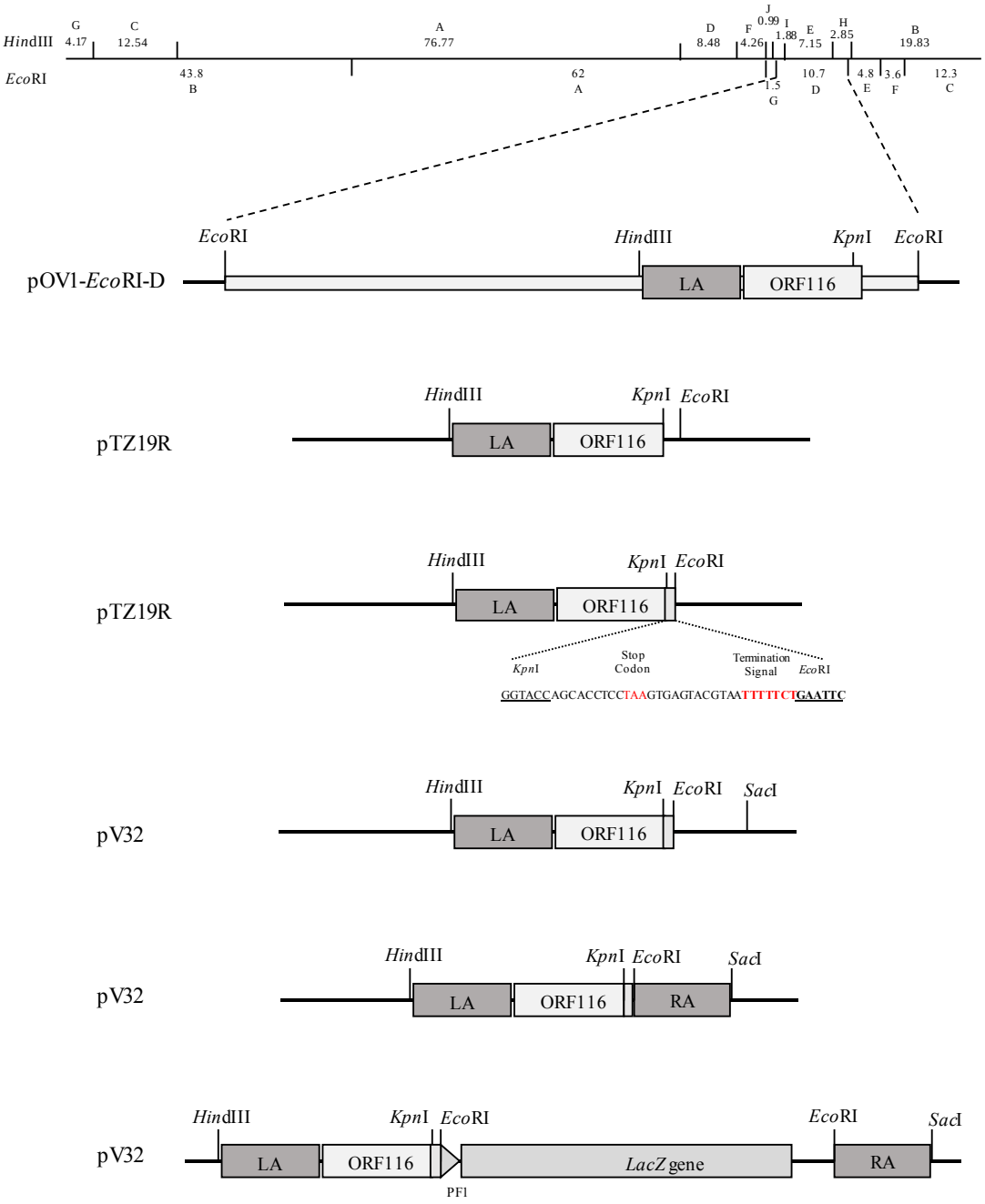

Figure 2.2. Sequences of cloning steps. Diagram showing the steps for construction of the final transfer vector used for the revertant-116 virus. The plasmid pOV1 contains the ORF116 gene and upstream sequence (left arm) both located between *Hin*dIII and *Kpn*I. The subfragment of *Hin*dIII/*Kpn*I was inserted into pTZ19R and an *Eco*RI/*Kpn*I linker was incorporated into pTZ19R. The *Hin*dIII/*Eco*RI fragment from pTZ19R was digested and inserted into pV32. Finally, a *LacZ* reporter gene was cloned into the same vector pV32 at the *Eco*RI restriction site generating the final construct used in homologous recombination.

digestion with *Hin*dIII and *Eco*RI restriction enzymes and cloned into the pV32 vector at the same sites. pV32 plasmid and the pTZ19R containing *Eco*RI/*Hin*dIII fragment were double digested with *Eco*RI and *Hin*dIII restriction enzymes and run on 1% gel then the pV32 vector and *Eco*RI/*Hin*dIII fragments from pTZ19R were excised and gel purified, then *Eco*RI/*Hin*dIII fragment was cloned into the pV32 vector. A fragment that spans 535 bp downstream of the ORF116 coding region (right arm with *Eco*RI and *Sac*I sites incorporated) which includes 373 bp of the ORF117 gene was PCR amplified from pVO1 plasmid using primers ORF116 right arm F 5'-CCCGAATTCGCATTTCGGAGTAACGTCGTA (*Eco*RI site underlined) and ORF116 right arm R 5'- CCAGAGCTCGGTCGTCGATCACCCAAGGGT (*Sac*I site underlined) then the PCR product was gel purified. The right arm was subjected first to double digestion with *Eco*RI and *Sac*I and cleaned up using a PCR Purification Kit (QIAGEN) then sequenced to check for errors before cloning into the pV32 vector at the *Eco*RI and *Sac*I restriction sites. Finally, the *E. coli* β-galactosidase gene (*lacZ*) placed under the control of a strong ORFV late promoter PF1 (Fleming, S. B. *et al.,* 1993) was cloned into an *Eco*RI site located between the ORF116 gene and the right arm. The correct orientation of *LacZ* gene was screened and confirmed by colony PCR (Bergkessel, M. *et al.,* 2013; Santos, C. N. S. *et al.,* 2014) in which a pair of primers (ORF116 linker F and R 5'-GCGCATCGTAACCGTGCATCTGCCAGTTTG) was used to yield a specific product of known size only if the *LacZ* gene was cloned in the correct orientation. The final plasmid construct was subjected to thorough restriction analysis to confirm the presence of all fragments within the construct and also to confirm the correct orientation of the *LacZ* gene. The final construct was sequenced utilizing primers used in constructing the transfer vector and all are depicted in Figure 3.4 A. Before the construct was used to generate the revertant virus, the function of *E. coli* β-galactosidase gene (*lacZ*) was checked in the LT-OV-NZ2 virus infected cells and the generation of blue colour was examined in the presence of X-Gal.

2.4.2 Transfection of Transfer Plasmid into Lamb Testes (LT)-Infected Cells

The final plasmid construct was used to generate the revertant-116 virus. LT cells were seeded at $2X10^6$ cell per 25-cm^2 flask. On the day of transfection, the cells were washed with PBS then infected with OV-NZ2Δ116 mutant as a parental virus at an MOI 0.5 per cell for 1 hour rocking every 15 min. After 1 hour of adsorption, MEM supplemented with 2% FCS was added and cells

incubated for 2 hours. After 2 hours post infection, the infected cells were transfected with the transfer vector using Lipofectamine 2000 (Invitrogen) according to manufacturer's instructions. The DNA:Lipid mixture was prepared by incubating 3 μg of the plasmid transfer vector into 0.5 ml of OPTI-MEM and 3 μl of Lipofectamine 2000 in 0.5 ml of OPTI-MEM for 30 min at room temperature. Then both contents were mixed and incubated for 15 min at RT. The infected cells were washed with PBS then with OPTI-MEM twice, 1 ml of transfection mixture was added and incubated overnight. Next day, the transfection mixture was removed and 4 ml of MEM medium with 2% FCS was added into the flask and incubated for 6 days until a complete cytopathic effect (CPE) observed. The cells were removed using a cell scraper and the whole content was transferred into a 15-ml tube then stored at -80 °C. The cells were disrupted by three freeze-thaw cycles and sonication. The cell debris was pelleted by low speed spin for 5 min at 4 °C and the supernatant transferred into a clean tube and stored at -80 °C.

2.4.3 Selection, Screening and Purification of Revertant-116 Virus

The *E. coli LacZ* gene was incorporated into the transfer vector downstream of ORF116 under control of the ORFV late promoter PF1 in order to provide a selection method for the identification of the resultant revertant-116 virus through the production of ß-galactosidase (ß-gal). The putative revertant-116 virus was screened and selected by their blue plaques in the presence of 5-bromo-4-chloro-3-indolyl-β-D-galactopyranoside (X-Gal) (200 μg/ml). The parental virus genome contains the *E. coli gusA* gene encoding ß-glucuronidase (GUS) that catalyses the production of blue colour in the presence of 5-bromo-4-chloro-3-indolyl glucuronide (X-Gluc). The resultant revertant-116 virus was subjected to plaque assay as explained above and detected by the X-Gal stain and distinguished from the parental virus by their blue plaque phenotype. A number of well-separated and strong blue-displayed plaques were picked with a sterilized pipette tip by piercing it through the agarose to the bottom of the well, scraping the monolayer and aspirating the agarose plug containing infected cells into the pipette then transferring it to a clean tube containing 200 μl of PBS then stored at -80 °C. They were subjected to three freeze-thaw cycles and sonication in order to break the cell membrane and release the intracellular infectious particles. Those putative revertant-116 virus isolates were amplified first in a 25-cm^2 flask of LT cells $2X10^6$ cell per flask using 50 μl of the virus isolate per flask. After adsorption, 5 ml of MEM 2% FCS was added then the flasks were incubated for

five days at 37 °C in 5% CO_2 atmosphere. Virus isolates showing a strong cytopathic effect (CPE) were chosen and their cells and supernatant harvested and transferred into 15-ml tubes then stored at -80 °C. They were subjected to three freeze-thaw cycles and sonication. The cell lysates were spun at 1500 rpm for 10 min at 4 °C and 50 µl of virus isolate was subjected to plaquing in 6-well plates as explained above. Well-separated and strong blue-displayed plaques were picked as explained above. Three rounds of plaque purification were performed to ensure complete removal of the parental virus and final pure revertant-116 virus obtained. PCR analysis was further conducted to ensure virus purity.

2.5 Analysis of Virus Growth Kinetics

One-step or multiple-step growth curves were conducted to characterize the growth of virus in HEK293, THP-1, NDF or HaCaT cells. Cells were seeded in 6-well plates at $4x10^5$ cells per well and incubated at 37 °C with 5% CO_2 overnight. On the day of infection, the medium was removed and cells washed with PBS. Then the cells were infected with sonicated virus using 200 µl inocula. After 1 hour of adsorption at 37 °C, the cells were incubated with 2 ml of medium, 2% FCS at 37 °C until harvesting time. To harvest virus, the cells were scraped off the surface and all contents were transferred to a 2-ml tube then stored at -80 °C. To release virus from cells, the samples were subjected to 3 cycles of thawing-freezing. The viral progeny was determined by plaque assay on LT cells.

2.6 Detection of Early Viral Protein Synthesis

Cells were infected with sonicated virus or for the inhibition study of early gene synthesis, the cells were infected with heat-inactivated virus in which virus inoculum was heated at 56 °C for 1 hour. Then the cells were incubated for 1 hour at 37 ºC with tipping every 10-15 min. After adsorption, 2 ml of medium containing 2% FCS was added. Then cells were incubated at 37 °C with 5% CO_2 until harvested. The cells were removed and transferred to a 1.5-ml tube and the cell suspension was centrifuged at 1200 rpm for 5 min, and the supernatant aspirated. OV119 viral protein expression was analysed by western blotting.

2.7 RNA Interference

Short interfering RNAs (siRNAs) including negative control siRNA are listed in Table 2.1 showing their sequences and sources. They were reconstituted in RNase-free water to final concentration of 100 μM for RIG-I and 20 μM for STING. Lipofectamine 2000 (ThermoFisher) was used to transfect siRNA into the cells according to the manufacturer's instructions. The cells were seeded at $2X10^4$ cells in a 24-well plate and incubated overnight at 37 °C. The cells were washed twice with PBS and 400 μl of OPTI-MEM added with no FCS or antibiotics. One hundred microliters of OPTI-MEM containing the siRNA:lipid mix was prepared and transfection carried out according to the manufacturer's instructions. Three siRNAs targeting a gene of interest were used and absence of siRNA (none, only Lipofectamine 2000) and negative control siRNA (NC) were included in each experiment as controls. The final concentration of siRNA used was 100 nM and 1 μl of Lipofectamine 2000 was used per well. The following day of transfection the cells 25 μl of FCS was added and the cells incubated for a further day. The knockdown effects were analysed by western blotting using antibody against the protein of interest. After 48 hours post transfection, the cells were used for the assays of IFN-β induction.

2.8 Western Immunoblotting

The cell pellets were washed with PBS twice and lysed in lysis buffer [1% Nonidot P-40 (NP-40), 150 mM NaCl, 50 mM Tris-HCl pH 7.5, 2 mM PMSF, 1 mM Na_3VO_4, 10 mM NaF, 1 tablet protease inhibitor (cOmplete, Mini, EDTA-free, Roche) per 10 ml] for early viral protein synthesis and siRNA knockdown experiments, whereas, for the experiments involving detection of phosphorylated proteins the cells were lysed in Phosphosafe Extraction reagent (Merck Millipore). The cell lysates were kept on ice for 30 min, then centrifuged at 16,000 rpm for 10 min at 4 °C. Supernatants were transferred to new 1.5-ml tubes. The concentration of protein extracted was determined using Pierce BCA Protein assay Kit (ThermoFisher) following the manufacturer's instructions.

Equal amounts of samples were prepared in loading buffer (LDS sample buffer 4X and reducing buffer 10X, novex, life technologies) then boiled for 8 min. The protein and molecular weight marker were resolved by Tris-glycine SDS-polyacrylamide gel electrophoresis (SDS-PAGE) using Mini-PROTEAN® Electrophoresis System (BioRad), then the separated proteins were

transferred onto nitrocellulose membranes (45 micron, Amersham) using a Mini Trans-Blot Cell (BioRad). The membrane was blocked with 5% skimmed milk in TBST buffer for 1 hour at room temperature, then the membrane was incubated with primary antibody in TBST containing 1% skimmed milk or 5% bovine serum albumin (BSA) for phosphorylated protein overnight at 4 °C with shaking. The membrane was then washed with TBST for three 5-min washes and incubated with HRP-conjugated secondary antibody in TBST containing 1 % skimmed milk for 1 hour at room temperature on a shaker. Then the membrane was washed with TBST for three 5-min washes and bands were detected using chemiluminescent substrate (Pierce, Thermo Scientific) and imaged by Odyssey imaging system (Li-Cor Biosciences). Bands were quantified using ImageJ software (version 1.51e) and normalized to those of the loading control. All primary and secondary antibodies are listed in Table 2.2.

2.9 Immunoprecipitation

Cells were washed twice with PBS and lysed with lysis buffer [1% Nonidot P-40 (NP-40), 150 mM NaCl, 50 mM Tris-HCl pH 8, 2 mM phenymethylsulfonyl Fluoride (PMSF), 1 mM Na_3VO_4, 10 mM NaF, 1 tablet protease inhibitor (cOmplete, Mini, EDTA-free, Roche) per 10 ml]. After 30 min of incubation on ice, the lysates were centrifuged at 13,000 rpm for 20 min at 4 °C then the supernatants were transferred into new tubes. Anti-RIG-I (cell signalling) (1:50) and normal rabbit IgG (Invitrogen) as negative control were added into the lysates. The antibodies and proteins mixtures were incubated overnight at 4 °C on a rotator. Fifty microliters of protein G Sepharose beads were added into the lysates and incubated for 2 hours at 4 °C on a rotator. Proteins bound to antibodies and protein G Sepharose were collected by centrifugation for 30 sec then washed three times with 750 µl of lysis buffer for 5 min at 4 °C on a rotator. The precipitated proteins were analysed by western blot analysis.

Table 2.1. Short interfering RNAs (siRNAs) sequences.

Gene	GenBank Accession No.	Nucleotide Position	siRNA No.	Sequence (5'-3'), sense and anti-sense [a]	Source
hRIG-I	NM_014314	2798	1	GACAUUUGAGAUUCCAGUU[dT][dT] AACUGGAAUCUCAAAUGUC[dT][dT]	SIGMA
		2381	2	GACUAGUAAUGCUGGUGUA[dT][dT] UACACCAGCAUUACUAGUC[dT][dT]	SIGMA
		1970	3	CAGCAAUGAGAAUCCUAAA[dT][dT] UUUAGGAUUCUCAUUGCUG[dT][dT]	SIGMA
hSTING (TMEM173)	NM_198282	1035	1	GCAUCAAGGAUCGGGUUU[TT] AAACCCGAUCCUUGAUGC[TT]	GENEPHARMA
		679	2	GCCCUUCACUUGGAUGCUU[TT] AAGCAUCCAAGUGAAGGGC[TT]	GENEPHARMA
		886	3	GCAUUACAACAACCUGCUA[TT] UAGCAGGUUGUUGUAAUGC[TT]	GENEPHARMA
Negative Control (NC)	-	-	-	UAGCGACUAAACACAUCAA[UU] UUGAUGUGUUUAGUCGCUA[UU]	Dharmacon Cat#D-001210-01

[a] Sequence in brackets indicate overhangs.

Table 2.2. Antibodies used in western blot analysis.

Primary Antibodies	Source	Catalog No.	Dilution used	Blocking Condition	Antibody incubation
Phospho-STING (Ser366) (D7C3S) Rabbit mAb	Cell Signaling Technology	19781	1:1000	1 hour at RT in 5 % BSA	Overnight at 4 °C in 5 % BSA in TBST on shaker
RIG-I (D14G6) Rabbit mAb	Cell Signaling Technology	3743	1:1000 1:50 (IP)*	1 hour at RT in 5 % skimmed milk	Overnight at 4 °C in 5 % BSA in TBST on shaker
STING (D2P2F) Rabbit mAb	Cell Signaling Technology	13647	1:1000	1 hour at RT in 5 % skimmed milk	Overnight at 4 °C in 5 % BSA in TBST on shaker
TBK1/NAK Rabbit mAb	Cell Signaling Technology	3013	1:1000	1 hour at RT in 5 % skimmed milk	Overnight at 4 °C in 5 % BSA in TBST on shaker
IRF3 (D83B9) Rabbit mAb	Cell Signaling Technology	4302	1:1000	1 hour at RT in 5 % skimmed milk	Overnight at 4 °C in 5 % BSA in TBST on shaker
Phospho-TBK1/NAK (Ser172) (D52C2) XP Rabbit mAb	Cell Signaling Technology	5483	1:1000	1 hour at RT in 5 % BSA	Overnight at 4 °C in 5 % BSA in TBST on shaker
Phospho-IRF3 (Ser396) (D601M) Rabbit mAb	Cell Signaling Technology	29047	1:1000	1 hour at RT in 5 % BSA	Overnight at 4 °C in 5 % BSA in TBST on shaker
Mouse monoclonal Anti-Flag M2 Ab	Sigma-Aldrich	F1804	1:1000	1 hour at RT in 5 % skimmed milk in TBST	Overnight at 4 °C in 1 % skimmed milk in TBST on shaker
Rb pAb to alpha Tubulin	Abcam	Ab4074	1:2000	1 hour at RT in 5 % skimmed milk in TBST	Overnight at 4 °C in 1 % skimmed milk in TBST on shaker
Actin (C-11)	Santa Cruz Biotechnology	Sc-1615	1:2000	1 hour at RT in 5 % skimmed milk in TBST	Overnight at 4 °C in 1 % skimmed milk in TBST on shaker
Rabbit Anti-OV119	(Harfoot, R. T., 2015)	-	1:2000	1 hour at RT in 5 % skimmed milk in TBST	Overnight at 4 °C in 1 % skimmed milk in TBST on shaker

Continued next page

Primary Antibodies	Source	Catalog No.	Dilution used	Blocking Condition	Antibody incubation
Normal rabbit IgG	Invitrogen	-	1:50 (IP)*	-	-

* Immunoprecipitation (IP).

Secondary Antibodies	Source	Catalog No.	Dilution used	Blocking Condition	Antibody incubation
Polyclonal goat anti-Rabbit Immunoglobulin/HRP	Dako	P0448	1:2000	-	1 hour at RT in 1 % skimmed milk on shaker
Anti-Mouse IgG, HRP-linked Antibody	Cell Signaling Technology	7076	1:2000	-	1 hour at RT in 1 % skimmed milk on shaker

2.10 Analysis of Viral Genomic DNA

2.10.1 Virus DNA Extraction

The protocol for viral DNA preparation was adapted from Mercer, A. A. *et al.* (1987). Virus stock was sucrose purified and the supernatant discarded and the pellet resuspended in 0.2 ml of ET buffer (0.25 M Tris, pH 7.5 and 0.01 M EDTA). A gradient of sodium diatrizoate (25% to 50%) was prepared in a Beckman Coulter Ultra-Clear Centrifuge tube (13x51 mm) using a peristaltic pump, then overlaid with 0.5 ml of 10% dextran and last the resuspended virus was laid on top. The virus was centrifuged at 22,000 rpm in an SW55Ti rotor for 18 hours at 4 °C. After centrifugation, the two visible bands were harvested separately by using a 1-ml pipette tip. The bands were diluted in 4 ml of ET buffer then layered on a 1 ml 40% sucrose cushion for another sucrose purification. The supernatant was discarded and the pellet was resuspended in 0.2 ml of TE buffer (0.01 M Tris, pH 8.0 and 0.001M EDTA). The purified virus pellet was digested by adding 10 µl of proteinase K (25 mg/ml) and 2.5 µl of 10% SDS then incubated for 2 hours at 56 °C. Another 2.5 µl of 10% SDS was added with 30 min incubation at 56 °C. After digestion, the virus DNA was layered onto a density gradient of guanidine HCl/Cesium chloride (1.35 g/ml to 1.55 g/ml) prepared in a Beckman Coulter Ultra-Clear Centrifuge tube (13x51 mm) by peristaltic pump then ultra-centrifuged at 35,000 rpm using an SW55Ti rotor for 18 hours at 20 °C. After centrifugation was completed, 0.5 ml of fractions were collected by 1-ml pipette tip and transferred into 1.5-ml tubes. All Fractions were checked by gel electrophoresis to identify the fractions containing virus DNA. Five µl from each fraction was mixed with 40 µl of TE buffer and 5 µl of loading dye then loaded onto a 0.7% gel and run for 1 hour at 75 V. Those fractions containing DNA were pooled, transferred into dialysis tubing and sealed at both ends with clips. The tubing was placed in 2 L of dialysis buffer (TE: 0.01 M Tris, pH8 and 0.001 M EDTA) in a cool room and stirred with a magnetic stirrer for 2 days, and changing the buffer every day. After dialysis, the dialyzed DNA was transferred into a 1.5-ml tube and stored at 4 °C.

2.10.2 Endonuclease Restriction of Viral DNA.

The concentration of viral DNA prep was determined by NanoDrop spectrophotometer. Viral DNA was digested in a reaction containing 5 µl (50 U) of restriction enzyme (Roche) and 28 µl of buffer in a total volume of 280 µl. The reaction was incubated at 37 °C for 2 hours, then the digested DNA was ethanol precipitated in 560 µl of absolute ethanol and 25 µl of 3 M sodium acetate (pH 5) at -20 °C overnight. The digested DNA was recovered by centrifuging at 13,000 rpm for 15 min. The

supernatant was discarded and the pellet washed with 70% ethanol and centrifuged at 13,000 rpm for 15 min. The pellet was air-dried then resuspended in 10 µl of TE buffer (pH 7.5) and 3 µl of loading dye added. Two hundred ml of 0.7% agarose gel containing 0.5 µg/ml ethidium bromide was prepared in a tray sized 15 cm x 24 cm. The digested virus DNA was run at 45 V overnight. The bands were visualized under UV light. The size of DNA fragments were compared to those predicted by GeneQuest (DNAStar, Inc).

2.10.3 PCR Amplification of Viral DNA

PCR amplification of the target region of viral DNA was performed with 40 cycles in a final volume of 50 µl containing 0.5 µl of Taq DNA Polymerase (Roche), 5 µl of 10X buffer, 1 µl of 0.2 mM dNTPs (Roche), 1 µl of each 10 pmol forward and reverse primer (see Table 2.3 for primer sets) and 5 µl of viral DNA. The cycling conditions were conducted in a PCR thermal cycler as follows: 15 sec at 94 °C (denaturation), 30 sec at 60 °C (annealing) and 45 sec at 72 °C (elongation). Initial denaturation was 2 min at 94 °C for one cycle and final elongation was 7 min at 72 °C for one cycle then cooled to 4 °C. Ten µl of PCR products mixed with 5 µl of loading dye were electrophoresed on a 1% agarose gel at 75 mV for 1 hr. The PCR products were visualized under UV light.

Table 2.3. Primers used in PCR analysis of viral DNA.

NO.	Sequence (5'-3')
Universal Primers for WT, KO and Rev.	
1_F	CTACGGCGCTTATGTGGACT
5_R	CCAGAGCTCGGTCGTCGATCACCCAAGGGT
Primers for WT	
1_F	CTACGGCGCTTATGTGGACT
2_R	TCTGAGGCACGCCATCTTTC
Primers for KO	
	Left Region of ORF116 locus
1_F	CTACGGCGCTTATGTGGACT
3_R	CACCATTGGCCACCACCTGCC
	Right Region of ORF116 locus
4_F	CAGCGTTGGTGGGAAAGCGCG
5_R	CCAGAGCTCGGTCGTCGATCACCCAAGGGT
Primers for Rev	
	Left Region of ORF116 locus
6_F	GTGCAGACTGTCCATGGTGT
7_R	TTGGGTAACGCCAGGGTTTT
	Right Region of ORF116 locus
8_F	CTCACGCGTGGCAGCATCAG
5_R	CCAGAGCTCGGTCGTCGATCACCCAAGGGT
Primers for GUS	
4_F	CAGCGTTGGTGGGAAAGCGCG
3_R	CACCATTGGCCACCACCTGCC

F, forward. R, reverse. WT, wild type. KO, knockout. Rev, revertant.
See Figure 3.7 for targeted regions and Figures 9.3, 9.4 and 9.5 for targeted sequences.

2.11 Cloning ORFV Virus ORF020 Gene into pAPEX3-Flag

The ORFV ORF020 gene (VACV homologue E3L) was PCR amplified from pVU215 using the forward primer 5'-AAGGCGCGCCTGGCCTGCGAGTGCGCGT containing an *Asc*I restriction site underlined and the reverse primer 5'-AAGGCGCGCCAAGCTGATGCCGCAGTTG containing an *Asc*I restriction site underlined. The ORF020 PCR amplified product was purified and digested with *Asc*I restriction enzyme. The ORF020 gene was cloned into the vector pAPEX3-flag at the *Asc*I restriction site and ORF020 gene correct orientation was confirmed by restriction analysis. The flag tag sequence was just before stop codon and kozak sequence was just before the first start codon. The cloned ORF020 was sequenced and confirmed there were no PCR errors.

2.12 Transient Expression of Proteins from Plasmids

The plasmids were prepared at large scale. The plasmids were transfected into the cells using Lipofectamine 2000 (Invitrogen) according to the manufacturer's instructions. After 24 hours post transfection, the cells were lysed in lysis buffer and protein expression was detected by western blotting using anti-flag antibody. The transfected cells were used for IFN-β signalling assays.

2.13 Generation of Cell Lines

Tissue culture flasks (75 cm^2) were seeded with cells of 20% confluency in 15 ml of complete medium and incubated overnight at 37 °C. Fifteen micrograms of each plasmid expressing OV-NZ2 ORF116, OV-NZ2 ORF020 or human RIG-I and 60 µl of Lipofectamine 2000 (Invitrogen) were pipetted into tubes of 1500 µl of OPTI-MEM separately then incubated at room temperature for 5 min. The contents were combined and incubated for 20 min at room temperature. The cells were washed twice with PBS and 5 ml of medium added with no FCS or antibiotics. The lipid:DNA mix was added to the cells according to the manufacturer's instructions and cells incubated for 1 hour at 37 °C with 5% CO_2. Then, 7 ml of complete medium was added. The cells were incubated for two days at 37 °C with 5% CO_2. Stable transfection cells expressing ORF116 and ORF020 proteins were selected using Hygromycin B (Sigma-Aldrich) at 0.1 mg/ml concentration, whereas cells expressing RIG-I were selected using geneticin (G418) (Gibco) at

1 mg/ml. Cells co-expressing RIG-I/ORF116 and RIG-I/ORF020 were selected by both antibiotics hygromycin B and geneticin at concentrations of 1 mg/ml and 0.1 mg/ml respectively. Stable transfection was maintained in selection medium until a stable cell line was obtained. After the cell line was generated, cell lysates were prepared using lysis buffer (1% Nonidot P-40 (NP-40), 150 mM NaCl, 50 mM Tris-HCl pH 8, 2mM PMSF, 1 mM Na_3VO_4, 10 mM NaF, 1 tablet proteinase inhibitor / 10 ml).

2.14 Poly(dA:dT) or Poly(I:C) Cell Stimulation

LyoVec was used as a transfection reagent as this drives the delivery of nucleic acids into the cytosol. The sterile lyophilized reagent was reconstituted with sterile Milli-Q H_2O according to the manufacturer's instructions. Sterile lyophilized poly(dA:dT) was resuspended with sterile endotoxin-free physiological H_2O provided at a concentration 1 µg/µl then aliquoted and stored at -20 °C. Sterile lyophilized Poly(I:C) was resuspended in 5 ml of sterile Milli-Q H_2O making a concentration of 1µg/µl, then aliquoted and stored at -20 °C. RNA Polymerase III inhibitor (powder) was dissolved in DMSO. Reagent details are shown in Table 9.1.

Sufficient LyoVec-nucleic acid complex was prepared for culture format and cell transfection was conducted according to the manufacturer's instructions. Following cell seeding and overnight culture, the cells were washed with PBS and fresh complete medium was added. The cells were stimulated with either poly(dA:dT) or poly(I:C) at the indicated concentration and incubated until the harvesting time indicated. For nucleic acid stimulation assays involving virus infection, the viral inoculum with appropriate MOI was prepared and cells were washed twice with PBS. Viral inoculum was added to the cells and incubated for 1 hour adsorption at 37 °C with tilting every 15 min. After 1 h of adsorption, fresh complete medium was added. It is important to note that infection follows poly(dA:dT) stimulation whereas this is vice versa for poly(I:C) stimulation unless otherwise indicated. For stimulation assays involving treatment with the RNA Polymerase III inhibitor (ML60218), cells were pre-treated with the appropriate concentration of ML60218 for 2 hours and the drug was maintained across the duration of the assay. The cells were incubated at 37 °C until harvesting time. The cells were harvested by detaching them by pipetting up and down (HEK293 cells) or by trypsinization (other cell types),

then transferred into a 2-ml tube. The cell pellets were centrifuged at 1200 rpm for 5 min at 4 ℃ then the supernatant removed and total RNA extraction from cell pellets carried out.

2.15 Total RNA Isolation and cDNA Synthesis

Total RNA was extracted from cell lysates using a Total RNA Mini Kit (Geneaid) according to the manufacturer's instructions. The quality and quantity of total RNA was evaluated with UV spectroscopy. One hundred nanogram of RNA sample was subjected to DNase I off-column treatment using PerfeCta DNase I (Quanta Biosciences) according to the manufacturer's instructions to degrade genomic DNA. The reaction was set up as follow: 16 µl of RNA, 2 µl of 10X reaction buffer and 2 µl of DNase I. The reaction was incubated at 37 °C for 30 min then 2 µl of 10X stop buffer was added and incubated at 65 °C for 10 min. The successful removal of DNA was confirmed by comparing with negative control reaction in which RNA sample has no reverse transcriptase. Then RNA samples were reversed transcribed into cDNA using SuperScript IV VILO Master Mix (Invitrogen) according to the manufacturer's instructions. The reaction was set up as follows: 11 µl of digested RNA sample, 4 µl of RT mix and made up to 20 µl with RNase-free water. The reaction was started with 25 °C for 10 min then cDNA synthesized at 50 °C for 10 min. The transcription was terminated at 85 °C for 5 min then cooled at 4 °C. cDNA was diluted 1:5 in Milli-Q H_2O.

2.16 Quantitative Real Time-PCR (qRT-PCR) and Data Analysis

Gene specific primers were designed by using qPrimerDepot and were produced by Invitrogen. Their sequences are shown in Table 2.4. Their target specificity was confirmed using NCBI Primer-BLAST. Their amplification specificity also was validated by melting curve analysis and agarose gel electrophoresis of PCR products. Their concentration and amplification efficiency was determined as well.

qRT-PCR was performed using PerfeCta SYBR Green FastMix, Low ROX (Quanta Biosciences) as a dye-based detection method and ABI QuantStudio 6 Flex Real Time PCR System. The reaction was set up in a 10 µl final volume at least in duplicate as follow: 5 µl of SYBR Mix, 0.1 µl of forward primer (200 nM), 0.1 µl of reverse primers (200 nM), 2 µl of cDNA and 2.8 µl of RNase-free water. A no template control was included in each assay. The plate was placed in the

thermal cycler and cycling conditions were, initial 95 °C for 2 min for one cycle, followed by 40 cycles of denaturation at 95 °C for 15 sec and annealing and extension at 60 °C for 30 sec. A melting curve was constructed at the end of the assay. The expression level of glyceraldehyde 3-phosphate dehydrogenase (GAPDH) was determined in each individual sample as a reference gene.

qRT-PCR Data analysis was conducted in which Ct values of gene of interest mRNA were normalized to the Ct value of GAPDH mRNA producing ΔCt values, then relating those normalized values to control producing ΔΔCt values. Stability of GAPDH expression was confirmed by assessing its Ct values across the time points, untreated and treated samples, and assure the Ct values are consistent. The expression fold was calculated by applying the formula $2^{-\Delta\Delta Ct}$ (Pfaffl, M. W., 2001). To obtain relative expression levels for comparison, the values of treated or infected samples were related to the values of untreated or uninfected samples respectively after considering the values of untreated or uninfected samples as 1.

2.17 Transcription of ORFV ORF116 Gene

HeLa cells were seeded at $4x10^5$ cells in a 6-well plate and incubated overnight at 37 °C. The cells were pre-treated with cyclohexamide (100 µg/ml), then the cells washed with PBS and mock infected or infected with virus at a multiplicity of infection 10. After 1 hour of adsorption, 2 ml of medium, 2% FCS was added to the cells and incubated until harvesting in the presence or absence of cyclohexamide (100 µg / ml). The cells were harvested by trypsinization and total RNA extracted. cDNA was synthesized and conventional PCR was conducted using 2 µl of cDNA and the following primers: ORF116 F 5'-ATGAGTAGTTCAAGTAGCGAGACC and ORF116 R 5'- GGAGGTGCTGGTACCAGTGGTAGTTTCAGT. The PCR product was visualized under UV light.

Table 2.4. Gene specific primers for qRT-PCR.

Gene	GenBank Accession Number	Sequence
IFN-β	NM_002176.4	F 5-'CCTGAAGGCCAAGGAGTACA R 5'-AAGCAATTGTCCAGTCCCAG
RIG-I	NM_014314	F 5'-GGCCCTTGTTGTTTTTCTCA R 5'-GAAGACCCTGGACCCTACCT
ISG56 (IFIT1)	NM_001270927.2	F 5'-GCCCTATCTGGTGATGCAGT R 5'-GCAGCCAAGTTTTACCGAAG
ISG54 (IFIT2)	NM_001547.5	F 5'-CAAGTTCCAGGTGAAATGGC R 5'-CGAACAGCTGAGAATTGCAC
ISG20	NM_001303233.2	F 5'-GCTTGCCTTTCAGGAGCTG R 5'-ATCACCGATTACAGAACCCG
IFI44	NM_006417.5	F 5'-TACCAGTTTAATCCCATGGAATCA R 5'-CAAATACAAATGCCACACAATGAA
OAS1	NM_001032409.3	F 5'- GAGACCCAAAGGGTTGGAGG R 5'- GTGTGCTGGGTCAGCAGAAT
OASL	NM_003733.3	F 5'-AAACAGCTCAGAAACGCCAC R 5'-CGGGTGCTGAAGGTAGTCAA
MDA5 (IFIH1)	NM_022168.4	F 5'-AGCTGACACTTCCTTCTGCC R 5'-GGGGCATGGAGAATAACTCA
IFI16	NM_001206567.2	F 5'-CATGAACGGTCCTGGAAAAT R 5'-TCCAGCAGTTTCTTCACCAA
DDX60	NM_017631.6	F 5'-AAGGTGTTCCTTGATGATCTCC R 5'-TGACAATGGGAGTTGATATTCC
GAPDH	NM_002046.7	F 5'-CTCTGCTGATGCCCCCATGTTC R 5'-GGTGGTGCAGGAGGCATTGCTG
IL-8	NM_000584.4	F 5'-AAATTTGGGGTGGAAAGGTT R 5'-TCCTGATTTCTGCAGCTCTGT
IL-6	NM_000600.5	F 5'-GTCAGGGGTGGTTATTGCAT R 5'-AGTGAGGAACAAGCCAGAGC
STING	NM_198282.4	F 5'-GAGCAGGCCAAACTCTTCTG R 5'-TGCCCACAGTAACCTCTTCC

2.18 Quantification of Cytokine IL-1β Secretion

Human IL-1β in supernatants was quantified by ELISA using Human IL-1β OptEIA ELISA Set II (BD, Biosciences). An ELISA microwell plate (Nunc) was coated at 50 µl per well with capture antibody and incubated overnight at 4 °C. Unbound capture antibody was removed by washing 3X in wash buffer (PBS+0.05% Tween-20). The wells were blocked with 200 µl per well with assay diluent (PBS+10% FCS) and incubated for 1 hour at room temperature. The plate was washed 3X with wash buffer and 50 µl of cell-free supernatant were added to each well and 50 µl of serial dilution of standard human IL-1β to produce a standard curve. Then the assay was incubated for 2 hours at room temperature. The plate was washed 5X with wash buffer and 50 µl per well of detection antibody then incubated for 1 hour at room temperature. The plate was washed 5X and 50 µl per well of enzyme reagent (Streptavidin-horseradish peroxidase conjugate) diluted 1:250 in assay diluent was added then incubated for 30 min at room temperature. The plate was washed 7X with wash buffer and 100 µl of TMB substrate added then incubated for 10 min in the dark at room temperature. The reaction was stopped by adding 50 µl per well of 2N H_2SO_4. The assay was then read with an ELISA microplate spectrophotometer at an absorbance of 450 nm then the IL-1β concentration was calculated based upon a standard curve.

2.19 Bioinformatic Analysis

DNA and amino acid sequences were obtained from the database of GenBank of the National Center for Biotechnology Information. The FASTA files of nucleotide sequences were imported into EditSeq, then all sequences were aligned with MegAlign (Lasergene 10).

2.20 Statistical Analysis

Each experiment was performed at least three times in replicate, unless otherwise stated. Quantitative data were visualized and analyzed using GraphPad Prism software ver.7.0e. Statistical analysis was performed by student's *t* test for pairwise comparisons or by two-way ANOVA when comparing more than two sets of values. Statistically significant differences are indicated in figure legends. The *P* value in assays of IFN-β mRNA relative expression was calculated after converting the values of untreated or uninfected samples to 1 and then relate the values of treated or infected samples to them for comparison in a way similar to studies conducted

previously (Brass, A. L. *et al.*, 2009; Mounce, B. C. *et al.*, 2013; Nagesh, P. T. *et al.*, 2016; Wang, S. *et al.*, 2014; Zupkovitz, G. *et al.*, 2006).

RESULTS I

3 RESULTS I: OV-NZ2 ORF116 Modulation of the Interferon Response

3.1 Immunomodulatory Genes discovered in Parapoxviruses

Poxviruses replicate in the cytoplasm of infected cells and during infection derivatives from the virus, mainly viral nucleic acids trigger host innate immunity upon detection. However, viruses have evolved strategies to counteract host detection inhibiting signalling molecules leading to the innate immune response (Bowie, A. G. *et al.*, 2008). Genes located within the termini are mostly nonessential and encode factors involved in host range, virulence and immune evasion. Table 3.1 shows examples of these proteins encoded by ORFV and VACV.

The identification of those immunomodulators was initially determined by analyzing their sequence similarity with host immune effectors. For example, the soluble viral receptors have homology to cellular IFN and interleukin receptors (Alcami, A. *et al.*, 1992; Alcamí, A. *et al.*, 1995; Alcamí, A. *et al.*, 2000; Colamonici, O. R. *et al.*, 1995; Symons, J. A. *et al.*, 1995). In other cases, the identification of such proteins was found based on ligand-binding characteristics such as the viral chemokine inhibitor that interacts with β chemokines although this inhibitor has no homologue with cellular chemokine receptors (Smith, C. A. *et al.*, 1997). In addition, structural analysis of viral factors was done to identify the structural similarity of these immunomodulators to host effectors. For example, apoptosis is regulated by Bcl-2 family proteins. Structural comparison analysis has revealed that poxviruses encode a number of α-helical proteins that adopt a Bcl-2 fold despite lacking sequence similarities to apoptosis-regulated cellular proteins (Franklin, E. *et al.*, 2013). The gene ORF125 of OV-NZ2 has the characteristic BH domain residues and Bcl-2-like fold structure, so it was predicted that this viral protein could act as an anti-apoptotic factor (Westphal, D. *et al.*, 2009).

Genomic analysis of the OV-NZ2 genome has shown that its double stranded DNA consists of a cluster of genes located in the variable terminal regions at both termini and it is widely believed that these genes are nonessential and involved in host cell manipulation. OV-NZ2 ORF116 is one of the genes located within these clusters. It contains an A/T rich sequence resembling an early promoter upstream from the coding sequence and has no transcription stop sequence T_5NT downstream from the translation stop codon. The predicted peptide has been shown to lack a

secretary signal peptide indicating that the gene most likely functions intracellularly and possibly targeting signalling pathways involved in the host response.

The functional analysis of OV-NZ2 ORF116 gene has been investigated previously (AlDaif, Master Thesis, University of Otago). The transcriptome of HeLa cells infected with OV-NZ2 wild type or OV-NZ2Δ116 has been analysed using microarray. The microarray data revealed a major effect on the expression pattern of a number of cellular genes by ORFV infection. Analysis of differential gene expression found that the expression level of a number of ISGs had been up-regulated in knockout virus infected cells to higher levels than in wild type infected cells. This observation may suggest that ORF116 is likely to be involved in modulating the antiviral effectors of the type I IFN response and targeting a number of cellular ISGs by blocking the production of type I IFN from infected cells or blocking the expression of ISGs.

The main objective of this chapter was to further validate the function of the gene ORF116 of OV-NZ2. A revertant-116 virus was constructed in which ORF116 gene was re-inserted at the deleted gene locus in the knockout-116 virus. Then the level of cellular ISG expression was examined in HeLa cells infected with revertant-116 and compared to cells infected with wild type and knockout-116 viruses. It is essential to re-insert the deleted gene to show that the phenotype of wild type can be restored. This will provide strong evidence that the observation in knockout mutant-infected cells was real and not an artefact of genetic modification of virus. It will also provide a strong basis for the role of the gene in question.

Table 3.1. Virus proteins interfering with cell signalling involved in innate immunity.

A. Orf virus proteins

Protein	References
ORF002	(Diel, D. G. *et al.*, 2011a)
	(Chen, D. *et al.*, 2016)
ORF024	(Diel, D. G. *et al.*, 2010)
ORF119	(Li, W. *et al.*, 2018)
	(Nagendraprabhu, P. *et al.*, 2017)
ORF121	(Diel, D. G. *et al.*, 2011b)
ORF073	(Khatiwada, S. *et al.*, 2017)
ORF020	(McInnes, C. J. *et al.*, 1998)

B. Vaccinia virus proteins [a]

Protein	References
N1	(Cooray, S. *et al.*, 2007)
	(DiPerna, G. *et al.*, 2004)
A46	(Bowie, A. *et al.*, 2000)
	(Stack, J. *et al.*, 2005)
A52	(Bowie, A. *et al.*, 2000)
	(Harte, M. T. *et al.*, 2003)
B14	(Chen, R. A. J. *et al.*, 2008)
	(Graham, S. C. *et al.*, 2008)
K7	(Schröder, M. *et al.*, 2008)
M2	(Gedey, R. *et al.*, 2006)
K1	(Shisler, J. L. *et al.*, 2004)
E3	(Valentine, R. *et al.*, 2010)
C4	(Ember, S. W. J. *et al.*, 2012)
A49	(Mansur, D. S. *et al.*, 2013)
A46	(Stack, J. *et al.*, 2005)
K7	(Schröder, M. *et al.*, 2008)
C6	(Unterholzner, L. *et al.*, 2011)
N2	(Ferguson, B. J. *et al.*, 2013)
C16	(Peters, N. E. *et al.*, 2013)
C4	(Scutts, S. R. *et al.*, 2018)

[a] Modified from (Perdiguero B, E. M., 2009; Randall, R. E. *et al.*, 2008)

3.2 Bioinformatic Analysis of ORF116

The *ORF116* gene of OV-NZ2 is located within the right terminus of the variable region of the virus genome between nucleotides 115865 and 116557 within the *Hin*dIII-H fragment (Mercer, A. A. *et al.*, 2006). It is a unique gene of 696 nucleotides encoding a predicted protein of 231 aa with a predicted molecular weight 24.27 kDa. Attempts were made to predict the two- or three-dimensional structure of OV-NZ2 ORF116 protein, but due to there being no homologues of OV-NZ2 ORF116, no structure could be predicted. An NCBI search for potential conserved domains was conducted to provide any suggestion of a putative function for OV-NZ2 ORF116 protein. From the search, no potential domains were identified, except a domain in DNA polymerase III subunits gamma and tau that showed resemblance with the OV-NZ2 ORF116 C-terminus (Appendix: Figure 9.1). The analysis of the amino acid sequence of OV-NZ2 ORF116 has shown no secretary signal peptide sequence which may suggest that this protein acts intracellularly. In addition, short sequences of amino acids were identified that have basic positively charged lysine (Lys, K) and arginine (Arg, R) amino acids following hydrophobic sequence of proline (Pro, P), isoleucine (Ile, I), alanine (Ala, A) and methionine (Met, M) at the N-terminus as indicated in Figure 3.2. This pattern of amino acid sequence is an indication of a classic signal peptide for protein localization to the mitochondria or nucleus.

OV-NZ2 ORF116 has no homologues outside the parapoxvirus genus. BLAST results have shown homologues at the nucleotide level only within ORFV species whereas at the amino acid level it is also weakly conserved with Pseudocowpox virus (PCPV) species. The nucleotide and amino acid sequence of OV-NZ2 ORF116 were aligned with other OV strains using the Clustal W alignment method as indicated in Figures 3.1 and 3.2. From the alignment analysis, OV-NZ2 ORF116 shows identity with ORF116 of OV-IA82, OV-D1701, OV-SY17, OV-B029, OV-HN3/12 and OV-NA1/11 at the nucleotide level from 92.5 % to 96.1 % and at the amino acid level from 78.0 % to 94.3 %, whereas ORF116 of OV-SA00, OV-NA17, OV-SJ1, OV-YX and OV-GO shows less identity at the nucleotide level from 65.0 % to 68.7 % and at the amino acid level from 52.4 % to 55.2 %.

The *ORF116* genes varies in size ranging from 585 to 717 nucleotides and all genes are transcribed toward the right terminus. The genes encode proteins of 194 to 238 amino acids with

predicted molecular weights of 21.6 to 26.5 kDa. Residues within the N-terminus are more strongly conserved than the C-terminus.

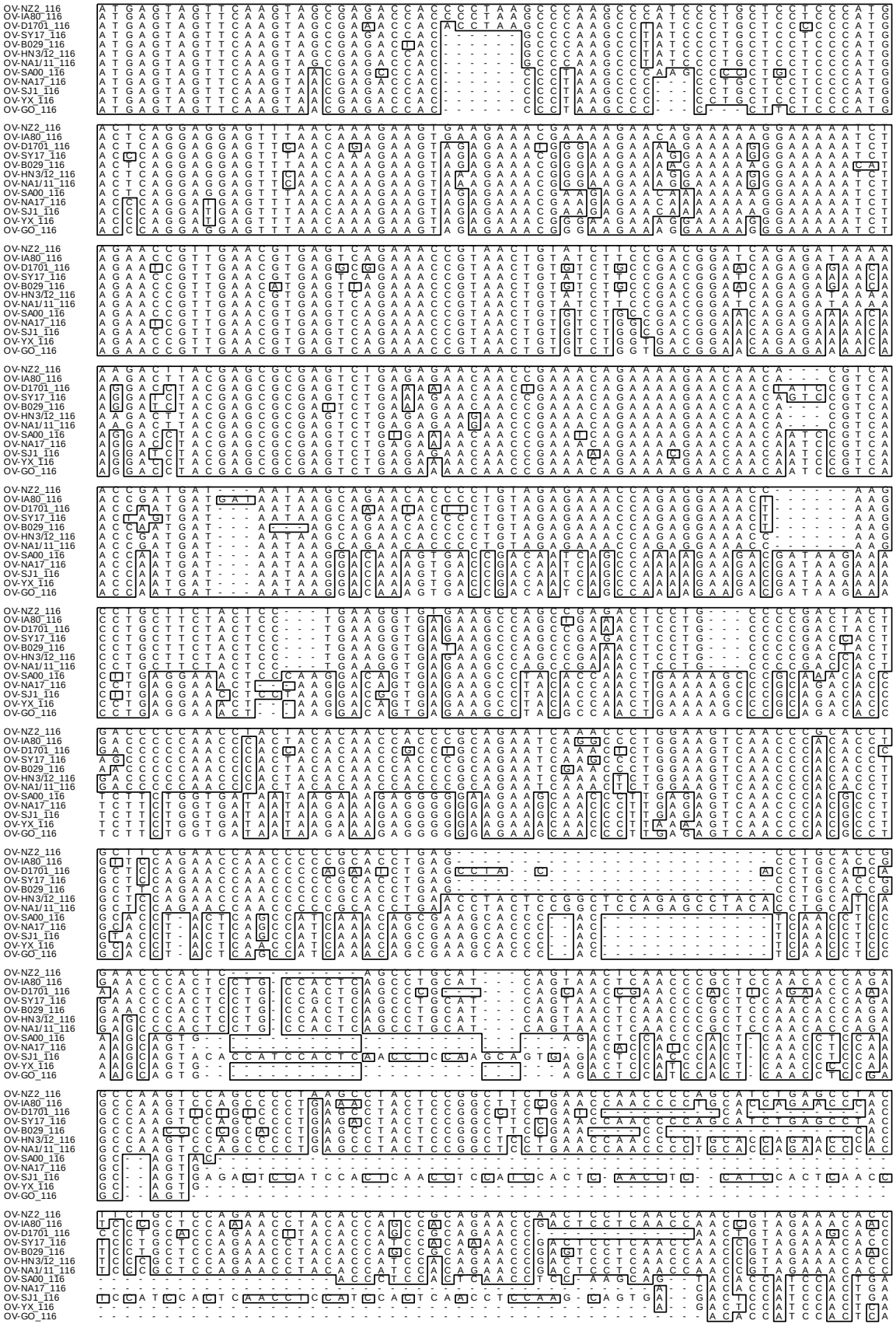

Continued next page

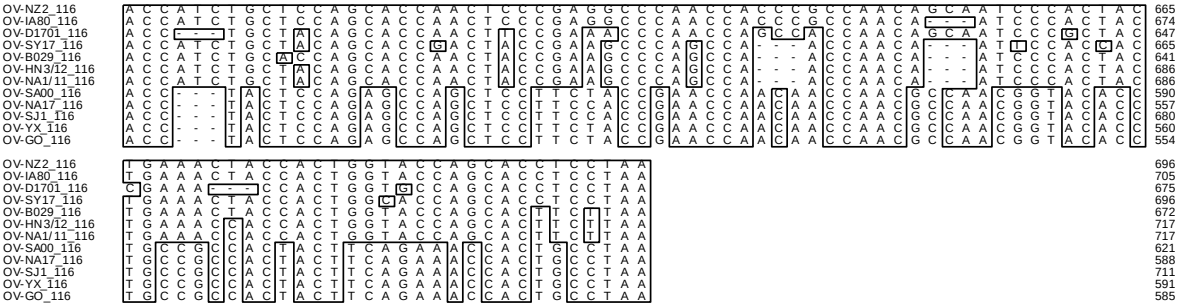

Figure 3.1. Clustal W alignment of ORFV ORF116 nucleotide sequences. Nucleotide sequence of OV-NZ2 ORF116 is aligned with ORF116 of ORFV strains: OV-IA82, OV-D1701, OV-SY17, OV-B029, OV-OV-HN3/12, OV-NA1/11, OV-SA00, OV-NA17, OV-SJ1, OV-YX, OV-GO. See Appendix: Table 9.2 for accession numbers. Nucleotides identical to those of OV-NZ2 ORF116 are boxed. Numbers on the right indicate nucleotide positions.

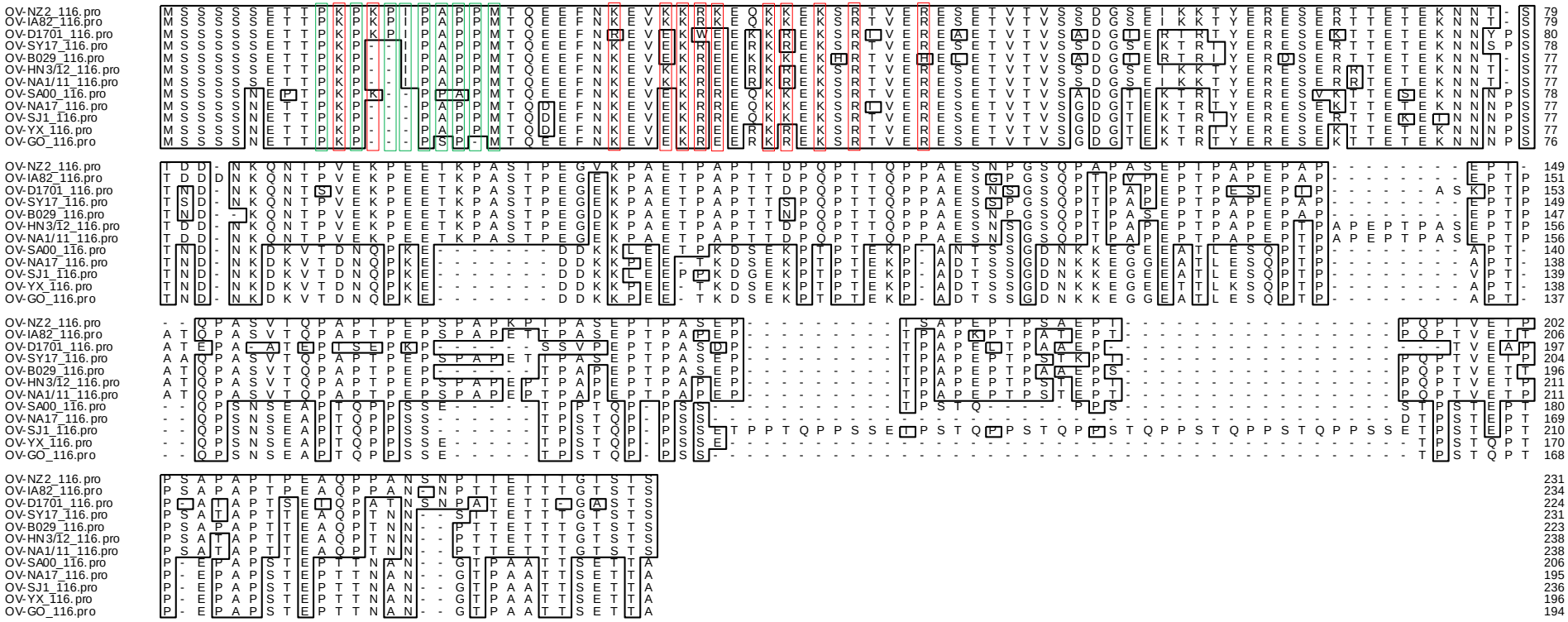

Figure 3.2. Clustal W alignment of ORFV ORF116 amino acid sequences. Amino acid sequence of OV-NZ2 ORF116 is aligned with ORF116 of ORFV strains: OV-IA82, OV-D1701, OV-SY17, OV-B029, OV-OV-HN3/12, OV-NA1/11, OV-SA00, OV-NA17, OV-SJ1, OV-YX, OV-GO. See Appendix: Table 9.2 for accession numbers. Amino acids identical to those of OV-NZ2 ORF116 are boxed. Numbers on the right indicate amino acid positions. The consensus sequences of basic positively charged amino acids are boxed in red. The consensus sequences of hydrophobic amino acids are boxed in green.

3.3 Generation of Revertant 116 virus

3.3.1 Overview

DNA homologous recombination is a naturally occurring event in virus-infected cells (Fenner, F., 1959; Fenner, F. *et al.*, 1958). Homologous recombination is widely used to generate recombinant poxviruses (Moss, B., 1991). It involves designing a transfer vector that has the gene of interest under a poxvirus promoter, flanking regions derived from poxvirus genome and a selection marker. The permissive cells are infected with the virus and transfected with the vector. Homologous recombination will occur between the vector and virus genome which will subsequently incorporate the gene into the virus genome as depicted in Figure 3.3. The resulting recombinant virus is selected and subjected to several rounds of plaque purification.

There are a number of methods for selecting and screening the resultant recombinant virus. The choice of selection method depends on the purpose of generating the recombinant virus. The most widely used method for VACV is utilizing homologous recombination into the thymidine kinase (*tk*) gene of VACV. An insertion of the gene of interest at the locus of the *tk* gene will disrupt the *tk* gene function and provide a means of selecting the recombinant virus with a tk^- phenotype in a tk^- cell line in the presence of 5-bromodeoxyuridine (BrdU) (Byrd, C. M. *et al.*, 2004). Other methods of selection include antibiotic resistance through the use of a suitable antibiotic resistance gene for instance neomycin or hygromycin in which only the resulting recombinant virus will replicate in the presence of the respective antibiotic (Franke, C. A. *et al.*, 1985).

In this study, the *E. coli* ß-galactosidase reporter gene was chosen as a selection marker. The ß-galactosidase gene was incorporated into the transfer vector to facilitate the identification of recombinant virus through the production of blue colour in the presence of X-Gal. OV-NZ2Δ116 virus, previously produced, has been used as a parental virus to generate the OV-NZ2-Rev116 virus. The knockout-116 contains an *E. coli* ß-glucuronidase reporter gene (*gusA*) to identify the virus through the production of blue colour in the presence of X-Gluc.

An OV-NZ2-Rev116 revertant virus was generated in which the ORF116 gene was re-inserted into the OV-NZ2Δ116 knockout at the same original locus of *ORF116* along with the reporter gene *LacZ* under the poxvirus PF1 promoter. Firstly the transfer vector carrying OV-NZ2 ORF116 and the reporter gene was constructed, then the cassette was introduced

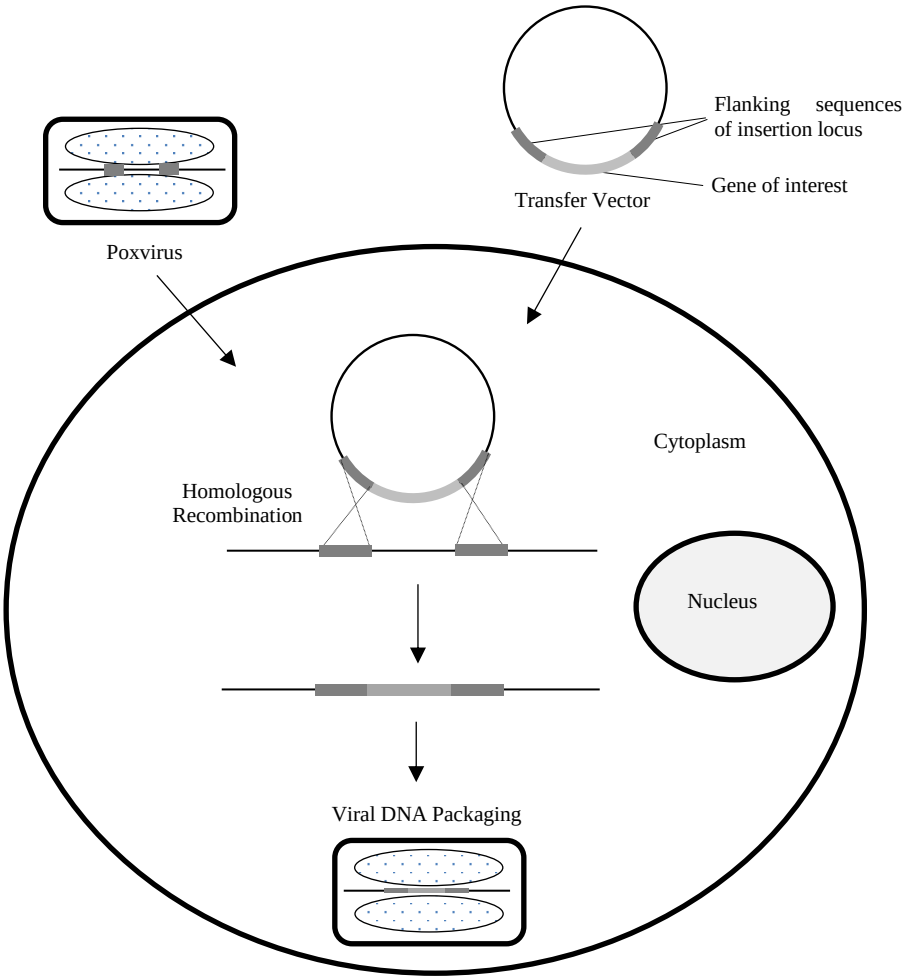

Figure 3.3. Generation of OV-NZ2-Rev116 by homologous recombination. LT cells were seeded at $2x10^6$ cell per 25-cm^2 flask. The cells were infected with OV-NZ2Δ116 at an MOI 0.5 for 2 hrs. Then 3 μg of the plasmid transfer vector containing ORF116 was transfected into the LT cells and incubated overnight. The next day, 4 ml of MEM 2% FCS was added into the flask and incubated for 6 days. The cells were scraped and transferred into 15-ml tube.

into the same locus of OV-NZ2Δ116 virus genome by homologous recombination. The resultant OV-NZ2-Rev116 virus was selected and purified in the presence of X-Gal staining then characterized. Finally, the expression levels of ISGs were investigated in OV-NZ2-, OV-NZ2Δ116- or OV-NZ2-Rev116-infected HeLa cell.

3.3.2 Construction of Transfer Vector Containing ORFV ORF116 and Reporter Gene

The transfer vector plasmid was constructed by genetic manipulation of several plasmids as detailed in materials and methods. A 1.255 kb *Hin*dIII-*Kpn*I subfragment containing the left arm and ORF116 except the last 13 nucleotides at the C-terminus was digested from pOV1-*Eco*RI-D then cloned into pTZ19R vector. This step was followed by incorporation of a linker which introduced *Kpn*I and *Eco*RI restriction sites, the 13 nucleotides not within the restriction fragment, a stop codon and a poxvirus early transcription termination signal T_5NT resulting in a DNA fragment containing the full length sequence of the 116 gene with *Hin*dIII and *Eco*RI restriction sites. This fragment was removed from pTZ19 and cloned into pV32 vector at the same sites. The right arm was PCR amplified and *Eco*RI and *Sac*I sites were introduced then cloned into pV32 at the *Eco*RI and *Sac*I restriction sites. Finally, the *E. coli* β-galactosidase gene (*lacZ*) placed under the control of a strong ORFV late promoter PF1 (Fleming, S. B. *et al.*, 1993) was cloned as a reporter gene into the *Eco*RI site located between the ORF116 gene and the right arm. The schematic representation of the final construct is shown in Figure 3.4 A.

In every step of cloning, restriction analysis was conducted to confirm the presence of a cloned fragment. The final transfer vector was thoroughly characterized in which the vector was subjected to restriction analysis as shown in Figure 3.4 B to confirm the correctness and intactness of all restriction fragments within the construct. The restriction analysis has shown the presence of all fragments. *Hin*dIII/*Kpn*I (left arm and ORF116), *Kpn*I/*Eco*RI (linker), *Eco*RI (*Lac*Z gene) and *Eco*RI/*Sac*I (right arm) digestions have produced fragment sizes of 1.2 kb, 0.03 kb, 3.4 kb and 0.53 kb respectively. Although the linker band 0.03 kb generated from *Kpn*I/*Eco*RI digestion is not visible maybe due to the low amount of DNA, this band was clearly visualized in the early steps of cloning.

Screening for clones carrying the correct orientation of the *LacZ* gene was conducted in order to obtain a construct harbouring *ORF116* and *Lac*Z that transcribed in the same direction. Colony PCR for clones was performed as explained in material and methods and the correct orientation of the *LacZ* gene clone was selected (data not shown). This was further confirmed by performing restriction analysis using either *Nde*I or *Sac*I restriction enzyme. These two enzymes can produce distinguishable bands from a single digestion of the construct. *Nde*I or *Sac*I digestion produced two distinguishable bands in the correct orientation of the *Lac*Z gene that differ from the incorrect one as shown in Figure 3.4 C.

Before the construct was used for generating the recombinant virus, the construct was sequenced using primers indicated in the schematic map of the construct in Figure 3.4 A and the sequencing data has shown the intactness of the construct (data not shown). The *LacZ* gene functionality and capability of producing blue colour in the presence of X-Gal was also tested. From the Figure 3.4 D, it is clear that the *Lac*Z gene was functional and a blue colour was produced in the presence of X-Gal.

3.3.3 Generation of Revertant-116 Virus

Revertant-116 virus was generated from the parental knockout-116 virus as described in materials and methods and has been identified and selected by their blue plaque phenotype in the presence of X-Gal and lack of blue colour in the presence of X-Gluc. The putative revertant-116 was subjected to several rounds of single plaque selection until a pure revertant virus was obtained as shown in the plaque assay in Figure 3.5. This result also confirmed that homologous recombination has replaced the *GUS* gene in the parental virus with the ORF116 and *LacZ* gene cassette at the same locus as the resultant revertant virus was detectable by the X-Gal stain but not by X-Gluc and vice versa with the parental knockout-116 virus. This data confirmed that the revertant-116 virus was obtained.

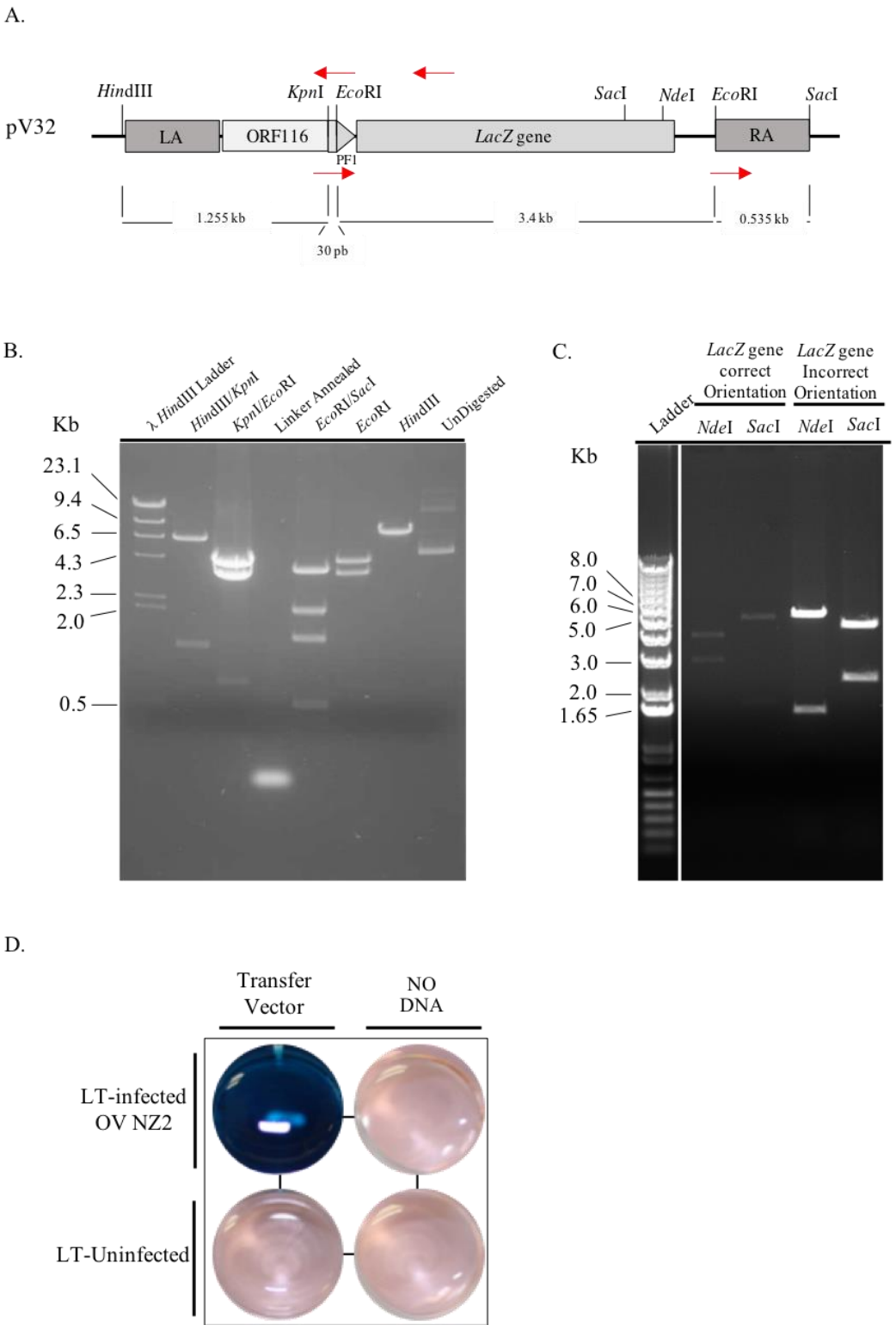

Figure 3.4. Restriction analysis of final construct. (**A**) Diagram showing the final construct used for generating OV-NZ2 ORF116 revertant. Red arrows indicated primers used for construct sequencing. (**B**) and (**C**) The construct was digested with the indicated restriction enzymes and separated by electrophoresis on a 1% agarose gel. A DNA molecular weight marker was run in parallel. The size of DNA fragments are indicated in kb. (**D**) The construct functionality was checked. LT cells were either mock infected or infected with ORFV wild type at an MOI 5 for 2 hrs then transfected with 1µg of construct per well for 48 hrs. The cells were stained with 70 µl of X-gal (20 mg/ml) for 24 hrs.

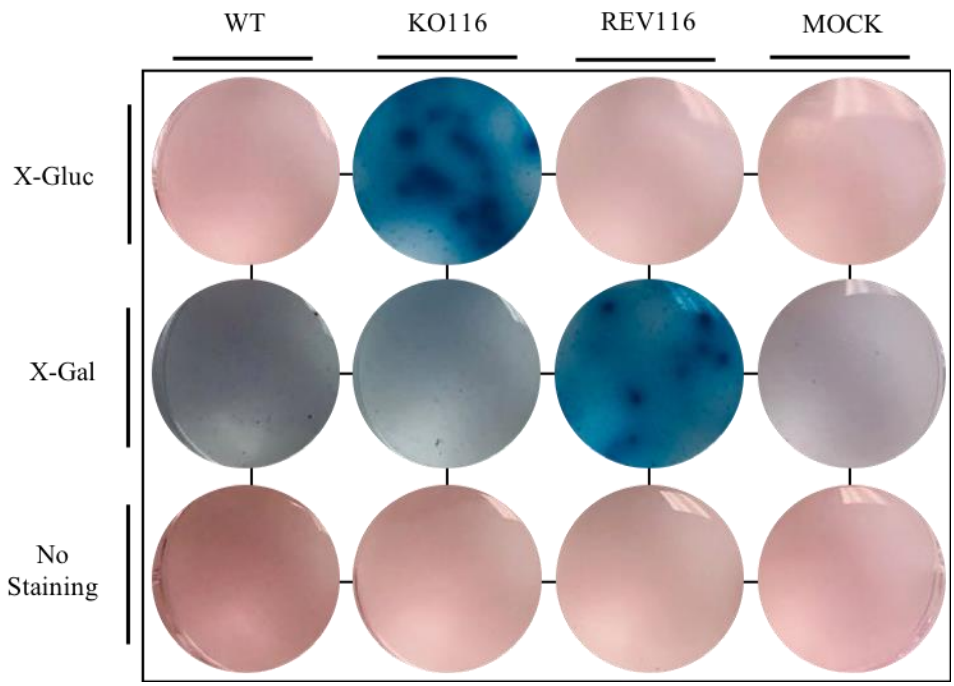

Figure 3.5. OV-NZ2-Rev116 virus selection and purification. The infected and transfected cells were subjected to 3 freeze-thaw cycles and screened for revertant virus plaques in a 6-well plate by staining with X-Gal. After three rounds of single plaque selection, a pure revertant virus was obtained.

3.3.4 Characterization of OV-NZ2-Rev116 virus

Restriction Analysis of Recombinant Viral DNA

Attempts were made to characterize the genomic DNA of OV-NZ2-Rev116 by restriction analysis to ensure no major changes to the genome apart from the targeted region had occurred and also to confirm no duplication or translocation of one genome end to the other had occurred (Fleming, S. B. *et al.*, 1995). *Hin*dIII digestion was used as it produced distinguishable bands. A *Hin*dIII cleavage map of OV-NZ-Rev116 genome is shown in Figure 3.6. *Hin*dIII-H digest was predicted to produce a shift from 4.75 kb in the OV-NZ2Δ116 (Appendix: Figure 9.2) to 6.28 kb in the OV-NZ2-Rev116 in the insertion site as proposed in Figure 3.6. Viral DNA of OV-NZ2-Rev116 including OV-NZ2 wild type and OV-NZ2Δ116 viruses was isolated as described in materials and methods and subjected to *Hin*dIII digestion, then the fragments were resolved on an agarose gel. However, DNA fragments were barely visible on the gel, due to technical difficulties in producing the large

amount of viral DNA required to perform this analysis. Several attempts were made to extract sufficient DNA from the three viruses and subject them to endonuclease digestion.

PCR analysis of Recombinant Viral DNA

PCR analysis of viral DNA was conducted to characterize the OV-NZ2-Rev116 genome along the with OV-NZ2 wild type and OV-NZ2Δ116 genomes. The sequences of *Hin*dIII/*Eco*RI fragments and primer targets for OV-NZ2 wild type, OV-NZ2Δ116 and OV-NZ2-Rev116 are depicted in Appendix: Figures 9.3, 9.4 and 9.5 respectively. PCR amplification of the entire cassette was conducted for the OV-NZ2-Rev116 genome and also for OV-NZ2 wild type and OV-NZ2Δ116 genomes by using one set of primers (1_F and 5_R). This set of primers spans the ORF116 locus and the flanking regions to produce PCR product sizes of 1.57 kb, 3.47 kb and 5.01 kb from the OV-NZ2 wild type, OV-NZ2Δ116 and OV-NZ2-Rev116 respectively (Figure 3.7 A, B and C). PCR amplification showed PCR products from all the viral genome templates and they had migrated at the expected sizes (Figure 3.8 A) despite faint bands obtained from OV-NZ2Δ116 and OV-NZ2-Rev116 genomes. Attempts were made to optimize the PCR reaction using the same set of primers (1_F and 5_R) but none were successful to obtain clearer bands from either viruses templates although this set of primers has shown efficient PCR amplification from plasmids and produced strong bands with the expected size (data not shown). Nevertheless, this result confirmed the insertion of the cassette within the OV-NZ2-Rev116 genome and replacement of the *GUS* gene from the parental virus OV-NZ2Δ116.

Two sets of primers were designed to target two regions of the ORF116 locus where genetic modification took place to the OV-NZ2-Rev116 genome as shown in Figure 3.7 C (See Appendix 9.5 for the targeted nucleotide sequences and sets of primers used). Primer 6_F and 7_R were used to span upstream of the ORF116 gene (left arm region) to the 5'- terminal end of the *LacZ* gene. The PCR amplification produced one product that migrated at the expected size of 0.99 kb (Figure 3.8 B lane 4). Primers 8_F and 5_R were used to target the region from the 3'- terminal end of *Lac*Z gene to the right arm. Similarly, PCR amplification produced only one band that migrated at the expected size of 1.37 kb (Figure 3.8 B lane 6). This further confirmed the correct insertion of the DNA fragments in the ORF116 locus and also confirmed the correct orientation of the *LacZ* gene.

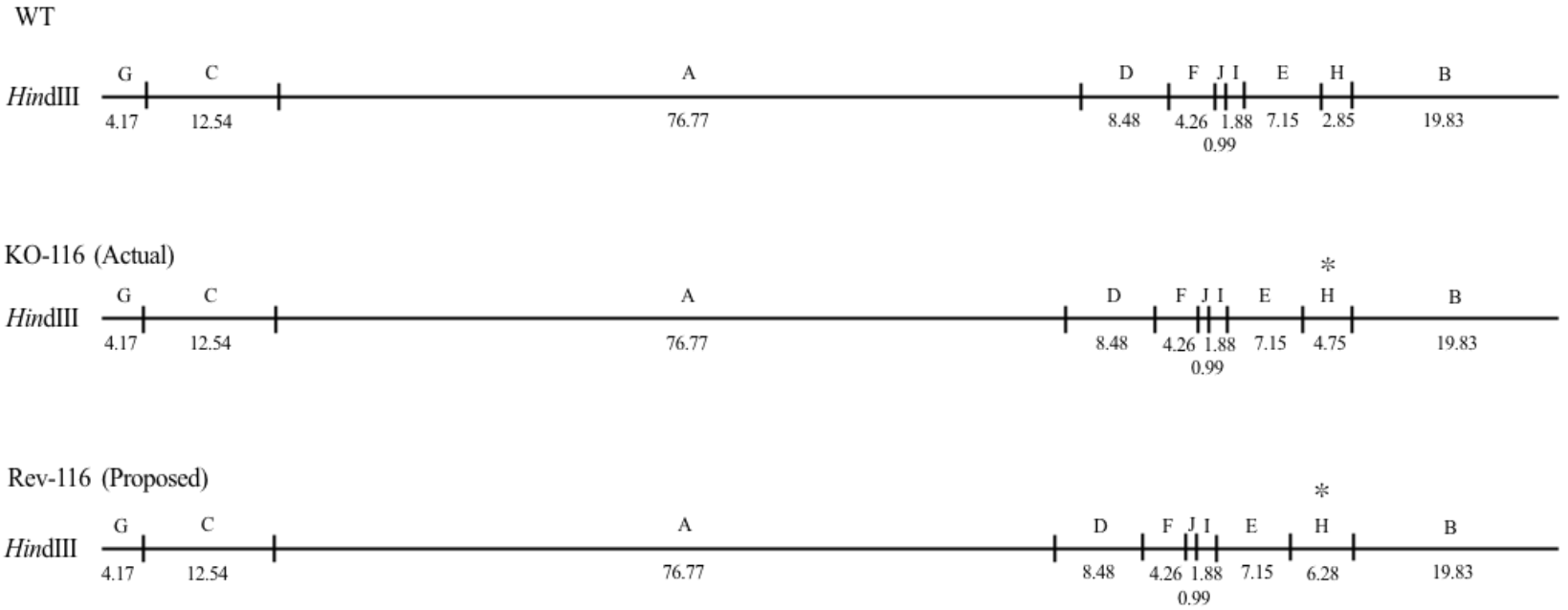

Figure 3.6. Restriction endonuclease maps of OV-NZ2, OV-NZ2Δ116 and OV-NZ2-Rev116 genomes. *Hin*dIII fragments of OV-NZ2 wild type (WT), OV-NZ2Δ116 (KO-116) and OV-NZ2-Rev116 (Rev-116) genomes were calculated using SeqBuilder (DNAStar Inc.). An asterisk indicates the fragment that would have been visualized with different sizes in all three viruses.

It was shown from the plaque assay (Figure 3.5) that the constructed OV-NZ2-Rev116 virus was pure and it was proposed that the homologous recombination during construction of the virus replaced the *GUS* gene in the OV-NZ2Δ116 parental virus with the *ORF116* gene and the *LacZ* gene at the same locus. To further confirm this, a pair of primes 4_F and 3_R was designed that recognizes only the *GUS* gene. PCR amplification of genomic DNA for all viruses using the same set of primers was performed and the PCR amplification produced only one band in the OV-NZ2Δ116 virus (Figure 3.8 B lane 8) but not in the OV-NZ2-Rev116 (Figure 3.8 B lane 9) or OV-NZ2 wild type (Figure 3.8 B lane 7) and that the fragment migrated at the expected size of 0.53 kb. This data confirmed that the OV-NZ2-Rev116 virus is pure and that the insertion has taken place at the correct locus.

PCR analysis of OV-NZ2Δ116 was also included. Two sets of primers (1_F and 3_R) and (4_F and 5_R) were designed to target the locus of ORF116 in the OV-NZ2Δ116 virus where the deletion of ORF116 occurred as indicated in Figure 3.7 B (See Appendix 9.4 for the targeted nucleotide sequences and sets of primers used). Primer 1_F and 3_R were used to span the upstream region of the *ORF116* gene (left arm region) to the 5'- terminal end of the *GUS* gene. PCR amplification produced one product that migrated at the expected size of 1.67 kb (Figure 3.8 B lane 3). Whereas primers 4_F and 5_R were used to target the region from downstream of the 5'- terminal end of the *GUS* gene to the right arm. Similarly the PCR amplification produced only one band that migrated at the expected size of 2.26 kb (Figure 3.8 B lane 5). The genomic DNA from OV-NZ2 wild type virus produced one band of 1.212 kb as predicted from primer 1_F and primer 2_R (Figure 3.8 B lane 2) (See Appendix 9.3 for the targeted nucleotide sequences and set of primers used).

PCR analysis have clearly shown that all the PCR products fit with the predicted sizes and has confirmed the correct insertion of the cassette. In addition, all PCR products were gel purified and sequenced. The sequencing showed the presence and intactness of the gene sequences inserted and correct order.

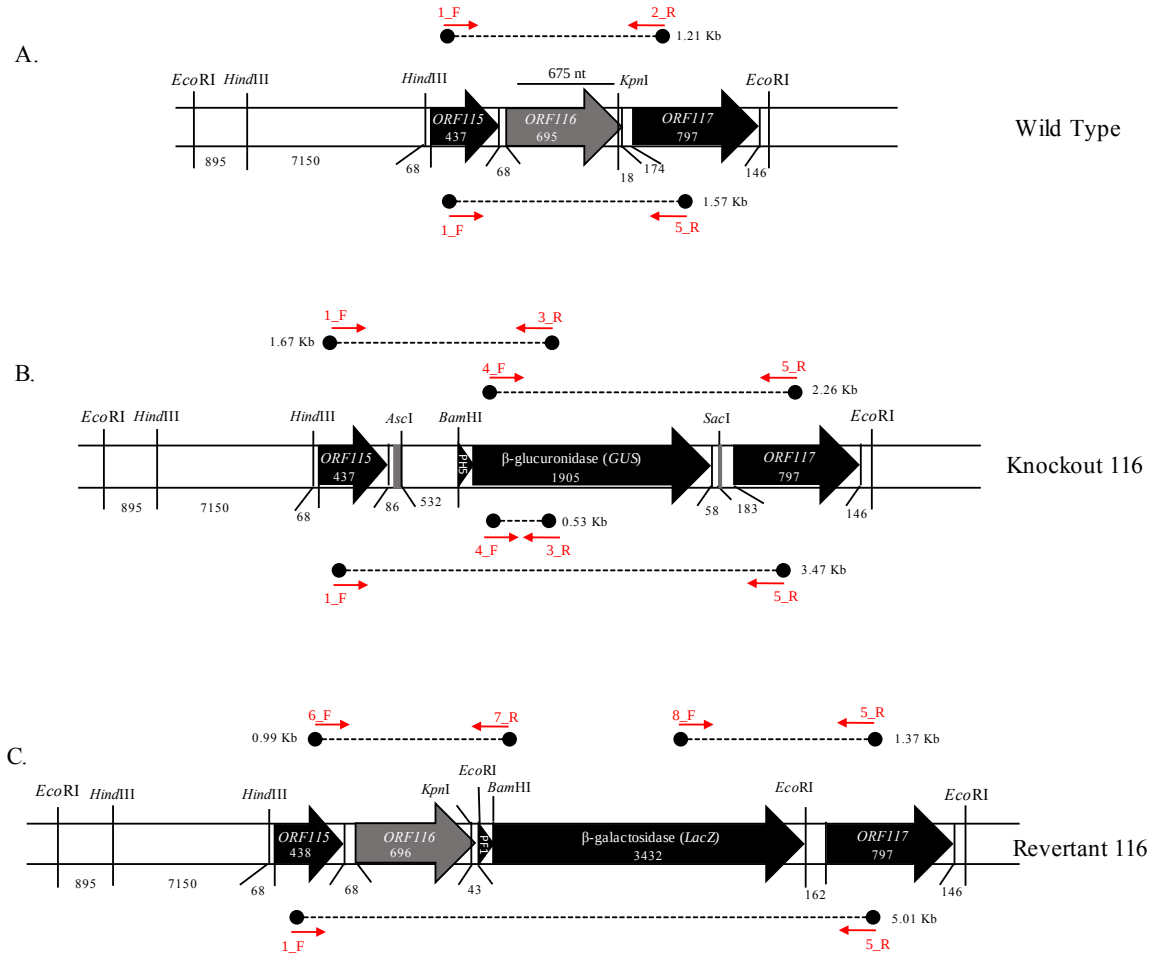

Figure 3.7. Schematic representation of the ORF116 locus within the OV-NZ2, OV-NZ2Δ116 and OV-NZ2-Rev116 genomes. (A) The solid line above ORF116 indicates 675 nt deleted from ORF116 during the construction of the OV-NZ2Δ116 virus and replacement with the *GUS* gene under the control of a vaccinia virus late promoter PH5 as shown in (B). **(B)** A schematic map of the OV-NZ2Δ116 virus. **(C)** OV-NZ2-Rev116 virus was constructed using the OV-NZ2Δ116 virus as a parental virus in which the *GUS* gene was replaced with a cassette containing ORF116 and the *LacZ* gene under the control of an ORFV virus late promoter PF1. Primers sets used in the characterization by PCR are indicated in red numbered arrows (also see Table 2.3). The amplified regions are depicted in dotted lines along with their predicted sizes.

A.

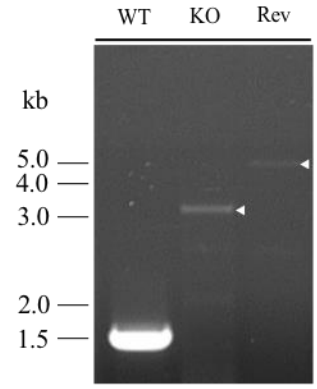

B.

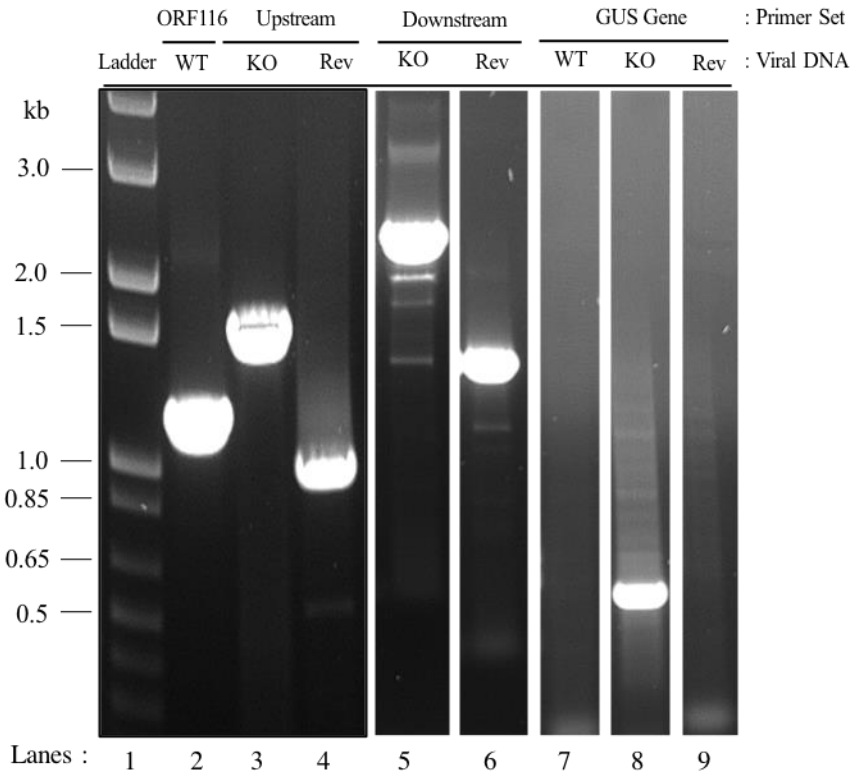

Figure 3.8. PCR analysis of viral DNA of OV-NZ2, OV-NZ2Δ116 and OV-NZ2-Rev116 genomes. Confirmation and characterization of purified OV-NZ2-Rev116 virus was conducted by PCR analysis. The PCR products derived from ORF116 loci of OV-NZ2 wild type, OV-NZ2Δ116 and OV-NZ2-Rev116 templates are shown using one set of primers (1_F and 5_R) targeting the whole loci (see Figure 3.7) (**A**) or different sets of primers targeting upstream or downstream regions as indicated by arrowheads in Figure 3.7, lane 2 (1_F and 2_R), lane 3 (1_F and 3_R), lane 4 (6_F and 7_R), lane 5 (4_F and 5_R), lane 6 (8_F and 5_R), lanes 7, 8 and 9 (4_F and 3_R) (**B**). Lane 1 is the molecular markers shown in kb.

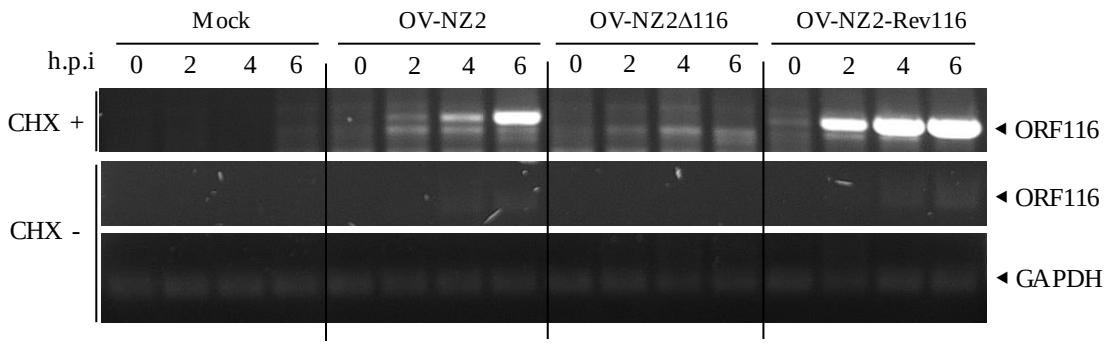

Figure 3.9. Transcription kinetics analysis of the ORF116 gene by RT-PCR. hNDF cells were either mock infected or infected with OV-NZ2 *wt*, OV-NZ2Δ116 or OV-NZ2Rev-116 virus at an MOI of 10 pfu per cell in the presence or absence cycloheximide (100 µg / ml). Total RNA was isolated at 0, 2, 4 and 6 h.p.i. Total RNA was treated with DNase I and purified. Transcriptional analysis of *ORF116* was performed by Reverse Transcription-PCR. Five hundred ng of total RNA was reverse transcribed into cDNA. One µl of cDNA product was PCR amplified, then 10 µl of PCR product was separated by electrophoresis on a 1% agarose gel containing ethidium bromide.

ORF116 is expressed early in OV-NZ2- and OV-NZ2-Rev116-infected cells

The kinetics of ORF116 transcription was investigated using reverse-transcription PCR. The cells were infected with OV-NZ2, OV-NZ2Δ116 or OV-NZ2-Rev116 at an MOI 10 in the presence or absence of cycloheximide (100 ng/ml). Cells were harvested at 0, 2, 4 and 6 h.p.i. Total RNA was isolated and subjected to RT-PCR. ORF116 (0.69 kb) was detected at 2 h.p.i. in the presence of cycloheximide in only OV-NZ2 and OV-NZ2Rev116 infections but not in OV-NZΔ116 infection and the level of expression increased at 4 and 6 hours post-infection as shown in Figure 3.9. Non-specific bands smaller than ORF116 bands were detected in three virus infections. Similarly, the expression of ORF116 in the absence of cycloheximide was detected in OV-NZ2 and OV-NZ2-Rev116 but not in OV-NZ2Δ116, albeit the bands are so faint due to weak staining with ethidium bromide. The RT-PCR data of ORF116 expression level in OV-NZ2 infection is relatively lower than the expression level of ORF116 in OV-NZ2-Rev116 at all time points and that could be due to differences in virus titre. A PCR product corresponding to transcription of the ORF116 gene was not detected in OV-NZ2Δ116 infection indicating the deletion of ORF116 in the OV-NZ2Δ116. This result has shown that ORF116 is intact and expressed at an early stage of OV-NZ2-Rev116 virus replication.

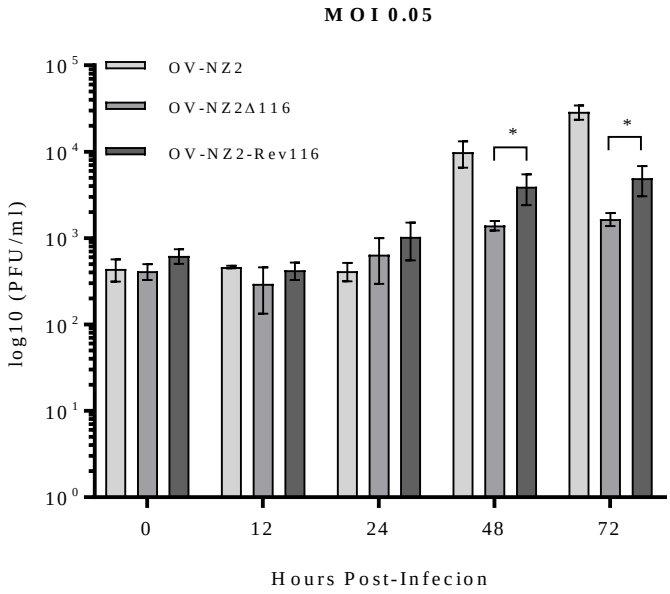

Figure 3.10. Growth analysis of OV-NZ2, OV-NZ2Δ116 and OV-NZ2-Rev116. hNDF cells were infected at an MOI of 0.05 pfu per cell with either OV-NZ2 *wt*, OV-NZ2Δ116 or OV-NZ2-Rev116 viruses. The virus progeny was determined on LT cells. Virus plaques were visualized by staining then counted and virus titres determined. Statistical analysis was performed using a student's *t* test. Data are representative of one experiment of three independent experiments. Error bars represent mean ±SD. Asterisks indicate probability $^{*}P \leq 0.05$ that were calculated from technical triplicates from one experiment.

Viruses Growth analysis

The growth of the OV-NZ2-Rev116 was characterized and compared to OV-NZ2 and OV-NZ2Δ116. The cells were infected with a low MOI 0.05 of virus to characterize the virus over multiple cycles. The cells were harvested at various time points and the virus progeny titrated in LT cells by plaque assay. The exponential phase was seen at 24 hours post-infection and the growth reached a plateau by 72 hours post-infection. OV-NZ2 replicated to higher levels than OV-NZ2-Rev116 and OV-NZ2Δ116. However, re-insertion of the ORF116 into the OV-NZ2Δ116 virus restored the phenotype of wild type replication to that of OV-NZ2 at 48 hours post-infection (Figure 3.10).

3.4 OV-NZ2 ORF116 Gene Modulation of the Type I Interferon Response

Having established that the OV-NZ2-Rev116 restored the growth phenotype of the wild type, the expression levels of ISGs were examined in HeLa cells infected with either OV-NZ2, OV-NZ2Δ116 or OV-NZ2Rev116. The three viruses were sucrose purified to remove any cytokines that might be present in the media.

HeLa cells were infected with either OV-NZ2, OV-NZ2Δ116 or OV-NZ2Rev116 at a MOI 10 for 0, 2, 4 and 6 hours post-infection, then total RNA was isolated from infected cells. Having met the accuracy and precision of the primers, the expression levels of ISGs (IFI44, IFI16, RIG-I, IFIH1, IFIT2, IFIT1, OAS1, OASL, DDX60, IL-6, IL-8, ISG20) were measured by qRT-PCR. The mRNA expression levels of these ISGs were normalized to the mRNA level of *GAPDH* gene then the fold change in mRNA level was calculated relative to the mRNA level of mock-infected cells. *GAPDH* gene expression was shown to remain stable across all time points and virus infections in HeLa cells so it was an ideal internal control in this study. Because fold differences were variable across biological replicates, only one of three biological replicates was presented.

qRT-PCR analysis revealed a change in the mRNA levels of the ISGs that was observed at 6 hours post-infection except for IL-8 and IFI16 at 2 and 4 hours post-infection. The qRT-PCR data of differential ISGs expression showed high expression levels in OV-NZΔ116 infection across all selected genes except DDX60. However, OV-NZ2-Rev116 infection restored the phenotype of the OV-NZ2 in which those ISGs have been altered and down-regulated at 2 and 4 h.p.i. for IL-8 and IFI16 and at 6 hours post-infection for ISG20, OASL, IL-6, IFIH1, RIG-I, IFIT2, IFI44 genes to the level similar to OV-NZ2, except DDX60 (Figure 3.11). The expression levels of ISGs OASL, IL-8, IFIH1, RIG-I, IFIT2 and IFI16 were restored by the revertant virus whereas the ISGs ISG20, IL-6 and IFI44 were partially restored by the virus. With regard to the genes IFIT1 and OAS1, although they have not been altered in HeLa infected with OV-NZ2, their expression levels were altered in HeLa-infected with OV-NZ2-Rev116. All the fold changes in the three viral infections related to mock infection or related to wild type infection from three independent experiments are shown in Table 3.2, 3.3, 3.4, 3.5, 3.6 and 3.7.

These results strongly suggest that ORF116 plays a role in modulating the IFN response and the up-regulation of ISG expression observed in OV-NZ2Δ116 infection was not due to an

unintended mutation introduced during the construction of the mutant virus. The modulation by antiviral effectors was more likely due to blocking the production of type I IFN response from infected cells or blocking the expression of ISGs or both. In the following chapters, an investigation was conducted to examine whether or not ORFV blocks type I IFN production from cells stimulated with either poly(dA:dT) or poly(I:C). Finally, ORF116 gene was examined to determine whether ORF116 blocks type I IFN production.

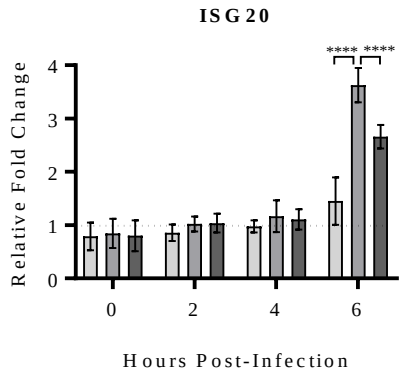

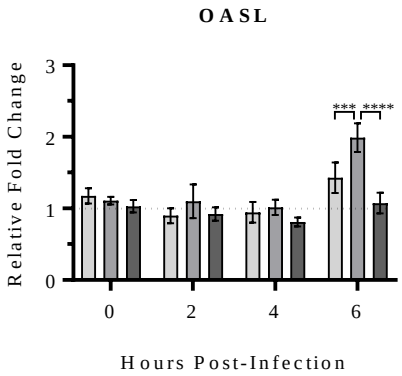

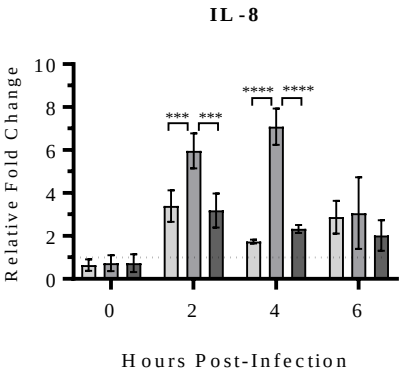

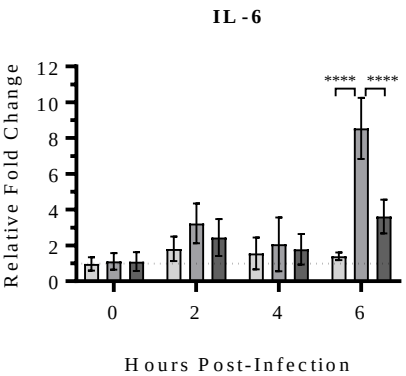

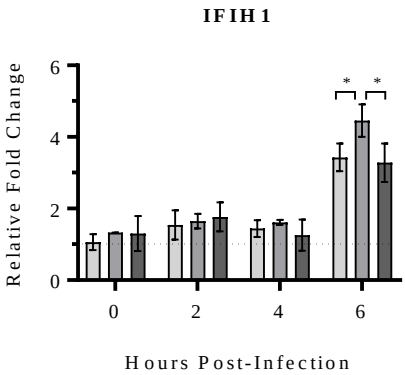

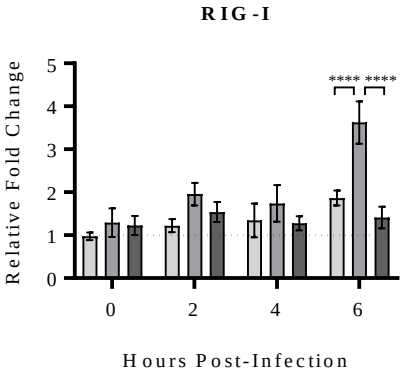

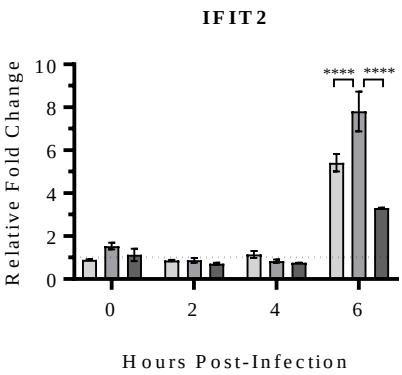

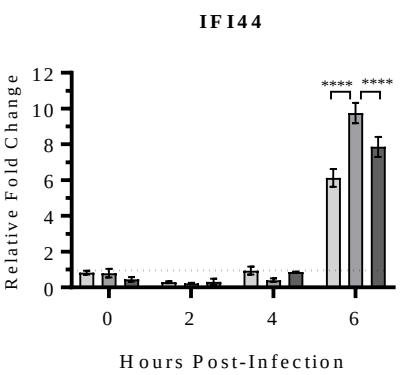

Continued next page

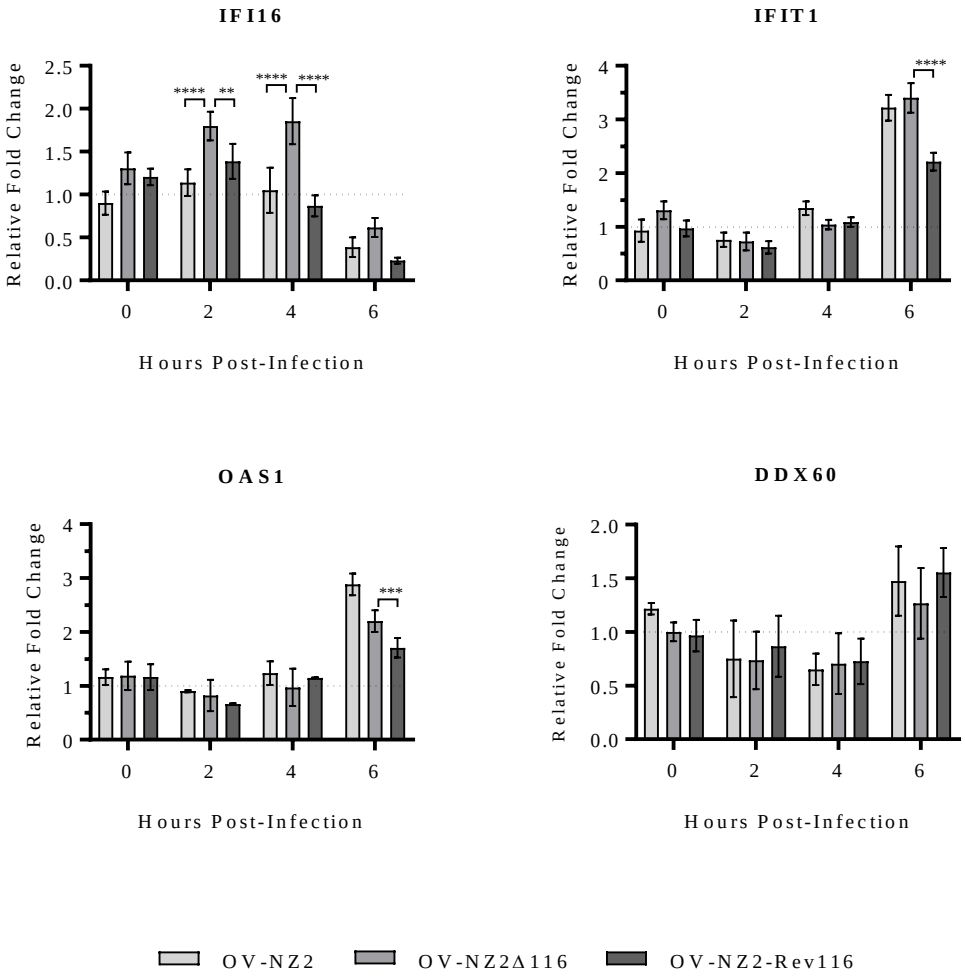

Figure 3.11. Analysis of change in the expression levels of ISGs after infecting HeLa cells with wild type virus OV-NZ2, knockout virus OV-NZ2Δ116 or revertant virus OV-NZ2-Rev116. HeLa cells were mock infected or infected with the indicated virus at an MOI of 10 pfu per cell. Infected cells were harvested at 0, 2, 4 and 6 hours post-infection and total RNA was extracted. qRT-PCR was performed in triplicate of technical replicate to quantify relative expression levels of the indicated genes. Data were normalized against GAPDH and are presented relative to mock-infected cells. Data are representative of experiment one of three independent experiments. Error bars represent mean ±SD. Statistical analysis was performed using two-way ANOVA. Asterisks indicate probability: $^{*}P \leq 0.0332$, $^{**}P \leq 0.0021$, $^{***}P \leq 0.0002$, $^{****}P \leq 0.0001$. *P* value was calculated from qRT-PCR triplicate of technical replicate of experiment one.

Table 3.2. Expression levels of interferon-stimulated genes (ISGs) in HeLa-infected cells from experiment one.

		mRNA expression analyzed by qRT-Real Time-PCR in HeLa cells infected with indicated virus relative to mock infection											
		OV-NZ2				OV-NZ2Δ116				OV-NZ2Rev116			
ISGs	GenBank	0 h.p.i.	2 h.p.i.	4 h.p.i.	6 h.p.i.	0 h.p.i.	2 h.p.i.	4 h.p.i.	6 h.p.i.	0 h.p.i.	2 h.p.i.	4 h.p.i.	6 h.p.i.
IFI44	NM_006417	0.82	0.28	0.94	**6.12**	0.79	0.22	0.40	**9.74**	0.45	0.30	0.85	**7.85**
RIG-I	NM_014314	0.97	1.22	1.34	**1.86**	1.29	1.95	1.74	**3.62**	1.22	1.54	1.27	**1.41**
IFI16	NM_001206567	0.90	**1.13**	**1.05**	0.38	1.30	**1.79**	**1.85**	0.61	1.20	**1.38**	0.86	0.23
IFIH1	NM_022168	1.06	1.53	1.44	**3.42**	1.32	1.64	1.61	**4.45**	1.29	1.76	1.25	**3.28**
IFIT1	NM_001548	0.92	0.75	1.34	**3.22**	1.30	0.72	1.03	**3.40**	0.96	0.61	1.08	**2.21**
IFIT2	NM_001547	0.90	0.87	1.14	**5.42**	1.53	0.87	0.83	**7.80**	1.12	0.71	0.75	**3.31**
OAS1	NM_001032409	1.16	0.90	1.23	**2.88**	1.18	0.82	0.97	**2.20**	1.16	0.66	1.14	**1.70**
OASL	NM_001261825	1.17	0.89	0.94	**1.42**	1.10	1.09	1.01	**1.98**	1.03	0.92	0.81	**1.07**
DDX60	NM_017631	1.21	0.75	0.65	1.47	1.00	0.73	0.70	1.26	0.96	0.86	0.72	1.55
ISG20	NM_002201	0.79	0.85	0.97	**1.45**	0.84	1.02	1.16	**3.62**	0.80	1.03	1.10	**2.65**
IL-8	NM_000584	0.64	**3.39**	**1.73**	2.87	0.73	**5.96**	**7.09**	3.06	0.72	**3.18**	**2.33**	2.02
IL-6	NM_0006000	0.96	1.81	1.55	**1.40**	1.11	3.23	2.06	**8.54**	1.10	2.44	1.78	**3.61**

Differentially expressed genes are indicated in bold.

Table 3.3. Fold change of interferon-stimulated genes (ISGs) determined by qRT-PCR relative to wild type from experiment one.

		Fold Change determined by qRT-PCR in HeLa cells infected with indicated virus relative to wild type virus infection							
		OV-NZ2Δ116				OV-NZ2Rev116			
ISGs	GenBank	0 h.p.i.	2 h.p.i.	4 h.p.i.	6 h.p.i.	0 h.p.i.	2 h.p.i.	4 h.p.i.	6 h.p.i.
IFI44	NM_006417	0.96	0.78	0.42	**1.59**	0.54	1.07	0.90	**1.28**
RIG-I	NM_014314	1.32	1.59	1.29	**1.94**	1.25	1.26	0.94	**0.75**
IFI16	NM_001206567	1.44	1.58	**1.76**	**1.60**	1.33	1.22	**0.81**	**0.60**
IFIH1	NM_022168	1.24	1.07	1.11	**1.30**	1.21	1.15	0.86	**0.95**
IFIT1	NM_001548	1.41	0.96	0.76	1.05	1.04	0.81	0.80	0.68
IFIT2	NM_001547	1.70	1.00	0.72	**1.43**	1.24	0.81	0.65	**0.61**
OAS1	NM_001032409	1.01	0.91	0.78	0.76	1.00	0.73	0.92	0.59
OASL	NM_001261825	0.94	1.22	1.07	**1.39**	0.88	1.03	0.86	**0.75**
DDX60	NM_017631	0.82	0.97	1.07	0.85	0.79	1.14	1.10	1.05
ISG20	NM_002201	1.06	1.20	1.19	**2.49**	1.01	1.21	1.13	**1.82**
IL-8	NM_000584	1.14	1.75	**4.09**	1.06	1.12	0.93	**1.34**	0.70
IL-6	NM_0006000	1.15	1.78	1.32	**6.10**	1.14	1.34	1.14	**2.57**

Differentially expressed genes are indicated in bold.

Table 3.4. Expression levels of interferon-stimulated genes (ISGs) in HeLa-infected cells from experiment two.

		mRNA expression analyzed by qRT-Real Time-PCR in HeLa cells infected with indicated virus relative to mock infection											
		OV-NZ2				OV-NZ2Δ116				OV-NZ2Rev116			
ISGs	GenBank	0 h.p.i.	2 h.p.i.	4 h.p.i.	6 h.p.i.	0 h.p.i.	2 h.p.i.	4 h.p.i.	6 h.p.i.	0 h.p.i.	2 h.p.i.	4 h.p.i.	6 h.p.i.
IFI44	NM_006417	0.91	1.11	1.21	**1.88**	1.21	0.77	0.91	**3.40**	1.16	1.23	0.96	**2.09**
RIG-I	NM_014314	1.61	1.75	1.67	**3.23**	1.71	1.90	1.25	**4.69**	1.68	2.13	1.63	**3.41**
IFI16	NM_001206567	0.95	0.82	0.91	0.62	0.97	0.89	0.92	0.55	1.15	0.94	1.08	0.71
IFIH1	NM_022168	0.51	0.28	0.29	**3.13**	0.38	0.40	0.47	**4.87**	0.53	0.32	0.25	**4.39**
IFIT1	NM_001548	0.56	1.11	1.39	**1.19**	0.52	0.45	0.84	**2.42**	0.45	0.92	0.98	**1.17**
IFIT2	NM_001547	1.25	098	0.71	**3.18**	1.29	0.65	1.42	**6.19**	0.97	0.40	0.90	**2.89**
OAS1	NM_001032409	1.61	1.10	1.50	**1.29**	1.42	1.06	1.39	**1.90**	1.07	1.01	1.06	**1.47**
OASL	NM_001261825	1.20	1.36	0.85	1.08	1.20	1.66	0.99	1.02	1.30	1.48	0.86	1.20
DDX60	NM_017631	1.25	1.02	0.64	1.22	1.04	0.91	0.86	1.05	1.07	1.10	0.79	1.52
ISG20	NM_002201	0.86	1.93	2.08	**2.74**	0.79	2.06	1.67	**3.34**	0.94	2.35	2.14	**2.88**
IL-8	NM_000584	0.83	**3.49**	**12.94**	2.79	0.68	**29.94**	**14.03**	5.66	1.27	**8.63**	**6.83**	4.85
IL-6	NM_0006000	1.76	2.96	3.29	**2.98**	2.06	2.66	3.36	**3.85**	2.05	3.54	3.37	**2.51**

Differentially expressed genes are indicated in bold.

Table 3.5. Fold change of interferon-stimulated genes (ISGs) determined by qRT-PCR relative to wild type from experiment two.

		Fold Change determined by qRT-PCR in HeLa cells infected with indicated virus relative to wild type virus infection							
		OV-NZ2Δ116				OV-NZ2Rev116			
ISGs	GenBank	0 h.p.i.	2 h.p.i.	4 h.p.i.	6 h.p.i.	0 h.p.i.	2 h.p.i.	4 h.p.i.	6 h.p.i.
IFI44	NM_006417	1.32	0.69	0.74	**1.80**	1.27	1.10	0.79	**1.10**
RIG-I	NM_014314	1.06	1.08	0.75	**1.45**	1.04	1.21	0.97	**1.05**
IFI16	NM_001206567	1.01	1.08	1.01	0.87	1.20	1.14	1.18	1.13
IFIH1	NM_022168	0.75	1.41	**1.60**	**1.55**	1.05	1.10	**0.86**	**1.40**
IFIT1	NM_001548	0.92	0.41	0.60	**2.03**	0.80	0.82	0.70	**0.98**
IFIT2	NM_001547	1.03	0.66	1.98	**1.94**	0.77	0.41	1.26	**0.90**
OAS1	NM_001032409	0.88	0.96	0.92	**1.46**	0.66	0.92	0.70	**1.13**
OASL	NM_001261825	1.00	1.22	1.16	0.94	1.08	1.09	1.00	1.11
DDX60	NM_017631	0.83	0.89	1.34	0.86	0.85	1.07	1.24	1.24
ISG20	NM_002201	0.91	1.06	0.80	**1.22**	1.09	1.21	1.03	**1.06**
IL-8	NM_000584	0.82	**8.55**	**1.08**	2.02	1.52	**2.46**	**0.52**	1.73
IL-6	NM_0006000	1.17	0.89	0.71	**1.29**	1.16	1.19	1.02	**0.84**

Differentially expressed genes are indicated in bold.

Table 3.6. Expression levels of interferon-stimulated genes (ISGs) in HeLa-infected cells from experiment three.

		mRNA expression analyzed by qRT-Real Time-PCR in HeLa cells infected with indicated virus relative to mock infection											
		OV-NZ2				OV-NZ2Δ116				OV-NZ2Rev116			
ISGs	GenBank	0 h.p.i.	2 h.p.i.	4 h.p.i.	6 h.p.i.	0 h.p.i.	2 h.p.i.	4 h.p.i.	6 h.p.i.	0 h.p.i.	2 h.p.i.	4 h.p.i.	6 h.p.i.
IFI44	NM_006417	0.80	0.77	0.74	**1.36**	0.77	0.87	0.87	**1.93**	0.79	0.84	0.79	**1.36**
RIG-I	NM_014314	0.85	0.84	1.09	2.06	0.92	0.99	0.86	1.86	0.92	0.99	0.99	1.98
IFI16	NM_001206567	0.85	1.01	0.77	**0.66**	0.67	1.07	0.92	**0.91**	0.77	1.02	0.85	**0.59**
IFIH1	NM_022168	0.86	0.75	0.76	**2.16**	0.87	0.91	0.88	**2.59**	0.89	0.88	0.81	**1.75**
IFIT1	NM_001548	1.04	0.83	0.72	**2.11**	0.97	0.89	0.87	**2.59**	0.98	0.91	0.90	**1.94**
IFIT2	NM_001547	1.01	0.74	0.52	**2.02**	1.02	0.93	0.71	**2.57**	1.03	0.80	0.55	**1.85**
OAS1	NM_001032409	0.53	0.72	0.47	**1.03**	0.81	1.23	1.43	**1.65**	0.72	0.94	1.39	**1.03**
OASL	NM_001261825	1.16	0.84	0.88	**1.09**	1.23	1.05	0.91	**1.64**	1.14	0.85	0.96	**1.12**
DDX60	NM_017631	0.97	0.65	0.95	0.72	0.71	0.62	0.76	0.73	0.68	0.56	0.73	0.73
ISG20	NM_002201	0.52	0.60	0.80	**1.09**	0.56	0.64	0.84	**2.41**	0.67	0.54	0.90	**1.17**
IL-8	NM_000584	0.80	**3.07**	**1.15**	0.80	0.75	**3.83**	**1.48**	0.84	0.70	**3.44**	**1.35**	0.84
IL-6	NM_0006000	1.06	**1.76**	0.99	1.18	1.09	**2.72**	0.99	1.10	1.06	**1.90**	1.06	0.97

Differentially expressed genes are indicated in bold.

Table 3.7. Fold change of interferon-stimulated genes (ISGs) determined by qRT-PCR relative to wild type from experiment three.

		Fold Change determined by qRT-PCR in HeLa cells infected with indicated virus relative to wild type virus infection							
		OV-NZ2Δ116				OV-NZ2Rev116			
ISGs	GenBank	0 h.p.i.	2 h.p.i.	4 h.p.i.	6 h.p.i.	0 h.p.i.	2 h.p.i.	4 h.p.i.	6 h.p.i.
IFI44	NM_006417	0.96	1.12	1.17	**1.42**	0.99	1.07	1.06	**1.00**
RIG-I	NM_014314	1.08	1.17	0.79	0.89	1.08	1.17	0.91	0.95
IFI16	NM_001206567	0.78	1.05	1.20	**1.38**	0.91	1.01	1.10	**0.90**
IFIH1	NM_022168	1.00	1.21	1.16	**1.19**	1.03	1.17	1.06	0.81
IFIT1	NM_001548	0.93	1.06	1.21	**1.22**	0.93	1.09	1.24	0.92
IFIT2	NM_001547	1.01	1.25	1.35	**1.26**	1.02	1.08	1.05	0.91
OAS1	NM_001032409	1.51	1.70	3.01	**1.60**	1.35	1.31	2.94	**1.00**
OASL	NM_001261825	1.06	1.25	1.03	**1.50**	0.98	1.01	1.09	**1.02**
DDX60	NM_017631	0.73	0.94	0.80	1.01	0.70	0.85	0.77	1.01
ISG20	NM_002201	1.06	1.06	1.04	**2.20**	1.28	0.89	1.11	**1.01**
IL-8	NM_000584	0.93	1.24	1.28	1.05	0.87	1.11	1.17	1.05
IL-6	NM_0006000	1.02	**1.54**	1.00	0.99	0.99	**1.08**	1.06	0.82

Differentially expressed genes are indicated in bold.

3.5 Discussion

In this study, a novel gene ORF116 expressed by OV-NZ2 was discovered that plays a role in innate immune modulation. ORF116 is highly conserved within ORFV strains and no homologues were found outside the *Parapoxvirus* genus. It is located within the right terminal region of the OV-NZ2 genome amongst a cluster of genes that are involved in immunomodulation. Amino acid sequence analysis of ORF116 shows that it lacks a peptide signal sequence which strongly suggests that this protein acts intracellularly and like the other genes in this region, is expressed early before DNA replication.

Previously, transcriptome analysis of HeLa cells infected with OV-NZ2 wild type or with OV-NZ2Δ116 knockout mutant by microarray revealed an up-regulation of a number of ISGs in knockout mutant virus-infected cells to higher levels than in OV-NZ2 wild type-infected cells, suggesting a major role played by ORF116 in modulating the IFN response (AlDaif, B., 2013). This observation prompted us to validate its role by making a revertant virus in which the ORF116 was re-inserted at the same locus in the mutant virus. The revertant virus was generated as described in materials and methods and its genome was characterized by PCR analysis. The analysis has shown the re-insertion of *ORF116* gene along with the *LacZ* reporter gene and virus purity was confirmed. The transcription of *ORF116* gene was detected at 2 h.p.i. by RT-PCR and it was expressed early before viral DNA replication since cycloheximide did not inhibit its expression. Growth of the wild type virus, knockout mutant and revertant in cell culture showed that the growth of revertant virus was restored compared to the knockout mutant virus, albeit not as efficiently as wild type virus. From three independent experiments, it has been shown that the expression levels of a number of ISGs (IFI44, IFI16, RIG-I, IFIT2, IFIT1, OAS1, OASL, IFIH1, IL-6, IL-8, ISG20, but not DDX60) analyzed by qRT-PCR in infected HeLa cells showed a differential expression pattern. The expression level of the selected ISG mRNAs except DDX60 were significantly higher in OV-NZ2Δ116 than OV-NZ2-infected cells and importantly than the OV-NZ2Rev116 revertant virus. It was clear that the re-insertion of the *ORF116* gene in the revertant restored the phenotype of wild type virus. The differential expression of these ISGs was detected at 6 h.p.i except for both IL-8 and IFI16 at 2 and 4 h.p.i. DDX60 has shown upregulation at 6 h.p.i. with no significant differential expression among the three viruses. Nevertheless, these data have confirmed the role of ORF116 in modulating the IFN response. In addition, the data suggests that the *ORF116* gene could either directly or cooperatively inhibit those ISGs by

direct interaction, or by interfering with the type I IFN signalling pathways, or by inhibiting the induction of type 1 IFN or all of the above.

The deletion of ORF116 from OV-NZ2 caused a slight attenuation in the growth of the mutant virus and from previous examination, the CPE was much slower and size of the virus plaques were smaller despite similar plaque morphology to wild type. All these observations could explain the up-regulation of ISGs examined and their action on virus replication. It is unlikely that ORF116 is a host range gene since the deletion showed a small effect on suppressing virus growth. A number of host range genes have been identified in poxviruses such as K1L, C7L, E3L and K3L which are essential for virus replication in a cell-type specific manner (Beattie, Elizabeth *et al.*, 1995; Langland, J. O. *et al.*, 2002; Meng, X. *et al.*, 2012; Nájera, J. L. *et al.*, 2006; Perkus, M. E. *et al.*, 1990; Shisler, J. L. *et al.*, 2004). K1L and C7L have been shown to target the IFN effector response (Meng, X. *et al.*, 2009). Taken together, the elevated levels of ISGs could explain its reduced replication levels in cell culture.

The analysis of the amino acid sequence of OV-NZ2 ORF116 has shown no evidence of a secretary signal peptide, but it was found that there is a tentative classical signal peptide for protein localization to mitochondria and nucleus. A clearer insight as to where the ORF116 protein localizes could be elucidated by co-localization studies. Further characterization of ORF116 protein was considered essential in understanding its role either by expressing ORF116 with a tag from a construct or constructing another recombinant virus that expresses ORF116 with a tag under its natural promoter as there was no antibody available against the protein. Given that the ORF116 protein acts intracellularly, it is more likely targeting signalling pathways. Sequence analysis of the promoter region of the altered ISGs has shown a number of GAAAN(N)(N)GAAA sequences within the region upstream of the TATA box, indicating a putative IRF-binding site. The promoter region of IFN-β contains an ISRE consisting of four sets of overlapping PRDII, PRDIII-I and PRDIV that are recognized by the transcription factors NF-κB, IRF3/7 and ATF-2/c-Jun respectively and many ISGs harbour ISRE-like sequences in their promoter region too. Sequence similarity was found between ISRE ($^{A}/_{G}$NGA**AA**NNGAAACT) of ISGs and the IRF-binding site (PRDIII-I) (G(A)A**AA**$^{G}/_{C}{}^{T}/_{C}$GAAA$^{G}/_{C}{}^{T}/_{C}$) of IFN-β and the 5' flanking AA sequence (in bold) is essential for the recognition by IRFs, not NF-κB (Darnell, J. *et al.*, 1994; Tanaka, N. *et al.*, 1993). These findings could be encouraging to investigate whether ORF116 is targeting IRF3 in particular or any molecules of signalling pathways that converge at IRF3.

It has not been determined yet whether the expression of those altered ISGs in the present study has been an effect of virus infection or IFN induction. Identifying how these ISGs induced could assist determining which pathways the ORF116 protein is targeting. ISGs are different in their inducibility in which some could be induced only by IFN such as IFITM1, some could be induced by both IFN and virus such as IFI15, and others could be induced only by virus such as ISG56 as IFN-β does. There is no definitive signature that determines whether a particular ISG gene is virus-inducible or IFN-inducible. DNA-protein binding studies could define the exact relationship by means of e.g. electrophoretic mobility shift assay (EMSA), footprinting or even crystal structure studies. Biochemists speculate that ISREs that contain only two repeats of GAAA is induced by IFN whereas those that contain three or four repeats is induced by IFN and virus (Maniatis, T. *et al.*, 1998). In addition, Wathelet, M. G. *et al.* (1992) provide an explanation for this dilemma by the existence of additional virus-inducible elements like PRDII and PRDIV.

A number of other virus infection studies, that have also shown manipulation of many of the ISGs were observed in this study. A comparison of NYVAC and MVA (a highly attenuated virus in which a 25 kb fragment containing non-essential genes is deleted) infections in either MDDC or HeLa cells at 6 h.p.i. revealed a distinct pattern in gene expression. The expression level of IFIT1, IFIT4, ISG15 and ISG20 was higher in MVA-infected MDDC than in NYVAC-infected MDDC (Guerra, S. *et al.*, 2007). Studies on Papillomavirus (HPV) type 31 has revealed downregulation of a number of ISGs including MX1, MX2, IFI27, IFIT1, IFIT2, OAS2, STAT1 and IFITM3 (Chang, Y. E. *et al.*, 2000). On the other hand, IFI44 and DDX60 were up-regulated in cells transfected with the genome of HPV type 11, 16 and 45 (Kaczkowski, B. *et al.*, 2012). Moreover, HIV-1-infected MDDC showed 18 ISGs that were up-regulated with no change in IFN expression (Harman, A. N. *et al.*, 2011).

From analysis of over 300 known ISGs we are gaining a clearer picture of which ISGs are specifically targeted by viruses, although the antiviral properties of many of them has not been delineated yet (Sadler, A. J. *et al.*, 2008). Those ISGs that are specifically manipulated by the ORFV ORF116 and that are also targeted by other viruses are discussed in detail below.

IFI16 is a member of the PYHIN protein family that act as a DNA sensor and recruits STING for IFN-β induction (Fernandes-Alnemri, T. *et al.*, 2009; Hornung, V. *et al.*, 2009; Rathinam, V. A. K. *et al.*, 2010; Unterholzner, L. *et al.*, 2010). IFI16 was up-regulated by OV-NZ2Δ116 infection but not by OV-NZ2 or OV-NZ2Rev116 at 2 and 4 h.p.i., suggesting a mechanism

used by OV-NZ2 to evade the DNA sensing pathway. At 6 h.p.i, the three viruses have downregulated IFI16 below the basal level at 6 h.p.i., suggesting virus-mediated IFI16 transcript depletion. IFI44 is induced by virus and IFN-α/β and localizes within the cytoplasm. It functions to aggregate microtubules, affecting early intracellular viral transport (Hallen, L. C. *et al.*, 2007; Honda, Y. *et al.*, 1990; Kitamura, A. *et al.*, 1994; Moens, B. *et al.*, 2012). The yield of Bunyamwera orthobunyavirus from cells expressing IFI44 was inhibited ≥ 10-fold (Carlton-Smith, C. *et al.*, 2012). Furthermore, the IFI44 expression level was increased by about 4 times in the knockout HSV-1Δ34.5-infected MEF cells compared with the wild type (Pasieka, T. J. *et al.*, 2006).

RIG-I and MDA5 are cytosolic antiviral molecules that play a major role in cytoplasmic sensing of virus RNA either from genome, replication by-products or transcripts (Yoneyama, M. *et al.*, 2004). Upon viral RNA recognition by RIG-I or MDA5, signalling cascades are triggered through MAVS leading to induction of type I IFN. They can play a major role in sensing DNA viruses. MYXV induces IFN-β expression in primary human macrophages (pHMs), but this expression was reduced in RIG-I-deficient pHMs (Wang, F. *et al.*, 2008). HSV-1 and adenovirus have shown more efficient replication in RIG-I mutant Huh-7.5.1 cells than wild type Huh-7 cells (Cheng, G. *et al.*, 2007). The role of MDA5 in sensing DNA viruses can be variable (Delaloye, J. *et al.*, 2009; Gitlin, L. *et al.*, 2006). The observations found in this study showed that OV-NZ2 is manipulating the transcriptional levels of both RIG-I and IFIH1 with a stronger effect on RIG-I expression. It would be interesting to study in depth the effect of ORF116 at the molecular level and understand the mechanism adopted by this gene to affect the RLR signalling cascade.

OAS is a family of ISGs consisting three enzymes OAS1-3 and OASL. OAS1-3 and 2-5A-dependent RNase (RNaseL) function in an antiviral role by initiating RNA degradation and inducing IFN expression (Kristiansen, H. *et al.*, 2011), whereas OASL is related to the OAS by its N-terminal OAS-like domain but lacks 2'-5' oligoadenylate synthetase activity. OASL is rapidly induced by virus infection or IFN and acts as an antiviral effector via its ubiquitin-like domain (UBL) (Hartmann, R. *et al.*, 1998; Marques, J. *et al.*, 2008; Melchjorsen, J. *et al.*, 2009). It has been also shown that OASL enhances RIG-I-mediated signalling (Zhu, J. *et al.*, 2014). This could suggest an interplay between OASL and RIG-I, observed in this study, in their expression or suppression caused by ORF116.

The ISG56/IFIT1 gene family is comprised of four members: ISG56/IFIT1, ISG54/IFIT2, ISG60/IFIT3 and ISG58/IFIT5 and they can be induced by IFN or virus infection to mediate translation inhibition (Fensterl, V. *et al.*, 2011). Their antiviral role against poxvirus has been recently demonstrated. A C9-deleted VACV mutant was IFN resistant in IFIT1/2/3 knockout cells and C9 mediates proteolysis of IFIT1/2/3 proteins without affecting their mRNAs levels (Liu, R. *et al.*, 2018; Liu, R. *et al.*, 2019). ORFV targets IFIT1 and IFIT2 but at the transcriptional level, suggesting different strategies of ISG antagonism amongst poxviruses. ISG20 is a $3' \rightarrow 5'$ exoribonuclease that degrades ssRNA and acts as an antiviral effector (Espert, L. *et al.*, 2005; Espert, L. *et al.*, 2004; Gongora, C. *et al.*, 2000). It is also believed that ISG20 can act as regulator through upregulation of IFIT1 and other ISGs (Weiss, C. M. *et al.*, 2018).

DDX60 contains a DEXD/H box RNA helicase domain and is involved in the antiviral response. In this study, DDX60 has not been altered by ORF116 and slightly upregulated at 6 h.p.i in all viruses. It could be altered by other viral factors or this ISG is not affecting ORFV replication. Its antiviral effect was shown in poliovirus-infected HeLa cells at 14 h.p.i and VSV-infected HEK293 cells (Miyashita, M. *et al.*, 2011).

Cytokines and chemokines are induced in response to infection to modulate the immune cells and attract them to the site of infection. IL-8 is a chemokine regulated by the transcription factor NF-κB and is rapidly induced in response to viral infection and other stimuli. It appears that the expression of ORF116 was important at a very early stage of infection (2 and 4 h.p.i) to inhibit IL-8 action, then masked by other viral factors after 4 h.p.i., indicating the importance of temporal activation of virus and host genes to fight for supremacy. The manipulation of IL-8 expression was also observed in OV-IA82-infected OFTu cells by ORF024 at the same time points 2 and 4 h.p.i (Diel, D. G. *et al.*, 2010). IL-6 is a pro-inflammatory cytokine induced at an early stage of infection and its manipulation was observed in CPXV and MPXV-infected HeLa cells at 6 h.p.i. (Bourquain, D. *et al.*, 2013).

To summarise, the role of the ORFV ORF116 gene was addressed in this part of the study and the results have shown its potential to modulate the IFN response. So far the results have shown that a number of ISGs are manipulated by ORF116 and prompted further studies to track its inhibitory effect and to determine its exact target within the IFN signalling pathway and delineate the precise mechanism of its action within the complex IFN system. Those ISGs are known to function as antiviral effectors and it would be interesting to investigate whether

they act as restriction factors against ORFV. ORF116 could have a direct specific effect on ISG expression, in particular it could be targeting IRF-3 within infected cells or it could have a role in inhibiting type I IFN production or signalling again by targeting IRF-3. From the above results a decision was made to look at the effect of ORFV infection on IFN-β production (see next two Chapters) as it would address an important aspect of ORFV biology in the first instance and in addition to examine the specific effects of ORF116 on IFN-β production in the context of the virus and from a protein expression vector.

RESULTS II

4 RESULTS II: Effect of ORFV Infection on IFN-β Expression (RIG-I-Dependent Pathway)

4.1 Overview

It is widely believed that replication of viruses, including OV-NZ2 virus, can generate dsRNA in the cytoplasm as a byproduct formed by base-pairing between converging intermediate viral transcripts during virus genome transcription. The generated dsRNA can be recognized by cytosolic RNA sensors leading to the expression of type I interferon.

To investigate the effect of OV-NZ2 virus infection on type I interferon expression, the HEK293 cell was chosen to represent a model of RNA-dependent IFN-β induction. As reported previously, HEK293 cells are known to lack DNA sensors except RNA polymerase III. RNA polymerase III recognizes dsDNA such as poly(dA:dT) and converts it into 5'-triphosphate dsRNA which is then solely recognized by RIG-I and not MDA5. These cells do not express the ER-residing STING adaptor and fail to respond to c-di-GMP, cyclic dinucleotide detected by STING (Burdette, D. L. *et al.*, 2011; McWhirter, S. M. *et al.*, 2009). Toll-like receptors (TLRs) are not expressed in this cell line either, however, it does express cytosolic RIG-I and MDA5 sensors. Only RIG-I, but not MDA5, detects 5'-triphosphate dsRNA derived from poly(dA:dT) by polymerase III. Recognition of nucleic acid material by the RIG-I receptor will trigger the RNA-dependent signalling pathway that leads to expression of type I interferon as shown in Figure 4.1.

4.2 Induction of IFN-β Expression in HEK293 Cells

An investigation was conducted to establish in the first instance the cellular response of HEK293 cell to exogenous nucleic acid material and detection of IFN-β expression. Synthetic dsDNA poly(dA:dT) or synthetic dsRNA poly(I:C) were used to stimulate the cytosolic RNA sensing pathway. The cells were transfected with either poly(dA:dT) or poly(I:C) and the induction of IFN-β was quantified by qRT-PCR. Kinetic analysis was performed to assess the time course of type I IFN induction and also to determine the optimal dose of nucleic acid to produce the IFN response. qRT-PCR data was normalized to the expression level of GAPDH, then compared to mock samples in each of the corresponding time points. Importantly, GAPDH showed no change in its expression level during the course of

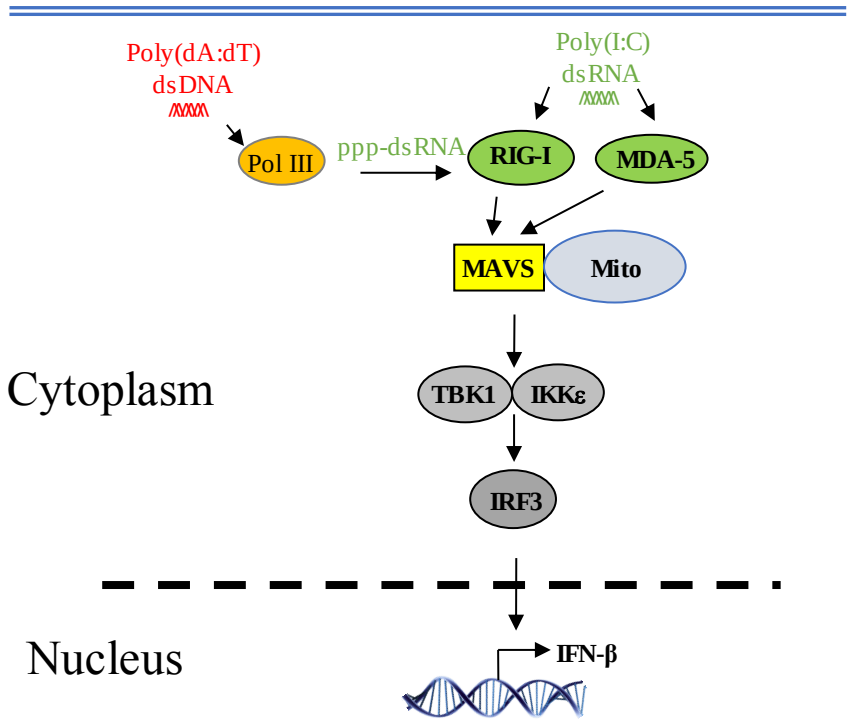

Figure 4.1. Experimental model to study RIG-I/MDA5 pathways involved in the induction of IFN-ß in HEK293 cells. RIG-like receptors are localized in the cytosol. RIG-I receptor senses short dsRNA and also ppp-dsRNA derived from polymerase III-transcribed poly(dA:dT), whereas MDA5 senses long dsRNA. Upon ligand binding, RLRs engage the adaptor MAVS located on the outer membrane of mitochondria then lead to the downstream signalling to TBK1/IKKε-phosphorylating IRF3 and IFN-β expression.

stimulation in HEK293 cells. Then, fold change of IFN-β induction was calculated as described in materials and methods.

The cells responded to both transfected poly(dA:dT) (Figure 4.2 A) and poly(I:C) (Figure 4.3 A) in which the induction of IFN-β expression was detected after 4 hours post stimulation and the induction increased reaching more than 7000 fold and 400 fold respectively at 25 hours post stimulation. The induction did not increase much beyond 25 hours post stimulation in either poly(dA:dT) or poly(I:C) treated cells (data not shown). Accordingly, the time point of 20 hours post stimulation was chosen in this study at which a strong IFN response was seen. The nucleic acid dose response was also investigated in HEK293 cells and the appropriate concentration required was also determined. The cells were stimulated with either poly(dA:dT) or poly(I:C) at different concentrations and harvested at different time points.

A.

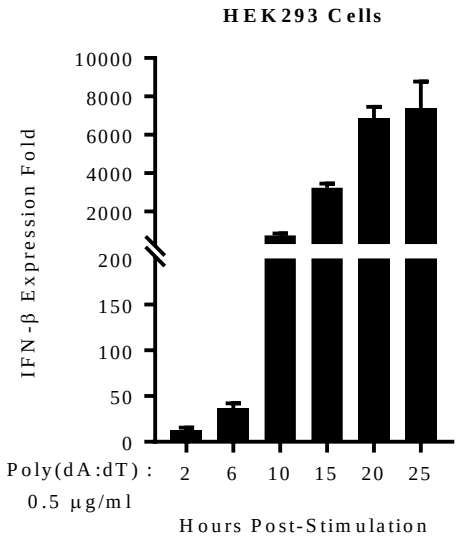

B.

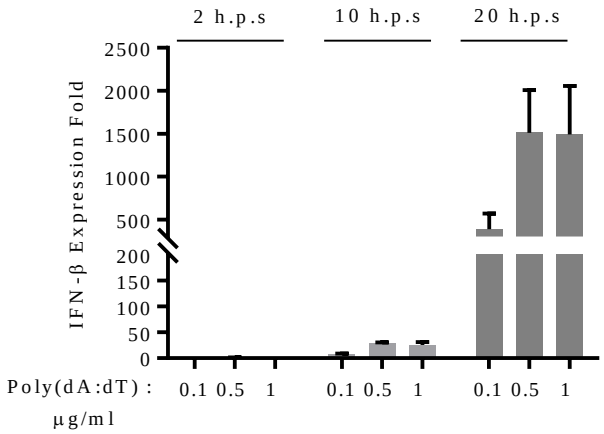

Figure 4.2. Induction of IFN-β by poly(dA:dT) in HEK293 cells. (**A**) and (**B**) HEK293 cells were seeded at $4x10^5$ cells in 6-well plates and stimulated with poly(dA:dT) at concentration indicated. Total RNA was isolated from cells at the time shown and IFN-β mRNA was quantified by qRT-PCR in triplicate. Expression fold was calculated as described in materials and methods. Data are from one representative experiment of four (**A**) and three (**B**) independent experiments conducted with technical replicate. Error bars represent mean ±SD.

Poly(dA:dT) stimulation showed that the IFN response was dose-dependent and the concentration of 0.5 µg/ml was sufficient to produce a strong response and accordingly this concentration was chosen in this study (Figure 4.2 B). Similarly, poly(I:C) stimulation showed a marked increase in response from 10 to 20 hours post stimulation (Figure 4.3 B and

C) and a concentration 1 μg/ml was sufficient to produce a strong response; accordingly the concentration of 1 μg/ml was chosen in this study.

HEK293 cells does not express the TLR3 receptor, as reported previously (de Bouteiller, O. *et al.*, 2005). It is a receptor that recognize dsRNA from either the extracellular or intracellular environment and triggers signalling through the endosomal pathway. In this study it has been hypothesized that poly(I:C) triggers the intracellular RNA sensing pathway through the cytosolic sensor. The transfection reagent LyoVec is known to deliver poly(I:C) into the cell cytosol resulting in exposing poly(I:C) to the cytosolic dsRNA sensor. To examine this hypothesis, poly(I:C) was delivered into HEK293 cells either complexed with cationic lipid LyoVec or without, then IFN-β mRNA was quantified by qRT-PCR. As expected, poly(I:C) alone did not induce IFN-β expression in comparison with poly(I:C) complexed with cationic lipid LyoVec (Figure 4.3 C). This result suggests that RNA sensing and signalling in HEK293 cells dose not involve the TLR3 receptor, or TLR3 does not recognize poly(I:C) or HEK293 cells do not express TLR3.

4.3 Poly(dA:dT)-mediated IFN-β Expression in HEK293 Cells through RNA Polymerase III

As HEK293 cells lack the expression of DNA sensors, however investigators have identified that RNA Polymerase III is expressed in these cells that can transcribe AT-rich dsDNA into 5'triphosphate dsRNA (Ablasser, A. *et al.*, 2009; Chiu, Y.-H. *et al.*, 2009) that serves as a ligand for the detection by RIG-I (Hornung, V. *et al.*, 2006). Therefore, the induction of IFN-β observed above was presumably through RIG-I/MDA5 and not through DNA sensors when the cells were stimulated with poly(dA:dT). This assumption was examined by inhibiting the function of RNA Polymerase III that is responsible for converting dsDNA to 5'-triphosphate dsRNA using an RNA Polymerase III inhibitor (ML-60218). HEK293 cells were treated with ML-60218 then stimulated with poly(dA:dT) or poly(I:C) and the induction of IFN-β quantified by qRT-PCR.

In poly(dA:dT)-stimulated ML-60218-treated cells, the induction of IFN-β expression was enhanced slightly at low concentrations of ML-60218 but then suppressed significantly at higher concentrations of ML-60218 in a dose-dependent manner (Figure 4.4), consistent with a previous report (Valentine, R. *et al.*, 2010). This slight enhancement of IFN-β induction in HEK293 cells treated with ML60218 was also previously observed (Tamassia, N. *et al.*,

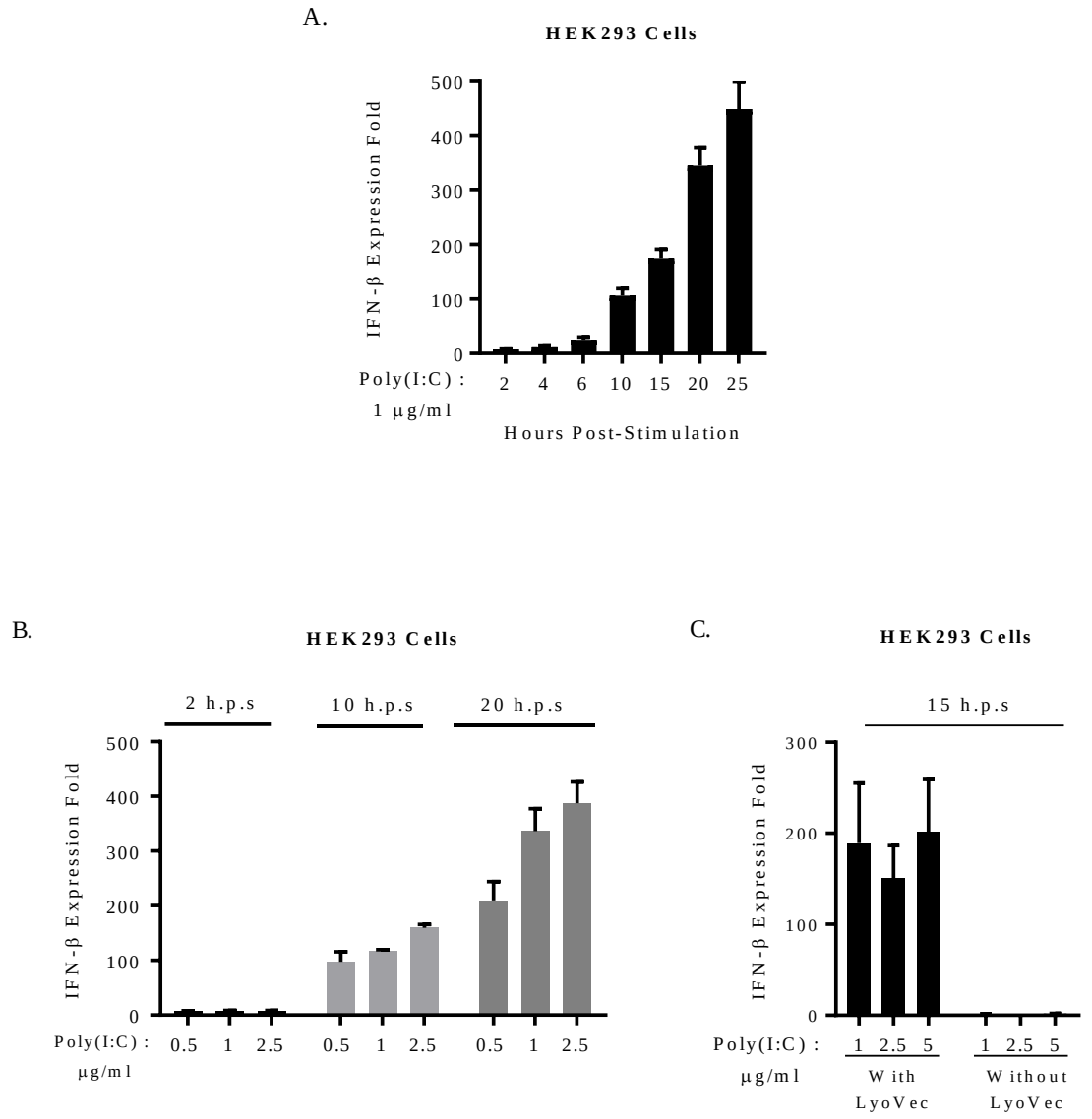

Figure 4.3 Induction of IFN-β by poly(I:C) in HEK293 cells. (**A**), (**B**) and (**C**) HEK293 cells were seeded at $4x10^5$ cells in 6-well plates and stimulated with poly(I:C) complexed with LyoVec (**A**), (**B**) and (**C**) or without LyoVec (**C**) at concentration indicated. Total RNA was isolated from cells at the time shown and IFN-β mRNA was quantified by qRT-PCR in triplicate. Expression fold was calculated as described in materials and methods. Data are from one representative experiment of three (**A**), three (**B**) and one (**C**) independent experiments conducted with technical replicate. Error bars represent mean ±SD.

2012). On the other hand, poly(I:C)-mediated IFN-β expression has not been affected by ML-60218 treatment and the IFN-β expression has remained stable at all concentrations (Figure 4.4). The inhibition of IFN-β induction in poly(dA:dT) stimulation was not due to potential toxicity of ML-60218, since the induction of IFN-β expression in poly(I:C) stimulation has

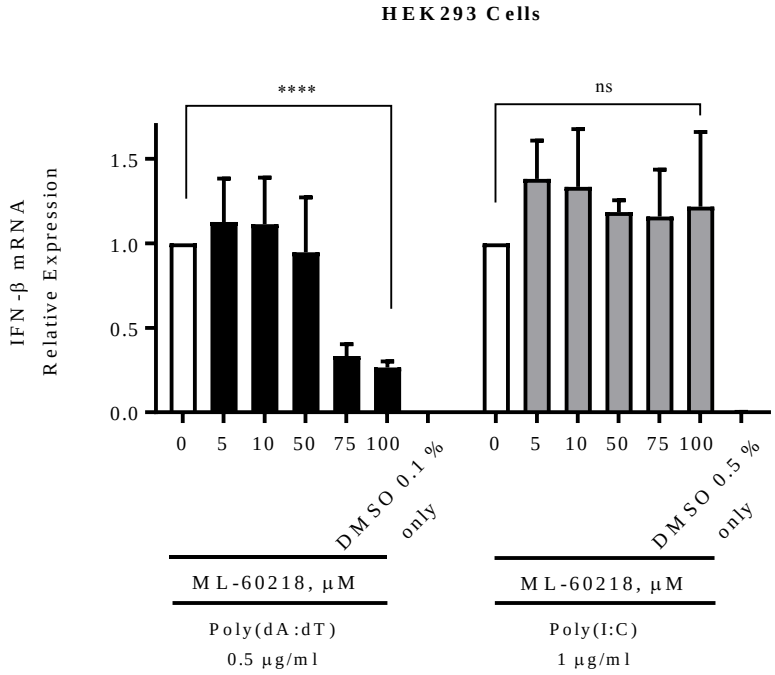

Figure 4.4. RNA Polymerase III is required for poly(dA:dT)-mediated IFN-β induction in HEK293 cells. HEK293 cells were seeded at $4x10^5$ in a 6-well plate. The cells were treated with ML-60218 at the indicated concentration for two hours and then stimulated with either poly(dA:dT) at a concentration of 0.5 µg/ml or poly(I:C) at a concentration of 1 µg/ml. The induction of IFN-ß expression was assessed by qRT-PCR after 24 hours post stimulation. qRT-PCR assay was conducted in triplicate. The level of IFN-β mRNA in untreated sample was considered 1 to compare the treated samples. Data are from three independent experiments conducted with technical replicate. Error bars represent mean ±SD. Statistical analysis was performed using Student's *t* test. Asterisks indicate probability: $^{ns}P \geq 0.1234$, $^{****}P \leq 0.0001$.

not been affected even at 100 µM. Besides, the cells' viability was examined visually under light microscopy and was not adversely affected. As DMSO was used as a solvent for ML-60218 and it was included in this assay as a control to exclude the notion of IFN-β induction was by DMSO. These results have shown that inhibition of RNA Polymerase III blocked the production of IFN-β through the suppression of 5'-triphosphate dsRNA production and have demonstrated that the poly(dA:dT) was transcribed to 5'-triphosphate dsRNA and triggers the induction of type I interferon through RIG-I in HEK293 cells.

4.4 Inhibitory Effect of OV-NZ2 Infection on IFN-β Expression in poly(dA:dT)-stimulated HEK293 Cells

It has been shown that HEK293 cells respond to transfected synthetic dsDNA and produce IFN-β through cytosolic nucleic acid sensing. Next, an investigation was conducted to test whether OV-NZ2 infection has an effect on type I interferon expression. HEK293 cells were stimulated with poly(dA:dT) at a concentration of 0.5 μg/ml for 4 hours, then the cells were infected with OV-NZ2 at different multiplicities of infection for 20 hours. qRT-PCR analysis was conducted from total RNA isolated from cells. The results showed that OV-NZ2 infection significantly suppressed IFN-β mRNA levels in HEK293 in a dose-dependent manner (Figure 4.5 A). The inhibition of IFN-β expression was highly significant at an MOI 5 and was used hereafter. The duration of OV-NZ2 IFN antagonism was investigated over 20 hours of virus infection. The cells were first stimulated for 4 hours with poly(dA:dT), then infected with OV-NZ2 at an MOI 5. The cells were harvested at different intervals and total RNA isolated. It has been shown that the inhibitory effect of OV-NZ2 lasted throughout the time course of the experiment (Figure 4.5 B). OV-NZ2 infection only, without stimulation, was also included and showed no noticeable induction of IFN-β expression (Figure 4.5 B). This result strongly suggested that the virus encodes factors that play a role in interfering with type I interferon expression.

4.5 Inhibitory Effect of OV-NZ2 Infection on IFN-β Expression in poly(I:C)-stimulated HEK293 Cells

It was also shown above that HEK293 cells produce IFN-β in response to a transfected synthetic viral mimic of dsRNA. Virus replication can produce an intermediate dsRNA in infected cells and could potentially be recognized by RNA sensors. The poly(I:C) used in this study was relatively small, about 0.3 kb (data not shown). It has been shown that RIG-I and MDA5 have differential preferences for the type of RNA molecules. MDA5 recognizes long poly(I:C) about 7 kb and RIG-I recognizes short poly(I:C) about 0.3 kb (Kato, H. *et al.*, 2008). HEK293 cells were first infected with OV-NZ2 for four hours, then stimulated with synthetic dsRNA poly(I:C). The cells were harvested and IFN-β mRNA was quantified by qRT-PCR. The data have shown that OV-NZ2 infection caused a significant inhibition in IFN-β expression in poly(I:C)-stimulated HEK293 cells and an MOI 5 was sufficient for the inhibitory effect as shown in Figure 4.6 A. Next, the duration of the OV-NZ2 inhibitory effect was addressed. HEK293 cells were first infected with OV-NZ2 at an MOI 5 for four hours

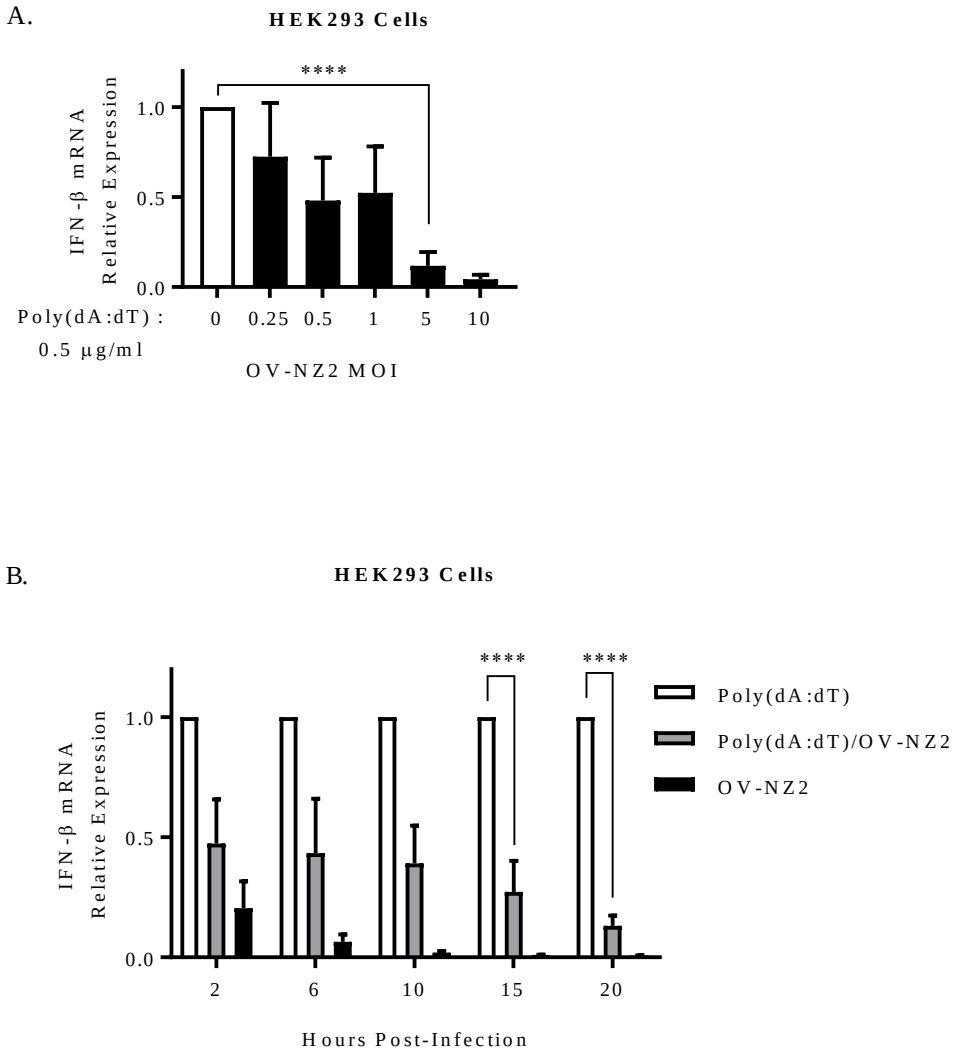

Figure 4.5. Inhibitory effect of OV-NZ2 Infection on IFN-β Induction in poly(dA:dT)-stimulated HEK293 cells. HEK293 cells were seeded at $4x10^5$ cells in 6-well plates and stimulated with poly(dA:dT) at concentration of 0.5 µg/ml for 4 hours. Then the cells were infected with virus for 20 hours at different MOI's as indicated in (**A**) or infected with the virus for indicated times at an MOI of 5 in (**B**). Total RNA was isolated from cells and IFN-β mRNA was quantified by qRT-PCR in triplicate. The level of IFN-β mRNA in uninfected sample was considered 1 to compare the infected samples. Data are from three independent experiments. Statistical analysis was performed using Student's *t* test in (A) and two-way ANOVA in (B). Error bars represent mean ±SD. Asterisks indicate probability $^{****}P \leq 0.0001$.

then stimulated with poly(I:C) and incubated until harvesting time. Similar to the inhibitory effect of OV-NZ2 infection in poly(dA:dT)-stimulated cells, OV-NZ2 inhibited the

A.

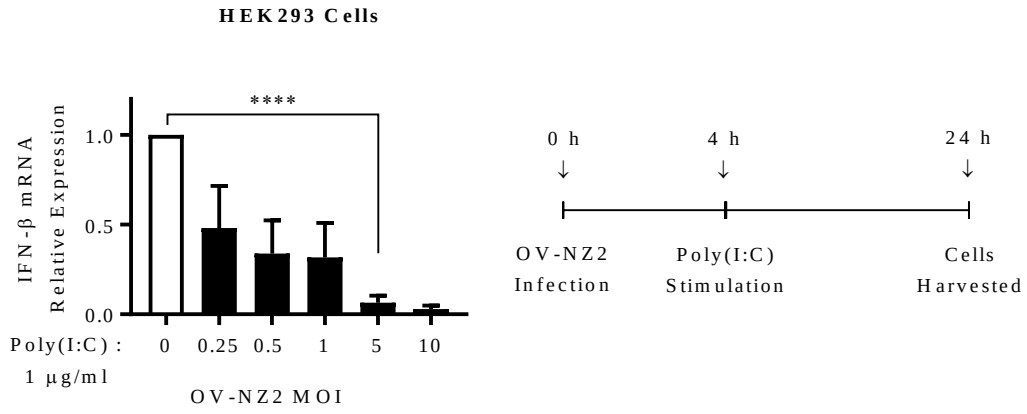

B.

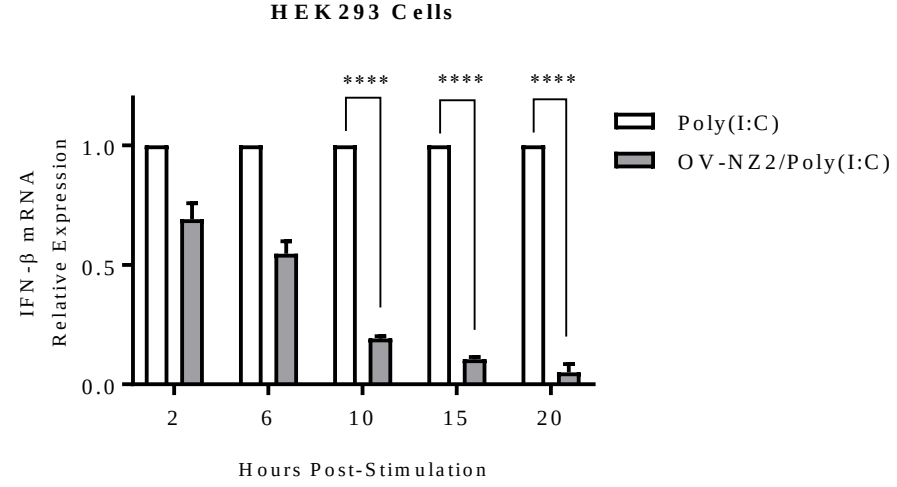

Figure 4.6 Inhibitory effect of OV-NZ2 Infection on IFN-β Induction in poly(I:C)-stimulated HEK293 cells. HEK293 cells were seeded at $4x10^5$ cells in a 6-well plate and first infected with OV-NZ2 for 4 hours at different MOI's as indicated in (**A**) or at an MOI of 5 in (**B**). After 4 hours post infection, the cells were stimulated with poly(I:C) at a concentration of 1 µg/ml and incubated for 20 hours in (**A**) or at the indicated time in (**B**). Total RNA was isolated from cells and IFN-β mRNA was quantified by qRT-PCR in triplicate. The level of IFN-β mRNA in uninfected sample was considered 1 to compare the infected samples. Data are from three independent experiments. Statistical analysis was performed using a Student's *t* test in (**A**) and two-way ANOVA in (**B**). Error bars represent mean ±SD. Asterisks indicate probability $^{****}P \leq 0.0001$.

expression of IFN-β in poly(I:C)-stimulated HEK293 cells over the time course of the experiment as shown in Figure 4.6 B.

It appears that OV-NZ2 has a different mechanism to counteract the poly(I:C)-induced IFN response that differs from the poly(dA:dT)-induced IFN response. The virus was able to

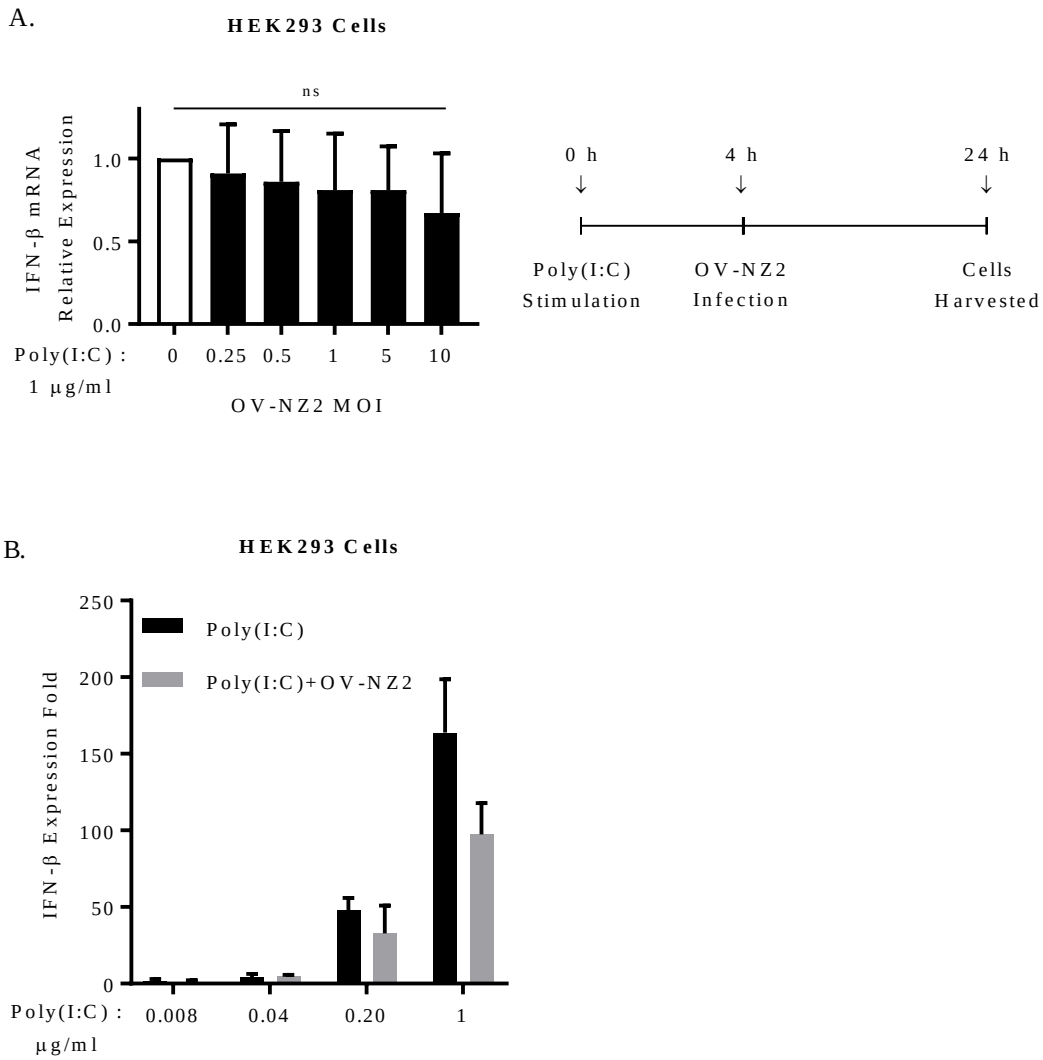

Figure 4.7. OV-NZ2 infection is required first to inhibit poly(I:C)-induced IFN-β expression in HEK293 cells. (**A**) HEK293 cells were seeded at $4x10^5$ cells in 6-well plates and stimulated with poly(I:C) at 1 µg/ml for 4 hours. Then the cells were mock infected or infected with OV-NZ2 at different MOI's indicated then the cells incubated for 20 hours post infection. Total RNA was isolated from the cells and IFN-ß mRNA was quantified by qRT-PCR in triplicate of technical replicate. The level of IFN-β mRNA in uninfected sample was considered 1 to compare the infected samples. Statistical analysis was performed using Student's *t* test. Data are from three independent experiments. Error bars represent mean ±SD. ns indicates probability $^{ns}P \geq 0.1234$. (**B**) HEK293 cells were seeded at $4x10^5$ cells in 6-well plates and stimulated with poly(I:C) at the concentrations indicated for 4 hours. Then the cells were mock infected or infected with OV-NZ2 at an MOI of 5 then the cells incubated for 20 hours post infection. Total RNA was isolated from the cells and IFN-ß mRNA was quantified by qRT-PCR in triplicate of technical replicate. Data are from one experiment. Error bars represent mean ±SD.

significantly suppress the expression of type I interferon in poly(dA:dT)-stimulated HEK293

cells following stimulation. On the other hand, the virus could not significantly suppress the poly(I:C)-induced IFN response when infection follows stimulation (Figure 4.7 A) and that was not because of an excessive response that the virus could not counteract (Figure 4.7 B). This may indicate that infection needs to precede poly(I:C) stimulation to express a specific antagonist to counteract the dsRNA-induced IFN response.

4.6 RIG-I Receptor is Required for IFN-β Expression in HEK293 Cells

RIG-I encodes a protein that contains DExD/H box RNA helicase and a caspase recruitment domain and it has been shown that this protein plays an essential role in regulation of dsRNA-induced signalling that leads to expression of type I interferon (Yoneyama, M. *et al.*, 2004).

From the results of IFN-β induction reported above, it was more likely that the RIG-I receptor plays a major role in the induction of IFN-β expression in HEK293 cells when stimulated with poly(dA:dT) or poly(I:C). The involvement of RIG-I in the IFN response was further investigated by using RNA interference (RNAi). Three different predesigned synthetic small interfering RNAs duplex (siRNA) were used to minimize the possibility of off-target effects. They were short 19 nucleotide siRNA with 2-base 3' overhangs and these features enable siRNA to bypass any possible interferon induction triggered by dsRNA transfection (Marques, J. T. *et al.*, 2006; Sioud, M., 2006).

It was anticipated that endogenous RIG-I is constantly expressed in the cytosol of HEK293 cells in order to detect any danger signal and then its level is increased by interferon upon induction. Western blot analysis has shown no sign of RIG-I protein detection in unstimulated cells (Figure 4.8 A) and this was consistent with previously published studies (Kok, K.-H. *et al.*, 2011; Zhu, J. *et al.*, 2014). However, immunoprecipitation using antibody against endogenous RIG-I showed a weak signal of RIG-I protein expression in some cases, indicating that the protein is present but at a very low level (Figure 4.8 A). The expression of endogenous RIG-I protein in poly(dA:dT)-stimulated HEK293 cells was barely detected at 15 hours post-stimulation but it was detectable at 24 hours post stimulation, whereas in poly(I:C) stimulation it was neither detectable at 15 nor at 24 hours post-stimulation (data not shown). It was speculated that HEK293 cells do not express STING, an adaptor for the DNA signalling pathway (see next Chapter for more detail). To exclude this possibility, western immunoblotting analysis was conducted and showed no sign of STING expression

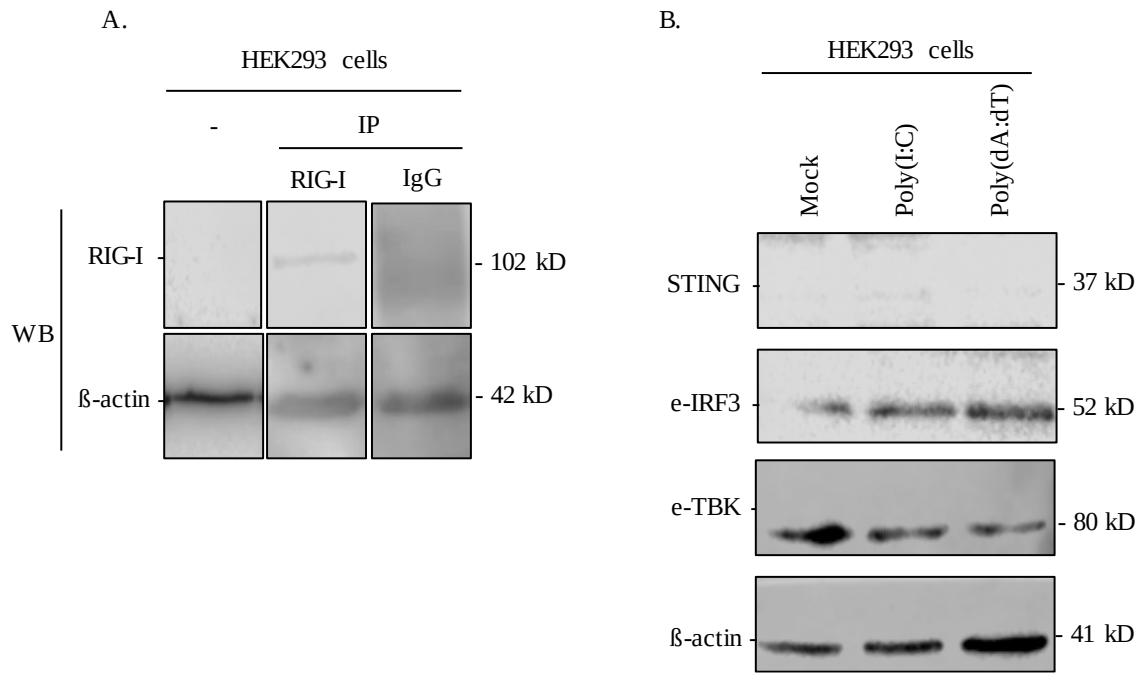

Figure 4.8. Detection of signalling proteins in HEK293 cells by western blotting. (**A**) HEK293 cell lysates were immunoprecipitated (IP) with anti-RIG-I antibody or IgG as a negative control and protein detected by anti-RIG-I. (**B**) HEK293 cells were mock stimulated or stimulated with 0.5 μg/ml of poly(dA:dT) or with 1 μg/ml of poly(I:C) for 15 hours. Cells were harvested and lysed. Ten μg of cell lysate was resolved on a 10 % SDS-polyacrylamide gel and proteins transferred onto nitrocellulose membrane. The membrane was incubated with antibody indicated and visualized by chemiluminescence.

either in mock or stimulated cells (Figure 4.8 B), consistent with observations by Zhang, Y. *et al.* (2014), and as expected the cells do express IRF3 and TBK1 molecules (Figure 4.8 B).

Next, an optimization of RIG-I siRNA transfection was conducted to determine the optimal conditions and concentrations of siRNA transfection that lead to depletion of RIG-I protein expression in HEK293 cells. It was found that siRNA#2 at 100 nM was sufficient to deplete the expression of RIG-I protein (data not shown). HEK293 cells were transiently transfected with three siRNA individually targeting distinct regions in RIG-I mRNA along with an siRNA negative control (NC) and absence of siRNA (none). Then the cells were stimulated either with poly(dA:dT) or poly(I:C) and IFN-β expression examined by qRT-PCR. The transfection of RIG-I siRNA caused a depletion in RIG-I protein in poly(dA:dT)-stimulated cells of about 70% (Figure 4.9 A and B). In addition, siRNA-mediated RIG-I silencing caused

about 70 – 80% of RIG-I mRNA depletion in either poly(dA:dT)- or poly(I:C)-stimulated HEK293 cells (Figure 4.9 C and D). As expected, the induction of IFN-β mRNA was abolished in both poly(dA:dT)- and poly(I:C)-stimulated cells after depleting RIG-I mRNA (Figure 4.10 A and B). These results strongly suggest that the RIG-I receptor is involved in the induction of IFN-β expression.

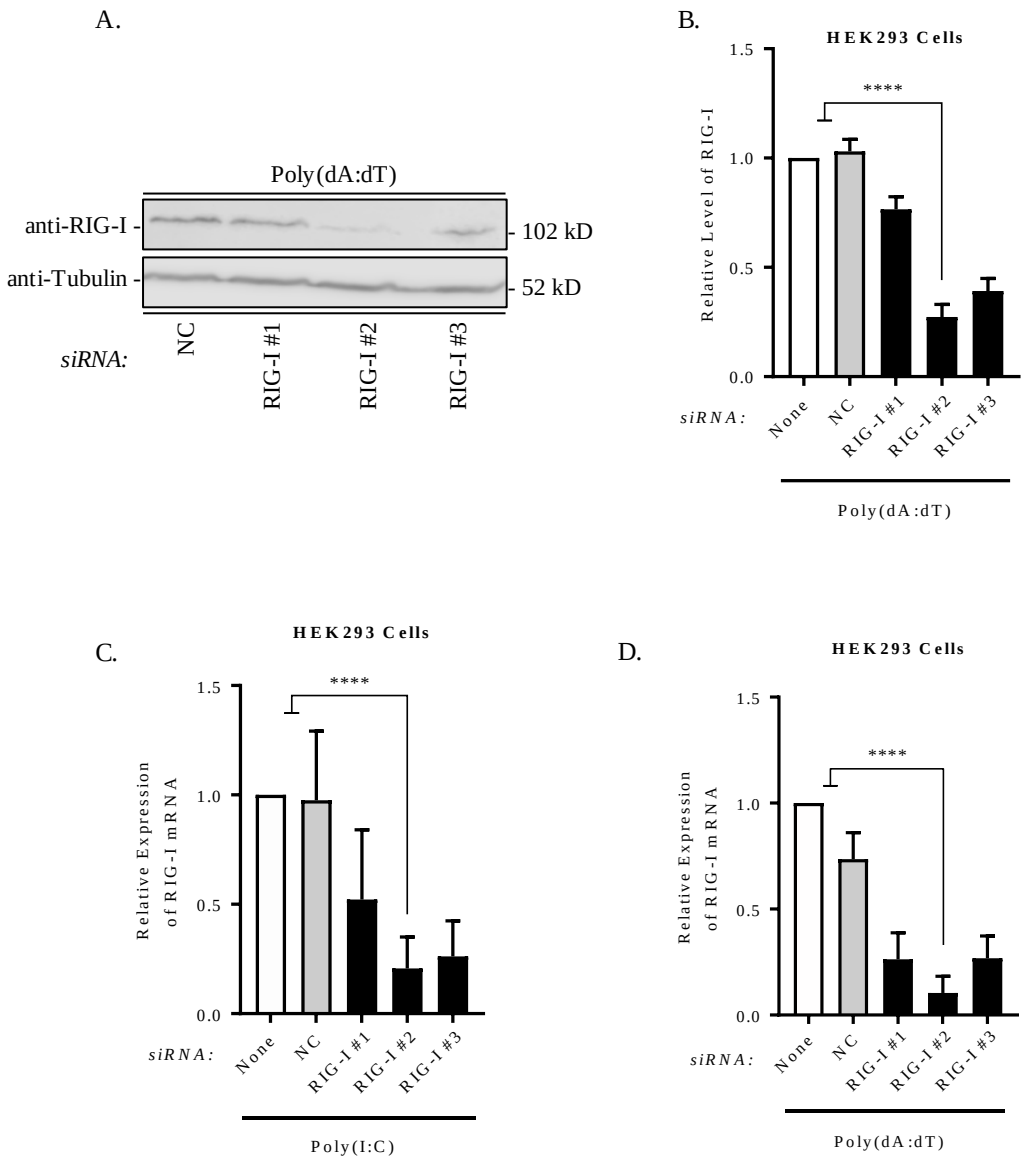

Figure 4.9. siRNA knockdown of RIG-I gene in HEK293 cells. HEK293 cells were transfected for 48 hours with three different siRNAs (100 nM) targeting distinct regions in mRNA of the RIG-I gene. Control conditions include mock transfection in the absence of siRNA (none) or transfection with a non-targeting control siRNA (NC). At 48 h.p.t., the transfected cells were stimulated with either poly(dA:dT) 0.5 µg/ml or poly(I:C) 1 µg/ml for 24 hrs. (**A**) Transfected cells were lysed in lysis buffer for western blot analysis of RIG-I protein expression using 40 µg of total protein. Western blot data is from one representative experiment of three independent experiments. (**B**) Expression of RIG-I protein was quantified from western blot and relative RIG-I expression levels were obtained by normalizing to a tubulin loading control then to a mock transfection control. (**C**) and (**D**) Expression level of RIG-I mRNA was determined in siRNA-transfected cells by qRT-PCR in triplicate of technical replicate either induced by poly(I:C) (**C**) or poly(dA:dT) (**D**). Data are from three independent experiments. Statistical analysis was performed using a Student's *t* test. Error bars represent mean ±SD. Asterisks indicate probability $^{****}P \leq 0.0001$.

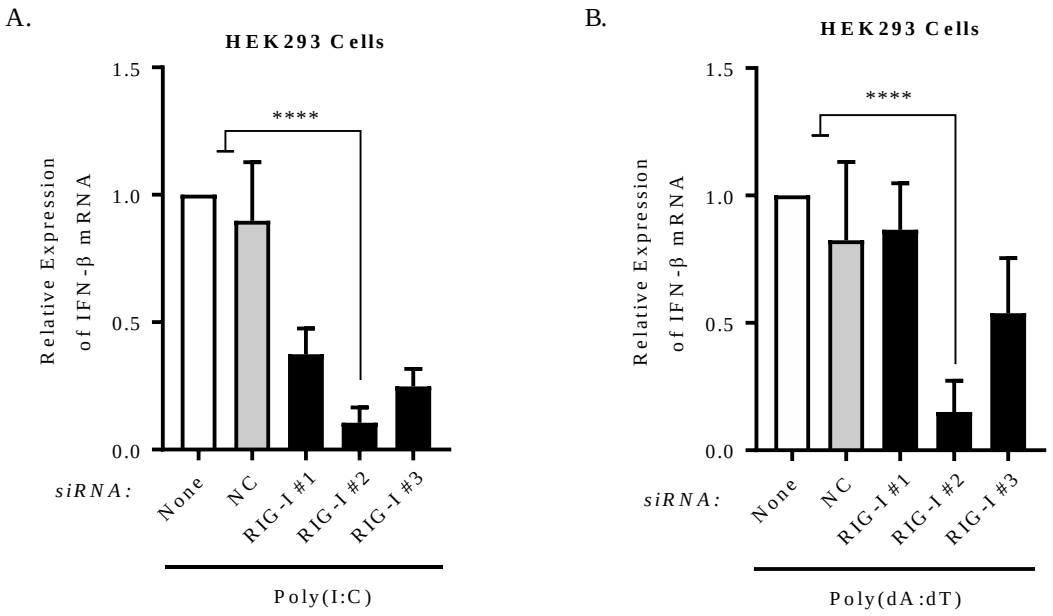

Figure 4.10 RIG-I is required in HEK293 cells for IFN-ß induction. HEK293 cells were transfected for 48 hours with three different siRNAs (100 nM) targeting distinct regions in mRNA of RIG-I gene. Control conditions include mock transfection in the absence of siRNA (none) or transfection with a non-targeting control siRNA (NC). At 48 h.p.t., the transfected cells were stimulated either with poly(I:C) 1 µg/ml (**A**) or poly(dA:dT) 0.5 µg/ml (**B**) for 24 hrs. Then the induction of IFN-ß expression was assessed by qRT-PCR in triplicate of technical replicate. Data are from three independent experiments. Statistical analysis was performed using Student's *t* test. Error bars represent mean ±SD. Asterisks indicate probability $^{****}P \leq 0.0001$.

The involvement of RIG-I in dsRNA-induced IFN-β in HEK293 cells was further confirmed by transient expression of the receptor. RIG-I protein was transiently expressed from pEF-BOS-RIG-I-flag in HEK293 cells at increasing amounts for 24 hours and the linearized empty vector was included as a control as well. Then the cells were mock stimulated or stimulated with poly(dA:dT) or poly(I:C) for 24 hours and cells harvested for total RNA and protein detection. qRT-PCR data showed that expression of RIG-I alone triggered the IFN signalling pathway at 0.5 and 1 µg, however, this induction of IFN-β was significantly enhanced by poly(dA:dT) or poly(I:C) stimulation by 5 and 10 fold respectively compared to untransfected cells and that was not observed in cells transfected with empty vector (Figure 4.11). These results further confirmed the involvement of RIG-I in dsRNA-induced IFN-β and the only sensor that poly(dA:dT) is working through is RIG-I. The expression of RIG-I protein from

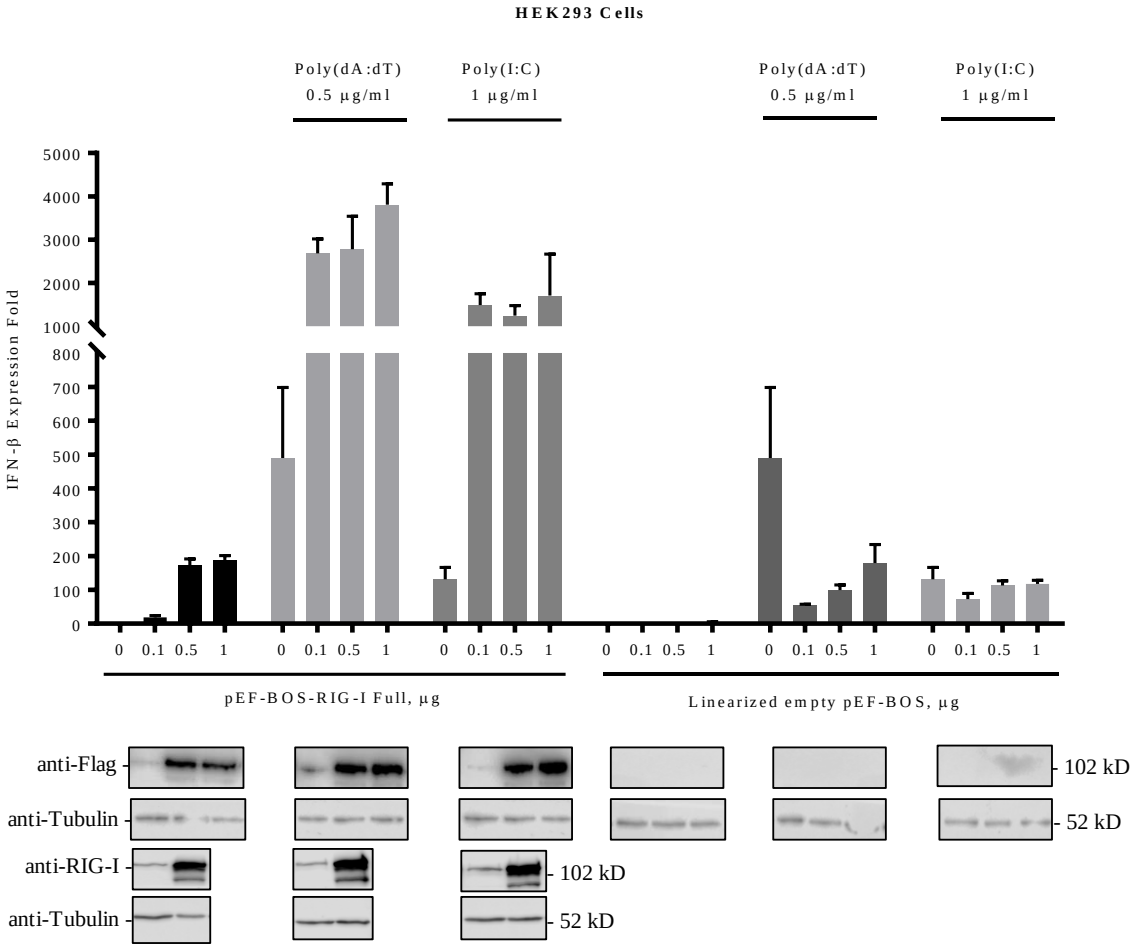

Figure 4.11 RIG-I is involved in the induction of IFN-β in HEK293 cells stimulated with either poly(dA:dT) or poly(I:C). HEK293 cells were seeded at $4x10^5$ in 6-well plates and transiently transfected either with human pEF-BOS-RIG-I full-Flag or linearized empty pEF-BOS as a control for 24 hrs at the indicated amounts. Then cells were either mock stimulated or stimulated with poly(dA:dT) 0.5 µg/ml or poly(I:C) 1 µg/ml for 24 hrs. The cells were harvested and lysed for total RNA and total protein. Induction of IFN-β mRNA was assessed in cells by qRT-PCR and expression fold was calculated as described in materials and methods. RIG-I protein expression level from the vector was also assessed by immunoblotting using either anti-flag or anti-RIG-I antibody. Data are from one experiment with technical replicate and qRT-PCR conducted in triplicate. Error bars represent mean ±SD.

the vector was also confirmed by western blotting using antibodies against flag or RIG-I (Figure 4.11).

4.7 Role of OV-NZ2 ORF020 (E3L homologue) on RIG-I-Dependent Signalling

A homolog of the VACV interferon resistance gene E3L, ORF020, was discovered in OV-NZ2 (McInnes, C. J. *et al.*, 1998). ORF020 is transcribed towards the left terminus of the virus genome. ORF020 was found to bind dsRNA; but not ssRNA, ssDNA or dsDNA and inhibits the activation of dsRNA-dependent protein kinase (PKR) (Haig, D. M. *et al.*, 1998). VACV E3L was shown to have the ability to inhibits the luciferase activity of an IFN-β-dependent promoter in poly(dA:dT)- stimulated 293T and HeLa cells (Valentine, R. *et al.*, 2010).

These reports raised the question whether OV-NZ2 ORF020 could be responsible, or partially responsible, for the inhibition of IFN-β expression observed in this study and more likely through interfering with RIG-I-dependent signalling (Figure 4.12). Transient expression of OV-NZ2 ORF020 could give a clearer insight as to how OV-NZ2 manipulates the IFN response. Therefore, an investigation was undertaken to examine the effect of ORF020 gene on RIG-I-dependent signalling by expression of ORF020 from a vector in HEK293 cells then stimulated with dsDNA poly(dA:dT) or dsRNA poly(I:C) and induction of IFN-β measured by qRT-PCR.

Firstly, a plasmid construct expressing OV-NZ2 ORF020 was generated in which the ORF020 gene was PCR amplified from a pVU2015 *Kpn*I-F fragment (Figure 4.13 A) and cloned into a pAPEX3-Flag vector at the *Asc*I restriction site as described in materials and methods. The correct orientation of ORF020 was confirmed by restriction analysis (data not shown) and the final construct was sequenced to confirm the integrity of the construct. Upon 24 hour post transfection, the expression of ORF020 was detected in HEK293 cells by western blotting using anti-flag antibody and the size of the band was around 24 kDa (Figure 4.13 B). ORF020 protein was previously expressed in *E. coli* as a thioredoxin fusion protein from the pTrxFus expression vector and produced a protein with a size about 41 kDa on Coomassie gel (Haig, D. M. *et al.*, 1998).

Secondly, the investigation determined the effect of OV-NZ2 ORF020 on IFN-β expression. ORF020 was expressed in HEK293 cells at increasing amount for 24 hours then cells stimulated with poly(dA:dT) or poly(I:C) and IFN-β mRNA quantified by qRT-PCR. Protein

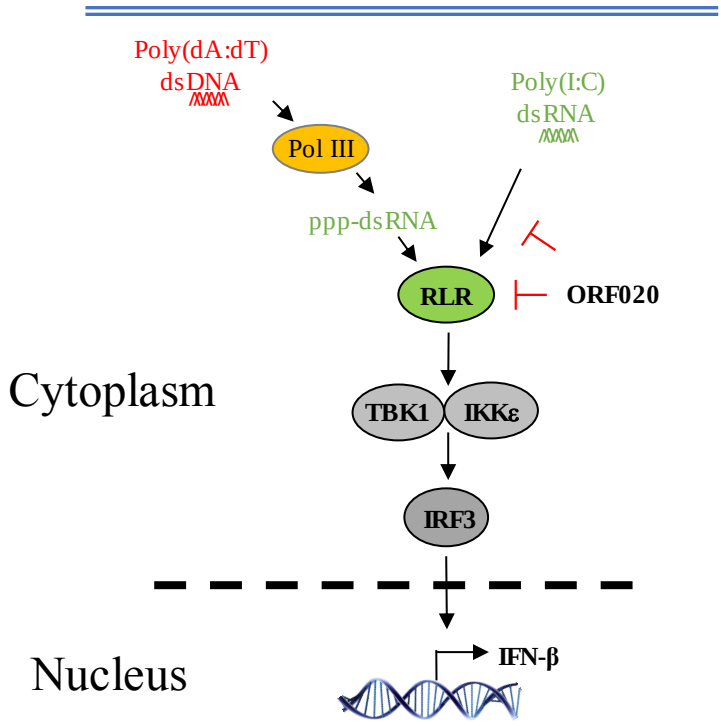

Figure 4.12 Schematic representation of potential effect of OV-NZ2 ORF020 on the induction of IFN-ß in HEK293 cells. Upon stimulation with poly(dA:dT), polymerase III will convert it to ppp-dsRNA then detected by RIG-I receptor leading to expression of IFN-β. Poly(I:C) stimulation will trigger RLR-dependent signalling pathway that leads to expression of IFN-β. OV-NZ2 ORF020 has a potential effect on the expression of IFN-β by targeting RLR signalling through either dsRNA or RIG-I leading to inhibition of IFN-β expression.

expression was detected by western blotting using anti-flag antibody. Expression of ORF020 without stimulation did not induce IFN signalling. However, IFN-β expression was inhibited by ORF020 in poly(dA:dT)- or poly(I:C)-stimulated cells in a dose-dependent manner compared to mock transfectants (Figure 4.14). Ideally this assay could have been improved by incorporating an empty vector control, however the preliminary finding implies that ORF020 plays a role in counteracting the IFN response by targeting RIG-I-like receptor-dependent signalling.

Having established that RIG-I expression enhanced IFN signalling and ORF020 expression suppressed the signalling, it was speculated that ORF020 has a role on RIG-I. An approach was taken to investigate the effect of ORF020 on RIG-I-dependent signalling by co-expressing an increasing amount of ORF020 and 0.1 μg of RIG-I-expressing plasmid in HEK293 cells and then observed the induction of IFN-β expression after stimulation with

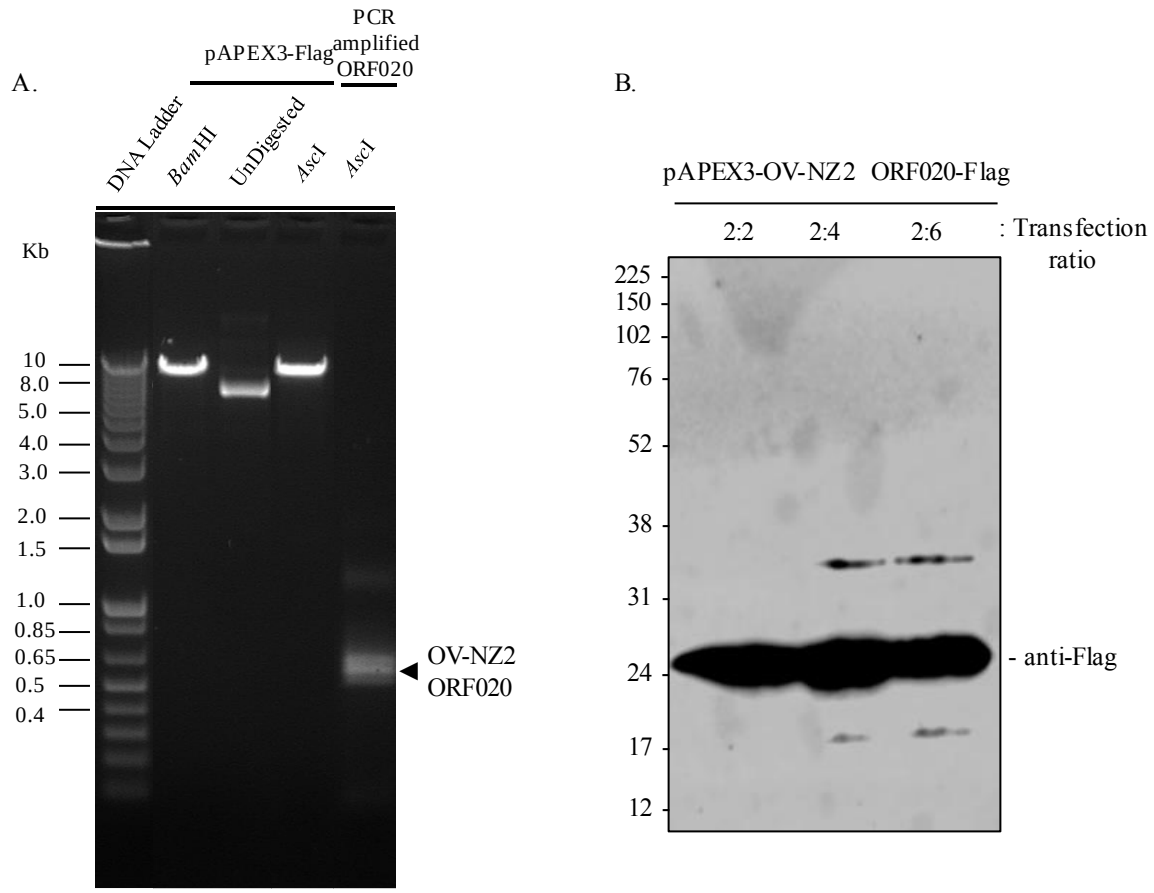

Figure 4.13. Electrophoresis of PCR amplified OV-NZ2 ORF020 gene and transient expression in HEK293 cells. (**A**) OV-NZ2 ORF020 was PCR amplified from the pVU215 plasmid using primers containing the *Asc*I site. PCR amplified ORF020 was firstly digested with *Asc*I then gel purified. The ORF020 was cloned into the vector pAPEX3-flag at the *Asc*I restriction site that included a start codon, downstream kozak sequence and stop codon downstream of the flag tag. The correct orientation of ORF020 gene was confirmed by restriction analysis and the integrity of the gene was also confirmed by sequencing. (**B**) Detection of ORF020 protein was assessed by western blot analysis. Two micrograms of the construct was transfected into HEK293 cell at different transfection ratios for 24 hours. Then 20 µl of cell lysate was resolved on a 10% of SDS-PAGE and protein detected by anti-flag antibody.

poly(dA:dT) or poly(I:C). The amount of plasmid expressing ORF020 was increased up to 2.5 µg in this assay rather than up to 1 µg as shown in Figure 4.14, whereas the amount of plasmid expressing RIG-I remained the same of 0.1 µg as this amount did not elicit the IFN response as shown in Figure 4.11. As shown in Figure 4.15, the expression of ORF020 in poly(dA:dT)- or poly(I:C)-stimulated cells transfected with RIG-I-expressing plasmid caused

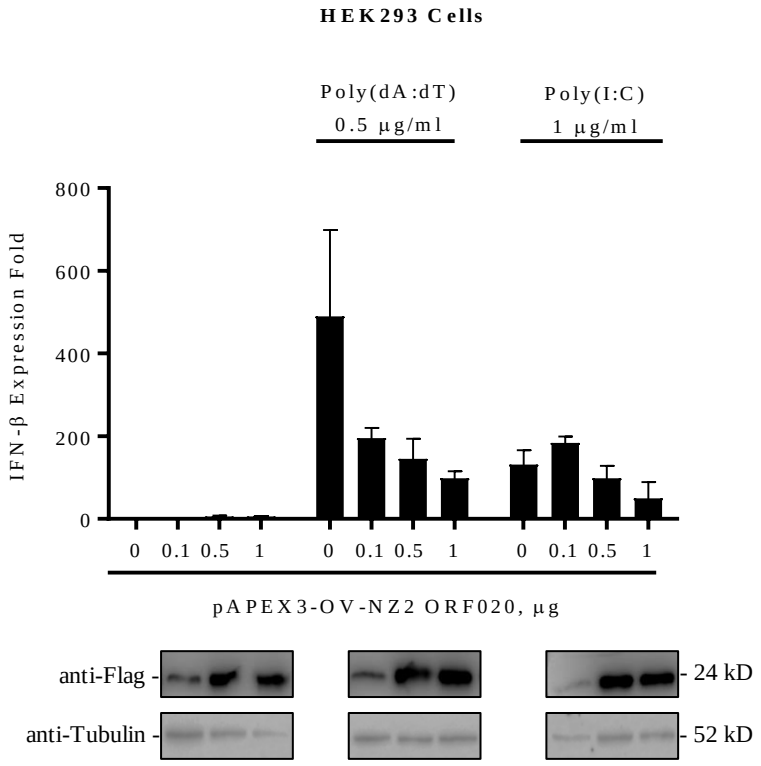

Figure 4.14. Effect of OV-NZ2 ORF020 expression on the induction of IFN-β in HEK293 cells stimulated with poly(dA:dT) or poly(I:C). Indicated amounts of OV-NZ2 ORF020 was expressed in HEK293 cells for 24 hours. Then cells were mock stimulated or stimulated with poly(dA:dT) or poly(I:C) for 24 hours. The induction of IFN-β mRNA was quantified by qRT-PCR in triplicate of technical replicate and expression fold was calculated as described in materials and methods. Data are from one experiment. Error bars represent mean ±SD. Equal amounts of total proteins were immunoblotted with anti-flag and tubulin was used as a loading control.

a suppression in IFN-β expression and it seems that the ORF020 protein has compromised RIG-I activity in enhancing IFN-β signalling. Taken together, these results have determined a new role for ORF020 in counteracting RLR-dependent signalling.

Due to the time constraints, the IFN assays that involved expression of RIG-I, ORF020 or RIG-I/ORF020 were only carried out once.

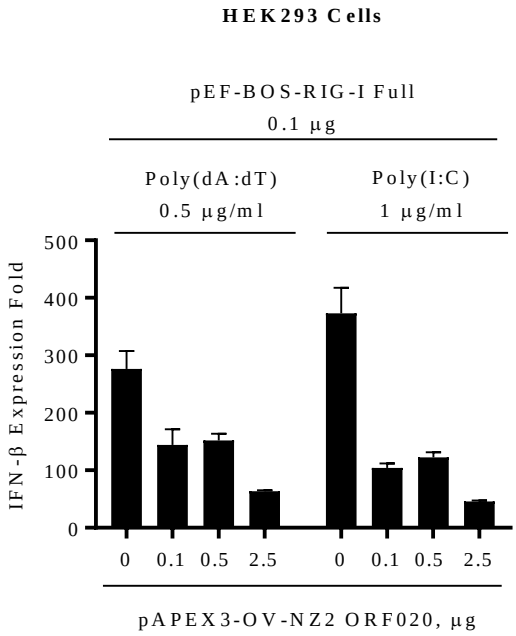

Figure 4.15 Effect of OV-NZ2 ORF020 expression on RIG-I-dependent sensing in HEK293 cells. Human RIG-I and OV-NZ2 ORF020 were co-expressed in HEK293 cells at concentration indicated for 24 hours. Then the cells were stimulated with poly(dA:dT) or poly(I:C) at concentration indicated for 24 hours. The induction of IFN-β was assessed in cells by qRT-PCR in triplicate of technical replicate and expression fold was calculated as described in materials and methods. Data are from one experiment. Error bars represent mean ±SD.

4.8 Detection of Phosphorylated-TBK and Phosphorylated-IRF3 in HEK293 Cells

IFN signalling pathways play a vital role in the regulation of the innate immune response. Upon recognition of PAMP through PRR, signalling pathways are activated leading to induction of type I IFN. Several signalling molecules are involved in this signalling cascade. TBK1 and IRF3 are an indisputably critical signalling axis and their involvement are supported by many lines of evidence. TBK1 is a critical kinase that gets auto-phosphorylated before transducing the signal to IRF3. IRF-3 is expressed constitutively in almost all cell types whereas most IRF family members are expressed only in specialized cell types. IRF-3 is known to regulate expression of IFN-β and interferon-stimulated genes upon its activation determined by phosphorylation, dimerization and translocation to the nucleus, hallmarks of

its activation. Therefore, it is not uncommon that viruses evolve to encode proteins that antagonize the function of TBK1 and IRF3.

It has been clearly shown that OV-NZ2 inhibits IFN-β expression. An attempt was made to understand the underlying mechanism and determine how the virus targets the IFN response. It was hypothesized that the virus either avoids cell receptor recognition or interferes with the signalling molecules. To test this hypothesis, an attempt was made to develop an assay and examine the activation of the signalling molecules (TBK1 and IRF-3) in HEK293 cells infected with OV-NZ2 by using western blot analysis. In the first instance, efforts were made to detect the phosphorylated forms of TBK1 and IRF-3 proteins in HEK293 cells upon stimulation with different concentrations of nucleic acid stimuli for different times points. However, none of these efforts were successful in detecting p-TBK1 or p-IRF-3 (data not shown). The Phosphorylated-TBK1 antibody used in this study detects Ser172 and it was intact as it was able to detect phosphorylated-TBK1 in THP-1 cells stimulated with LPS (Appendix: Figure 9.6), while phosphorylated-IRF-3 antibody detects Ser396. A previous report has shown differential phosphorylation of IRF-3 serine sites (Ser396 or Ser386) in HEK293 cells when stimulated with DNA or RNA molecules (Burleigh, K. *et al.*, 2019). It seems that TBK1 or IRF-3 are phosphorylated at low levels in some cell types when stimulated with poly(dA:dT) making the phosphorylated protein hardly detectable by western blotting (personal communication).

4.9 Early Viral Gene Synthesis was Required for Inhibition of IFN-β Expression in HEK293 Cells

It was hypothesized that the inhibitory effect of OV-NZ2 on IFN-β expression observed was caused by newly synthesized viral protein. An investigation was conducted to test this hypothesis and also to assist in identifying the virus gene(s) involved. A well-established approach widely used in poxvirus studies was undertaken in which the translation of early poxvirus gene transcripts is inhibited without interfering with virus gene transcription.

Of these inhibitors, adenosine N1-oxide (ANO) is a potent and selective inhibitor of poxvirus early protein synthesis due to selective incorporation of the adenosine analogue into viral mRNA resulting in inhibition of viral protein synthesis, consequently inhibiting viral DNA replication and late gene expression. In this study, the detection of OV119 by western blotting was used as an indication of virus early gene production. OV119 is a characterized OV-NZ2 early gene that produces a protein of 31 kDa (Harfoot, R. T., 2015). The optimal amount of

ANO was first determined in HEK293 cells infected with OV-NZ2 and it was found that a concentration of 5 μg/ml caused strong inhibition of OV 119 protein production (Appendix: Figure 9.7). Then IFN-β induction was assessed in ANO-treated HEK293 cells. From the data obtained, ANO seemed to interfere with IFN-β signalling (data not shown); therefore, the option of ANO treatment was excluded in this study.

Cycloheximide (CHX) is a common protein synthesis inhibitor that blocks the elongation phase of eukaryotic translation by binding the ribosome resulting in inhibition of eEF2-mediated translocation, leading to inhibition of virus and host protein synthesis. It is important to note that the required proteins to be inhibited in this study were virus proteins not host proteins. CHX will inhibit cellular protein translation and there might be newly synthesized host proteins required in IFN-β signalling. This notion was supported by work by Smith, E. J. *et al.* (2001). Their work was about testing the requirement for protein synthesis for activation of IRF7 in HEK293T cells upon infection with NDV, they found that cycloheximide treatment for more than 3 hours caused inhibition of IRF7 phosphorylation and they attributed this to the potential blockage of short-lived cellular protein synthesis. From the above findings, a CHX approach was also excluded in this study.

Cytosine arabinoside (AraC) is an inhibitor of viral DNA replication and therefore late protein expression, while early protein expression remains intact. However, prolonged exposure of cells to AraC is unknown and the cells in the proposed assay would need to be incubated for a lengthy time upon stimulation to see a response.

Ultraviolet (UV) light is a practical tool to generate non-replicating virus in which the viral genome gets cross-linked after exposure to UV (Tsung, K. *et al.*, 1996). However, this approach was not appropriate in this study as protein synthesis inhibition by UV treatment is proportional to the size of virus genes and that may cause a blockage in transcription of other early viral genes (Pelham, H. R. B., 1977; Tsung, K. *et al.*, 1996). Therefore, the investigation using UV treatment was not included in this study.

Lastly, inactivating virus by heat has been shown to render VACV non-infectious (Kaplan, C., 1958). Non-infectious particles generated from heat treatment have been characterized previously (Harper, J. M. *et al.*, 1978). They have shown that the machinery of gene transcription of the virus was relatively insensitive and virus could infect the cell and transcribe early genes but their protein synthesis was impaired. Besides, this approach has been used before to study the host immune response to heat-inactivated VACV (Cao, H. *et*

al., 2012) and it has been used also in an influenza virus study (Diebold, S. S. *et al.*, 2004). Since the life cycle of ORFV parallels VACV, it was encouraging to utilize a heat inactivation approach in this study to inactivate early protein synthesis of OV-NZ2. These reports have shown that the optimal temperature and duration of heat treatment is 55 °C for 1 hour, accordingly, these parameters were used in this study to inactivate OV-NZ2.

First of all, the growth of the OV-NZ2 wild type was characterized in HEK293 cells. The cells were infected with the virus at an MOI of 5, then the cells were harvested at various time points and the virus progeny quantified by plaque assay on LT cells. OV-NZ2 shows efficient replication in HEK293 cells (Figure 4.16). The virus showed a distinguishable eclipse phase at 6 hours post infection and exponential growth started at 12 hours post infection until 48 hours post infection then reached a plateau from day 2 giving about 100-fold increase in the virus progeny. This growth characteristics of OV-NZ2 in HEK293 cells was identical to growth in primary host LT cells and HeLa cells (unpublished data).

OV-NZ2 virus inocula were prepared at a multiplicity of infection 5 then the inocula were split into two in which one was treated with heat at 55 °C for 1 hour (referred to as heat inactivated virus) and the other left without treatment (referred to as untreated virus). The early viral gene protein synthesis in HEK293 cells infected either with untreated or heat inactivated virus was examined using OV119 protein as an indicator. The cells were either infected with untreated virus or heat inactivated virus then the cells harvested at 0, 2, 4 and 6 hour post infection. The cell lysates were subjected to western blotting using anti-OV119 antibody. The synthesis of OV119 was detected at 4 hours post infection and the level of OV119 protein increased at 6 hours post infection as shown in Figure 4.17. However, the induction of OV119 protein was completely abolished with heat inactivated virus that has lost early protein synthesis (Figure 4.17). The cytopathic effect (CPE) of infected HEK293 cells was also examined under light microscope. Untreated virus induced clear CPE at 4 hours post infection and increased at 6 hours post infection, whereas, as expected, the heat inactivated virus did not induce CPE (data not shown).

Having established the above, the investigation then assessed the induction of IFN-β expression in HEK293 cells infected with untreated or heat inactivated virus infection. The OV-NZ2-Rev116 virus and OV-NZ2Δ116 were included in this assay to assess whether ORF116 gene has any direct effect on IFN-β induction (see Chapter 3). The cells were infected with either untreated or heat inactivated virus after poly(dA:dT) stimulation or before

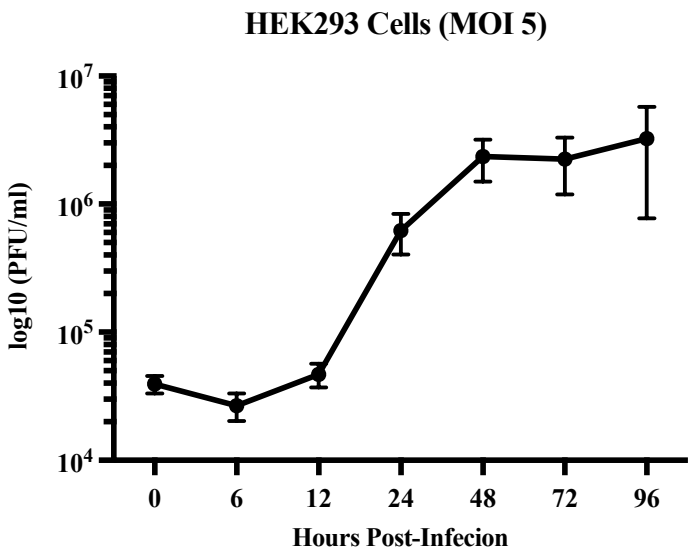

Figure 4.16. One-step growth analysis of OV-NZ2 in HEK293. HEK293 cells were seeded at $4x10^5$ and incubated overnight. At the day of infection, cells were washed with PBS then infected at an MOI of 5 pfu per cell with OV-NZ2 wild type. After 1hr adsorption, cells were washed with PBS to remove unattached virus then 2 ml of DMEM 2 % FCS was added. At various times post-infection, media and infected cells were collected. After three cycles of freezing and thawing, the virus was sonicated and viral titres determined by serial dilution and infection of LT cells. Virus plaques were visualized by staining with neutral red, counted then PFU/ml calculated.

poly(I:C) stimulation. Same virus preparations were used in poly(dA:dT)- and poly(I:C)-stimulated cells and equal amount was assured. Then IFN-β mRNA was quantified by qRT-PCR. The data showed that all live viruses were able to significantly inhibit the induction of IFN-β expression when cells were stimulated with poly(dA:dT) or poly(I:C) and this ability was not retained when cells were infected with heat inactivated virus (Figures 4.18). None of the viruses, untreated or heat inactivated, have induced the expression of IFN-β in un-stimulated cells. These data demonstrated that the virus gene responsible is an early gene(s) and the IFN inhibitory effect requires *de novo* synthesis early viral proteins. With regard to the role of ORF116, the induction of IFN-β has shown no significant difference among the viruses, suggesting that ORF116 has no role or it has been masked by other possible viral factors.

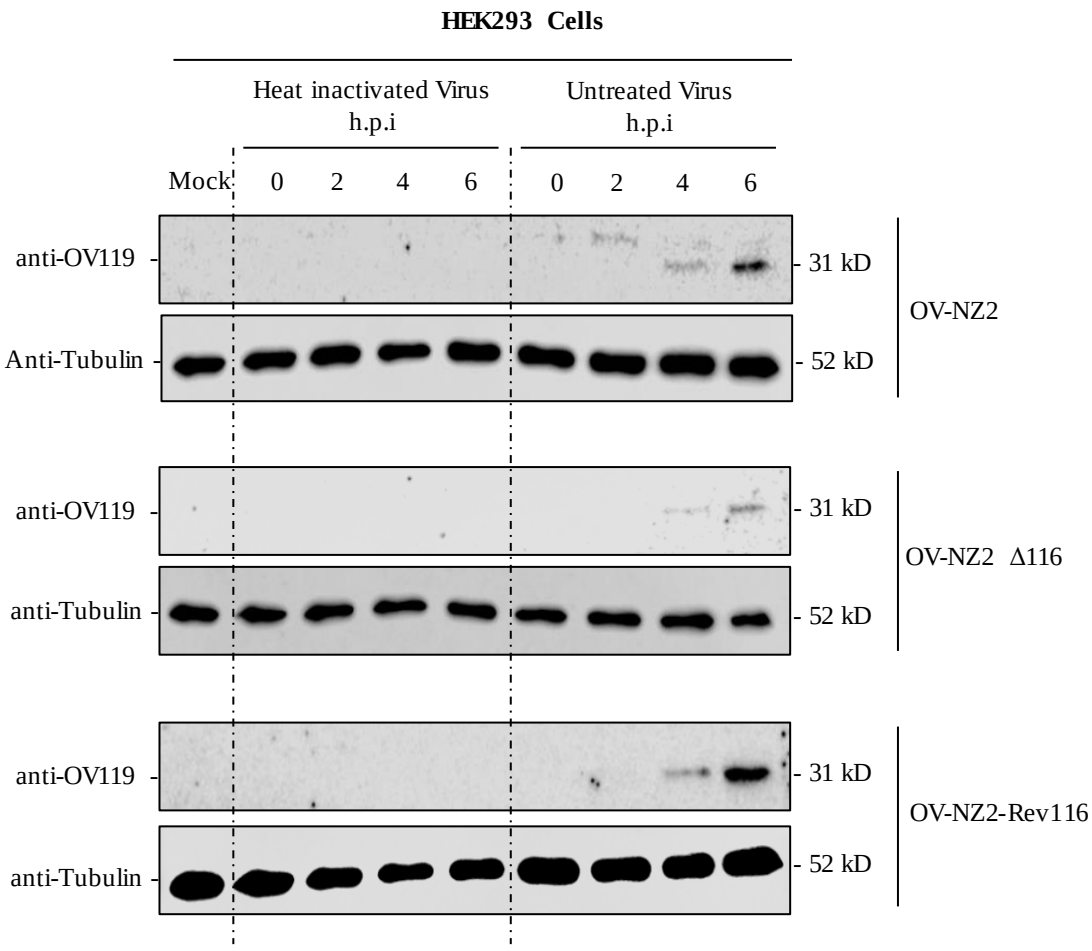

Figure 4.17 Detection of ORFV early protein synthesis in HEK293 cells infected with heat inactivated or untreated virus. HEK293 cells were seeded at $4x10^4$ in a 24-well plate. On the day of infection, virus inocula of OV-NZ2, OV-NZ2Δ116 or OV-NZ2Rev116 were prepared at an MOI of 5, then split into two. One was subjected to heat treatment in water bath at 55 ℃ for 1 hour and the other one left untreated. HEK293 cells were infected with heat inactivated or untreated OV-NZ2, OV-NZ2Δ116 or OV-NZ2Rev116. The cells were harvested and lyzed at 0, 1, 2, 4 and 6 hour post infection. Five microgram of total protein was resolved on a 10 % SDS-polyacrylamide gel and proteins transferred onto nitrocellulose membrane. The membrane was incubated with anti-OV119 antibody and proteins detected by chemiluminescence. The membranes were stripped and incubated with anti-tubulin as a loading control.

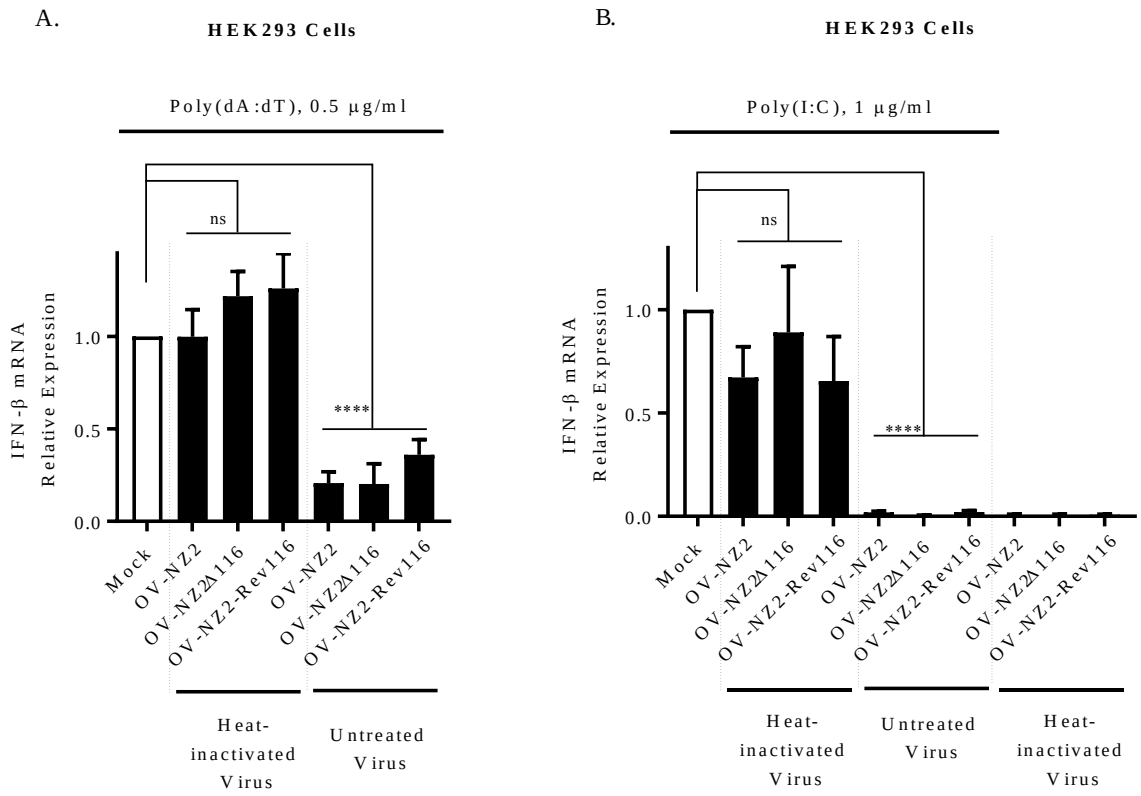

Figure 4.18 Induction of IFN-β by poly(dA:dT) or poly(I:C) in HEK293 cells infected with heat- inactivated or untreated virus. HEK293 cells were seeded at $4x10^4$ cells in a 24-well plate. (**A**) Cells were stimulated with poly(dA:dT) at 0.5 µg/ml and incubated for 4 hours then cells infected with either heat-inactivated or untreated virus:OV-NZ2, OV-NZ2Δ116 or OV-NZ2-Rev116 at an MOI of 5 and incubated for 20 hours. (**B**) Cells were infected with either heat-inactivated or untreated virus: OV-NZ2, OV-NZ2Δ116 or OV-NZ2-Rev116 at an MOI of 5 for 4 hours then cells stimulated with poly(I:C) at 1 µg/ml or left unstimulated and incubated for 20 hours. After incubation, cells were harvested and total RNA was isolated from the cells and IFN-ß mRNA was quantified by qRT-PCR in triplicate of technical replicate. The level of IFN-β mRNA in uninfected sample was considered 1 to compare the infected samples. Data are from three independent experiments. Error bars represent mean ±SD. Statistical analysis was performed using a Student's *t* test. Asterisks indicate probability: $^{ns}P \geq 0.1234$, $^{****}P \leq 0.0001$.

4.10 Effect of Stably Expressed ORF116 on the Induction of Type I Interferon

The manipulation of ISGs observed in the presence of ORF116 suggests that ORF116 is playing a role in modulating the IFN response and it was speculated either by blocking the production of type I interferon from infected cells or directly blocking ISG expression or both (see Chapter 3). However the data obtained from the infection of OV-NZ2, OV-NZ2Δ116 or OV-NZ2-Rev116 was not conclusive about the role of ORF116 on the inhibition of IFN-β (Figure 4.18). To delineate this further the role of ORF116 in isolation from other virus genes was investigated by making cell lines that stably express ORF116 then stimulated with either poly(dA:dT) or poly(I:C). Generating a cell line stably expressing the protein of interest would avoid introducing foreign nucleic acid material into the cells which may elicit an immune response.

A construct of pAPEX3-ORF116-Flag was utilized in which *ORF116* was cloned into pAPEX3-Flag at the *Bam*HI restriction site. The construct was first characterized by restriction analysis and sequencing, and the transient expression of ORF116 was detectable in HEK293 cells by immunoblotting analysis using anti-flag antibody. The predicted size from the amino acid sequence is about 25 kDa, however the size of the peptide detected was larger, probably due to post-translational modification. In addition to this, based on the observations shown in Figures 4.14 and 4.15, *OV-NZ2 ORF020* and human *RIG-I* genes were also included in this assay.

Attempts were made to stably express ORF116 and ORF020 individually in HeLa cells or with RIG-I in HEK293 cells. Generating a stable expressing cell line in HeLa cells would further validate the data obtained from OV-NZ2Δ116 infection in HeLa (Figure 3.11). Whereas generating a stable expressing cell line in HEK293 would provide insight into how the virus manipulates the induction of type I IFN.

pAPEX3 transfectants were selected with hygromycin B at a concentration of 0.1 mg/ml as this concentration was determined previously and shown to be suitable for selection of resistant clones that can kill non-transfectants without causing toxicity to the transfectants. pEF-BOS transfectants were selected with geneticin (G418) at a concentration of 1 mg/ml as determined from the kill curve in this study, consistent with previous reports. Co-transfection was selected by both antibiotics hygromycin B and G418 at the same concentration. All cell

lines were incubated in complete selection media for three months to insure resistant clones were generated.

The transient expression of the three proteins from constructs was confirmed, then cell lines were generated as detailed in material and methods. HeLa cells were transfected either with *ORF116* or *ORF020* and then subjected to antibiotic selection. Whereas HEK293 cells were transfected either with *ORF116*, *ORF020* or *RIG-I* or co-transfected with *RIG-I* then subjected to antibiotic selection. In pAPEX3 transfection, the cell death in control transfection was observed within a week then complete death was observed within two weeks. Whereas same sign of cell death was noticed in pEF-BOS transfection in the first week, complete death was observed after three weeks. After cell lines were generated, they were subjected to western blot analysis to detect the expression of proteins using anti-flag antibody as shown in Figure 4.19 A. Both HeLa-transfected *116* and HeLa-transfected *020* cell lines have shown hygromycin B resistance, but the expression of both proteins was not detectable, more likely the genes were silenced. HEK293-*020* and HEK293-*RIG-I* have also shown hygromycin B and geneticin resistance respectively, but no proteins were detectable on western blot. Nevertheless, HEK293-*116* has shown hygromcin B resistance and the protein was detectable. The co-transfection of *ORF116* and *RIG-I* in HEK293 cells has shown only *ORF116* protein expression but not RIG-I protein, whereas in the co-transfection of *ORF020* and *RIG-I* in HEK293, neither of the proteins were detectable (Figure 4.19 A).

The only cell line that successfully generated stably expressing protein was in HEK293 cells that express the OV-NZ2 ORF116 protein. This cell line was then used to investigate whether ORF116 has a role on the inhibition of type I IFN. The mock cells or cells expressing ORF116 were mock stimulated or stimulated with poly(dA:dT) or poly(I:C) then IFN-β mRNA was quantified by qRT-PCR. The data has shown that ORF116 suppressed the induction of IFN-β expression by about 50% either in poly(dA:dT)- or poly(I:C)-stimulated ORF116-expressing cells (Figure 4.19 B). This data strongly suggests a role played by ORF116 on IFN-β expression and the data in Figure 4.18 could suggest that ORF116 function was masked by other viral immunomodulators.

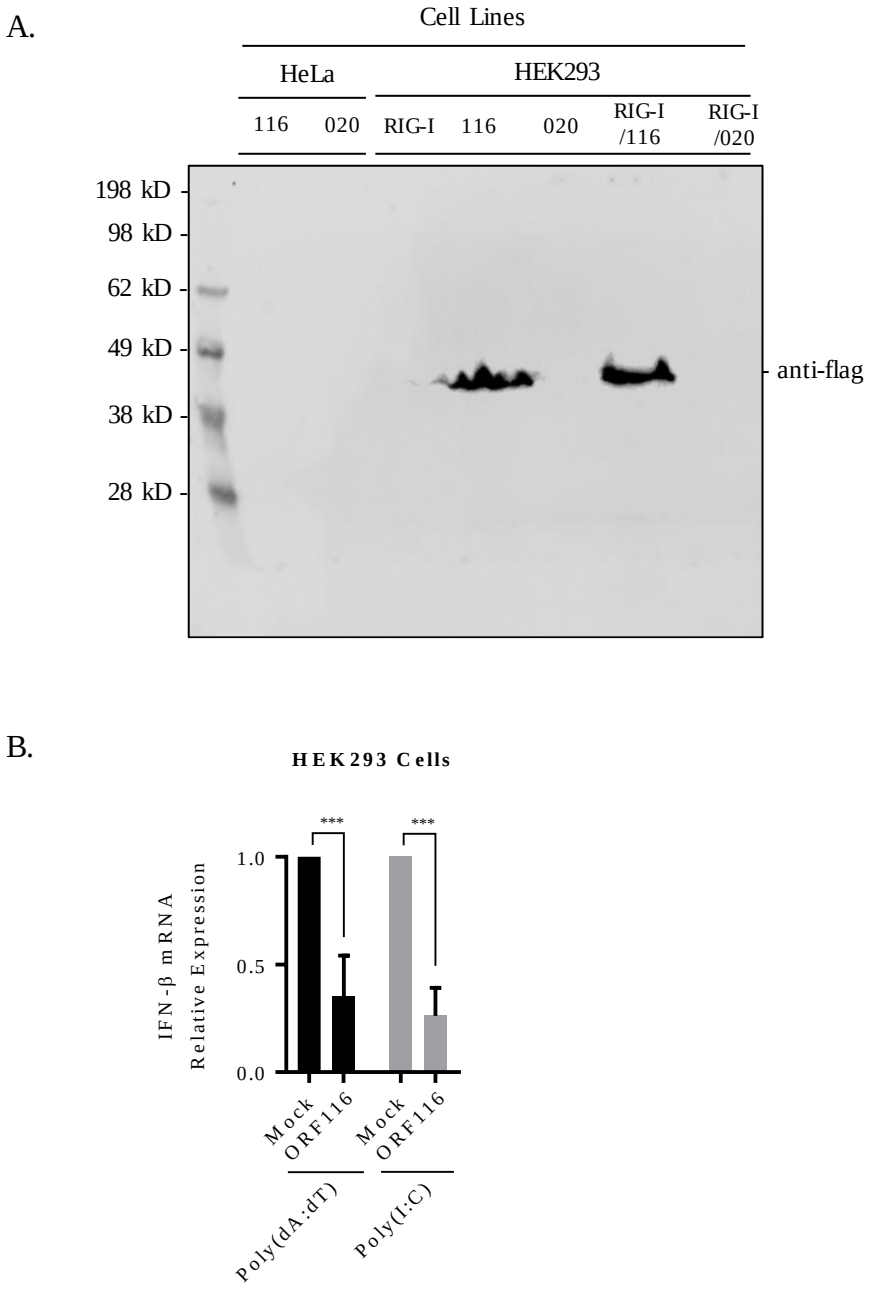

Figure 4.19. Effect of stable protein expression on the induction of IFN-β. (A) Detection of stable protein expression from cell lines by western blot. HeLa or HEK293 cells were stably transfected with indicated plasmids as described in materials and methods. One hundred µg of total protein was resolved on 10 % SDS-PAGE and proteins detected using anti-flag antibody. **(B)** Induction of IFN-ß by poly(dA:dT) and poly(I:C) in HEK293 cell line stably expressing ORF116. The cells were seeded at $4x10^5$ cells in a 6-well plate and stimulated with poly(dA:dT) or poly(I:C) and incubated for 20 hours post stimulation. Total RNA was isolated from cells and IFN-ß mRNA was quantified by qRT-PCR. The level of IFN-β mRNA in untransfected sample was considered 1 to compare the transfected samples. Data are from three independent experiments. Error bars represent mean ±SD. Statistical analysis was performed using the Student's *t* test. Asterisks indicate probability $^{***}P \leq 0.0002$.

4.11 Discussion

This is the first study that demonstrates inhibition of IFN-β expression by ORFV, a critical cytokine in the host antiviral response. Since ORFV replicates in the cytoplasm of the host cell and likely produces dsRNA from convergent transcription, makes it a potential target for cytosolic RNA-dependent sensing. Here, the objective of this part of the study was to investigate the effect of ORFV infection on type I IFN expression upon dsRNA sensing by RIG-I. HEK293 cells proved to be an excellent model to carry out this study in which they were permissive for ORFV, only expressed cytoplasmic RNA sensors RIG-I and MDA-5, responsive to exogenously delivered synthetic dsRNA that mimics virally produced dsRNA and importantly they do not express Toll-like Receptors or cytoplasmic DNA sensors, except for RNA Polymerase III, a feature that was exploited in this study.

Here, it was shown that ORFV clearly interferes with IFN signalling in HEK293 cells triggered either by poly(dA:dT) or poly(I:C) causing significant inhibition of IFN-β expression. These results strongly suggest that ORFV produces molecules that interfere with the signalling pathway leading to expression of IFN-β. It is likely that those viral molecules are synthesised early, and are not structural proteins as demonstrated in assays using heat-inactivated virus. Inhibition of signalling could be direct or it could be indirect. Poxviruses in particular orthopoxviruses directly target pathways that led to IFN production and suggests that the inhibition observed in our assays is likely to be direct although indirect mechanisms may also be possible. The inhibitory effect on IFN-β by ORFV in this study does not appear to be because of a general shutdown of transcription by the virus as the expression of the internal control GAPDH did not change in mock cells compared with infected cells. It is important to note that an attempt to detect IFN-β protein secretion was not conducted because the focus of this study was to investigate the effect of virus infection on IFN signalling pathway that lead to IFN-β expression but not the positive feedback loop effect of IFN. qRT-PCR technique was used to provide accurate quantification of mRNA and provided physiological relevance across different sample conditions.

ORFV, as for other poxviruses, encodes multiple factors at an early stage of infection to counteract the innate immune response at multiple levels including type I IFN induction. It was not unexpected that ORFV infection does not induce type I IFN expression and this could be due to the expression of viral inhibitors or failing to trigger IFN signalling in cell culture. Accordingly, it was essential to trigger the response of the IFN system to examine whether

the virus could inhibit the IFN response or not. In this study, synthetic dsDNA poly(dA:dT) and synthetic dsRNA poly(I:C) were chosen as inducers on the basis of their ability to activate the cytosolic DNA- or RNA-dependent IFN pathways respectively and mimic viral nucleic acids.

The data of kinetic induction of IFN-β has shown that the induction of this cytokine by poly(dA:dT) or poly(I:C) was marginal at early time points post stimulation, then the response was enhanced from 6 hours and increased up to 20 - 25 hours. Poly(dA:dT) induced the expression of IFN-β by about 8000 fold whereas poly(I:C) induced the response by about 500 fold. This fold difference in stimulation could be attributed to the continuous production of dsRNA through the polymerase III-dependent pathway in poly(dA:dT)-transfected HEK293 cells. It was observed that where cells were first stimulated with poly(dA:dT) for four hours then infected with the virus that this resulted in more than 50% and 80% inhibition in IFN-β production by 15 and 20 hours post-infection respectively whereas using poly(I:C) stimulation, in which cells were first infected with virus then stimulated led to more than 80% and 90% inhibition of IFN-β production at 15 and 20 hours post infection respectively.

Surprisingly, it was observed that when infection followed poly(I:C) stimulation, the virus could not significantly inhibit the response and the possible explanation for this could be that the virus might need first to express factors such as ORF020 (VACV E3L homologue) to sequester dsRNA and interfere with dsRNA engagement with receptors. From a comparison between the inhibitory effect of poly(dA:dT)- and poly(I:C)-stimulated cells, it was found that when virus infection preceded stimulation, stronger inhibition was found. It would have been interesting to have conducted the poly(dA:dT) assay by infecting cells before stimulating with poly(dA:dT) to determine whether there was even greater inhibition of IFN. To the best of our knowledge, there are few studies that have utilized a stimulation-infection approach to investigate the effect of virus on the IFN response, apart from assays involving transient expression of individual virus genes. Huang, J. *et al.* (2018) and Marq, J.-B. *et al.* (2009) have utilized this approach in their study, however, the virus infection was prior dsDNA stimulation. Studies have shown that IFN-α/β mRNA is constitutively expressed but at a very low level in the absence of virus or other inducers and this low level of induction is believed to provide weak signalling critical to elicit a stronger response upon virus infection or nucleic acid detection (Takaoka, A. *et al.*, 2006). Thus, when cells are stimulated first, this should not alter the physiological role of IFN signalling until IFN induction is noticeably

increased above the basal level. Here, the cells were infected with the virus at 4 hours post stimulation with poly(dA:dT) which was sufficient time to allow the virus to express all the necessary factors before the induction of IFN-β enters the exponential phase.

It was of great interest to examine specifically where ORFV was inhibiting the dsRNA signalling pathway. The aim was to simplify the model used to a single signalling pathway if possible and to subsequently investigate points of intervention by the virus. The fact that HEK293 cells express RNA polymerase III made this possible using poly(dA:dT). This allowed studies to be carried out specifically on the RIG-I pathway. The RNA polymerase III was blocked to see if this was the case using a specific RNA polymerase III inhibitor (ML-60218), the results showed that poly(I:C) could stimulate but poly(dA:dT) could not in which the induction decreased from about 400 fold to 100 fold. Furthermore, siRNA effectively knocked down RIG-I and blocked IFN-β induction by poly(dA:dT) and poly(I:C), besides, overexpression of RIG-I from a construct remarkably enhanced signalling by poly(dA:dT) or poly(I:C) further confirming the involvement of the RIG-I sensor. In addition its likely that poly(I:C) stimulated RIG-I and not MDA-5 because of its small size. The unavailability of constructs expressing full length MDA-5 or other intermediate signalling molecules prevented studies to examine the effects of ORFV on molecules involved in the IFN signalling pathway. Assays involving the co-expression signalling molecules with ORFV individual genes could also help to provide insight into which signalling factors ORFV targets and the viral genes responsible. Nevertheless, this data narrowed it down to the RIG-I pathway only, via RIG-I sensing and RNA polymerase III-dsDNA sensing pathways.

My data strongly suggested that the inhibition of IFN-β induction was through the RIG-I-dependent pathway in HEK293 cells. This pathway is well defined and operates through MAVS-TBK1/IKKε-IRF3. IRF3 is a key transcription factor for type I IFN induction and it is ubiquitously and constitutively expressed in many cell types. Many studies suggest that the primary role of IRF3 is to initiate the induction of IFN-β at an early stage of the response and is more favoured than IRF7. It is generally believed that the induction of IFN-β is mediated first through IRF3 whereas IRF7 is induced by IFN-β at a later stage and participates in initiating the expression of IFN-α by way of a positive-feedback loop as demonstrated in $IRF3^{-/-}$ or IFN-$\beta^{-/-}$ deficient mice studies (Erlandsson, L. *et al.*, 1998; Sato, M. *et al.*, 2000). When IRF3 is activated, it undergoes sequential posttranslational modification including phosphorylation and the essential kinases for its phosphorylation are TBK1 and IKKε

(Fitzgerald, K. A. *et al.*, 2003; Hemmi, H. *et al.*, 2004; Sharma, S. *et al.*, 2003). These kinases form complexes upon activation with other subunits NAP1, SINTBAD, TANK and DDX3 through TRAF3 downstream of the MAVS adaptor (Kawai, T. *et al.*, 2005; Meylan, E. *et al.*, 2005).

It has been shown that VACV produces multiple factors that block this IFN signalling pathway. For example, C6 interferes with the subunits NAP1, SINTBAD, TANK and prevents TBK1/IKKε-dependent activation of IRF3 and IRF7 (Unterholzner, L. *et al.*, 2011), whereas K7 can interfere with IRF3 activation by interacting with DDX3, an adaptor of TBK1/IKKε (Oda, S. *et al.*, 2009; Schröder, M. *et al.*, 2008; Soulat, D. *et al.*, 2008). N2 acts downstream of IRF3 phosphorylation and inhibits activation of IRF3 after translocation into the nucleus through an unknown mechanism (Ferguson, B. J. *et al.*, 2013). ORFV encodes a number of novel unknown genes and it is possible that some of the factors produced are involved in the blockage of IFN-β production. The block in IFN-β caused by ORFV was striking and it was felt that it was worth attempting to find where the block might have occurred by examining the phosphorylation status of proteins in the signalling cascade.

In this study, attempts were made to detect the phosphorylated forms of endogenous TBK1 and IRF3 in order to track down at which stage of the cytosolic signalling pathway of type I IFN induction the virus was targeting, however, it proved difficult to detect the physiological levels of both proteins in HEK293 cells in response to poly(dA:dT) stimulation. This reflected a limitation of the tools available for this work and not necessarily a technical issue. Poly(I:C) stimulation in the same cells was not tested in this study to investigate TBK1 and IRF3 phosphorylation. The antibodies anti-S396 and anti-S172 have been widely used in many studies to detect phosphorylated IRF3 and TBK1 respectively and to the best of our knowledge, only a few have reported the detection of poly(dA:dT)-induced phosphorylated IRF3 and TBK1 by these antibodies (Liu, D. *et al.*, 2019; Yang, K. *et al.*, 2015). The C-terminal region of human IRF3 has several phosphorylation sites organized into two clusters: two serine sites Ser385/Ser386 and five serine-threonine sites: Ser396/Ser398/Ser402/Thr404/Ser405. Servant, M. J. *et al.* (2003) have found that the S396 residue is sufficient to activate IRF3 whereas Mori, M. *et al.* (2004) found S386 to be a critical residue however, these two studies did not use poly(dA:dT) as an inducer for IRF3 activation. Further anti-S386 as used against phosphorylated IRF3 by Burleigh, K. *et al.* (2019) in HEK293 cells could be useful. The possible reasons that phosphorylated IRF3 could not be

detected here were that phosphorylation of IRF3 residues is stimulus- and cell type-dependent or possibly the phosphorylated IRF3 level was well below the detectable limit. This could also be the case for phosphorylated TBK1. An Enzyme-linked immunosorbent assay (ELISA) technique for the detection of protein phosphorylation could be an alternative approach. It is more sensitive than western blotting and detects precisely low abundant phosphorylated proteins. Besides, it can accurately quantify phosphorylated proteins across different sample treatments. In addition assays for IRF3 dimerization and nuclear translocation in the context of ORFV infection could be conducted to determine signalling events.

In an attempt to determine gene(s) involved in the inhibition of IFN-β induction, the manipulation of ISGs by ORF116 prompted an investigation to examine whether this gene modulates IFN-β production. Preliminary data showed that ORF116 expressed from a cell line caused about a 50% reduction in IFN-β induction in poly(dA:dT)- or poly(I:C)-stimulated cells compared to mock stimulated cells. Although the result was promising unfortunately an empty vector control had not been made at the time the assay was conducted which would have provided strong evidence that this gene inhibits IFN-β production. In contrast the ORF116 deletion mutant showed no difference in IFN-β inhibition in comparison with OV-NZ2 *wt* and OV-NZ2-Rev116 in poly(dA:dT)- or poly(I:C)-stimulated cells. A possible explanation could be that the ORF116 effect is masked by other factors expressed by the virus acting on the RIG-I signalling pathway. An intriguing possibility is that ORF116 is targeting IRF-3 as both the RIG-I signalling pathway and direct induction of ISG expression (IFN independent) both operate through IRF-3.

Assays were undertaken to determine whether IFN-β inhibition requires new virus protein synthesis. A heat inactivation approach was utilized over chemical inactivation e.g. binary ethyleneimine and β-propiolactone to inhibit virus early protein synthesis without affecting viral particle fusion and the early gene transcriptional machinery. The heat-inactivated virus failed to inhibit the expression of IFN-β in cells stimulated with poly(dA:dT) or poly(I:C), suggesting that inhibition requires new virus protein synthesis. Interestingly some variation were observed in fold change of IFN-β induction between the three heat-inactivated viruses in poly(I:C)-stimulated cells. The heat-inactivated virus preparation used in poly(I:C)-stimulated was the same as in poly(dA:dT)-stimulated; besides, equal amounts of input virus was assured. This difference in IFN-β induction was more likely due to genetic differences between the viruses. A variation of IFN-α induction between some live parental and

recombinant viruses or between low MOI or high MOI has been reported by other investigators (Büttner, M. *et al.*, 1995).

ORF020 is a dsRNA-binding protein expressed early during virus infection. The strategy of dsRNA sequestration is not only used by poxviruses but also by other dsDNA viruses such as HSV (US11) (Poppers, J. *et al.*, 2000) and RNA viruses such as IAV (NS1) (Lu, Y. *et al.*, 1995) to prevent the activation of PKR and OAS. ORF020 was shown to bind dsRNA and prevent the activation of PKR and OAS, however, its importance in blocking dsRNA-mediated induction of type I IFN was not investigated. A number of viruses that have been reported to block the induction of IFN may do so by sequestering dsRNA such as HBV core antigen (Twu, J. S. *et al.*, 1989; Whitten, T. M. *et al.*, 1991). Here, ORF020 was studied in isolation of other virus genes by expressing it from a vector in HEK293 cells. From the ectopic expression of ORF020, the gene was able to block the production of IFN-β in a dose-dependent manner in cells stimulated with poly(I:C) or poly(dA:dT) and this observation was consistent with those of shown for VACV E3L (Marq, J.-B. *et al.*, 2009; Valentine, R. *et al.*, 2010). In addition, ORF020 was found to compete with RIG-I signalling in a co-expression experiment. Although the experiment needs to be repeated and include an empty vector control, these two observations imply a critical role played by this gene in manipulating the RIG-I-dependent IFN response. The exact mechanism of IFN-β inhibition has yet to be elucidated, however, possible effects of ORF020 could be predicted based on studies of the VACV E3L homologue (Chang, H. W. *et al.*, 1992). Besides dsRNA-binding activity, E3L has multiple functions including inhibition of IRF3 and IRF7 activation and preventing the induction of type I IFN (Smith, E. J. *et al.*, 2001; Xiang, Y. *et al.*, 2002). It has been shown that the activation of IRF3 during VACV infection was PKR-dependent and that response was antagonized by VACV E3L (Zhang, P. *et al.*, 2008). The role of E3L as an IFN antagonist was further demonstrated in E3-transgenic mice that showed resistance to viruses (Domingo-Gil, E. *et al.*, 2008). It is speculated that ORF020 could act similarly to VACV E3L in antagonizing the IFN response. Further studies on ORF020 will provide further insight into the mechanism of ORFV evasion of cytosolic RNA sensing. Further studies could involve screening ORFV early genes by cloning them into expression vectors and determining their potential to inhibit IFN-β expression and also using pull-down experiments to find their cellular binding partners.

In summary, the effect of ORFV infection on the dsRNA-dependent IFN response was investigated and it was found for first time that the virus was able to block IFN-β production at the transcriptional level. Furthermore, the IFN antagonism employed by the virus has been caused by viral early genes. It was also shown that IFN-β inhibition was via RIG-I-dependent signalling in HEK293 cells. The exact mechanism that ORFV employs to interfere with RIG-I-dependent signalling and cellular molecules targeted by the virus are not yet known. Whether simply sequestering dsRNA is the main strategy or whether other as yet unknown factors such as the range of factors that VACV employs (A46, C6, K7, and N2) has yet to be determined.

RESULTS III

5 RESULTS III: Effect of ORFV Infection on IFN-β Expression (DNA Sensor-Dependent Pathway)

5.1 Overview

Upon ORFV infection, genomic DNA is exposed to the cytoplasm after the viral core is uncoated. Recent reports have shown that viral genomic DNA, such as VACV, can elicit an IFN response by inducing type I interferons in a TLR9-independent manner. This observation suggested that there is another mechanism of DNA sensing that can recognize DNA in the cytosol (Hochrein, H. *et al.*, 2004; Ishii, K. J. *et al.*, 2006). TLR9 recognizes only unmethylated CpG DNA in the endosome and requires a specific pathway to elicit the IFN response: MyD88/IRAK1 and IRAK4/TRAF6/IRF7 (Honda, K. *et al.*, 2004; Kawai, T. *et al.*, 2004). Besides, its expression is predominantly in immune cells such as plasmacytoid dendritic cells (Ishii, K. J. *et al.*, 2006; Stetson, D. B. *et al.*, 2006).

It has previously been shown that double stranded DNA oligonucleotides such as a 70-base pair oligonucleotide from VACV or IFN-stimulatory DNA (ISD) induce type I IFN in macrophages through STING (Ishikawa, H. *et al.*, 2009; Unterholzner, L. *et al.*, 2010). The STING adaptor is an ER resident protein that facilitates an innate immune response. It has been clearly shown that detection of intracellular DNA by DNA receptors results in induction of type I interferon in a STING-dependent manner through the STING-TBK1-IRF3 axis (Figure 5.1) (Burdette, D. L. *et al.*, 2012; Ishikawa, H. *et al.*, 2008; Ishikawa, H. *et al.*, 2009).

In order to investigate the effect of OV-NZ2 infection on the DNA sensing pathway, an appropriate cell type was sought to provide an ideal model system of DNA-dependent sensing in which they respond to poly(dA:dT) and provide a consistent measurement of the effect of stimulation and most importantly these cell types are permissive for virus growth, at least viral early gene synthesis.

ORFV causes an infection in the skin of the natural host and the predominant cell type residing in the epidermis are keratinocytes. Keratinocytes are highly specialized cells triggering the innate immune response and work as immune sentinels. HaCaT cells are a human keratinocyte cell line and it was initially tested and showed a strong induction of IFN-β expression upon stimulation with poly(dA:dT), but it showed no sign of OV-NZ2 infection, no early gene synthesis or virus replication (Appendix: Figure 9.8). Accordingly, this cell line was not appropriate and excluded from this study.

THP-1 is a human leukemia monocytic cell line and is commonly used in cytosolic DNA sensing studies (Jønsson, K. L. *et al.*, 2017; Unterholzner, L. *et al.*, 2010). THP-1 cells were first examined in their response to poly(dA:dT) and OV-NZ2 infectivity. They have shown a strong immune response upon stimulation with poly(dA:dT) and although the virus synthesizes its early proteins, it does not replicate in these cells.

Human neonatal dermal fibroblast (hNDF) cells were found to be an appropriate model in this study to investigate the effect of OV-NZ2 virus on STING-dependent IFN-β expression. This cell type expresses STING and respond to poly(dA:dT) transfection, besides, they are permissive for virus replication. The investigation carried out in this part of the study to examine the effect of OV-NZ2 infection on the DNA-sensing pathway were mostly conducted on hNDF cells. These highly specialized cells not only express STING-dependent DNA sensors but also express RNA sensors and those sensors either work through the endosomal pathway such as TLR3 or cytosolic pathway such as RIG-I and MDA5, which makes the system more complex to investigate (Figure 5.1).

5.2 Induction of IFN-β Expression in THP-1 Cells stimulated with Poly(dA:dT)

The cellular response to synthetic dsDNA poly(dA:dT) and induction of IFN-β expression were first investigated in THP-1 cells. THP-1 are a monocyte-like suspension cell line and they need to be differentiated into macrophage-like cells to respond to the stimulus. The cells were differentiated by PMA, a widely used reagent, and the cell morphological phenotype was examined by light microscopy determined by adherence to the surface, their macrophage-like phenotype and that they had stopped proliferating.

Determination of the PMA concentration was essential to determine the optimal priming conditions. THP-1 cells were primed with an increasing amount of PMA (5, 50, 100 and 300 ng/ml) for 3, 24, 48, 72 or 96 hours before being washed with PBS followed by resting the cells for up to 96 hours. The cells phenotype was assessed every day by light microscopy. At 24 hours, macrophage-like cells started to appear and the cells appeared more macrophage-like at 48-72 hours and this observation was observed irrespective of the presence or absence of PMA. By 96 hours of priming, the cells started to become larger in size and behave as activated macrophages (data not shown). With regard to the concentration, below 100 ng/ml of PMA was not enough to prime the cells even up to 4 days while above 100 ng/ml was enough to efficiently prime the cells. So the conditions of priming used in this assay were

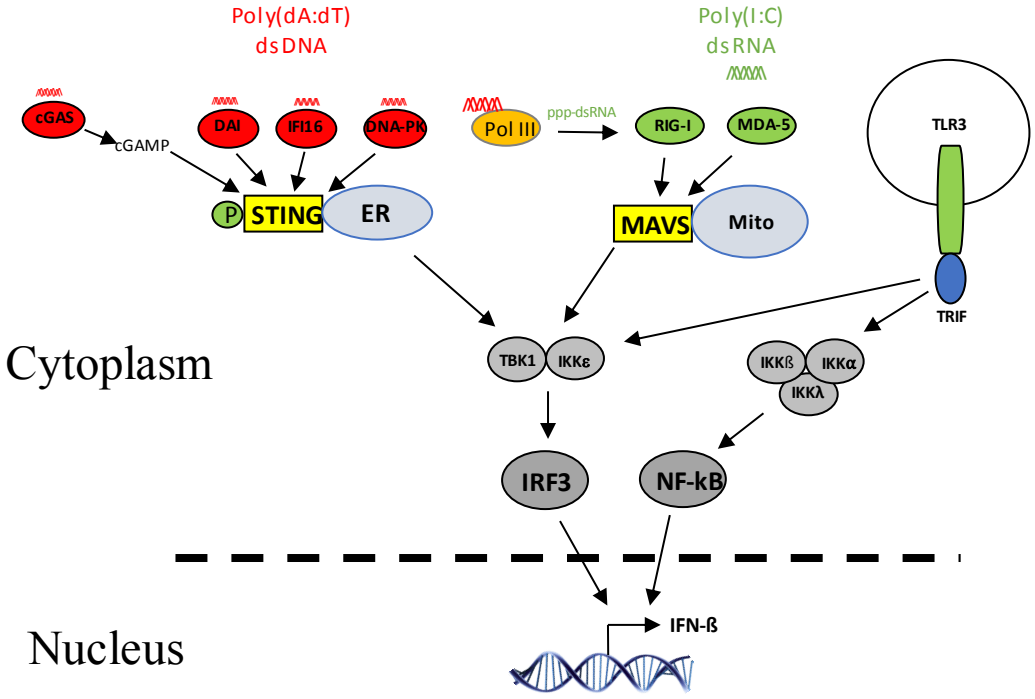

Figure 5.1. Experimental model to study the effect of OV-NZ2 on STING-dependent pathway of IFN-ß expression. A diagram representing DNA sensing mechanism and RNA-sensing mechanism. The DNA sensors cGAS, DAI, IFI16, DNA-PK and Pol III are localized in the cytosol and utilized the adaptor STING residing on the endoplasmic reticulum. They detect DNA in the cytosol and trigger the STING-dependent signalling leading to the activation of TBK1/IKKε and IRF3 that result in IFN-β expression. A unique feature with cGAS in which it synthesize the production of cGAMP dinucleotides that bind STING. RIG-like receptors are localized in the cytosol and utilize the adaptor MAVS. RIG-I receptor senses short dsRNA and also ppp-dsRNA derived from polymerase III-transcribed poly(dA:dT), whereas MDA5 senses long dsRNA. Upon ligand binding, RLRs engage the adaptor MAVS located on the outer membrane of mitochondria then lead to the downstream signalling to TBK1/IKKε-phosphorylating IRF3 and IFN expression. TLR3 is localized in the endosome and utilizes the adaptor TRIF. Upon recognising dsRNA, it can lead to IFN-β expression through TBK1/IKKβ-IRF3 and IKKα/IKKβ/IKKλ-NF-κB axis.

300 ng/ml of PMA for 3 hours of exposure then the cells were washed and incubated for 2 to 3 days of resting. Similar conditions are described by Starr, T. *et al.* (2018).

The investigation then assessed the cellular response to poly(dA:dT) and its ability to stimulate cytosolic DNA sensing pathways in THP-1 cells. The cells were first primed with PMA, then transfected with poly(dA:dT) and the induction of IFN-β mRNA was quantified

by qRT-PCR. Kinetic analysis was also performed to assess the time course of type I IFN induction. It was shown that the induction of IFN-β was detectable at about 2 hours post-stimulation then continued to accumulate up to 15 to 20 hours post-stimulation reaching about 800 fold followed by a slight increase over the next 5 hours (Figure 5.2 A). The optimal dose of poly(dA:dT) was also determined in THP-1 cells in which the primed cells were transfected with increasing amounts of poly(dA:dT) then IFN-β mRNA was quantified by qRT-PCR at various time points. The induction of IFN-β was detected at 2 hours post stimulation and increased over 10 and 15 hours. A distinguishable dose-dependent difference was observed at 10 hours post stimulation for poly(dA:dT) whereas at 15 hours the responses of all poly(dA:dT) concentrations (0.1, 0.5 and 1 μg/ml) had reached a similar level (Figure 5.2 B). Fold change of IFN-β induction was calculated as described in materials and methods. Because fold differences were huge and that have led to large differences across biological replicates, *p* values could not be used and one of three biological replicates is presented.

5.3 Inhibitory Effect of ORFV Infection on IFN-β Expression in THP-1 Cells stimulated with Poly(dA:dT)

As expected, THP-1 cells responded to poly(dA:dT) and produced type I interferon. Next, the effect of OV-NZ2 infection on IFN-β expression was investigated in THP-1 cells. The cells were primed with PMA and treated with poly(dA:dT) then infected with OV-NZ2 and IFN-β expression examined. Initially, the stimulation was conducted at intervals of 2, 4, 6, 10, 15 and 20 hours post infection and it was found that the virus showed to some extent an inhibitory effect on IFN-β expression with a bimodal pattern (data not shown). Attempts were made to thoroughly optimize the assay by looking at the duration of poly(dA:dT) stimulation before infecting cells or vice versa and by looking at the duration of virus infection before stimulating cells with poly(dA:dT). None of these attempts showed any differences (data not shown). Nevertheless, it was noticed that from three biological repeats the virus showed a consistent inhibition of IFN-β expression specifically at 10 hours post infection (Figure 5.3). OV-NZ2 can infect PMA-primed THP-1 cells and synthesize early viral proteins (Figure 5.4 A) but the cells were not permissive for virus replication (Figure 5.4 B). Other reports have shown the synthesis of a VACV late gene D8 in THP-1 infected with VACV strains COP or WR but not MVA (Georgana, I. *et al.*, 2018; Meade, N. *et al.*, 2019). These data have shown that OV-NZ2 counteracts the IFN response triggered by DNA sensing signalling. As the virus does not replicate in THP-1 but can express early genes, this IFN response antagonism observed was more likely caused by early viral genes.

A.

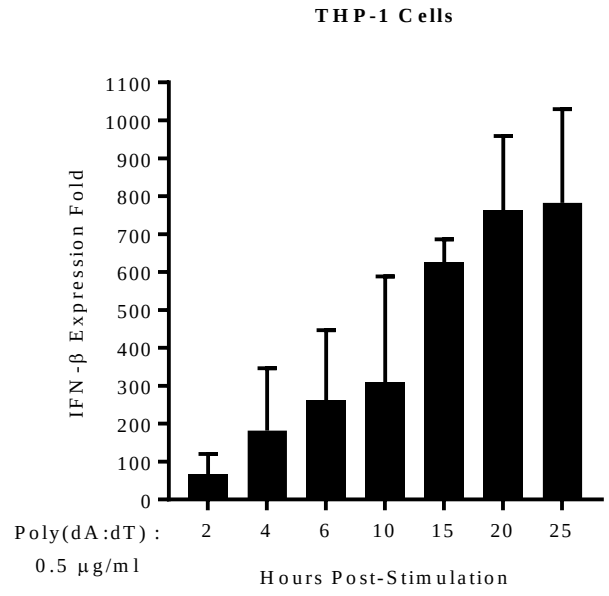

B.

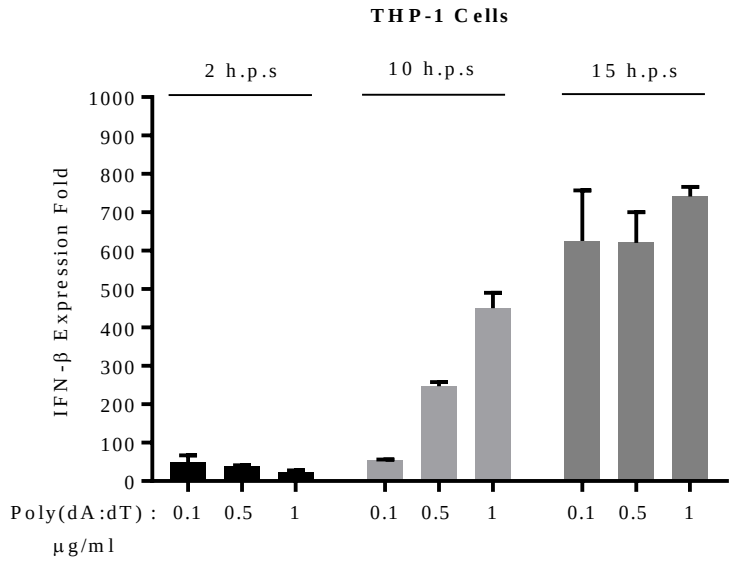

Figure 5.2 IFN-β induction in THP-1 cells. **(A)** and **(B)** THP-1 cells were seeded at $1x10^6$ cells in 6-well plates. After overnight incubation, the cells were first primed with PMA (300 ng/ml) for three hours then the medium changed and left for resting for three days. At day 3, cells were stimulated with poly(dA:dT) at a concentration of 0.5 µg/ml **(A)** or 0.1, 0.5 or 1 µg/ml **(B)** and incubated until the harvesting times indicated. Total RNA was isolated from the cells and IFN-β mRNA was quantified by qRT-PCR in triplicate of technical replicate. Expression fold was calculated as described in materials and methods. Data are from one representative experiment of three independent experiments. Error bars represent mean ±SD.

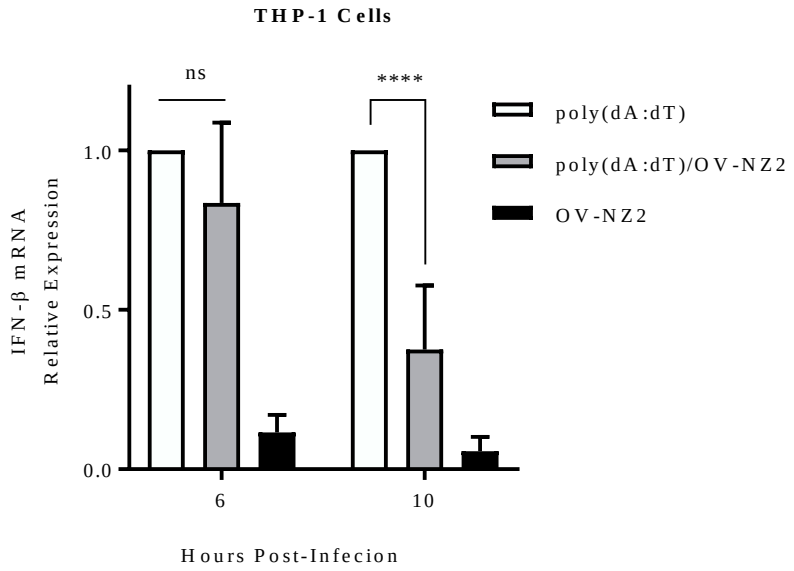

Figure 5.3. Effect of OV-Z2 virus infection effect on IFN-β Induction in THP-1 cells. THP-1 cells were seeded at $1x10^6$ cells in 6-well plates. After overnight incubation, the cells were first primed with PMA (300 ng/ml) for three hours then the medium changed and left for three days. At day 3, cells were stimulated with 0.5 µg/ml poly(dA:dT) and incubated for 4 hours. Then cells were infected at an MOI of 5 with OV-NZ2. At 6 and 10 hours post-infection, total RNA was isolated from cells and IFN-β mRNA was quantified by qRT-PCR. qPCR was conducted in triplicate. The level of IFN-β mRNA in uninfected sample was considered 1 to compare the infected samples. Statistical analysis was performed using Student's *t* test. Data are from three independent experiments. Error bars represent mean ±SD. Asterisks indicate probability: $^{ns}P \geq 0.1234$, $^{****}P \leq 0.0001$.

5.4 OV-NZ2 does not Inhibit IL-1β Release from Poly(dA:dT)-stimulated THP-1 Cells

Cytosolic DNA sensing can also activate the inflammasome pathway leading to the secretion of IL-1ß and IL-18 (Hornung, V. *et al.*, 2009). They are pro-inflammatory cytokines and initiate the immune response when they bind to their receptors (Sims, J. E. *et al.*, 2010). Pro-inflammatory stimuli such as MPA and LPS induce expression of inactive pro-forms of IL-1β and IL-18. Maturation of these precursors requires the proteolytic cleavage of caspase-1 in particular, after it gets activated by the inflammasome, to release active forms of IL-1β and IL-18. Activation of the inflammasome AIM2-ASC pathway was found to be crucial for

A.

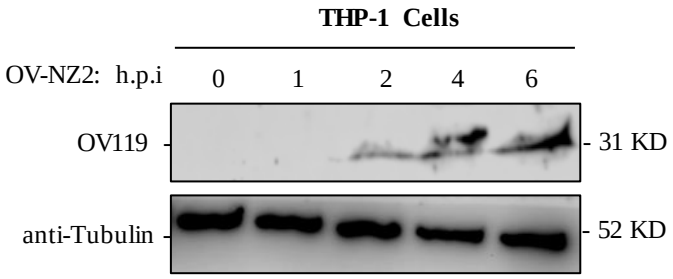

B.

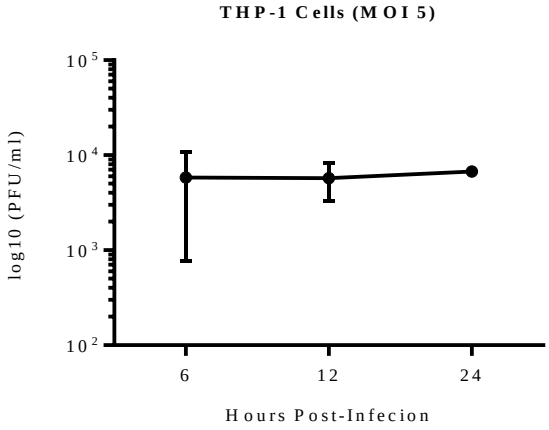

Figure 5.4. Characteristics of OV-NZ2 early gene protein synthesis and virus replication in THP-1 cells. THP-1 cells were seeded at $1x10^6$ cells in 6-well plates. After overnight incubation, the cells were first primed with PMA (300 ng/ml) for three hours then the medium changed and left for three days. **(A)** Cells were washed with PBS then infected with OV-NZ2 at am MOI of 10. Cells were lysed at the indicated times and 10 µl of cell lysate was resolved on a 10 % SDS-polyacrylamide gel for western blotting. The membrane was incubated with anti-OV119 antibody and proteins detected by chemiluminescence. Tubulin was used as a protein loading control. **(B)** THP-1 cells were infected at an MOI of 5 with OV-NZ2. At various times post-infection, media and infected cells were collected. After three cycles of freezing and thawing, the virus was sonicated and viral titres determined by serial dilution and infection of LT cells. Virus plaques were visualized by staining with neutral red and counted, then PFU/ml calculated.

innate immunity to DNA viruses (Rathinam, V. A. K. *et al.*, 2010). Therefore, it was of interest to investigate the effect of OV-NZ2 on inflammasome signalling.

THP-1 is the most commonly used cell type for the study of inflammasome activation. The investigation was conducted by measuring the release of IL-1β into the medium. THP-1 cells were primed with PMA before carrying out the experiment to promote monocytic differentiation and induce pro-IL-1ß expression. The kinetics of IL-1β secretion was first examined in THP-1 cells in which the cells were stimulated with an increasing amount of poly(dA:dT) and cell media collected at intervals. The secretion of IL-1β was determined by ELISA. From the Figure 5.5 A, the secretion of IL-1β was detected at about 4 to 6 hours post stimulation then accumulated over time until it reached a plateau by 20 hours post stimulation in a dose-dependent manner.

Having established the above, an investigation of the virus effect on inflammasome signalling was conducted. The cells were either unstimulated or stimulated with poly(dA:dT) for 4 hours, then either mock infected or infected with OV-NZ2. After 20 hours of incubation, the secretion of IL-1β was measured by ELISA. As shown in Figure 5.5 B, the virus did not inhibit the release of IL-1β in poly(dA:dT)-stimulated cells as there was no difference in IL-1β levels between uninfected and infected stimulated cells, and this observation was seen even at a lower dose of virus or poly(dA:dT) used (data not shown). It was not entirely unexpected that OV-NZ2 has induced the release of IL-1β. VACV (Western Reserve strain) was found to trigger the inflammasome and induced the release of IL-1ß from bone marrow-derived macrophage cells (Rathinam, V. A. K. *et al.*, 2010); however, VACV expresses secretory soluble viral receptors (B15R and B18R) that sequester IL-1β and disable it from binding to its receptors (Alcami, A. *et al.*, 1992; Smith, G. L. *et al.*, 1991).

5.5 Detection of Phosphorylated-TBK in THP-1 Cells

As explained in section 4.8, efforts were made to detect the phosphorylated-forms of TBK1 proteins in THP-1 cells upon stimulation with poly(dA:dT). None of these efforts were successful to detect p-TBK1 in poly(dA:dT)-stimulated cells but it was detectable in LPS-stimulated cells (Appendix: Figure 9.6).

A.

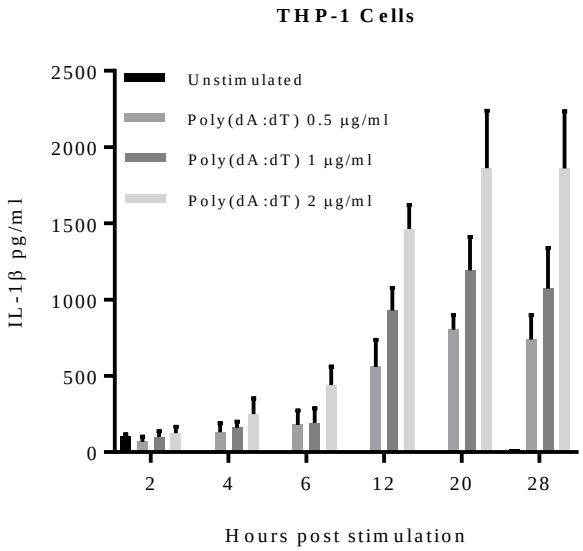

B.

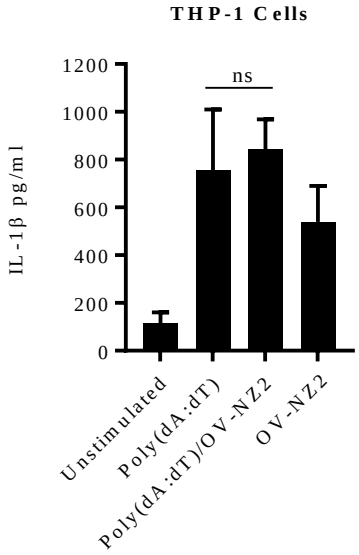

Figure 5.5 OV-NZ2 does not inhibit the release of IL-1β from THP-1 cells. (**A**) The THP-1 cells were primed with PMA (300 ng/ml) for 3 hours. After three days, the cells were unstimulated or stimulated with poly(dA:dT) 0.5, 1 or 2 µg/ml for the indicated time. (**B**) The THP-1 cells were primed with PMA (300 ng/ml) for 3 hours. After three days, the cells were unstimulated or stimulated with poly(dA:dT) 0.5 µg/ml for four hours, then cells mock infected or infected with the virus at an MOI of 5 and incubated for 20 hours. Supernatants in (**A** and **B**) were collected and analysed for IL-1β secretion by using ELISA. ELISA was conducted in duplicate. Statistical analysis was performed using a Student's *t* test. Data are from two independent experiments with three ELISA assays (**A**) and three independent experiments (**B**). Error bars represent mean ±SD. ns indicates probability $^{ns}P \geq 0.1234$.

5.6 Induction of IFN-β Expression in hNDF Cells stimulated with Poly(dA:dT) or Poly(I:C)

Human neonatal dermal fibroblast (hNDF) cells were another cell type used to represent the model of cytosolic DNA sensing in this study. In first instance, the cellular response to poly(dA:dT) or poly(I:C) and induction of type I IFN in these cells was assessed. The cells were transfected with poly(dA:dT) or poly(I:C) and the induction of IFN-ß was quantified by qRT-PCR. Kinetic analysis of IFN induction was also performed to assess the time course for type I IFN induction. Fold change of IFN-β induction was calculated as described in materials and methods. Because fold differences were huge and that have led to large differences across biological replicates, *p* values could not be used and one of three biological replicates was presented.

It was shown that poly(dA:dT) induced IFN-β expression at about 4 hours post-stimulation and IFN-β expression continued to accumulate up to 10 hours post stimulation with a slight increase at 15 hours reaching more than 10000 fold (Figure 5.6 A). The strongest response was observed at 10 to 15 hours of post-stimulation irrespective of slight decrease or increase at 20 hours post stimulation across the biological replicates. The optimal dose response for poly(dA:dT) was also assessed in hNDF cells, in which the cells were transfected with increasing amounts of poly(dA:dT) then IFN-β mRNA quantified by qRT-PCR at various time. Poly(dA:dT) induced a distinguishable dose-dependent response at 10 hours post-stimulation and the concentration of 0.5 μg/ml was sufficient to produce a strong response with no difference compared to 1 μg/ml (Figure 5.6 B). At 15 hours post stimulation across biological replicates, the three doses have produced variable levels of response in which they produced similar pattern as in 10 hours post stimulation or produced similar level of responses.

With regard to poly(I:C) stimulation, poly(I:C) induced IFN-β expression in hNDF cells that was detectable at 4 hours post-stimulation, then increased over time to 15 hours post-stimulation reaching about 2000 fold (Figure 5.7 A). A dose response assay was also conducted that showed a distinguishable dose-dependent response at 10 hours post stimulation and the concentration of 1 μg/ml was sufficient to produce a strong response (Figure 5.7 B). At 15 hours post stimulation, poly(I:C) produced a similar pattern to poly(dA:dT). There was no difference in the level of response beyond the concentration of 1 μg/ml (Figure 5.7 C).

A.

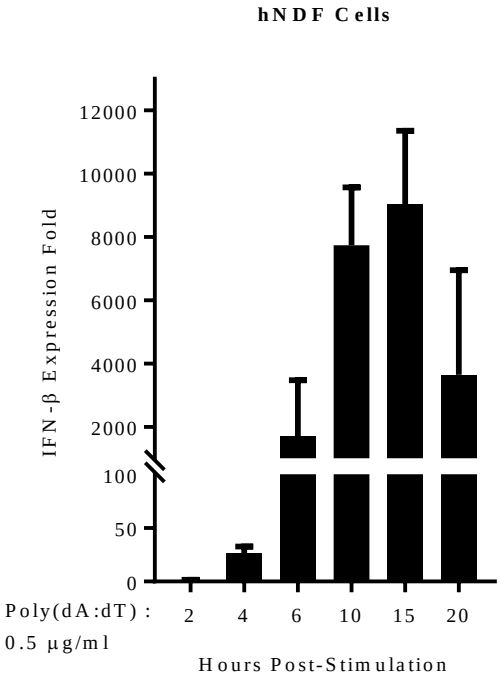

B.

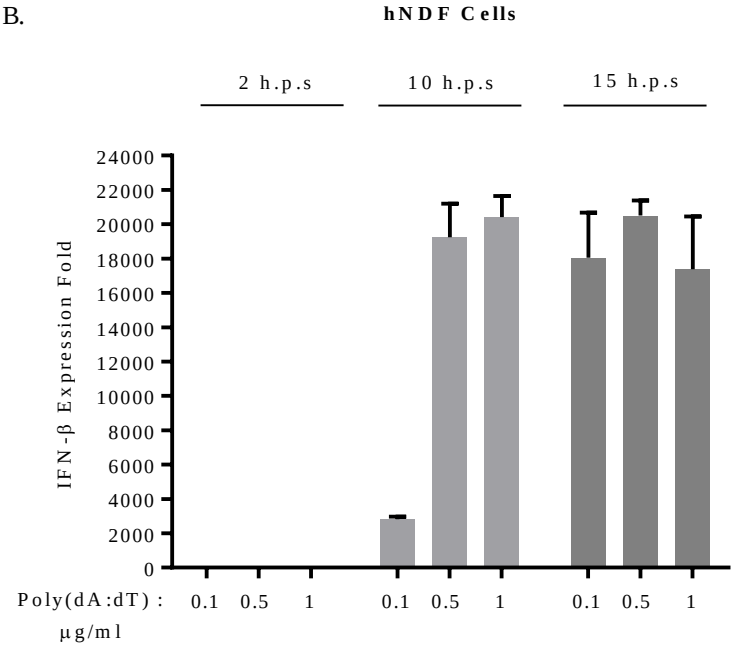

Figure 5.6 IFN-β Induction in hNDF cells with poly(dA:dT). (**A**) and (**B**) hNDF cells were seeded at $4x10^5$ cells in 6-well plates. Cells were stimulated with poly(dA:dT) at a concentration of 0.5 µg/ml (**A**) or 0.1, 0.5 or 1 µg/ml (**B**) and incubated for the times indicated. Total RNA was isolated from the cells and IFN-β mRNA was quantified by qRT-PCR in triplicate of technical replicate. Expression fold was calculated as described in materials and methods. Data are from one representative experiment of three independent experiments. Error bars represent mean ±SD.

As explained in section 4.2, poly(I:C) was delivered into hNDF cells either complexed to

cationic lipid LyoVec, or not, then IFN-β mRNA was quantified by qRT-PCR. Poly(I:C) activated the IFN signalling pathway when complexed to LyoVec. In contrast, free poly(I:C) did not lead to induction of IFN-β expression (Figure 5.7 C). This result suggests that the TLR3 receptor does not detect the poly(I:C) in this assay system and that the IFN-β expression observed was through cytosolic RNA receptors. TLR3 detects dsRNA not only in the endosome, but also from the extracellular environment, and then is taken-up through the endosomal pathway. The cationic lipid LyoVec transfection reagent consists of a combination of phosphonoloipid DTCPTA for cell membrane interaction and neutral lipid DiPPE for nucleic acid fusion with the cell membrane. The mechanism of nucleic acid uptake into the cell using these types of cationic lipids was proposed previously in which the lipid facilitates the nucleic acid transfection and escape from the endosome into the cytoplasm (Fasbender, A. *et al.*, 1997; Guillaume-Gable, C. *et al.*, 1998).

5.7 Inhibitory Effect of ORFV Infection on IFN-β Expression in hNDF Cells stimulated with Poly(dA:dT)

Having established that hNDF cells responded to transfected synthetic dsDNA and produce type I interferon, next an investigation was conducted to test whether OV-NZ2 infection has an effect on type I interferon expression. hNDF cells were stimulated with poly(dA:dT) at a concentration of 0.5 μg/ml for 4 hours then infected with OV-NZ2 at different MOI's for 10 hours. qRT-PCR analysis was conducted from total RNA isolated. The data have shown that OV-NZ2 infection significantly suppressed IFN-β expression in a dose-dependent manner (Figure 5.8 A). The inhibition of IFN-β expression was highly effective at an MOI of 5 and was used hereafter.

The duration of OV-NZ2 IFN antagonism was also investigated over 15 hours of virus infection. The cells were first stimulated with poly(dA:dT) for 4 hours then infected with OV-NZ2 at an MOI of 5. It was shown that the inhibitory effect was significant at 10 hours post infection (Figure 5.8 B). OV-NZ2 infection in unstimulated cells was included to examine whether the virus induces interferon or not. As shown in Figure 5.8 B, infection did not induce IFN-β expression in unstimulated cells across all time points. Overall, this result strongly suggests that the virus encodes modulatory proteins that play a role in interfering with type I interferon signalling upon stimulation with poly(dA:dT).

A.

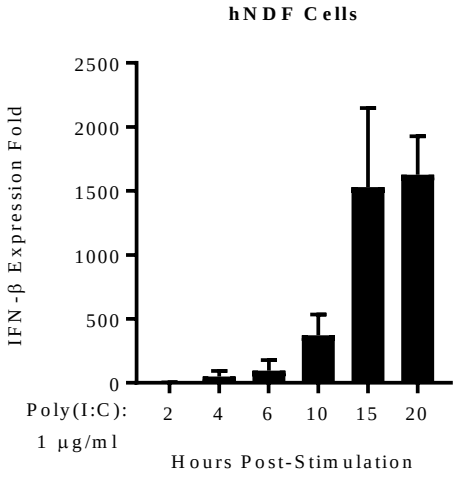

B.

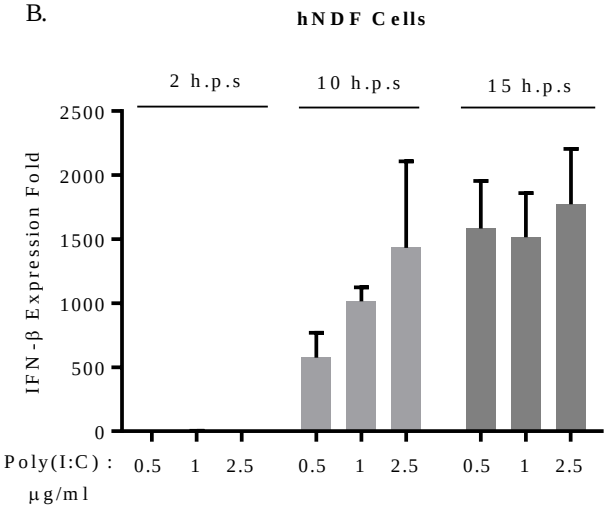

C.

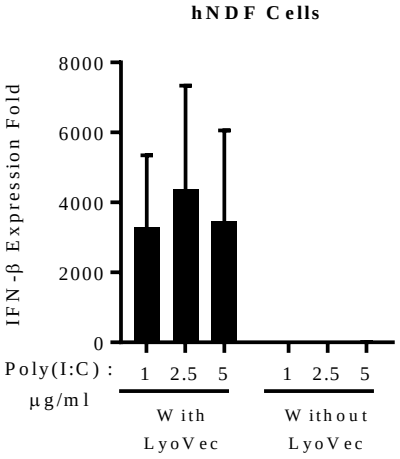

Figure 5.7. IFN-ß Induction in hNDF cells with poly(I:C). (**A**), (**B**) and (**C**) hNDF cells were seeded at $4x10^5$ cells in 6-well plates and stimulated with poly(I:C) complexed with LyoVec (**A**), (**B**) and (**C**) or without LyoVec (**C**) at concentration indicated. Total RNA was isolated from cells at the time shown and IFN-β mRNA was quantified by qRT-PCR in triplicate of technical replicate. Expression fold was calculated as described in materials and methods. Data are from one representative experiment of three (**A**), three (**B**) and one (**C**) independent experiments conducted with technical duplicate. Error bars represent mean ±SD.

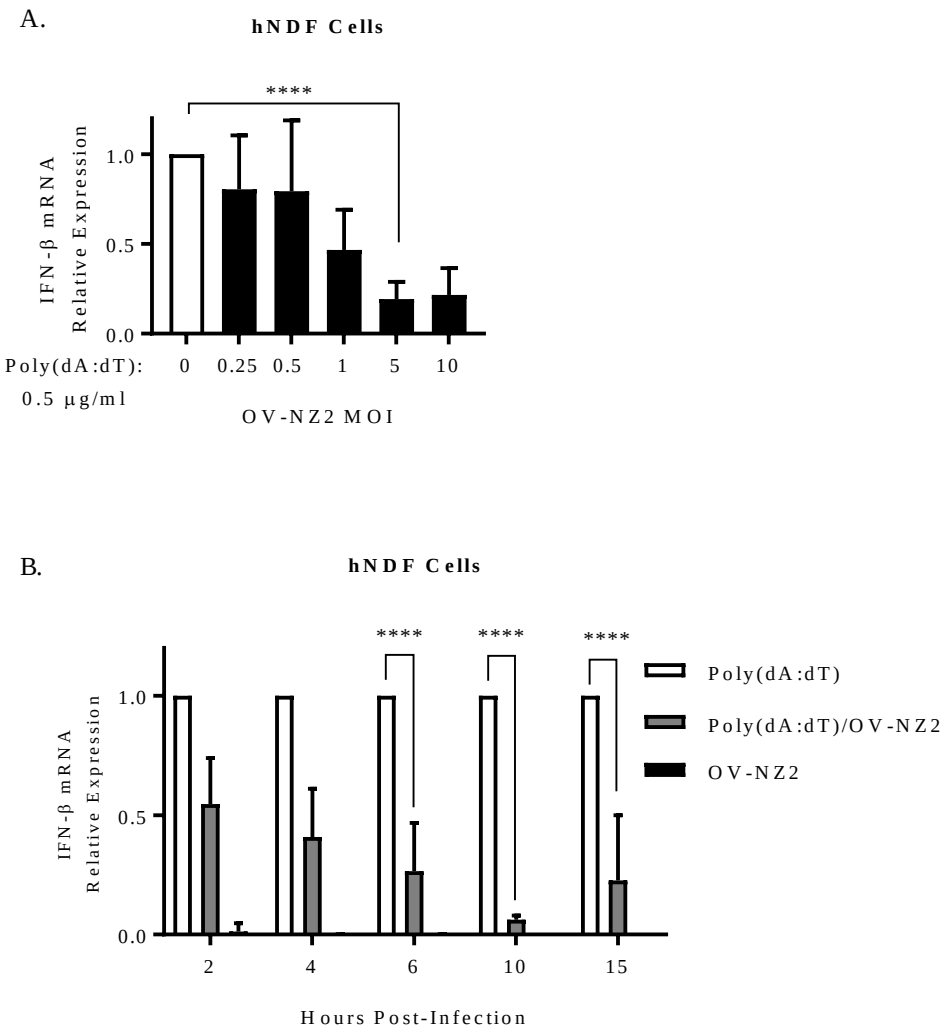

Figure 5.8. Inhibitory effect of OV-NZ2 infection on IFN-β induction in hNDF cells stimulated with poly(dA:dT). hNDF cells were seeded at $4x10^5$ cells in 6-well plates and stimulated with poly(dA:dT) (500 ng/ml) for 4 hrs. Then cells were infected with the virus at multiple MOIs as indicated for 10 hours (**A**) or at an MOI of 5 for indicated times (**B**). Total RNA was isolated from cells and IFN-ß mRNA was quantified by qRT-PCR in triplicate of technical replicate. The level of IFN-β mRNA in uninfected sample was considered 1 to compare the infected samples. Statistical analysis was performed using Student's *t* test **(A)** and two-way ANOVA **(B)**. Data are from three independent experiments. Error bars represent mean ±SD. Asterisks indicate probability $^{****}P \leq 0.0001$.

5.8 Inhibitory Effect of ORFV Infection on IFN-β Expression in hNDF Cells stimulated with Poly(I:C)

hNDF cells respond to transfected poly(I:C) by producing type I IFN. Although this chapter primarily investigates the effect of OV-NZ2 infection in poly(dA:dT)-stimulated hNDF cells, poly(I:C) stimulation was included so as to better understand virus manipulation of the IFN response because it is known that this cell type expresses RNA sensors that could detect an intermediate dsRNA produced during virus replication.

hNDF cells were first infected with OV-NZ2 at different MOI's for 4 hours then stimulated with synthetic dsRNA poly(I:C) and IFN-β mRNA quantified by qRT-PCR. The data show that OV-NZ2 infection caused a slight increase in the induction of IFN-β expression in poly(I:C)-stimulated hNDF cells at an MOI of 0.25 to 1 then a significant inhibition at 10 (Figure 5.9 A). This virus dose-dependent increase of IFN-β expression observed at MOIs 0.25, 0.5 and 1 was probably due to dsRNA intermediates generated during virus replication that elicit the IFN response and could not be counteracted unless the cells were infected with a higher dose of virus. Next, the duration of the OV-NZ2 inhibitory effect was addressed. The cells were first infected with OV-NZ2 at a multiplicity of infection 10 for 4 hours then stimulated with poly(I:C). Similar to the inhibitory effect of OV-NZ2 infection in poly(dA:dT)-stimulated cells, OV-NZ2 inhibited the expression of IFN-β induced by poly(I:C) and inhibition occurred across all time points (Figure 5.9 B).

Similar to the observation found in HEK293 cells, when poly(I:C) stimulation preceded virus infection (see Section 4.5), the virus could not inhibit the expression of IFN-β in hNDF cells (Figure 5.10 A and B). This observation may indicate that the virus might have another mechanism to counteract the poly(I:C)-induced IFN response in hNDF cells.

A.

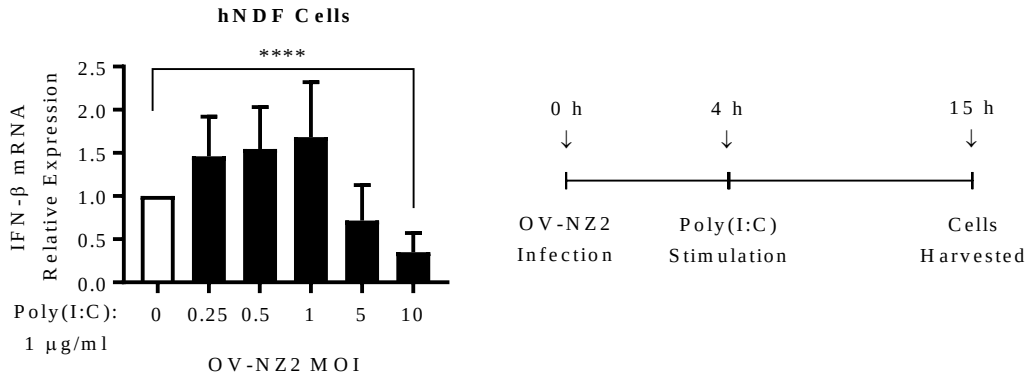

B.

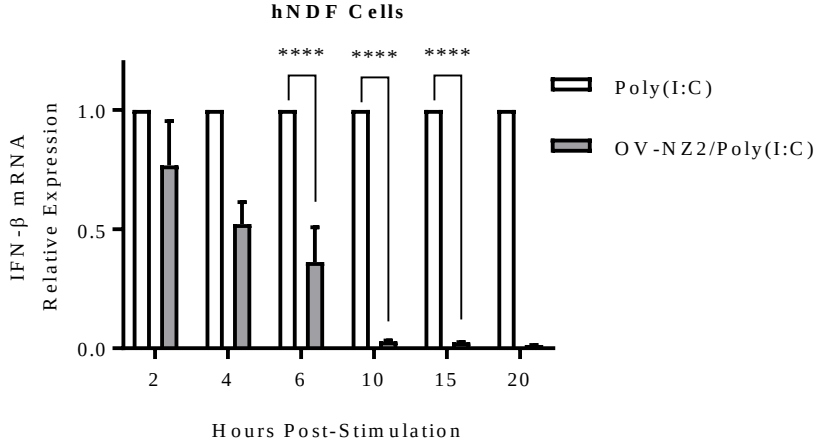

Figure 5.9. Inhibitory effect of OV-NZ2 infection on IFN-β Induction in hNDF cells stimulated with poly(I:C). hNDF cells were seeded at $4x10^5$ cells in 6-well plates. The cells were mock infected or infected with OV-NZ2 at different MOI's as indicated (**A**) or an MOI of 10 (**B**) for 4 hours then stimulated with 1 µg/ml of poly(I:C). The cells were incubated for 10 hours (**A**) or for times indicated (**B**). Total RNA was isolated and IFN-β mRNA quantified by qRT-PCR in triplicate of technical replicate. The level of IFN-β mRNA in uninfected sample was considered 1 to compare the infected samples. Statistical analysis was performed using the Student's *t* test **(A)** and two-way ANOVA **(B)**. Data are from three independent experiments. Error bars represent mean ±SD. Asterisks indicate probability $^{****}P \leq 0.0001$.

A.

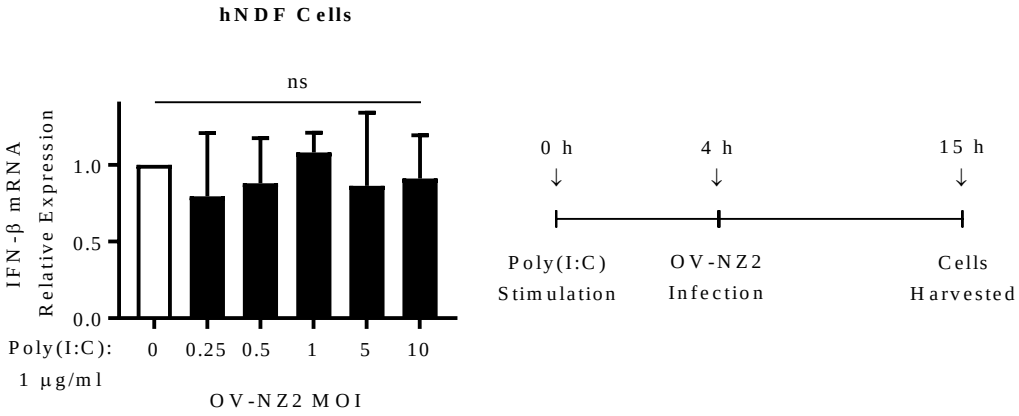

B.

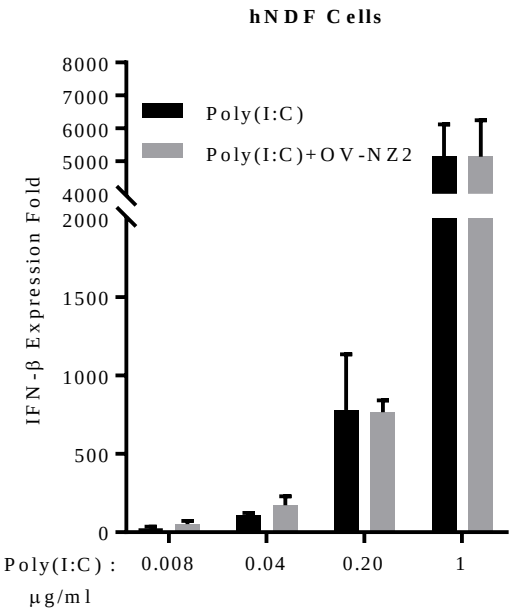

Figure 5.10. OV-NZ2 infection is required first to inhibit the IFN-β induction in poly(I:C)-stimulated hNDF cells. (**A**) hNDF cells were seeded at $4x10^5$ cells in 6-well plates and stimulated with poly(I:C) at 1 µg/ml for 4 hours. Then the cells were mock infected or infected with OV-NZ2 at different MOI's indicated then the cells incubated for 10 hours post infection. Total RNA was isolated from the cells and IFN-ß mRNA was quantified by qRT-PCR in triplicate. The level of IFN-β mRNA in uninfected sample was considered 1 to compare the infected samples. Statistical analysis was performed using student *t* test. Data are from three independent experiments. Error bars represent mean ±SD. Asterisks indicate probability $^{ns}P \geq 0.1234$. (**B**) hNDF cells were seeded at $4x10^5$ cells in 6-well plates and stimulated with poly(I:C) at the concentration indicated for 4 hours. Then the cells were mock infected or infected with OV-NZ2 at an MOI of 10 then the cells incubated for 10 hours post infection. Total RNA was isolated from the cells and IFN-ß mRNA was quantified by qRT-PCR in triplicate. Data are from one experiments. Error bars represent mean ±SD.

5.9 Detection of STING and RIG-I Expression Proteins in hNDF Cells

Several receptors have been proposed to be important for cytosolic DNA detection and those receptors depend on STING. It is a critical component in the DNA sensing pathway that conveys the upstream DNA sensing to downstream signalling events leading to induction of type I IFN.

Detection of STING and RIG-I protein expression in hNDF cells were investigated by western blotting in mock cells or cells stimulated with either poly(dA:dT) or poly(I:C). STING was detectable in unstimulated cells and it was noticed that the levels changed when the cells were stimulated with poly(dA:dT) or poly(I:C) (Figure 5.11). The STING level decreased when cells were stimulated with poly(dA:dT). A similar observation was found in poly(dA:dT)-stimulated HeLa cells (data not shown) and poly(dA:dT)-stimulated MEF cells (Abe, T. *et al.*, 2014; Liu, D. *et al.*, 2019), more likely due to ubiquitination of STING as reported previously (Ni, G. *et al.*, 2017). The IRF3 level also decreased when cells were stimulated with poly(dA:dT), a similar observation found in poly(dA:dT)-stimulated HeLa cells (data not shown). On the other hand, STING increased when cells were stimulated with poly(I:C), possibly due to autocrine and paracrine effects of type I IFN induction as found by Liu, Y. *et al.* (2016). RIG-I protein expression was not detectable in unstimulated hNDF cells but the protein was strongly induced in poly(dA:dT)- or poly(I:C)-stimulated hNDF cells (Figure 5.11). Similar to the observation found in HEK293 cells, the RIG-I protein was inducible in hNDF cells.

The regulation of STING is complex and involves several events to function. Upon cGAS-produced 2’3’-cGAMP, binding to STING results in translocation of STING from the endoplasmic reticulum compartment to the perinuclear region where autophosphorylated TBK1 is recruited to STING, allowing the phosphorylation of STING. Phosphorylated STING recruits IRF3 where IRF3 is phosphorylated by TBK1 leading to IRF3 dimerization, nuclear translocation and eventually induction of type I IFN (Liu, S. *et al.*, 2015; Tanaka, Y. *et al.*, 2012). In this study, attempts were made to investigate the effect of OV-NZ2 on the STING-TBK1-IRF3 axis of the DNA-sensing pathway by examining the phosphorylation events of these proteins in the context of virus infection. However, none of phospho-STING, phospho-TBK1 or phospho-IRF3 were detectable by western blotting in hNDF cells (data not shown).

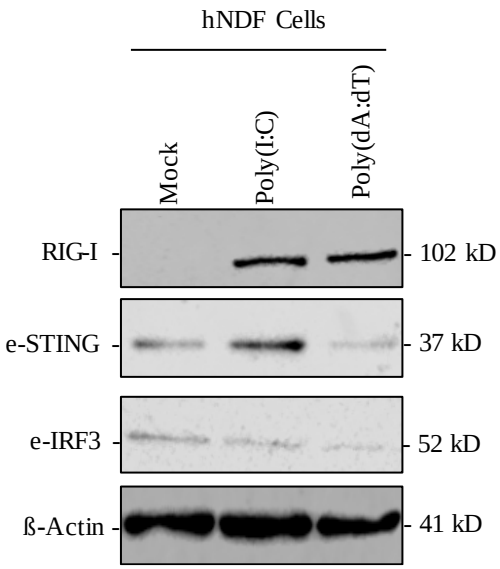

Figure 5.11. Detection of RIG-I, STING and IRF3 molecules in hNDF cells by western blotting. hNDF cells were mock or stimulated with either 0.5 μg/ml of poly(dA:dT) or poly(I:C) for 15 hrs. Equal amounts of cell lysate were resolved on a 10 % SDS-polyacrylamide gel for western blotting. Proteins were detected with the antibodies indicated. Proteins were visualized by chemiluminescence on an odyssey Fc imaging system.

5.10 Poly(dA:dT)-mediated IFN-β Expression is through the STING Adaptor in hNDF Cells

The importance of the STING-dependent pathway in mediating DNA-induced type I interferon was investigated in this study by knocking down the STING gene using RNAi then to examine the induction of type I interferon in response to poly(dA:dT). It is important to mention that since the transfected poly(dA:dT) could be transcribed by RNA polymerase III to 5'ppp-dsRNA and recognized by RIG-I leading to activation of the RNA-dependent pathway, RIG-I gene knockdown or STING/RIG-I double knockdown was included. Interestingly, an immunoprecipitation study on 293T cells has shown that RIG-I, but not MDA5, could bind with STING in a co-transfection experiment, suggesting that they function cooperatively (Ishikawa, H. *et al.,* 2008).

In this study, three different predesigned synthetic small interfering RNAs duplex (siRNA) targeting either STING or RIG-I genes were used to minimize the possibility of off-target effects. They were 19 nucleotide siRNA with 2-base 3' overhangs and these features enable

siRNA to bypass any possible interferon induction triggered by dsRNA transfection (Marques, J. T. *et al.*, 2006; Sioud, M., 2006). The optimal concentration of STING siRNA required to efficiently silence the gene without producing toxicity was determined in which the cells were transfected with a series of STING siRNA amounts (10, 50, 100, 200 and 300 nM) and cells incubated for two days post transfection. From western blotting, it was found that 100 nM siRNA produced maximal depletion of the STING protein and a concentration beyond 100 nM did not cause further depletion in STING (data not shown).

hNDF cells were either transiently mock transfected (none) or negative control (NC) or transfected with three siRNAs individually targeting STING. Then after 2 days post transfection, the protein level was examined by western blotting and the protein band quantified. Western blot analysis showed a depletion of STING (Figure 5.12 A). The protein bands were quantified by imageStudioLite and it was found that about a one third depletion was caused by siRNA #1 and about a half depletion was caused by siRNA #2 (Figure 5.12 B). The depletion was not caused by off-target effects as siRNA #3 did not deplete STING. The level of STING mRNA was also examined and found to be consistent with the protein level (Figure 5.12 C).

Having established this, IFN-β induction was examined in STING knockdown cells after stimulation with either poly(dA:dT) or poly(I:C). As expected, the induction of IFN-β mRNA reduced significantly in the poly(dA:dT)-stimulated STING-depleted cells by about 50% compared to controls but not completely, more likely due to the involvement of the RIG-I-dependent sensing through the cytosolic DNA-dependent RNA polymerase III response (Figure 5.12 E). On the other hand, the induction of IFN-β expression did not change in poly(I:C)-stimulated STING-depleted cells, indicating other RNA sensors, such as RIG-I, are involved in IFN-β expression in hNDFs (Figure 5.12 D). This result strongly suggests that STING-dependent sensing is involved in the induction of IFN-β by poly(dA:dT) and STING is required to induce the IFN response in hNDF cells and might suggest that the inhibitory effect caused by OV-NZ2 was more likely due to counteracting STING activation.

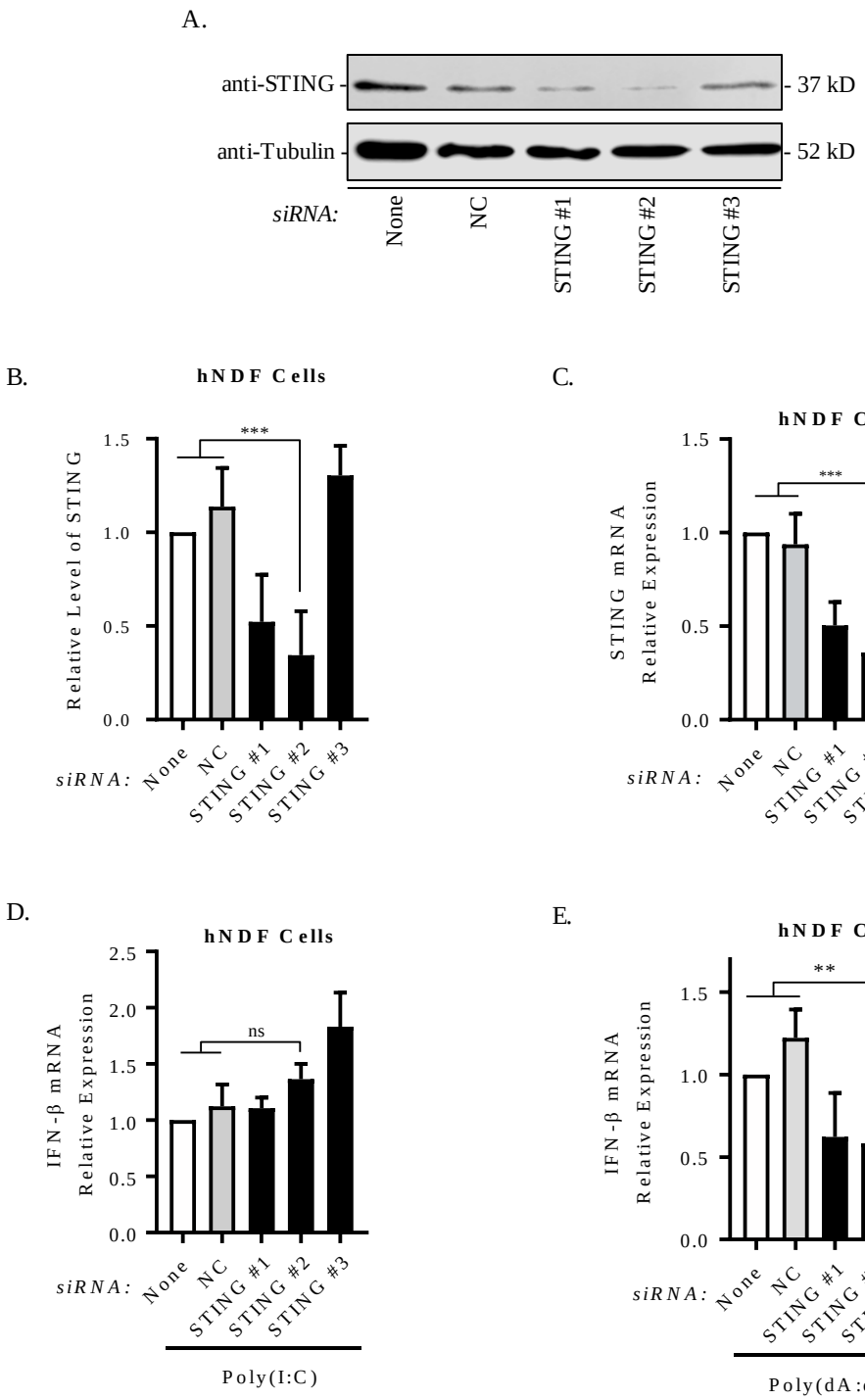

Caption is in the next page

Figure 5.12. STING is required for IFN-β induction in poly(dA:dT)-stimulated hNDF cells, but not with poly(I:C). hNDF cells were transfected with siRNA (100 nM) targeting the STING gene for 48 hrs. Three siRNAs were used to minimize the possibility of off-target effects. Control conditions included mock transfection in the absence of siRNA (none) or transfection with a non-targeting control siRNA (NC). At 48 h.p.t., the transfected cells were stimulated with either poly(dA:dT) 0.5 µg/ml for 15 hours or poly(I:C) 1 µg/ml for 20 hrs. Transfected cells were lyzed for analysis of target protein expression by western blotting (**A**).Target protein band intensity was quantified and plotted after being normalized to the loading control (**B**) and the mRNA level of STING was assessed (**C**). The induction of IFN-β was assessed in the transfected cells by qRT-PCR after 20 hours post stimulation with poly(I:C) (**D**) and 15 hours post stimulation with poly(dA:dT) (**E**). qRT-PCR was conducted in triplicate of technical replicate. Statistical analysis was performed using two-way ANOVA. Data are from three independent experiments. Error bars represent mean ±SD. Asterisks indicate probability: $^{ns}P \geq 0.1234$, $^{**}P \leq 0.0021$, $^{***}P \leq 0.0002$, $^{****}P \leq 0.0001$.

5.11 Other RNA Sensors are Involved in IFN-β Expression in hNDF Cells

Due to the complexity of nucleic acid detection and signalling in the cytosol of hNDFs, RNA sensors were considered in this study. It was speculated that the RIG-I receptor plays a major role in the induction of IFN-β expression in these cells when stimulated with poly(dA:dT) or poly(I:C). To test this hypothesis, knockdown of RIG-I by siRNA was conducted. Three different predesigned synthetic small interfering RNAs (siRNA) were used to minimize the possibility of off-target effects. The optimal concentration of RIG-I siRNA required in hNDF cells was also determined by transfecting the cells with a series of RIG-I siRNA amounts (10, 50 and 100 nM). The western blotting data showed that a concentration of 100 nM siRNA#2 produced significant depletion in RIG-I protein in hNDFs (data not shown).

hNDF cells were transiently transfected with siRNA targeting RIG-I then the RIG-I protein level was determined by western blot analysis 2 days post transfection. Before western blotting was conducted, stimulation was required to induce RIG-I expression in transfected cells. RIG-I siRNA transfection caused a noticeable protein depletion compared to the control (Figure 5.13 A) and that depletion was about 70% as shown in Figure 5.13 B. The level of RIG-I mRNA in the transfected cells was examined in poly(dA:dT)- or poly(I:C)-stimulated cells and it was found that the level RIG-I mRNA was reduced by about 50% in both poly(dA:dT) and poly(I:C) stimulation (Figure 5.13 C and D).

The induction of IFN-β expression was examined in the RIG-I-depleted cells after stimulation with either poly(dA:dT) or poly(I:C). The RIG-I-depleted cells showed no significant reduction in IFN-β expression when cells were stimulated with poly(dA:dT) (Figure 5.13 F), but only a slight decrease, possibly because a proportion of poly(dA:dT) was transcribed to 5'ppp-dsRNA but could not trigger the RNA-sensing pathway through RIG-I. On the other hand, the induction of IFN-β expression in RIG-I-depleted cells did not change when stimulated with poly(I:C) (Figure 5.13 E), suggesting other RNA sensors involved independently of TLR3 such as protein kinase R (PKR) (Diebold, S. S. *et al.*, 2003; Yang, Y. L. *et al.*, 1995).

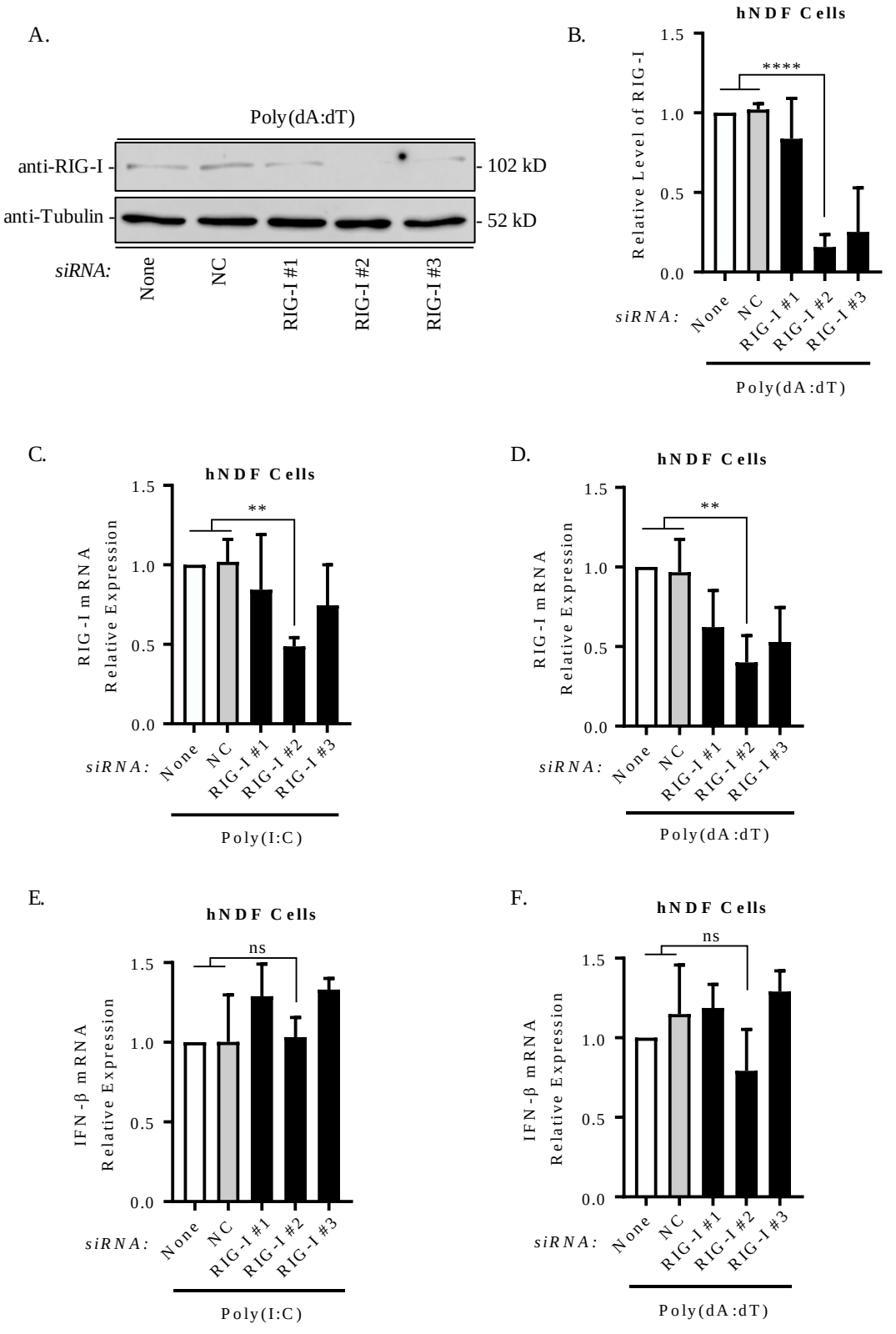

Caption is in the next page

Figure 5.13 RIG-I siRNA knockdown has no significant effect on poly(dA:dT)- or poly(I:C)-induced IFN-ß in hNDF cells. hNDF cells were transfected with siRNA (100 nM) targeting the RIG-I gene for 48 hrs. Three siRNAs were used to minimize the possibility of off-target effects. Control conditions included mock transfection in the absence of siRNA (none) or transfection with a non-targeting control siRNA (NC). At 48 h.p.t., the transfected cells were stimulated with either poly(dA:dT) 0.5 µg/ml for 15 hours or poly(I:C) 1 µg/ml for 20 hours. Transfected cells were lyzed for analysis of target protein expression by western blotting (**A**) and qPCR (**C** and **D**). Target protein band intensity was quantified and plotted after being normalized to the loading control (**B**). The induction of IFN-β was assessed in the transfected cells by qRT-PCR after 20 hours post stimulation with poly(I:C) (**E**) and 15 hours post stimulation with poly(dA:dT) (**F**). qRT-PCR was conducted in triplicate of technical replicate. Statistical analysis was performed using two-way ANOVA. Data are from three independent experiments. Error bars represent mean ±SD. Asterisks indicate probability: $^{ns}P \geq 0.1234$, $^{**}P \leq 0.0021$, $^{****}P \leq 0.0001$.

5.12 Stronger Reduction of IFN-β Expression in hNDF Cells with Double Knockdown of STING and RIG-I When Stimulated with Poly(dA:dT)

RNA interference data have shown that knockdown of STING has caused a reduction in IFN-β expression but not complete suppression and that was probably because poly(dA:dT) has been converted to 5'pppdsRNA by RNA polymerase III making it a ligand for RIG-I. This assumption was tested by conducting a double knockdown targeting STING and RIG-I genes resulting in shut down of DNA-dependent and RIG-I-dependent pathways when stimulated with poly(dA:dT). Then the induction of IFN-β expression was examined.

hNDF cells were transfected with pooled siRNAs#2 of STING and RIG-I for 2 days post transfection. Then the level of target proteins was determined by western blotting upon 24 hours of poly(I:C) stimulation. From the double knockdown, the level of STING protein was reduced by about 80% and the level of RIG-I was undetectable (Figure 5.14 A and B). The mRNA levels of both genes in STING/RIG-I-depleted cells was also determined after stimulation with poly(dA:dT) or poly(I:C). The mRNA level of both genes reduced by more than 50% for both poly(dA:dT) and poly(I:C) (Figure 5.14 C and D).

The induction of IFN-β expression was then investigated in the STING/RIG-I-depleted hNDF cells after stimulation with poly(dA:dT) or poly(I:C). As expected, a significant reduction in IFN-β induction was observed in poly(dA:dT)-stimulated cells after depleting STING and RIG-I simultaneously (Figure 5.14 E) and this reduction was even stronger than for STING only-depleted cells (Figure 5.13 E). This result strongly suggests that poly(dA:dT) is working only through STING-dependent and RIG-I-dependent pathways. On the other hand, poly(I:C) stimulation did not cause a significant reduction in IFN-β expression in STING/RIG-I-depleted hNDFs (Figure 5.14 F) and reduced slightly compared to a single knockdown as shown in Figure 5.12 D and Figure 5.13 E. The inhibitory effect of OV-NZ2 has not been affected even in STING/RIG-I-depleted cells either after stimulation with poly(dA:dT) or poly(I:C) (Figure 5.14 E and F).

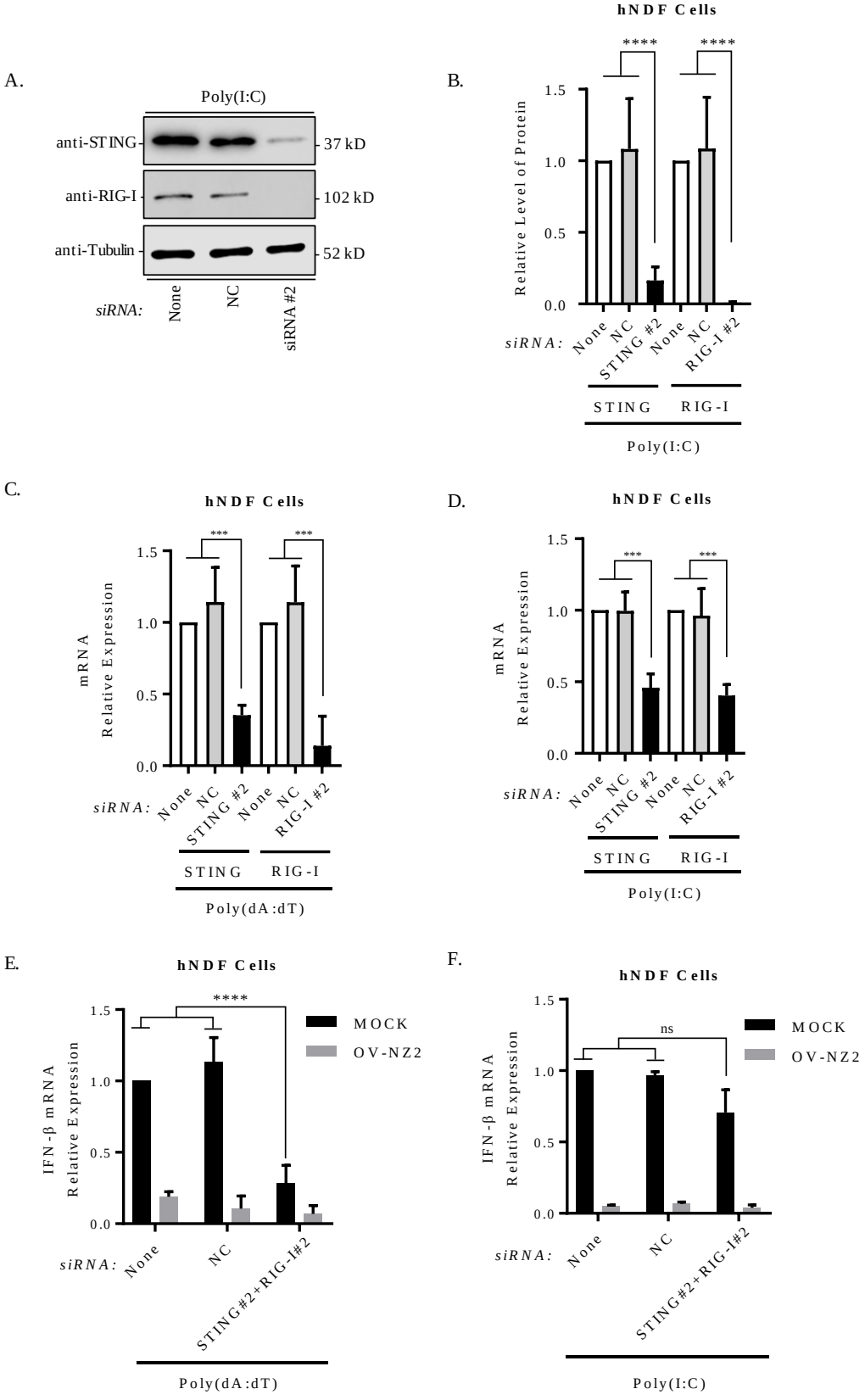

Caption is in the next page

Figure 5.14. STING/RIG-I siRNA double knockdown has a significant effect on poly(dA:dT)-induced IFN-ß expression in hNDF cells. hNDF cells were co-transfected with siRNA (100 nM) targeting the STING and RIG-I genes for 48 hrs. Three siRNAs were used to minimize the possibility of off-target effects. Control conditions included mock transfection in the absence of siRNA (none) or transfection with a non-targeting control siRNA (NC). At 48 h.p.t., the transfected cells were stimulated with either poly(dA:dT) 0.5 µg/ml for 15 hours or poly(I:C) 1 µg/ml for 20 hrs. Transfected cells were lysed for analysis of target protein expression by western blotting (**A**) and mRNA by qRT-PCR (**C** and **D**). Target protein band intensity was quantified and plotted after normalization to the loading control (**B**). The induction of IFN-ß was assessed in the siRNA transfected cells by qRT-PCR in triplicate after 15 hours post stimulation with poly(dA:dT) (**E**) and 20 hours post stimulation with poly(I:C) (**F**) in infected or uninfected cells. Statistical analysis was performed using two-way ANOVA. Data are from three independent experiments. Error bars represent mean ±SD. Asterisks indicate probability: $^{ns}P \geq 0.1234$, $^{***}P \leq 0.0002$, $^{****}P \leq 0.0001$.

5.13 Virus Early Gene Synthesis is Required to Inhibit IFN-β Expression in hNDF Cells

An investigation was carried out to determine whether the virus inhibitory effect observed in hNDF cells, when stimulated with poly(dA:dT), required new early viral gene protein synthesis. The approach of heat inactivation was utilized (as explained in Section 4.9) to inactivate early viral protein synthesis of OV-NZ2 including OV-NZ2Rev116 and OV-NZ2Δ116 (see Chapter 3) in an attempt to identify whether ORF116 has a role in the inhibitory effect on IFN-β expression in hNDF cells.

One-step growth of OV-NZ2 wild type was characterized in hNDF cells in which the cells were infected with virus at an MOI of 5. Then the cells were harvested at various times and the virus progeny quantified by plaque assay on LT cells. The virus showed exponential growth starting at 12 hours post infection until 48 hours post infection, then reached a plateau from day 2 until day 4 giving about a 5-fold increase in the virus progeny (Figure 5.15).

Next, early viral gene protein synthesis in hNDF cells infected with either OV-NZ2, OV-NZ2-Rev116 or OV-NZ2Δ116 was investigated using the OV119 protein as an indicator (Harfoot, R. T., 2015). Virus inocula were prepared at an MOI of 5 then the inocula were split into two in which one was treated with heat at 55 °C for 1 hour and the other was left without heat treatment. The cells were either infected with untreated virus or heat inactivated virus then the cells harvested at 0, 2, 4 and 6 hour post infection. The cell lysates were subjected to western blotting using anti-OV119 antibody. As shown in Figure 5.16, the synthesis of OV119 was detected at 4 hours post infection and increased further at 6 hours post infection. However, the induction of OV119 protein was completely abolished in heat inactivated virus infection indicating that heat inactivation destroyed early protein synthesis. It is worth noting that the cytopathic effect (CPE) of infected hNDF cells was also examined under light microscopy and found that the untreated virus induced a clear CPE at 4 hours post infection that increased at 6 hours post infection, whereas the heat inactivated virus did not induce CPE (data not shown).

Given that the heat inactivation has inactivated virus early gene protein synthesis, the investigation then assessed the induction of IFN-β expression in hNDF cells infected with untreated or heat inactivated virus. The cells were infected with either untreated or heat inactivated virus after poly(dA:dT) stimulation or before poly(I:C) stimulation, then IFN-β

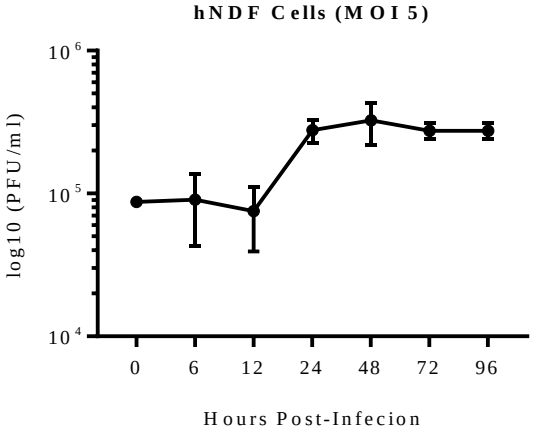

Figure 5.15. One-step growth analysis of OV-NZ2 in hNDF cells. hNDFs were seeded at $4x10^5$ and incubated overnight. Cells were infected at an MOI of 5 with OV-NZ2. After 1hr adsorption, cells were washed with PBS to remove unattached virus then 2 ml of DMEM 2 % FCS was added to hNDF infected cells. At various times post-infection, media and infected cells were collected. After three cycles of freezing and thawing, the virus was sonicated and viral titres determined by serial dilution and plaque assay on LT cells.

mRNA was quantified by qRT-PCR. As seen in Figure 5.17 A and B, the untreated viruses were able to significantly inhibit the induction of IFN-β expression in poly(dA:dT)- or poly(I:C)-stimulated cells. On the other hand, the ability of IFN-β inhibition was not retained in stimulated cells infected with the heat inactivated viruses indicating that the inhibitory effect of OV-NZ2 on IFN-β expression requires *de novo* early viral proteins (Figure 5.17 A and B). Unlike in HEK293 cells (see Figure 4.18), all heat-inactivated viruses induced the expression of IFN-β in un-stimulated cells, more likely due to the presence of virus RNA generated from gene transcription which may further validate the intactness of virus transcription machinery even after heat treatment. It is important to note that the variation in level of IFN-β induction in unstimulated cells infected with heat inactivated viruses was not because of an inhibitory effect caused by the virus as the same preparations of viruses have not caused variations in poly(dA:dT)- or poly(I:C)-stimulated cells. Overall, the data demonstrate that the gene responsible for the inhibitory effect was an early gene(s) and this effect was not caused by viral structural proteins. In addition, ORF116 did not seem to have a direct effect on IFN-β induction or it does but masked by other viral factors.

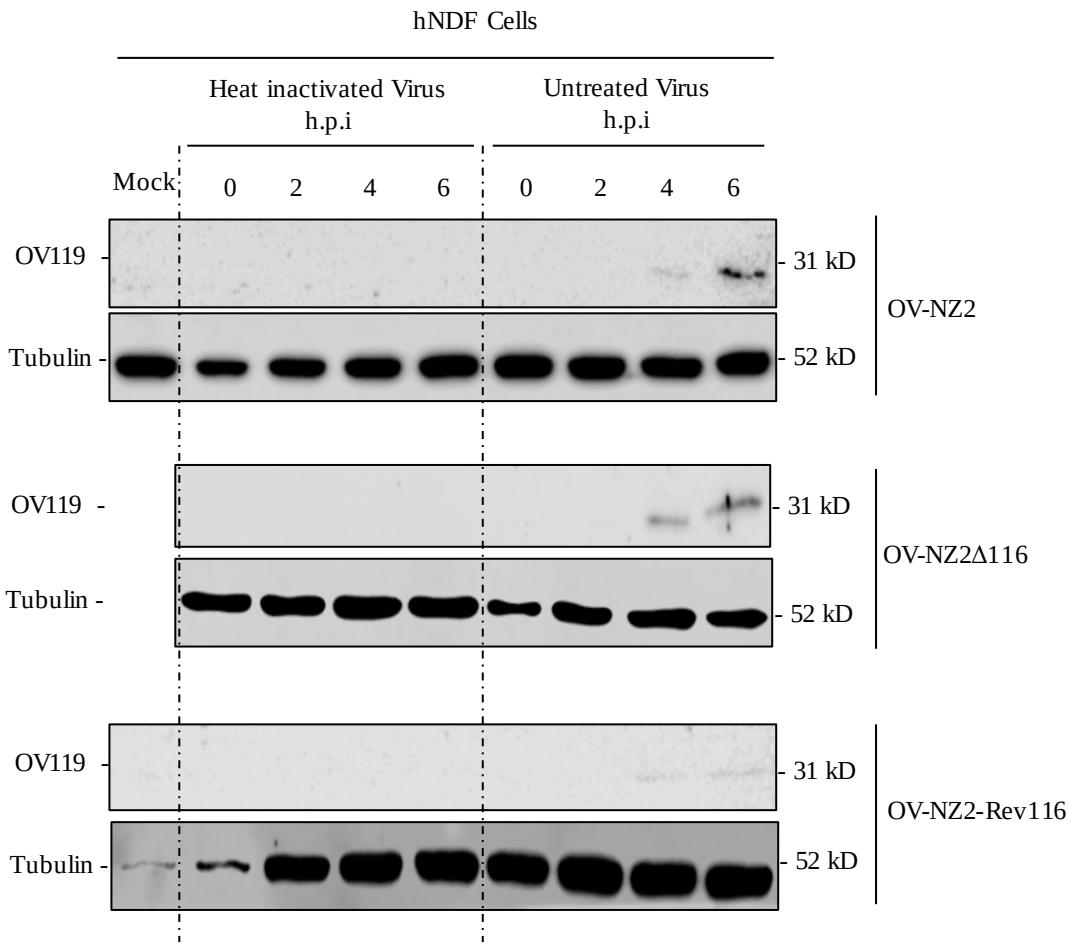

Figure 5.16. Detection of ORFV early protein synthesis in hNDF cells infected with heat inactivated or untreated virus. hNDF cells were seeded at $4x10^4$ in a 24-well plate. On the day of infection, virus inocula of OV-NZ2, OV-NZ2Δ116 or OV-NZ2Rev116 were prepared at an MOI of 5, then split into two. One half was subjected to heat treatment at 55 °C for 1 hour and the other half left untreated and the cells were then infected with the heat inactivated or untreated virus. The cells were harvested and lyzed at time points 0, 1, 2, 4 and 6 hour post infection. Equal amounts of total protein were resolved on a 10% SDS-polyacrylamide gel for western blotting. The membrane was incubated with anti-OV119 antibody or anti-tubulin antibody as a loading control and proteins detected by chemiluminescence.

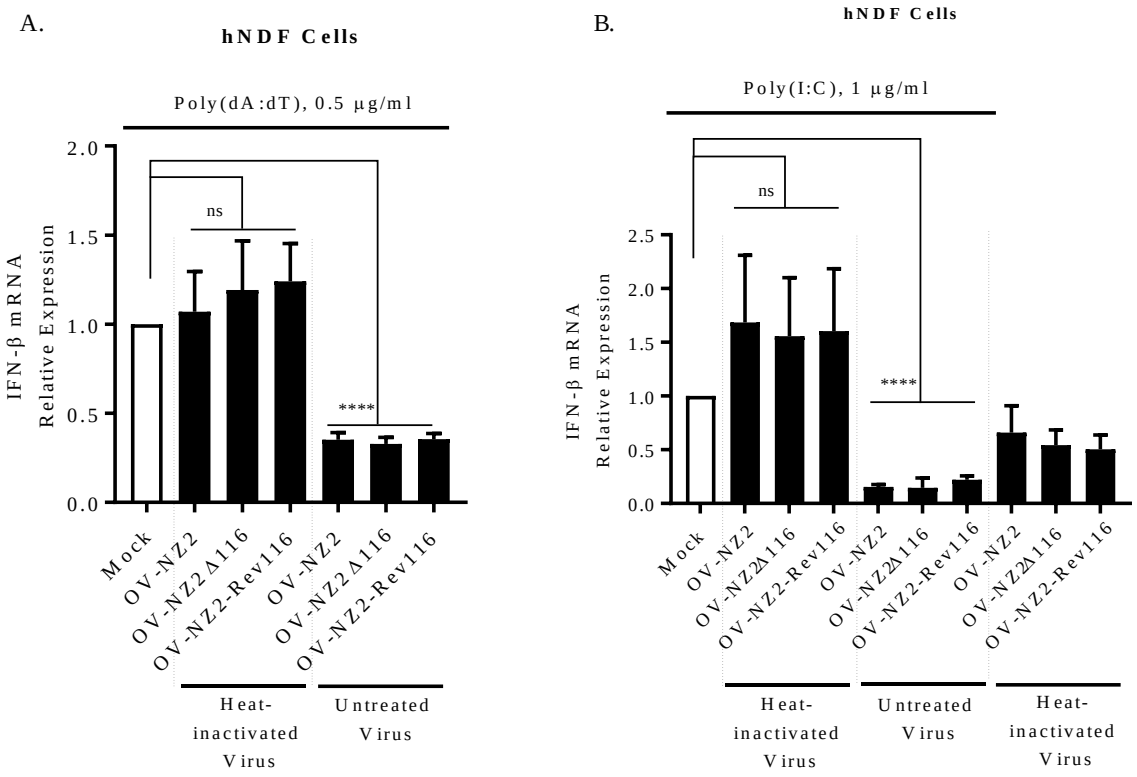

Figure 5.17. Induction of IFN-β by poly(dA:dT) or poly(I:C) in hNDF cells infected with heat -inactivated or untreated virus. hNDFs were seeded at $4x10^4$ cells in a 24-well plate. (**A**) Cells were stimulated with poly(dA:dT) at 0.5 µg/ml and incubated for 4 hours then cells infected with either heat-inactivated or untreated virus: OV-NZ2, OV-NZ2Δ116 or OV-NZ2-Rev116 at an MOI of 5 and incubated for 15 hours. (**B**) Cells were infected with either heat-inactivated or untreated virus: OV-NZ2, OV-NZ2Δ116 or OV-NZ2-Rev116 at an MOI of 10 for 4 hours then cells stimulated with poly(I:C) at 1 µg/ml or left unstimulated and incubated for 20 hours. After incubation, cells were harvested and total RNA was isolated from the cells and IFN-ß mRNA was quantified by qRT-PCR in triplicate of technical replicate. The level of IFN-β mRNA in uninfected sample was considered 1 to compare the infected samples. Data are from three independent experiments. Error bars represent mean ±SD. Statistical analysis was performed using a Student's *t* test. Asterisks indicate probability: $^{ns}P \geq 0.1234$, $^{****}P \leq 0.0001$.

5.14 Discussion

ORFV replicates in the cytoplasm of the host cell and the release of its genomic DNA into the cytoplasm, makes it a potential target for cytosolic DNA-dependent recognition. Here, the objective of this part of the study was to investigate the effect of ORFV infection on type I IFN expression upon cytosolic dsDNA sensing. The dsDNA sensing pathway was studied in hNDF cells, a primary cell type in which a strong IFN-β response could be induced by poly(dA:dT) and in which ORFV replicates. It was shown that ORFV interferes with the IFN response in these cells induced by poly(dA:dT) causing potent inhibition of IFN-β expression. This study shows for first time that ORFV has evolved a strategy to evade DNA-dependent signalling that requires the adaptor STING. These results strongly suggest that ORFV produces molecules that interfere with the signalling pathway leading to expression of IFN-β and it is likely that those molecules are synthesised early, as demonstrated in assays using heat-inactivated virus. This inhibition could be direct or it could be indirect. Poxviruses in particular orthopoxviruses directly target pathways that lead to IFN production and suggests that the inhibition observed in the present study is likely to be direct although indirect mechanisms may also be possible.

ORFV virus infects the skin of its host and specifically replicates in keratinocytes (Fleming, S. B. *et al.*, 2015). Primary keratinocytes reside in the epidermal layer of skin forming more than 90% of epidermal cells. Beneath the epidermis is the underlying dermal layer which harbours dermal fibroblasts. These two cell types act as sentinel cells and have the capability to activate the innate immune response against DNA viruses (Nestle, F. O. *et al.*, 2009). An appropriate cell type was sought to provide a model for this study to investigate the effect of ORFV infection on cytosolic DNA-mediated IFN-β expression. Because primary keratinocytes, which have been shown to be a strong producer of IFN-α/β (Fujisawa, H. *et al.*, 1997) were not available, the investigation initially made use of a keratinocyte (HaCaT) cell line. Although they are responsive to poly(dA:dT) by high production of IFN-β peaking at 6 hours post stimulation (Almine, J. F. *et al.*, 2017), they were not permissive for ORFV replication. Here, hNDFs were chosen as a model for this study for the following reasons. They express STING, are permissive for ORFV replication and importantly their DNA sensors were responsive to poly(dA:dT). It is almost impossible to find a cell type or cell line that expresses only cytosolic STING-dependent DNA sensors without RNA sensors. Other cell types were also sought to demonstrate inhibition of IFN-β by ORFV. A THP-1 cell line,

was also used in this study since other investigators have used these cells to study the interaction between DNA virus infection and cytosolic DNA sensing (Jønsson, K. L. *et al.*, 2017; Unterholzner, L. *et al.*, 2010). In natural infection, immune cells such as monocytes, cDCs and pDCs infiltrate into the ORFV lesion and get abortively infected by ORFV. Other poxviruses such as PPVO and myxoma virus abortively infect pDCs and induce the expression of IFN-β (Dai, P. *et al.*, 2011; von Buttlar, H. *et al.*, 2014) and other poxviruses such as VACV and modified vaccinia virus Ankara (MVA) infect pDCs and inhibit the production of IFN-β owing to multiple viral inhibitors (Dai, P. *et al.*, 2014).

As noted from the kinetics of IFN-β induction in hNDF cells, the exponential phase of IFN-β was observed at 4 hours post-poly(dA:dT) stimulation, whereas there was a further delay of about two hours upon poly(I:C) stimulation, indicating a stronger activation of the pathway by poly(dA:dT) than poly(I:C), consistent with studies by Unterholzner, L. *et al.* (2011). Poly(dA:dT) caused faster and stronger stimulation of IFN-β induction than poly(I:C), possibly due to the fact that poly(dA:dT) stimulation can lead to activation not only of the cytosolic DNA sensing pathways but also cytosolic RNA sensing pathways by the conversion of poly(dA:dT) to dsRNA via RNA polymerase III. This period of time before the exponential phase of IFN-β induction appears to have given the virus time to express its early genes and block the pathway. Unfortunately in this study phosphorylated TBK1 and IRF3 could not be detected by western blotting, and hence the kinetics of TBK1 and IRF3 phosphorylation could not be determined. This may have provided clues as to, if, where and when the virus blocked signalling.

The critical adaptor for DNA-mediated signalling is STING, that conveys upstream DNA sensing to the downstream signalling pathway through the kinases TBK1/IKKε and IKKα/IKKβ and transcription factors IRF3 and NF-κB (Ishikawa, H. *et al.*, 2009). STING regulation is complex and takes place through different regulatory mechanisms. It undergoes different post-translational modifications upon activation: dimerization, translocating from the ER to the signalling compartment, phosphorylation by TBK1 and further trafficking for subsequent degradation (Dobbs, N. *et al.*, 2015; Ishikawa, H. *et al.*, 2009). In this study, I attempted to investigate the effect of ORFV infection on STING-dependent signalling. Firstly, efforts were made to detect the phosphorylated forms of TBK1 and IRF3 in hNDF cells by western blotting upon stimulation with poly(dA:dT), but none of these attempts were successful for the possible reasons discussed in the previous chapter. Then the study moved

on to investigate STING in hNDF cells. The total protein was detected in untreated cells but the phosphorylated form could not be detected upon stimulating cells with poly(dA:dT). The phosphorylated form of endogenous STING has been detected by others in THP-1 cells when cells were stimulated with herring testis DNA (HT-DNA) (Liu, S. *et al.*, 2015). The approach to overcome this issue could be by expressing STING from a construct as shown in other studies. The antibody used against phosphorylated STING was anti-Ser366 and this residue was shown to be important for IRF3 activation and type I IFN induction (Liu, S. *et al.*, 2015; Tanaka, Y. *et al.*, 2012). Interestingly, it was noticed that endogenous total STING protein was degraded at 15 hours post stimulation with poly(dA:dT), but not with poly(I:C), in hNDFs. This observation has also been seen by others in which total STING was degraded when cells were stimulated with dsDNA or infected with HSV-1 (Konno, H. *et al.*, 2013). Fifteen hours of stimulation produced strong induction of IFN-β and it would have been interesting to have examined the kinetics of STING protein regulation in hNDF cells over this time course and then to have assessed this in ORFV-infected cells. It is believed that this mechanism of STING regulation acts as a negative regulator to prevent the deleterious consequences of the innate immune response on the host (Abe, T. *et al.*, 2013). In addition, a STING dimerization assay could have been performed to investigate the effect of ORFV infection on the activity of STING. If constructs expressing full length of IFN signalling molecules such as STING were available during the course of this study, this tool could have also been used to investigate the effects of ORFV on signalling.

An RNA interference (RNAi) strategy was applied to dissect out critical elements of the signalling pathways that led to the induction of IFN-β in hNDF cells by poly(dA:dT) and poly(I:C). Single or double knockdown of STING and RIG-I by siRNA showed no effect on the production of IFN-β when cells were stimulated with poly(I:C), indicating involvement of STING-independent pathways and other RNA sensors operating. The TLR3-TRIF dependent signalling pathway was not assessed and the assumption of TLR3 activation by poly(I:C) was not investigated. Importantly STING was shown to be involved when knocked down and cells stimulated with poly(dA:dT) in which the production of IFN-β decreased by ~50%, although it was not definitively shown that the pathway studied here was a cytoplasmic dsDNA sensing pathway. Complete inhibition of IFN-β production in the STING-depleted cells was improbable due to other pathways operating but could be due to the incomplete abolishment of STING protein by siRNA. An ideal approach would be to eliminate this

ambiguity by gene knockout. The data have shown that ORFV blocked the signalling of STING-dependent pathways however, further investigations are required to confirm this.

As discussed in the previous chapter, the inhibitory effect by ORFV observed in this study was not because of a cytotoxic effect induced by infection or general cellular shutdown of transcription. It has been shown by others that poly(dA:dT) stimulation can lead to not only induction of IFN-β and inflammasome activation but also to pyroptoic cell death with signs of plasma membrane swelling and blebbing by light microscopy. This phenomena only happens in immune cells that express ASC and caspase-1, critical signalling molecules for inflammasome activation (Fernandes-Alnemri, T. *et al.*, 2009; Hornung, V. *et al.*, 2009; Rathinam, V. A. K. *et al.*, 2010). Here, a viability assay for poly(dA:dT)-stimulated hNDF cells was not conducted, however, the cells were examined by light microscopy during the time course of IFN-β induction and signs of swelling and blebbing of the plasma membrane or cell death were not observed.

Assays were undertaken to determine whether IFN-β inhibition requires new virus protein synthesis. A heat inactivation approach was utilized over chemical inactivation e.g. binary ethyleneimine and β-propiolactone to inhibit virus early protein synthesis without affecting viral particle fusion and early gene transcriptional machinery as described previously. Heat-inactivated OV-NZ2 including OV-NZ2Δ116 and OV-NZ2-Rev116 failed to inhibit the expression of IFN-β in cells stimulated with poly(dA:dT) or poly(I:C), suggesting that the inhibition requires virus new protein synthesis. Surprisingly, poly(I:C)-induced IFN-β in cells infected with heat-inactivated viruses was higher than mock-infected cells by about half for some unknown reason. The approach of heat inactivation of VACV has been studied in detail previously and it was shown that the viral transcripts produced were long uncapped partially double stranded RNA and untranslatable (Harper, J. M. *et al.*, 1978) and it has been used previously for such studies (Parekh, N. J. *et al.*, 2019). Furthermore Cao, H. *et al.* (2012) have confirmed inhibition of early viral gene synthesis from VACV expressing GFP under control p7.5 promoter. The GFP expression was significantly reduced upon heat inactivation indicating abolished early viral protein production. Here, the inhibition of early viral gene synthesis during heat-inactivated ORFV infection was confirmed by western blotting.

Unlike untreated ORFV, heat-inactivated ORFVs OV-NZ2, OV-NZ2Δ116, and OV-NZ2-Rev116 induced the expression of type I IFN in unstimulated cells. It could be that this was through cytosolic RNA sensing as the production of early viral RNA transcripts were

presumably intact. Alternatively, heat-inactivated ORFV has been taken up by endosomes and the viral particles processed then the viral DNA released into the cytoplasm and sensed by cytosolic DNA sensors. Interestingly inactivated parapoxvirus ovis (PPVO, Orf virus strain D1701), known as Baypamun, is used to treat disease susceptible livestock, the basis of which is its immunostimulatory and antiviral activity (Siegemund, S. *et al.*, 2009; von Buttlar, H. *et al.*, 2014; Weber, O. *et al.*, 2003).

It was of interest to identify ORFV genes involved in inhibiting IFN-β expression. A potential candidate *ORF116* was included in this study. There was no difference between the *ORF116* deletion mutant compared with OV-NZ2 wild type and OV-NZ2-Rev116 in either poly(dA:dT)- or poly(I:C)-stimulated cells. This assay might not be sufficient to draw a definitive conclusion about the role of ORF116 because its effect could be masked by other factors expressed by the virus acting on the DNA signalling pathway. Like other poxviruses, it is possible that ORFV could encode multiple proteins that target the same signalling pathway to close-down the innate immune response. VACV is known to encode several proteins targeting distinct components involved in the signalling of type I IFN. Other approaches to address this question could involve expressing ORF116 from a construct in a DNA-signalling dependent cell system. Although the RNA binding protein ORF020 (E3L homologue) was shown to inhibit IFN-β expression in HEK293 cells, it was not considered in this part of study as it does not bind dsDNA (McInnes, C. J. *et al.*, 1998) and does not contain an N-terminal Z-DNA binding domain.

A molecular gene screen of ORFV factors that inhibit IFN-β could help to identify those factors that inhibit signalling. This approach has been used for other poxviruses. Based on the results obtained here, strongly suggests that ORFV targets the DNA sensing pathway(s). VACV devotes a considerable number of factors that target this pathway. DNA-PK is a heterotrimeric complex consisting of heterodimer Ku70 and Ku80 and catalytic subunit DNA-PKcs. Besides its DNA repair function, it acts as a DNA sensor operating via STING (Ferguson, B. J. *et al.*, 2012). VACV C16 and C4 were shown to antagonize the activation of DNA-PK by interacting with the Ku heterodimer and thereby disrupting the binding of the Ku heterodimer to DNA, resulting in inhibition of DNA-PK-mediated DNA sensing (Peters, N. E. *et al.*, 2013; Scutts, S. R. *et al.*, 2018). Interestingly, the VACV vv811 strain lacking 55 ORFs including C16 was effective at inhibiting DNA-induced STING activation, albeit with slight activation of IRF3 phosphorylation (Georgana, I. *et al.*, 2018; Perkus, M. E. *et al.*,

1991). To the best of our knowledge, this is the only DNA sensor identified so far to be directly targeted by poxviruses. VACV N1L is another viral protein that has been shown to interfere with DNA sensing by inhibiting the activation of TBK1. N1L, expressed from MVA, caused a reduction in IFN-β expression, possibly through STING (DiPerna, G. *et al.*, 2004). VACV C6 was described as an inhibitor of IFN-β expression by preventing activation of IRF3 and IRF7 at the level of TBK1/IKKε and interfering with kinase-associated scaffold proteins NAP1, TANK and SINTBAD (Unterholzner, L. *et al.*, 2011). Georgana, I. *et al.* (2018) have found that poxviruses like VACV, CPXV and ECTV, but not MVA, were able to interfere with DNA-induced STING signalling by inhibiting STING dimerization and phosphorylation. ORFV does not have homologs of the above VACV factors that are known to target the DNA sensing pathway, however, based on the findings of this study ORFV appears to be targeting cytosolic DNA sensing pathway(s) and it is possible that some of the unknown genes in ORFV are involved. The STING-mediated antiviral response is also targeted by DNA viruses replicating in the nucleus. HSV-1 did not induce the expression of IFN-β in HFF cells and antagonized the response by encoding VP22 protein acting upstream of the cGAS/STING pathway by interfering with enzymatic activity of cGAS (Huang, J. *et al.*, 2018), whereas KSHV vIRF1/K9 disrupts the TBK1-STING interaction resulting in inhibition of STING function (Ma, Z. *et al.*, 2015). The data obtained in the present study are consistent with the published reports for other poxviruses and other DNA viruses

The transfection of THP-1 cells with dsDNA poly(dA:dT) induces the expression of pro-inflammatory cytokines in THP-1 cells via activation of the inflammasome. Assays were performed to investigate whether or not ORFV blocked the secretion of IL-1β; however, this was found not to be the case. It was shown that the virus could express its early genes in THP-1 cells but could not replicate. Despite the above results, ORFV has however evolved strategies to block inflammatory cytokine production. It encodes a vIL-10 that inhibits the synthesis of pro-inflammatory cytokines IL-1β and TNF from LPS-stimulated PMA-primed THP-1 cells and many other cell types (Fleming, S. B. *et al.*, 1997; Imlach, W. *et al.*, 2002; Wise, L. *et al.*, 2007).

An important aspect of dsDNA sensor activation that was not followed up here, would be to demonstrate whether ORFV DNA induces the expression of IFN-β and which region of the virus genome acts as a PAMP. Experimental work could have included testing ORFV repeat DNA to induce the response, but due to time constraints was not conducted. For VACV the

expression of IFN-β was observed upon transfection with one repeat (70 bp) from the left terminus of the VACV (WR) genome (Almine, J. F. *et al.*, 2017; Unterholzner, L. *et al.*, 2010). A similar observation was also found in murine γ-herpesvirus 68 in which a 100-bp repetitive region within its genome containing a high percentage of GC content was found to be required and sufficient to induce type I IFN (Sanchez, D. J. *et al.*, 2008). ORFV encodes many repeats within the termini and such fragments could have been used to test their inducibility of IFN-β. Obtaining pure intact virus genomic DNA and efficient transfection of virus DNA molecules are both essential factors to conduct this assay successfully and that could be the reason for the majority of studies that have focused on inducibility of type I IFN using synthetic DNA or a fragment of the genome and not natural complete virus DNA. Upon identifying the direct involvement of virus DNA in induction of IFN, might also contribute towards identifying potential DNA sensor(s). The mechanism of the cytosolic DNA sensing system has not been fully elucidated and those DNA sensors discovered so far are not fully characterized, however, a possible approach would be to carry out a single or multiple gene knockdown or over-expression for those known cytosolic DNA sensors in several cell types then assess IFN induction.

In summary, IFN-β is a key cytokine of the innate antiviral response that is produced early during viral infection, thus poxviruses encode factors to disrupt IFN signalling at multiple levels. Here, this study provides preliminary evidence to show that ORFV possesses a mechanism to target IFN signalling in hNDF cells induced by poly(dA:dT) however it is yet to be proven that this is through cytoplasmic dsDNA sensing.

GENERAL DISCUSSION

6 GENERAL DISCUSSION

Despite the differences of mammalian viruses in structure, diseases they induce and replication strategies, they all trigger common cellular components during infection to initiate an innate immune response to a lesser or greater degree. An essential component of this response is induction of type I interferon. The IFN response, a powerful cellular defence against viral infection, results in the up-regulation of many ISGs whose products have antiviral activity. Not surprisingly, viruses have evolved a variety of strategies to evade the IFN response. Studies with poxviruses have demonstrated the role of multiple viral modulators that control the host IFN response by targeting type I IFN producing signalling pathways that are activated through cytosolic nucleic acid PRRs. ORFV has evolved strategies to counteract type I IFN expression. In this study, IFN-β was investigated specifically because it is a key cytokine produced early by most cell types, particularly fibroblasts, as a first line of defence against viral infection during the innate immune response. It has been shown for the first time that ORFV has the ability to inhibit signalling pathways that lead to the production of IFN-β that involve cytoplasmic RNA and DNA sensors. In addition, IFN antagonism employed by the virus involves the expression of early genes, however, the exact mechanism that ORFV employs to interfere with signalling are not yet known. It is likely that the inhibition of IFN-β will reflect a general inhibition of the type I IFN response in the cell types used in this study and this could be a reflection of such inhibition *in vivo*. The data presented here provide a new evasion mechanism for ORFV virus that allows it to replicate in the complex skin immune environment. Many other viruses also target type I IFN. VACV also utilizes early gene factors to inhibit IFN-β (Waibler, Z. *et al.*, 2009). Mouse cytomegalovirus, a DNA herpesvirus, inhibits IFN-β by targeting IRF3 activation (Le, V. T. K. *et al.*, 2008) and some RNA viruses such as dengue virus target IFN-β at the transcriptional level (Rodriguez-Madoz, J. R. *et al.*, 2010).

HEK293 and hNDF cells were used in this study as model systems to investigate the effects of ORFV infection on RNA sensing and DNA sensing respectively. For HEK293 cells I was able to define accurately the RNA sensing pathway that IFN-β induction operates through, whereas in the model of DNA sensing system, it still requires thorough examination to determine precisely the sensors and pathways involved. hNDF cells are more specialised than HEK293 cells as they express multiple nucleic acid sensing systems that lead to expression of IFN-β. Both cell types responded to poly(dA:dT) and poly(I:C) and produced high level

of IFN-β expression. In HEK293 cells, it was clearly shown that poly(dA:dT) triggered RIG-I-dependent signalling via Polymerase III, whereas it was not established whether poly(I:C) triggered RIG-I or the MDA5 sensor or both in HEK293 cells. hNDF cells express multiple RNA sensors, apart from RIG-I and MDA5, and these sensors have different properties (see Tables 1.4, 1.5 and 1.6), as a result, it could not be concluded which RNA sensors were involved in poly(I:C)-stimulated hNDF cells. Sentinel cells, including hNDF cells, express a range of DNA sensors in cytosol or endosome and it is not known yet the exact signature of DNA molecules that these sensors recognize. Having said that, it has been shown previously that poly(dA:dT) was recognized by many cytosolic DNA sensors in different cell types (see Table 1.3). As time permitted, the involvement of STING and RIG-I in the induction of IFN-β in HEK293 and hNDF cells were examined. Unlike HEK293, hNDF cells express STING that is critical for signalling where cytosolic DNA sensors are involved and it was shown that a reduction of IFN-β induction occurred when STING was depleted in poly(dA:dT) stimulated cells. Depletion of RIG-I alone did not cause significant inhibition in IFN-β expression when both STING and RIG-I were depleted in hNDF cells. In contrast, knockdown of RIG-I or inhibition of Polymerase III in HEK293 cells significantly altered the expression of IFN-β in poly(dA:dT)-stimulated cells. In both models, the synthesis of virus early proteins was required to inhibit the expression of IFN-β.

ORFV exclusively replicates in the cytoplasm of infected cells, rendering exposure to the host cytosolic nucleic acid detection system. TLRs, on the other hand, may play less of a role as they are located in endosomal compartments. Skin-resident keratinocytes act as sentinel cells that have the capability to activate the innate immune response against DNA viruses (Fleming, S. B. *et al.*, 2015; Nestle, F. O. *et al.*, 2009) and it has been shown that these cells are strong producers of IFN-α/β (Almine, J. F. *et al.*, 2017; Fujisawa, H. *et al.*, 1997; Schnipper, L. E. *et al.*, 1984; Torseth, J. W. *et al.*, 1987). Primary keratinocytes express a number of cytosolic DNA sensors such as ZBP1(DAI), IFI16, cGAS, STING and AIM2 and also TLRs such as TLR3 and TLR9 (Almine, J. F. *et al.*, 2017; Devos, M. *et al.*, 2020; Kopfnagel, V. *et al.*, 2011; Lebre, M. C. *et al.*, 2007). In spite of this, ORFV infects keratinocytes and causes a localized infection that persists for weeks. The above PRRs, strongly suggests that ORFV virus counteracts signalling that is either triggered by DNA or RNA in the cytoplasm perhaps the most important target being DNA sensing as the virus DNA will be first exposed to the cytoplasm, whereas dsRNA byproducts are generated post genomic replication when intermediate/late gene transcription is initiated.

The ORFV genome has about 64 % G-C content, and this is possibly due to mutational bias from unknown evolutionary pressures (Singer, G. A. C. *et al.*, 2000; Sueoka, N., 1988). TLR9 recognizes unmethylated CpG-containing ssDNA and it was found previously that ORFV detection was TLR9-dependent (von Buttlar, H. *et al.*, 2014), however, the virus was chemically inactive and the underlying mechanism might be different from live virus. The DNA or RNA structure of virus nucleic acids does not always reveal the class of sensors involved in viral nucleic acid detection since there are DNA viruses found to target RNA sensors and RNA viruses that target DNA sensors (Ma, Z. *et al.*, 2016). In time investigations will determine the sensors involved in virus detection, and structural analysis of nucleic acids sensors will unravel their sequence specificity. In my study although the DNA used for the model was AT rich and not GC rich, ORFV was nevertheless able to inhibit signalling which suggests that the target molecule(s) is where the DNA sensory pathways converge possibly at IRF-3 or a factor common to all the DNA sensory signalling pathways.

It is unknown whether IFN-β inhibition in this study was exerted by a single gene or multiple genes and whether targeting was directed at one component or several components of the signalling pathways. There are so far two early genes, ORF020 and ORF116, that have been shown to be potentially responsible for the inhibition of IFN. ORF116 was clearly shown to manipulate ISG expression by a mechanism that could be either a direct specific effect on ISGs or could have a role in inhibiting IFN-β production or signalling. It is intriguing to speculate that ORF116 could be targeting IRF-3 that is involved in both a direct induction of ISGs (type I IFN independent) and IFN-β production signalling pathways. It is strongly believed that ORF020 has an inhibitory effect on RIG-I-dependent signalling that leads to the expression of type I IFN. Nevertheless, further functional characterization of the interaction between ORF116 and ORF020 and the host is required to better understand their role on IFN modulation. There are likely to be many more ORFV genes involved in inhibiting type I IFN expression based on studies from other poxviruses. For instance, VACV encodes several genes A46, C6, C16, C4, K7, N1 and N2 that target different components of IFN signalling that leads to expression of type I IFN. ORFV could possess a similar mechanism to target factors where IFN signalling pathways converge. A large scale screen of ORFV ORFs is required to identify those gene(s) that inhibit type I IFN induction. In this study, it was confirmed that the inhibitory effect was caused by an early gene and the ORFs located in the terminal regions might be selected, as these two regions are rich in immunomodulatory genes. The appropriate strategy for this is that those ORFs are first cloned individually into

mammalian expression vectors then transfected individually into cells and the expression of type I IFNs assessed upon stimulation.

It is now clear from this study that ORFV has the ability to target all arms of the IFN response. The data presented here has revealed the potency of ORFV to inhibit IFN-β expression even when cells are stimulated with mimetic synthetic nucleic acids dsRNA or dsDNA however recent findings suggest that ORFV does not have the same potency to inhibit other arms of the IFN response such as those involved in effector immunity. VACV KIL and C7L were shown to have a role in inhibiting the IFN effector response by targeting SAMD9, a potent inhibitor of poxvirus replication that targets viral protein synthesis and deletion of these two genes makes the virus sensitive to IFN (Meng, X. *et al.*, 2009; Meng, X. *et al.*, 2012). Unusually members of the parapoxvirus genus lack homologues of KIL and C7L however despite this, ORFV can partially restore the growth phenotype of a VACV C7L/K1L deletion mutant in HeLa cells (Riad, S. *et al.*, 2020) suggesting that it has evolved an alternative strategy to target SAMD9. Moreover the potency of the IFN inhibitory effect was not found to be as strong as VACV and may partly explain why ORFV does not cause systemic infection and is restricted to the skin only. In addition ORFV does encode ORFV *ORF020* an orthologue of VACV E3L that binds dsRNA and inhibits the activation of PKR (Haig, D. M. *et al.*, 1998; McInnes, C. J. *et al.*, 1998) however its role as a virulence factor is unknown and this study has identified a new factor ORF116 that manipulates a number of ISGs expressed in HeLa cells, but its direct effect is yet to be determined. ORFV has also been shown to inhibit type I IFN signalling. The IFN-α/β receptor, JAK1, Tyk2, STAT1 and STAT2 are the major components of type I IFN signalling and it is not surprising that at least one or more of these components are targeted by almost all viruses (Fleming, S. B., 2016). ORFV does not produce soluble IFN receptor homologues or IFN binding proteins to disable the IFN from binding to its receptor that are encoded by orthopoxviruses (Colamonici, O. R. *et al.*, 1995) however ORFV encodes a homologue of VH1 that targets STAT1 and ORFV potently inhibits the JAK/STAT signalling pathway (Harvey, R. *et al.*, 2015).

Poxviruses are some of the largest of the DNA viruses harbouring from 130 to 200 genes. Relatively, half of those are involved in host range, virulence and immunomodulation. It is believed that the virus may require many inhibitors to target all possible signalling pathways that ultimately lead to the induction of type I IFN. There is a general view that multiple viral inhibitors of the IFN system encoded by poxviruses have non-redundant function. The virus

needs to counteract the complex signalling pathways and any cross talk between different pathways. As some poxviruses have a broad host range, this will require encoding different viral inhibitors tailored to target specific signalling pathways or components or at different stages of infection. It is possible that each viral inhibitor could have multiple functions.

Future studies could focus on the underlying mechanisms by which the ORFV causes IFN inhibition and the IFN signalling components targeted to obtain further insight into the nature of this virus-host interaction. Expressing IFN signalling molecules individually from vectors in cells could aid the identification of components of the RIG-I-dependent sensing signalling pathways targeted by ORFV. Further work is needed to conclusively demonstrate that ORFV targets cytoplasmic DNA sensor signalling pathways and also to identify which DNA sensors are involved in detecting ORFV. This could be demonstrated by utilizing knockout cells that are deficient in expressing critical cytosolic DNA signalling molecules or DNA sensors. Overall, understanding those underlying mechanisms will not only unravel viral strategies to evade immune sensing but may also lead to the discovery of potential antiviral therapeutics.

FUTURE DIRECTIONS

7 FUTURE DIRECTIONS

The novel observations reported in this thesis have opened up many research questions for future study and some are listed below in order of priority:

- Investigate the colocalization of 116 protein in the infected cell.
- Conduct 116 binding protein pull-down assays and identify 116 protein partners by mass spectrometry.
- Look at the effect of 116 gene expression from vector on the production of IFN-β released with dsDNA such as poly(dA:dT) and viral DNA.
- Determine the mechanism of how the virus inhibits the IFN induction and which factors, interfere with the signalling molecules that lead to IFN induction and ISG expression.
- Look at the effect of ORFV virus on signalling pathways that lead to IFN production primarily those pathways that require DNA sensors and whether there are any differences between different cell types.
- A series of siRNA knockdown for RNA or DNA sensors to determine any potential receptors involved in ORFV virus detection.
- Identify endogenous active forms of the pathways that ORFV virus is targeting in different cell types by using western immunoblotting.
- Examine the cellular transcriptome from viral infection of other cell lines e.g. hNDF and HEK293 using wild type, knockout and revertant viruses and looking at gene expression levels of specific ISGs using qPCR.
- Examine cellular gene expression and transcriptome by applying new advanced technology e.g. RNA-seq or NanoString technology. Deep RNA sequencing will enable us to obtain high resolution data of both the viral and cellular transcriptome simultaneously.
- Produce an antibody against ORF116 to detect it in the infected cells.
- Knocking down the affected ISGs genes using siRNA could determine the antiviral effectors targeted by ORF116.
- Conduct an in vivo study on animal models to determine the virulence of ORF116 using the wild type, ORF116 deletion mutant and revertant viruses.

8 REFERENCES

Abe, T., & Barber, G. N. (2014). Cytosolic-DNA-Mediated, STING-Dependent Proinflammatory Gene Induction Necessitates Canonical NF-κB Activation through TBK1. *Journal of Virology, 88*(10), 5328-5341.

Abe, T., Harashima, A., Xia, T., Konno, H., Konno, K., Morales, A., Ahn, J., Gutman, D., & Barber, Glen N. (2013). STING Recognition of Cytoplasmic DNA Instigates Cellular Defense. *Molecular Cell, 50*(1), 5-15.

Ablasser, A., Bauernfeind, F., Hartmann, G., Latz, E., Fitzgerald, K. A., & Hornung, V. (2009). RIG-I-dependent sensing of poly(dA:dT) through the induction of an RNA polymerase III–transcribed RNA intermediate. *Nature Immunology, 10*(10), 1065-1072.

Ablasser, A., Goldeck, M., Cavlar, T., Deimling, T., Witte, G., Röhl, I., Hopfner, K.-P., Ludwig, J., & Hornung, V. (2013). cGAS produces a 2′-5′-linked cyclic dinucleotide second messenger that activates STING. *Nature, 498*(7454), 380-384.

Akira, S. (2003). Toll-like Receptor Signaling. *Journal of Biological Chemistry, 278*(40), 38105-38108.

Alcami, A., & Smith, G. L. (1992). A soluble receptor for interleukin-1β encoded by vaccinia virus: A novel mechanism of virus modulation of the host response to infection. *Cell, 71*(1), 153-167.

Alcamí, A., & Smith, G. L. (1995). Vaccinia, cowpox, and camelpox viruses encode soluble gamma interferon receptors with novel broad species specificity. *Journal of Virology, 69*(8), 4633-4639.

Alcamí, A., Symons, J. A., & Smith, G. L. (2000). The Vaccinia Virus Soluble Alpha/Beta Interferon (IFN) Receptor Binds to the Cell Surface and Protects Cells from the Antiviral Effects of IFN. *Journal of Virology, 74*(23), 11230-11239.

AlDaif, B. (2013). *Functional analysis of the Orf virus ORF116 gene: a potential modulator of the interferon response* (Master of Science Master's Thesis), University of Otago, Dunedin, New Zealand. Retrieved from http://hdl.handle.net/10523/4621

Alexopoulou, L., Holt, A. C., Medzhitov, R., & Flavell, R. A. (2001). Recognition of double-stranded RNA and activation of NF-κB by Toll-like receptor 3. *Nature, 413*(6857), 732-738.

Alff, P. J., Sen, N., Gorbunova, E., Gavrilovskaya, I. N., & Mackow, E. R. (2008). The NY-1 Hantavirus Gn Cytoplasmic Tail Coprecipitates TRAF3 and Inhibits Cellular

Interferon Responses by Disrupting TBK1-TRAF3 Complex Formation. *Journal of Virology, 82*(18), 9115-9122.

Almine, J. F., O'Hare, C. A. J., Dunphy, G., Haga, I. R., Naik, R. J., Atrih, A., Connolly, D. J., Taylor, J., Kelsall, I. R., Bowie, A. G., Beard, P. M., & Unterholzner, L. (2017). IFI16 and cGAS cooperate in the activation of STING during DNA sensing in human keratinocytes. *Nature Communications, 8*(1), 14392.

Alspach, E., Lussier, D. M., & Schreiber, R. D. (2019). Interferon γ and Its Important Roles in Promoting and Inhibiting Spontaneous and Therapeutic Cancer Immunity. *Cold Spring Harbor Perspectives in Biology, 11*(3), a028480.

Andersen, J., VanScoy, S., Cheng, T. F., Gomez, D., & Reich, N. C. (2008). IRF-3-dependent and augmented target genes during viral infection. *Genes Immun, 9*(2), 168-175.

Andrejeva, J., Childs, K. S., Young, D. F., Carlos, T. S., Stock, N., Goodbourn, S., & Randall, R. E. (2004). The V proteins of paramyxoviruses bind the IFN-inducible RNA helicase, mda-5, and inhibit its activation of the IFN-β promoter. *Proceedings of the National Academy of Sciences of the United States of America, 101*(49), 17264-17269.

Ank, N., West, H., & Paludan, S. R. (2006). IFN-λ: Novel Antiviral Cytokines. *Journal of Interferon & Cytokine Research, 26*(6), 373-379.

Barber, G. N. (2011). Innate immune DNA sensing pathways: STING, AIMII and the regulation of interferon production and inflammatory responses. *Current Opinion in Immunology, 23*(1), 10-20.

Barral, P. M., Sarkar, D., Fisher, P. B., & Racaniello, V. R. (2009). RIG-I is cleaved during picornavirus infection. *Virology, 391*(2), 171-176.

Baum, A., Sachidanandam, R., & García-Sastre, A. (2010). Preference of RIG-I for short viral RNA molecules in infected cells revealed by next-generation sequencing. *Proceedings of the National Academy of Sciences, 107*(37), 16303-16308.

Beattie, E., Denzler, K. L., Tartaglia, J., Perkus, M. E., Paoletti, E., & Jacobs, B. L. (1995). Reversal of the interferon-sensitive phenotype of a vaccinia virus lacking E3L by expression of the reovirus S4 gene. *Journal of Virology, 69*(1), 499-505.

Beattie, E., Paoletti, E., & Tartaglia, J. (1995). Distinct Patterns of IFN Sensitivity Observed in Cells Infected with Vaccinia K3L- and E3L- Mutant Viruses. *Virology, 210*(2), 254-263.

Bergkessel, M., & Guthrie, C. (2013). Colony PCR. *Methods Enzymol, 529*, 299-309.

Biolatti, M., Dell'Oste, V., Pautasso, S., von Einem, J., Marschall, M., Plachter, B., Gariglio, M., De Andrea, M., & Landolfo, S. (2016). Regulatory Interaction between the Cellular Restriction Factor IFI16 and Viral pp65 (pUL83) Modulates Viral Gene Expression and IFI16 Protein Stability. *Journal of Virology, 90*(18), 8238-8250.

Bochud, P.-Y., Hersberger, M., Taffé, P., Bochud, M., Stein, C. M., Rodrigues, S. D., Calandra, T., Francioli, P., Telenti, A., Speck, R. F., Aderem, A., & Study, f. t. S. H. C. (2007). Polymorphisms in Toll-like receptor 9 influence the clinical course of HIV-1 infection. *AIDS, 21*(4), 441-446.

Boehme, K. W., & Compton, T. (2004). Innate Sensing of Viruses by Toll-Like Receptors. *Journal of Virology, 78*(15), 7867-7873.

Bourquain, D., & Nitsche, A. (2013). Cowpox virus but not Vaccinia virus induces secretion of CXCL1, IL-8 and IL-6 and chemotaxis of monocytes in vitro. *Virus Research, 171*(1), 161-167.

Bowie, A., Kiss-Toth, E., Symons, J. A., Smith, G. L., Dower, S. K., & O'Neill, L. A. J. (2000). A46R and A52R from vaccinia virus are antagonists of host IL-1 and toll-like receptor signaling. *Proceedings of the National Academy of Sciences, 97*(18), 10162-10167.

Bowie, A. G., & Haga, I. R. (2005). The role of Toll-like receptors in the host response to viruses. *Molecular Immunology, 42*(8), 859-867.

Bowie, A. G., & Unterholzner, L. (2008). Viral evasion and subversion of pattern-recognition receptor signalling. *Nature Reviews Immunology, 8*(12), 911-922.

Boyle, K., & Traktman, P. (2009). Poxviruses. In K. D. Raney, M. Gotte, & C. E. Cameron (Eds.), *Viral Genome Replication* (pp. 225-247). Boston, MA: Springer US.

Brass, A. L., Huang, I. C., Benita, Y., John, S. P., Krishnan, M. N., Feeley, E. M., Ryan, B. J., Weyer, J. L., van der Weyden, L., Fikrig, E., Adams, D. J., Xavier, R. J., Farzan, M., & Elledge, S. J. (2009). The IFITM Proteins Mediate Cellular Resistance to Influenza A H1N1 Virus, West Nile Virus, and Dengue Virus. *Cell, 139*(7), 1243-1254.

Broder, C. C., & Earl, P. L. (1999). Recombinant vaccinia viruses. *Molecular Biotechnology, 13*(3), 223-245.

Brzostek-Racine, S., Gordon, C., Van Scoy, S., & Reich, N. C. (2011). The DNA Damage Response Induces IFN. *The Journal of Immunology, 187*(10), 5336-5345.

Buller, R. M., & Palumbo, G. J. (1991). Poxvirus pathogenesis. *Microbiological Reviews, 55*(1), 80-122.

Bürckstümmer, T., Baumann, C., Blüml, S., Dixit, E., Dürnberger, G., Jahn, H., Planyavsky, M., Bilban, M., Colinge, J., Bennett, K. L., & Superti-Furga, G. (2009). An orthogonal proteomic-genomic screen identifies AIM2 as a cytoplasmic DNA sensor for the inflammasome. *Nature Immunology, 10*(3), 266-272.

Burdette, D. L., Monroe, K. M., Sotelo-Troha, K., Iwig, J. S., Eckert, B., Hyodo, M., Hayakawa, Y., & Vance, R. E. (2011). STING is a direct innate immune sensor of cyclic di-GMP. *Nature, 478*(7370), 515-518.

Burdette, D. L., & Vance, R. E. (2012). STING and the innate immune response to nucleic acids in the cytosol. *Nature Immunology, 14*(1), 19-26.

Burleigh, K., Maltbaek, J. H., Cambier, S., Green, R., Gale, M., James, R. C., & Stetson, D. B. (2019). Human DNA-PK activates a STING-independent DNA sensing pathway. *bioRxiv*, 587501.

Büttner, M., Czerny, C. P., Lehner, K. H., & Wertz, K. (1995). Interferon induction in peripheral blood mononuclear leukocytes of man and farm animals by poxvirus vector candidates and some poxvirus constructs. *Veterinary Immunology and Immunopathology, 46*(3), 237-250.

Byrd, C. M., & Hruby, D. E. (2004). Construction of Recombinant Vaccinia Virus. In S. N. Isaacs (Ed.), *Vaccinia Virus and Poxvirology: Methods and Protocols* (pp. 31-40). Totowa, NJ: Humana Press.

Cai, X., Chiu, Y.-H., & Chen, Zhijian J. (2014). The cGAS-cGAMP-STING Pathway of Cytosolic DNA Sensing and Signaling. *Molecular Cell, 54*(2), 289-296.

Camus-Bouclainville, C., Fiette, L., Bouchiha, S., Pignolet, B., Counor, D., Filipe, C., Gelfi, J., & Messud-Petit, F. (2004). A Virulence Factor of Myxoma Virus Colocalizes with NF-κB in the Nucleus and Interferes with Inflammation. *Journal of Virology, 78*(5), 2510-2516.

Cao, H., Dai, P., Wang, W., Li, H., Yuan, J., Wang, F., Fang, C.-M., Pitha, P. M., Liu, J., Condit, R. C., McFadden, G., Merghoub, T., Houghton, A. N., Young, J. W., Shuman, S., & Deng, L. (2012). Innate Immune Response of Human Plasmacytoid Dendritic Cells to Poxvirus Infection Is Subverted by Vaccinia E3 via Its Z-DNA/RNA Binding Domain. *PLoS ONE, 7*(5), e36823.

Carlton-Smith, C., & Elliott, R. M. (2012). Viperin, MTAP44, and Protein Kinase R Contribute to the Interferon-Induced Inhibition of Bunyamwera Orthobunyavirus Replication. *Journal of Virology, 86*(21), 11548-11557.

Carty, M., & Bowie, A. G. (2010). Recent insights into the role of Toll-like receptors in viral infection. *Clinical & Experimental Immunology, 161*(3), 397-406.

Chakrabarti, A., Banerjee, S., Franchi, L., Loo, Y.-M., Gale, M., Núñez, G., & Silverman, Robert H. (2015). RNase L Activates the NLRP3 Inflammasome during Viral Infections. *Cell Host & Microbe, 17*(4), 466-477.

Chang, H. W., Watson, J. C., & Jacobs, B. L. (1992). The E3L gene of vaccinia virus encodes an inhibitor of the interferon-induced, double-stranded RNA-dependent protein kinase. *Proceedings of the National Academy of Sciences of the United States of America, 89*(11), 4825-4829.

Chang, Y. E., & Laimins, L. A. (2000). Microarray Analysis Identifies Interferon-Inducible Genes and Stat-1 as Major Transcriptional Targets of Human Papillomavirus Type 31. *Journal of Virology, 74*(9), 4174-4182.

Chawla-Sarkar, M., Lindner, D. J., Liu, Y.-F., Williams, B. R., Sen, G. C., Silverman, R. H., & Borden, E. C. (2003). Apoptosis and interferons: Role of interferon-stimulated genes as mediators of apoptosis. *Apoptosis, 8*(3), 237-249.

Chen, D., Zheng, Z., Xiao, B., Li, W., Long, M., Chen, H., Li, M., Rock, D. L., Hao, W., & Luo, S. (2016). Orf Virus 002 Protein Targets Ovine Protein S100A4 and Inhibits NF-κB Signaling. *Frontiers in Microbiology, 7*, 1389-1389.

Chen, H., Sun, H., You, F., Sun, W., Zhou, X., Chen, L., Yang, J., Wang, Y., Tang, H., Guan, Y., Xia, W., Gu, J., Ishikawa, H., Gutman, D., Barber, G., Qin, Z., & Jiang, Z. (2011). Activation of STAT6 by STING Is Critical for Antiviral Innate Immunity. *Cell, 147*(2), 436-446.

Chen, Q., Sun, L., & Chen, Z. J. (2016). Regulation and function of the cGAS–STING pathway of cytosolic DNA sensing. *Nature Immunology, 17*(10), 1142-1149.

Chen, R. A. J., Ryzhakov, G., Cooray, S., Randow, F., & Smith, G. L. (2008). Inhibition of IκB Kinase by Vaccinia Virus Virulence Factor B14. *PLOS Pathogens, 4*(2), e22.

Cheng, G., Zhong, J., Chung, J., & Chisari, F. V. (2007). Double-stranded DNA and double-stranded RNA induce a common antiviral signaling pathway in human cells. *Proceedings of the National Academy of Sciences, 104*(21), 9035-9040.

Chi, X., Zeng, X., Li, W., Hao, W., Li, M., Huang, X., Huang, Y., Rock, D. L., Luo, S., & Wang, S. (2015). Genome analysis of orf virus isolates from goats in the Fujian Province of southern China. *Frontiers in Microbiology, 6*, 1135.

Chiu, Y.-H., MacMillan, J. B., & Chen, Z. J. (2009). RNA Polymerase III Detects Cytosolic DNA and Induces Type I Interferons through the RIG-I Pathway. *Cell, 138*(3), 576-591.

Chow, K. T., Jr., M. G., & Loo, Y.-M. (2018). RIG-I and Other RNA Sensors in Antiviral Immunity. *Annual Review of Immunology, 36*(1), 667-694.

Christensen, M. H., Jensen, S. B., Miettinen, J. J., Luecke, S., Prabakaran, T., Reinert, L. S., Mettenleiter, T., Chen, Z. J., Knipe, D. M., Sandri-Goldin, R. M., Enquist, L. W., Hartmann, R., Mogensen, T. H., Rice, S. A., Nyman, T. A., Matikainen, S., & Paludan, S. R. (2016). HSV-1 ICP27 targets the TBK1-activated STING signalsome to inhibit virus-induced type I IFN expression. *The EMBO Journal, 35*(13), 1385-1399.

Civril, F., Deimling, T., de Oliveira Mann, C. C., Ablasser, A., Moldt, M., Witte, G., Hornung, V., & Hopfner, K.-P. (2013). Structural mechanism of cytosolic DNA sensing by cGAS. *Nature, 498*(7454), 332-337.

Colamonici, O. R., Domanski, P., Sweitzer, S. M., Larner, A., & Buller, R. M. L. (1995). Vaccinia Virus B18R Gene Encodes a Type I Interferon-binding Protein That Blocks Interferon α Transmembrane Signaling. *Journal of Biological Chemistry, 270*(27), 15974-15978.

Cooray, S., Bahar, M. W., Abrescia, N. G. A., McVey, C. E., Bartlett, N. W., Chen, R. A.-J., Stuart, D. I., Grimes, J. M., & Smith, G. L. (2007). Functional and structural studies of the vaccinia virus virulence factor N1 reveal a Bcl-2-like anti-apoptotic protein. *Journal of General Virology, 88*(6), 1656-1666.

Cristea, I. M., Moorman, N. J., Terhune, S. S., Cuevas, C. D., O'Keefe, E. S., Rout, M. P., Chait, B. T., & Shenk, T. (2010). Human Cytomegalovirus pUL83 Stimulates Activity of the Viral Immediate-Early Promoter through Its Interaction with the Cellular IFI16 Protein. *Journal of Virology, 84*(15), 7803-7814.

Cuchet-Lourenço, D., Anderson, G., Sloan, E., Orr, A., & Everett, R. D. (2013). The Viral Ubiquitin Ligase ICP0 Is neither Sufficient nor Necessary for Degradation of the Cellular DNA Sensor IFI16 during Herpes Simplex Virus 1 Infection. *Journal of Virology, 87*(24), 13422-13432.

Daffis, S., Samuel, M. A., Suthar, M. S., Gale, M., & Diamond, M. S. (2008). Toll-Like Receptor 3 Has a Protective Role against West Nile Virus Infection. *Journal of Virology, 82*(21), 10349-10358.

Dai, P., Cao, H., Merghoub, T., Avogadri, F., Wang, W., Parikh, T., Fang, C.-M., Pitha, P. M., Fitzgerald, K. A., Rahman, M. M., McFadden, G., Hu, X., Houghton, A. N., Shuman, S., & Deng, L. (2011). Myxoma virus induces type I interferon production in murine plasmacytoid dendritic cells via a TLR9/MyD88-, IRF5/IRF7-, and IFNAR-dependent pathway. *Journal of Virology, 85*(20), 10814-10825.

Dai, P., Wang, W., Cao, H., Avogadri, F., Dai, L., Drexler, I., Joyce, J. A., Li, X.-D., Chen, Z., Merghoub, T., Shuman, S., & Deng, L. (2014). Modified vaccinia virus Ankara triggers type I IFN production in murine conventional dendritic cells via a cGAS/STING-mediated cytosolic DNA-sensing pathway. *PLOS Pathogens, 10*(4), e1003989.

Damon, I. K. (2007). Poxviruses. In D. E. G. David M. Knipe, Robert A. Lamb, Stephen E. Straus, Peter M. Howley, Malcolm A. Martin, Bernard Roizman (Ed.), *Fields Virology* (5 ed., Vol. 2, pp. 2947-2976). Philadelphia: Wolters Kluwer-Lippincott Williams & Wilkins.

Darnell, J., Kerr, I., & Stark, G. (1994). Jak-STAT pathways and transcriptional activation in response to IFNs and other extracellular signaling proteins. *Science, 264*(5164), 1415-1421.

Datta, A., Sinha-Datta, U., Dhillon, N. K., Buch, S., & Nicot, C. (2006). The HTLV-I p30 Interferes with TLR4 Signaling and Modulates the Release of Pro- and Anti-inflammatory Cytokines from Human Macrophages. *Journal of Biological Chemistry, 281*(33), 23414-23424.

Davies, M. V., Chang, H. W., Jacobs, B. L., & Kaufman, R. J. (1993). The E3L and K3L vaccinia virus gene products stimulate translation through inhibition of the double-stranded RNA-dependent protein kinase by different mechanisms. *Journal of Virology, 67*(3), 1688-1692.

Davies, M. V., Elroy-Stein, O., Jagus, R., Moss, B., & Kaufman, R. J. (1992). The vaccinia virus K3L gene product potentiates translation by inhibiting double-stranded-RNA-activated protein kinase and phosphorylation of the alpha subunit of eukaryotic initiation factor 2. *Journal of Virology, 66*(4), 1943-1950.

Davis, Meredith E., Wang, May K., Rennick, Linda J., Full, F., Gableske, S., Mesman, Annelies W., Gringhuis, Sonja I., Geijtenbeek, Teunis B. H., Duprex, W. P., & Gack, Michaela U. (2014). Antagonism of the Phosphatase PP1 by the Measles Virus V Protein Is Required for Innate Immune Escape of MDA5. *Cell Host & Microbe, 16*(1), 19-30.

Davis, W. G., Bowzard, J. B., Sharma, S. D., Wiens, M. E., Ranjan, P., Gangappa, S., Stuchlik, O., Pohl, J., Donis, R. O., Katz, J. M., Cameron, C. E., Fujita, T., & Sambhara, S. (2012). The 3′ Untranslated Regions of Influenza Genomic Sequences Are 5′PPP-Independent Ligands for RIG-I. *PLoS ONE, 7*(3), e32661.

de Bouteiller, O., Merck, E., Hasan, U. A., Hubac, S., Benguigui, B., Trinchieri, G., Bates, E. E. M., & Caux, C. (2005). Recognition of Double-stranded RNA by Human Toll-like Receptor 3 and Downstream Receptor Signaling Requires Multimerization and an Acidic pH. *Journal of Biological Chemistry, 280*(46), 38133-38145.

de Veer, M. J., Holko, M., Frevel, M., Walker, E., Der, S., Paranjape, J. M., Silverman, R. H., & Williams, B. R. G. (2001). Functional classification of interferon-stimulated genes identified using microarrays. *Journal of Leukocyte Biology, 69*(6), 912-920.

Deane, D., McInnes, C. J., Percival, A., Wood, A., Thomson, J., Lear, A., Gilray, J., Fleming, S., Mercer, A., & Haig, D. (2000). Orf Virus Encodes a Novel Secreted Protein Inhibitor of Granulocyte-Macrophage Colony-Stimulating Factor and Interleukin-2. *Journal of Virology, 74*(3), 1313-1320.

Deddouche, S., Goubau, D., Rehwinkel, J., Chakravarty, P., Begum, S., Maillard, P. V., Borg, A., Matthews, N., Feng, Q., van Kuppeveld, F. J. M., & Reis e Sousa, C. (2014). Identification of an LGP2-associated MDA5 agonist in picornavirus-infected cells. *eLife, 3*, e01535.

Delaloye, J., Roger, T., Steiner-Tardivel, Q.-G., Le Roy, D., Knaup Reymond, M., Akira, S., Petrilli, V., Gomez, C. E., Perdiguero, B., Tschopp, J., Pantaleo, G., Esteban, M., & Calandra, T. (2009). Innate Immune Sensing of Modified Vaccinia Virus Ankara (MVA) Is Mediated by TLR2-TLR6, MDA-5 and the NALP3 Inflammasome. *PLOS Pathogens, 5*(6), e1000480.

Delhon, G., Tulman, E. R., Afonso, C. L., Lu, Z., de la Concha-Bermejillo, A., Lehmkuhl, H. D., Piccone, M. E., Kutish, G. F., & Rock, D. L. (2004). Genomes of the Parapoxviruses Orf Virus and Bovine Papular Stomatitis Virus. *Journal of Virology, 78*(1), 168-177.

Dell'Oste, V., Gatti, D., Gugliesi, F., De Andrea, M., Bawadekar, M., Lo Cigno, I., Biolatti, M., Vallino, M., Marschall, M., Gariglio, M., & Landolfo, S. (2014). Innate Nuclear Sensor IFI16 Translocates into the Cytoplasm during the Early Stage of In Vitro Human Cytomegalovirus Infection and Is Entrapped in the Egressing Virions during the Late Stage. *Journal of Virology, 88*(12), 6970-6982.

Der, S. D., & Lau, A. S. (1995). Involvement of the double-stranded-RNA-dependent kinase PKR in interferon expression and interferon-mediated antiviral activity. *Proceedings of the National Academy of Sciences, 92*(19), 8841-8845.

Der, S. D., Zhou, A., Williams, B. R. G., & Silverman, R. H. (1998). Identification of genes differentially regulated by interferon α, β, or γ using oligonucleotide arrays. *Proceedings of the National Academy of Sciences, 95*(26), 15623-15628.

Devos, M., Tanghe, G., Gilbert, B., Dierick, E., Verheirstraeten, M., Nemegeer, J., de Reuver, R., Lefebvre, S., De Munck, J., Rehwinkel, J., Vandenabeele, P., Declercq, W., & Maelfait, J. (2020). Sensing of endogenous nucleic acids by ZBP1 induces keratinocyte necroptosis and skin inflammation. *Journal of Experimental Medicine, 217*(7). doi:10.1084/jem.20191913

Diebold, S. S., Kaisho, T., Hemmi, H., Akira, S., & Reis e Sousa, C. (2004). Innate Antiviral Responses by Means of TLR7-Mediated Recognition of Single-Stranded RNA. *Science, 303*(5663), 1529-1531.

Diebold, S. S., Massacrier, C., Akira, S., Paturel, C., Morel, Y., & Reis e Sousa, C. (2006). Nucleic acid agonists for Toll-like receptor 7 are defined by the presence of uridine ribonucleotides. *European Journal of Immunology, 36*(12), 3256-3267.

Diebold, S. S., Montoya, M., Unger, H., Alexopoulou, L., Roy, P., Haswell, L. E., Al-Shamkhani, A., Flavell, R., Borrow, P., & Sousa, C. R. e. (2003). Viral infection switches non-plasmacytoid dendritic cells into high interferon producers. *Nature, 424*(6946), 324-328.

Diel, D. G., Delhon, G., Luo, S., Flores, E. F., & Rock, D. L. (2010). A Novel Inhibitor of the NF-κB Signaling Pathway Encoded by the Parapoxvirus Orf Virus. *Journal of Virology, 84*(8), 3962-3973.

Diel, D. G., Luo, S., Delhon, G., Peng, Y., Flores, E. F., & Rock, D. L. (2011a). A nuclear inhibitor of NF-kappaB encoded by a poxvirus. *Journal of Virology, 85*(1), 264-275.

Diel, D. G., Luo, S., Delhon, G., Peng, Y., Flores, E. F., & Rock, D. L. (2011b). Orf virus ORFV121 encodes a novel inhibitor of NF-kappaB that contributes to virus virulence. *Journal of Virology, 85*(5), 2037-2049.

Diner, B. A., Lum, K. K., Javitt, A., & Cristea, I. M. (2015). Interactions of the Antiviral Factor Interferon Gamma-Inducible Protein 16 (IFI16) Mediate Immune Signaling and Herpes Simplex Virus-1 Immunosuppression. *Molecular & Cellular Proteomics, 14*(9), 2341-2356.

Diner, Elie J., Burdette, Dara L., Wilson, Stephen C., Monroe, Kathryn M., Kellenberger, Colleen A., Hyodo, M., Hayakawa, Y., Hammond, Ming C., & Vance, Russell E. (2013). The Innate Immune DNA Sensor cGAS Produces a Noncanonical Cyclic Dinucleotide that Activates Human STING. *Cell Reports*, *3*(5), 1355-1361.

DiPerna, G., Stack, J., Bowie, A. G., Boyd, A., Kotwal, G., Zhang, Z., Arvikar, S., Latz, E., Fitzgerald, K. A., & Marshall, W. L. (2004). Poxvirus Protein N1L Targets the I-κB Kinase Complex, Inhibits Signaling to NF-κB by the Tumor Necrosis Factor Superfamily of Receptors, and Inhibits NF-κB and IRF3 Signaling by Toll-like Receptors. *Journal of Biological Chemistry, 279*(35), 36570-36578.

Dobbs, N., Burnaevskiy, N., Chen, D., Gonugunta, Vijay K., Alto, Neal M., & Yan, N. (2015). STING Activation by Translocation from the ER Is Associated with Infection and Autoinflammatory Disease. *Cell Host & Microbe, 18*(2), 157-168.

Domingo-Gil, E., Pérez-Jiménez, E., Ventoso, I., Nájera, J. L., & Esteban, M. (2008). Expression of the E3L Gene of Vaccinia Virus in Transgenic Mice Decreases Host Resistance to Vaccinia Virus and Leishmania major Infections. *Journal of Virology, 82*(1), 254-267.

Dreux, M., Garaigorta, U., Boyd, B., Décembre, E., Chung, J., Whitten-Bauer, C., Wieland, S., & Chisari, Francis V. (2012). Short-Range Exosomal Transfer of Viral RNA from Infected Cells to Plasmacytoid Dendritic Cells Triggers Innate Immunity. *Cell Host & Microbe, 12*(4), 558-570.

Duan, X., Ponomareva, L., Veeranki, S., Panchanathan, R., Dickerson, E., & Choubey, D. (2011). Differential Roles for the Interferon-Inducible IFI16 and AIM2 Innate Immune Sensors for Cytosolic DNA in Cellular Senescence of Human Fibroblasts. *Molecular Cancer Research, 9*(5), 589-602.

Ember, S. W. J., Ren, H., Ferguson, B. J., & Smith, G. L. (2012). Vaccinia virus protein C4 inhibits NF-κB activation and promotes virus virulence. *Journal of General Virology, 93*(10), 2098-2108.

Equils, O., Schito, M. L., Karahashi, H., Madak, Z., Yarali, A., Michelsen, K. S., Sher, A., & Arditi, M. (2003). Toll-Like Receptor 2 (TLR2) and TLR9 Signaling Results in HIV-Long Terminal Repeat Trans-Activation and HIV Replication in HIV-1 Transgenic Mouse Spleen Cells: Implications of Simultaneous Activation of TLRs on HIV Replication. *The Journal of Immunology, 170*(10), 5159-5164.

Erlandsson, L., Blumenthal, R., Eloranta, M.-L., Engel, H., Alm, G., Weiss, S., & Leanderson, T. (1998). Interferon-beta is required for interferon-alpha production in mouse fibroblasts. *Current Biology, 8*(4), 223-226.

Espert, L., Degols, G., Lin, Y.-L., Vincent, T., Benkirane, M., & Mechti, N. (2005). Interferon-induced exonuclease ISG20 exhibits an antiviral activity against human immunodeficiency virus type 1. *Journal of General Virology, 86*(8), 2221-2229.

Espert, L., Rey, C., Gonzalez, L., Degols, G., Chelbi-Alix, M. K., Mechti, N., & Gongora, C. (2004). The exonuclease ISG20 is directly induced by synthetic dsRNA via NF-κB and IRF1 activation. *Oncogene, 23*(26), 4636-4640.

Evans, M. J., Hartman, S. L., Wolff, D. W., Rollins, S. A., & Squinto, S. P. (1995). Rapid expression of an anti-human C5 chimeric Fab utilizing a vector that replicates in COS and 293 cells. *Journal of Immunological Methods, 184*(1), 123-138.

Fahy, A. S., Clark, R. H., Glyde, E. F., & Smith, G. L. (2008). Vaccinia virus protein C16 acts intracellularly to modulate the host response and promote virulence. *Journal of General Virology, 89*(10), 2377-2387.

Fasbender, A., Marshall, J., Moninger, T. O., Grunst, T., Cheng, S., & Welsh, M. J. (1997). Effect of co-lipids in enhancing cationic lipid-mediated gene transfer in vitro and in vivo. *Gene Therapy, 4*(7), 716-725.

Feng, Q., Hato, Stanleyson V., Langereis, Martijn A., Zoll, J., Virgen-Slane, R., Peisley, A., Hur, S., Semler, Bert L., van Rij, Ronald P., & van Kuppeveld, Frank J. M. (2012). MDA5 Detects the Double-Stranded RNA Replicative Form in Picornavirus-Infected Cells. *Cell Reports, 2*(5), 1187-1196.

Feng, Q., Langereis, M. A., Lork, M., Nguyen, M., Hato, S. V., Lanke, K., Emdad, L., Bhoopathi, P., Fisher, P. B., Lloyd, R. E., & van Kuppeveld, F. J. M. (2014). Enterovirus 2Apro Targets MDA5 and MAVS in Infected Cells. *Journal of Virology, 88*(6), 3369-3378.

Fenner, F. (1959). Genetic studies with mammalian poxviruses. II. Recombination between two strains of vaccinia virus in single HeLa cells. *Virology, 8*, 499-507.

Fenner, F., & Comben, B. M. (1958). Genetic studies with mammalian poxviruses: I. Demonstration of recombination between two strains of vaccinia virus. *Virology, 5*(3), 530-548.

Fenner, F., & Nakano, J. H. (1988). Poxviridae: The Poxviruses *Laboratory Diagnosis of Infectious Diseases Principles and Practice: VOLUME II Viral, Rickettsial, and Chlamydial Diseases* (pp. 177-210). New York, NY: Springer New York.

Fensterl, V., & Sen, G. C. (2011). The ISG56/IFIT1 Gene Family. *Journal of Interferon & Cytokine Research, 31*(1), 71-78.

Ferguson, B. J., Benfield, C. T. O., Ren, H., Lee, V. H., Frazer, G. L., Strnadova, P., Sumner, R. P., & Smith, G. L. (2013). Vaccinia virus protein N2 is a nuclear IRF3 inhibitor that promotes virulence. *Journal of General Virology, 94*(9), 2070-2081.

Ferguson, B. J., Mansur, D. S., Peters, N. E., Ren, H., & Smith, G. L. (2012). DNA-PK is a DNA sensor for IRF-3-dependent innate immunity. *eLife, 1*, e00047.

Fernandes-Alnemri, T., Yu, J.-W., Datta, P., Wu, J., & Alnemri, E. S. (2009). AIM2 activates the inflammasome and cell death in response to cytoplasmic DNA. *Nature, 458*(7237), 509-513.

Fiola, S., Gosselin, D., Takada, K., & Gosselin, J. (2010). TLR9 Contributes to the Recognition of EBV by Primary Monocytes and Plasmacytoid Dendritic Cells. *The Journal of Immunology, 185*(6), 3620-3631.

Fitzgerald, K. A., McWhirter, S. M., Faia, K. L., Rowe, D. C., Latz, E., Golenbock, D. T., Coyle, A. J., Liao, S.-M., & Maniatis, T. (2003). IKKε and TBK1 are essential components of the IRF3 signaling pathway. *Nature Immunology, 4*(5), 491-496.

Fleming, S. B. (2016). Viral Inhibition of the IFN-Induced JAK/STAT Signalling Pathway: Development of Live Attenuated Vaccines by Mutation of Viral-Encoded IFN-Antagonists. *Vaccines, 4*(3), 23. doi:10.3390/vaccines4030023

Fleming, S. B., Blok, J., Fraser, K. M., Mercer, A. A., & Robinson, A. J. (1993). Conservation of gene structure and arrangement between vaccinia virus and orf virus. *Virology, 195*(1), 175-184.

Fleming, S. B., Lyttle, D. J., Sullivan, J. T., Mercer, A. A., & Robinson, A. J. (1995). Genomic analysis of a transposition-deletion variant of orf virus reveals a 3.3 kbp region of non-essential DNA. *The Journal of general virology, 76 (Pt 12)*, 2969-2978.

Fleming, S. B., McCaughan, C., Lateef, Z., Dunn, A., Wise, L. M., Real, N. C., & Mercer, A. A. (2017). Deletion of the Chemokine Binding Protein Gene from the Parapoxvirus Orf Virus Reduces Virulence and Pathogenesis in Sheep. *Front Microbiol, 8*, 46.

Fleming, S. B., McCaughan, C. A., Andrews, A. E., Nash, A. D., & Mercer, A. A. (1997). A homolog of interleukin-10 is encoded by the poxvirus orf virus. *Journal of Virology, 71*(6), 4857-4861.

Fleming, S. B., & Mercer, A. A. (2007). Genus Parapoxvirus. In A. A. Mercer, A. Schmidt, & O. Weber (Eds.), *Poxviruses* (pp. 127-165). Basel: Birkhäuser Basel.

Fleming, S. B., Wise, L. M., & Mercer, A. A. (2015). Molecular genetic analysis of orf virus: a poxvirus that has adapted to skin. *Viruses, 7*(3), 1505-1539.

Franke, C. A., Rice, C. M., Strauss, J. H., & Hruby, D. E. (1985). Neomycin resistance as a dominant selectable marker for selection and isolation of vaccinia virus recombinants. *Molecular and Cellular Biology, 5*(8), 1918-1924.

Franklin, E., & Khan, A. R. (2013). Poxvirus antagonism of innate immunity by Bcl-2 fold proteins. *Journal of Structural Biology, 181*(1), 1-10.

Friederichs, S., Krebs, S., Blum, H., Wolf, E., Lang, H., von Buttlar, H., & Büttner, M. (2014). Comparative and retrospective molecular analysis of Parapoxvirus (PPV) isolates. *Virus Res, 181*, 11-21.

Fujisawa, H., Kondo, S., Wang, B., Shivji, G. M., & Sauder, D. N. (1997). The Expression and Modulation of IFN-α and IFN-β in Human Keratinocytes. *Journal of Interferon & Cytokine Research, 17*(12), 721-725.

Furr, S. R., Moerdyk-Schauwecker, M., Grdzelishvili, V. Z., & Marriott, I. (2010). RIG-I mediates nonsegmented negative-sense RNA virus-induced inflammatory immune responses of primary human astrocytes. *Glia, 58*(13), 1620-1629.

Gack, M. U., Albrecht, R. A., Urano, T., Inn, K.-S., Huang, I. C., Carnero, E., Farzan, M., Inoue, S., Jung, J. U., & García-Sastre, A. (2009). Influenza A Virus NS1 Targets the Ubiquitin Ligase TRIM25 to Evade Recognition by the Host Viral RNA Sensor RIG-I. *Cell Host & Microbe, 5*(5), 439-449.

Gack, M. U., Shin, Y. C., Joo, C.-H., Urano, T., Liang, C., Sun, L., Takeuchi, O., Akira, S., Chen, Z., Inoue, S., & Jung, J. U. (2007). TRIM25 RING-finger E3 ubiquitin ligase is essential for RIG-I-mediated antiviral activity. *Nature, 446*(7138), 916-920.

Gao, D., Wu, J., Wu, Y.-T., Du, F., Aroh, C., Yan, N., Sun, L., & Chen, Z. J. (2013). Cyclic GMP-AMP Synthase Is an Innate Immune Sensor of HIV and Other Retroviruses. *Science, 341*(6148), 903-906.

Gariano, G. R., Dell'Oste, V., Bronzini, M., Gatti, D., Luganini, A., De Andrea, M., Gribaudo, G., Gariglio, M., & Landolfo, S. (2012). The Intracellular DNA Sensor IFI16 Gene Acts as Restriction Factor for Human Cytomegalovirus Replication. *PLOS Pathogens, 8*(1), e1002498.

Gedey, R., Jin, X.-L., Hinthong, O., & Shisler, J. L. (2006). Poxviral Regulation of the Host NF-κB Response: the Vaccinia Virus M2L Protein Inhibits Induction of NF-κB Activation via an ERK2 Pathway in Virus-Infected Human Embryonic Kidney Cells. *Journal of Virology, 80*(17), 8676-8685.

Georgana, I., Sumner, R. P., Towers, G. J., & Maluquer de Motes, C. (2018). Virulent Poxviruses Inhibit DNA Sensing by Preventing STING Activation. *Journal of Virology, 92*(10), e02145-02117.

Gilliet, M., Cao, W., & Liu, Y.-J. (2008). Plasmacytoid dendritic cells: sensing nucleic acids in viral infection and autoimmune diseases. *Nature Reviews Immunology, 8*(8), 594-606.

Gitlin, L., Barchet, W., Gilfillan, S., Cella, M., Beutler, B., Flavell, R. A., Diamond, M. S., & Colonna, M. (2006). Essential role of mda-5 in type I IFN responses to polyriboinosinic:polyribocytidylic acid and encephalomyocarditis picornavirus. *Proceedings of the National Academy of Sciences, 103*(22), 8459-8464.

Goebel, S. J., Johnson, G. P., Perkus, M. E., Davis, S. W., Winslow, J. P., & Paoletti, E. (1990). The complete DNA sequence of vaccinia virus. *Virology, 179*(1), 247-266.

Goffic, R. L., Balloy, V., Lagranderie, M., Alexopoulou, L., Escriou, N., Flavell, R., Chignard, M., & Si-Tahar, M. (2006). Detrimental Contribution of the Toll-Like Receptor (TLR)3 to Influenza A Virus–Induced Acute Pneumonia. *PLOS Pathogens, 2*(6), e53.

Gongora, C., Degols, G., Espert, L., Hua, T. D., & Mechti, N. (2000). A unique ISRE, in the TATA-less human Isg20 promoter, confers IRF-1-mediated responsiveness to both interferon type I and type II. *Nucleic Acids Research, 28*(12), 2333-2341.

Gorden, K. K. B., Qiu, X. X., Binsfeld, C. C. A., Vasilakos, J. P., & Alkan, S. S. (2006). Cutting Edge: Activation of Murine TLR8 by a Combination of Imidazoquinoline Immune Response Modifiers and PolyT Oligodeoxynucleotides. *The Journal of Immunology, 177*(10), 6584-6587.

Goubau, D., Schlee, M., Deddouche, S., Pruijssers, A. J., Zillinger, T., Goldeck, M., Schuberth, C., Van der Veen, A. G., Fujimura, T., Rehwinkel, J., Iskarpatyoti, J. A., Barchet, W., Ludwig, J., Dermody, T. S., Hartmann, G., & Reis e Sousa, C. (2014). Antiviral immunity via RIG-I-mediated recognition of RNA bearing 5′-diphosphates. *Nature, 514*(7522), 372-375.

Goutagny, N., Jiang, Z., Tian, J., Parroche, P., Schickli, J., Monks, B. G., Ulbrandt, N., Ji, H., Kiener, P. A., Coyle, A. J., & Fitzgerald, K. A. (2010). Cell Type-Specific Recognition of Human Metapneumoviruses (HMPVs) by Retinoic Acid-Inducible Gene I (RIG-I) and TLR7 and Viral Interference of RIG-I Ligand Recognition by HMPV-B1 Phosphoprotein. *The Journal of Immunology, 184*(3), 1168-1179.

Gowen, B. B., Hoopes, J. D., Wong, M.-H., Jung, K.-H., Isakson, K. C., Alexopoulou, L., Flavell, R. A., & Sidwell, R. W. (2006). TLR3 Deletion Limits Mortality and Disease Severity due to Phlebovirus Infection. *The Journal of Immunology, 177*(9), 6301-6307.

Graham, S. C., Bahar, M. W., Cooray, S., Chen, R. A. J., Whalen, D. M., Abrescia, N. G. A., Alderton, D., Owens, R. J., Stuart, D. I., Smith, G. L., & Grimes, J. M. (2008). Vaccinia Virus Proteins A52 and B14 Share a Bcl-2–Like Fold but Have Evolved to Inhibit NF-κB rather than Apoptosis. *PLOS Pathogens, 4*(8), e1000128.

Grandvaux, N., Servant, M. J., tenOever, B., Sen, G. C., Balachandran, S., Barber, G. N., Lin, R., & Hiscott, J. (2002). Transcriptional Profiling of Interferon Regulatory Factor 3 Target Genes: Direct Involvement in the Regulation of Interferon-Stimulated Genes. *Journal of Virology, 76*(11), 5532-5539.

Gregory, S. M., West, J. A., Dillon, P. J., Hilscher, C., Dittmer, D. P., & Damania, B. (2009). Toll-like receptor signaling controls reactivation of KSHV from latency. *Proceedings of the National Academy of Sciences, 106*(28), 11725-11730.

Gringhuis, S. I., Hertoghs, N., Kaptein, T. M., Zijlstra-Willems, E. M., Sarrami-Forooshani, R., Sprokholt, J. K., van Teijlingen, N. H., Kootstra, N. A., Booiman, T., van Dort, K. A., Ribeiro, C. M. S., Drewniak, A., & Geijtenbeek, T. B. H. (2017). HIV-1 blocks the signaling adaptor MAVS to evade antiviral host defense after sensing of abortive HIV-1 RNA by the host helicase DDX3. *Nature Immunology, 18*(2), 225-235.

Guerra, S., Cáceres, A., Knobeloch, K.-P., Horak, I., & Esteban, M. (2008). Vaccinia virus E3 protein prevents the antiviral action of ISG15. *PLOS Pathogens, 4*(7), e1000096.

Guerra, S., Nájera, J. L., González, J. M., López-Fernández, L. A., Climent, N., Gatell, J. M., Gallart, T., & Esteban, M. (2007). Distinct Gene Expression Profiling after Infection of Immature Human Monocyte-Derived Dendritic Cells by the Attenuated Poxvirus Vectors MVA and NYVAC. *Journal of Virology, 81*(16), 8707-8721.

Guggemoos, S., Hangel, D., Hamm, S., Heit, A., Bauer, S., & Adler, H. (2008). TLR9 Contributes to Antiviral Immunity during Gammaherpesvirus Infection. *The Journal of Immunology, 180*(1), 438-443.

Guillaume-Gable, C., Floch, V., Mercier, B., Audrezet, M.-P., Gobin, E., Le Bolc'h, G., Yaouanc, J.-J., Clement, J.-C., Abbayes, H. D., Leroy, J.-P., Morin, V., & Ferec, C. (1998). Cationic Phosphonolipids as Nonviral Gene Transfer Agents in the Lungs of Mice. *Human Gene Therapy, 9*(16), 2309-2319.

Haas, T., Metzger, J., Schmitz, F., Heit, A., Müller, T., Latz, E., & Wagner, H. (2008). The DNA Sugar Backbone 2′ Deoxyribose Determines Toll-like Receptor 9 Activation. *Immunity, 28*(3), 315-323.

Haasnoot, J., de Vries, W., Geutjes, E.-J., Prins, M., de Haan, P., & Berkhout, B. (2007). The Ebola Virus VP35 Protein Is a Suppressor of RNA Silencing. *PLOS Pathogens, 3*(6), e86.

Habjan, M., Andersson, I., Klingström, J., Schümann, M., Martin, A., Zimmermann, P., Wagner, V., Pichlmair, A., Schneider, U., Mühlberger, E., Mirazimi, A., & Weber, F. (2008). Processing of Genome 5′ Termini as a Strategy of Negative-Strand RNA Viruses to Avoid RIG-I-Dependent Interferon Induction. *PLoS ONE, 3*(4), e2032.

Haig, D. M., McInnes, C. J., Thomson, J., Wood, A., Bunyan, K., & Mercer, A. (1998). The orf virus OV20.0L gene product is involved in interferon resistance and inhibits an interferon-inducible, double-stranded RNA-dependent kinase. *Immunology, 93*(3), 335-340.

Halfmann, P., Neumann, G., & Kawaoka, Y. (2011). The Ebolavirus VP24 protein blocks phosphorylation of p38 mitogen-activated protein kinase. *The Journal of infectious diseases, 204 Suppl 3*(Suppl 3), S953-S956.

Hallen, L. C., Burki, Y., Ebeling, M., Broger, C., Siegrist, F., Oroszlan-Szovik, K., Bohrmann, B., Certa, U., & Foser, S. (2007). Antiproliferative activity of the human IFN-alpha-inducible protein IFI44. *J Interferon Cytokine Res, 27*(8), 675-680.

Hanahan, D. (1983). Studies on transformation of Escherichia coli with plasmids. *J Mol Biol, 166*(4), 557-580.

Harfoot, R. T. (2015). *Characterization of ORFV119* (Doctor of Philosophy Doctoral Thesis), University of Otago, Dunedin, New Zealand. Retrieved from http://hdl.handle.net/10523/5706

Harman, A. N., Lai, J., Turville, S., Samarajiwa, S., Gray, L., Marsden, V., Mercier, S. K., Jones, K., Nasr, N., Rustagi, A., Cumming, H., Donaghy, H., Mak, J., Gale, M., Jr., Churchill, M., Hertzog, P., & Cunningham, A. L. (2011). HIV infection of dendritic cells subverts the IFN induction pathway via IRF-1 and inhibits type 1 IFN production. *Blood, 118*(2), 298-308.

Harper, J. M., Parsonage, M. T., Pelham, H. R., & Darby, G. (1978). Heat inactivation of vaccinia virus particle-associated functions: properties of heated particles in vivo and in vitro. *Journal of Virology, 26*(3), 646-659.

Harte, M. T., Haga, I. R., Maloney, G., Gray, P., Reading, P. C., Bartlett, N. W., Smith, G. L., Bowie, A., & O'Neill, L. A. J. (2003). The Poxvirus Protein A52R Targets Toll-like Receptor Signaling Complexes to Suppress Host Defense. *The Journal of Experimental Medicine, 197*(3), 343-351.

Hartmann, R., Olsen, H. S., Widder, S., Jørgensen, R., & Justesen, J. (1998). p59OASL, a 2′–5′ oligoadenylate synthetase like protein: a novel human gene related to the 2′–5′ oligoadenylate synthetase family. *Nucleic Acids Research, 26*(18), 4121-4127.

Harvey, R., McCaughan, C., Wise, L. M., Mercer, A. A., & Fleming, S. B. (2015). Orf virus inhibits interferon stimulated gene expression and modulates the JAK/STAT signalling pathway. *Virus Research, 208*, 180-188.

Hasan, U. A., Bates, E., Takeshita, F., Biliato, A., Accardi, R., Bouvard, V., Mansour, M., Vincent, I., Gissmann, L., Iftner, T., Sideri, M., Stubenrauch, F., & Tommasino, M. (2007). TLR9 Expression and Function Is Abolished by the Cervical Cancer-Associated Human Papillomavirus Type 16. *The Journal of Immunology, 178*(5), 3186-3197.

Hatada, E., Saito, S., & Fukuda, R. (1999). Mutant Influenza Viruses with a Defective NS1 Protein Cannot Block the Activation of PKR in Infected Cells. *Journal of Virology, 73*(3), 2425-2433.

Hautaniemi, M., Ueda, N., Tuimala, J., Mercer, A. A., Lahdenperä, J., & McInnes, C. J. (2010). The genome of pseudocowpoxvirus: comparison of a reindeer isolate and a reference strain. *The Journal of general virology, 91*(Pt 6), 1560-1576.

Hautaniemi, M., Vaccari, F., Scagliarini, A., Laaksonen, S., Huovilainen, A., & McInnes, C. J. (2011). Analysis of deletion within the reindeer pseudocowpoxvirus genome. *Virus Res, 160*(1-2), 326-332.

Heil, F., Hemmi, H., Hochrein, H., Ampenberger, F., Kirschning, C., Akira, S., Lipford, G., Wagner, H., & Bauer, S. (2004). Species-Specific Recognition of Single-Stranded RNA via Toll-like Receptor 7 and 8. *Science, 303*(5663), 1526-1529.

Hemmi, H., Kaisho, T., Takeuchi, O., Sato, S., Sanjo, H., Hoshino, K., Horiuchi, T., Tomizawa, H., Takeda, K., & Akira, S. (2002). Small anti-viral compounds activate immune cells via the TLR7 MyD88–dependent signaling pathway. *Nature Immunology, 3*(2), 196-200.

Hemmi, H., Takeuchi, O., Sato, S., Yamamoto, M., Kaisho, T., Sanjo, H., Kawai, T., Hoshino, K., Takeda, K., & Akira, S. (2004). The Roles of Two IκB Kinase-related

Kinases in Lipopolysaccharide and Double Stranded RNA Signaling and Viral Infection. *The Journal of Experimental Medicine, 199*(12), 1641-1650.

Hertzog, P., Forster, S., & Samarajiwa, S. (2011). Systems Biology of Interferon Responses. *Journal of Interferon & Cytokine Research, 31*(1), 5-11.

Hochrein, H., Schlatter, B., O'Keeffe, M., Wagner, C., Schmitz, F., Schiemann, M., Bauer, S., Suter, M., & Wagner, H. (2004). Herpes simplex virus type-1 induces IFN-α production via Toll-like receptor 9-dependent and -independent pathways. *Proceedings of the National Academy of Sciences of the United States of America, 101*(31), 11416-11421.

Honda, K., Yanai, H., Mizutani, T., Negishi, H., Shimada, N., Suzuki, N., Ohba, Y., Takaoka, A., Yeh, W.-C., & Taniguchi, T. (2004). Role of a transductional-transcriptional processor complex involving MyD88 and IRF-7 in Toll-like receptor signaling. *Proceedings of the National Academy of Sciences of the United States of America, 101*(43), 15416-15421.

Honda, K., Yanai, H., Takaoka, A., & Taniguchi, T. (2005). Regulation of the type I IFN induction: a current view. *International Immunology, 17*(11), 1367-1378.

Honda, Y., Kondo, J., Maeda, T., Yoshiyama, Y., Yamada, E., Shimizu, Y. K., Shikata, T., & Ono, Y. (1990). Isolation and purification of a non-A, non-B hepatitis-associated microtubular aggregates protein. *Journal of General Virology, 71*(9), 1999-2004.

Horan, K. A., Hansen, K., Jakobsen, M. R., Holm, C. K., Søby, S., Unterholzner, L., Thompson, M., West, J. A., Iversen, M. B., Rasmussen, S. B., Ellermann-Eriksen, S., Kurt-Jones, E., Landolfo, S., Damania, B., Melchjorsen, J., Bowie, A. G., Fitzgerald, K. A., & Paludan, S. R. (2013). Proteasomal Degradation of Herpes Simplex Virus Capsids in Macrophages Releases DNA to the Cytosol for Recognition by DNA Sensors. *The Journal of Immunology, 190*(5), 2311-2319.

Hornung, V., Ablasser, A., Charrel-Dennis, M., Bauernfeind, F., Horvath, G., Caffrey, D. R., Latz, E., & Fitzgerald, K. A. (2009). AIM2 recognizes cytosolic dsDNA and forms a caspase-1-activating inflammasome with ASC. *Nature, 458*(7237), 514-518.

Hornung, V., Ellegast, J., Kim, S., Brzózka, K., Jung, A., Kato, H., Poeck, H., Akira, S., Conzelmann, K.-K., Schlee, M., Endres, S., & Hartmann, G. (2006). 5'-Triphosphate RNA Is the Ligand for RIG-I. *Science, 314*(5801), 994-997.

Hoshino, K., Sugiyama, T., Matsumoto, M., Tanaka, T., Saito, M., Hemmi, H., Ohara, O., Akira, S., & Kaisho, T. (2006). IκB kinase-α is critical for interferon-α production induced by Toll-like receptors 7 and 9. *Nature, 440*(7086), 949-953.

Hou, F., Sun, L., Zheng, H., Skaug, B., Jiang, Q.-X., & Chen, Zhijian J. (2011). MAVS Forms Functional Prion-like Aggregates to Activate and Propagate Antiviral Innate Immune Response. *Cell, 146*(3), 448-461.

Howell, M. D., Gallo, R. L., Boguniewicz, M., Jones, J. F., Wong, C., Streib, J. E., & Leung, D. Y. M. (2006). Cytokine Milieu of Atopic Dermatitis Skin Subverts the Innate Immune Response to Vaccinia Virus. *Immunity, 24*(3), 341-348.

Huang, J., You, H., Su, C., Li, Y., Chen, S., & Zheng, C. (2018). Herpes Simplex Virus 1 Tegument Protein VP22 Abrogates cGAS/STING-Mediated Antiviral Innate Immunity. *Journal of Virology, 92*(15), e00841-00818.

Huang, X. X., McCaughan, G. W., Shackel, N. A., & Gorrell, M. D. (2007). Up-regulation of proproliferative genes and the ligand/receptor pair placental growth factor and vascular endothelial growth factor receptor 1 in hepatitis C cirrhosis. *Liver International, 27*(7), 960-968.

Hull, C. M., & Bevilacqua, P. C. (2016). Discriminating Self and Non-Self by RNA: Roles for RNA Structure, Misfolding, and Modification in Regulating the Innate Immune Sensor PKR. *Accounts of Chemical Research, 49*(6), 1242-1249.

Hurst, T., & Bowie, A. G. (2008). Innate immune signaling pathways: lessons from vaccinia virus. *Future Virology, 3*(2), 147-156.

Hutchens, M., Luker, K. E., Sottile, P., Sonstein, J., Lukacs, N. W., Núñez, G., Curtis, J. L., & Luker, G. D. (2008). TLR3 Increases Disease Morbidity and Mortality from Vaccinia Infection. *The Journal of Immunology, 180*(1), 483-491.

Ikegame, S., Takeda, M., Ohno, S., Nakatsu, Y., Nakanishi, Y., & Yanagi, Y. (2010). Both RIG-I and MDA5 RNA Helicases Contribute to the Induction of Alpha/Beta Interferon in Measles Virus-Infected Human Cells. *Journal of Virology, 84*(1), 372-379.

Imlach, W., McCaughan, C. A., Mercer, A. A., Haig, D., & Fleming, S. B. (2002). Orf virus-encoded interleukin-10 stimulates the proliferation of murine mast cells and inhibits cytokine synthesis in murine peritoneal macrophages. *Journal of General Virology, 83*(5), 1049-1058.

Inn, K.-S., Lee, S.-H., Rathbun, J. Y., Wong, L.-Y., Toth, Z., Machida, K., Ou, J.-H. J., & Jung, J. U. (2011). Inhibition of RIG-I-Mediated Signaling by Kaposi's Sarcoma-Associated Herpesvirus-Encoded Deubiquitinase ORF64. *Journal of Virology, 85*(20), 10899-10904.

Iqbal, M., Poole, E., Goodbourn, S., & McCauley, J. W. (2004). Role for bovine viral diarrhea virus Erns glycoprotein in the control of activation of beta interferon by double-stranded RNA. *Journal of Virology, 78*(1), 136-145.

Isaacs, A., Lindenmann, J., & Andrewes, C. H. (1957). Virus interference. I. The interferon. *Proceedings of the Royal Society of London. Series B - Biological Sciences, 147*(927), 258-267.

Ishii, K. J., Coban, C., Kato, H., Takahashi, K., Torii, Y., Takeshita, F., Ludwig, H., Sutter, G., Suzuki, K., Hemmi, H., Sato, S., Yamamoto, M., Uematsu, S., Kawai, T., Takeuchi, O., & Akira, S. (2006). A Toll-like receptor–independent antiviral response induced by double-stranded B-form DNA. *Nature Immunology, 7*(1), 40-48.

Ishii, K. J., Kawagoe, T., Koyama, S., Matsui, K., Kumar, H., Kawai, T., Uematsu, S., Takeuchi, O., Takeshita, F., Coban, C., & Akira, S. (2008). TANK-binding kinase-1 delineates innate and adaptive immune responses to DNA vaccines. *Nature, 451*(7179), 725-729.

Ishikawa, H., & Barber, G. N. (2008). STING is an endoplasmic reticulum adaptor that facilitates innate immune signalling. *Nature, 455*(7213), 674-678.

Ishikawa, H., Ma, Z., & Barber, G. N. (2009). STING regulates intracellular DNA-mediated, type I interferon-dependent innate immunity. *Nature, 461*(7265), 788-792.

Iwakiri, D., Zhou, L., Samanta, M., Matsumoto, M., Ebihara, T., Seya, T., Imai, S., Fujieda, M., Kawa, K., & Takada, K. (2009). Epstein-Barr virus (EBV)–encoded small RNA is released from EBV-infected cells and activates signaling from toll-like receptor 3. *The Journal of Experimental Medicine, 206*(10), 2091-2099.

Jakobsen, M. R., Bak, R. O., Andersen, A., Berg, R. K., Jensen, S. B., Jin, T., Laustsen, A., Hansen, K., Østergaard, L., Fitzgerald, K. A., Xiao, T. S., Mikkelsen, J. G., Mogensen, T. H., & Paludan, S. R. (2013). IFI16 senses DNA forms of the lentiviral replication cycle and controls HIV-1 replication. *Proceedings of the National Academy of Sciences, 110*(48), E4571-E4580.

Jarmin, S., Manvell, R., Gough, R. E., Laidlaw, S. M., & Skinner, M. A. (2006). Avipoxvirus phylogenetics: identification of a PCR length polymorphism that discriminates between the two major clades. *The Journal of general virology, 87*(Pt 8), 2191-2201.

Jiang, W., Lederman, M. M., Mohner, R. J., Rodriguez, B., Nedrich, T. M., Harding, C. V., & Sieg, S. F. (2008). Impaired Naive and Memory B-Cell Responsiveness to TLR9 Stimulation in Human Immunodeficiency Virus Infection. *Journal of Virology, 82*(16), 7837-7845.

Jiang, Z., Mak, T. W., Sen, G., & Li, X. (2004). Toll-like receptor 3-mediated activation of NF-κB and IRF3 diverges at Toll-IL-1 receptor domain-containing adapter inducing IFN-β. *Proceedings of the National Academy of Sciences of the United States of America, 101*(10), 3533-3538.

Jin, T., Perry, A., Jiang, J., Smith, P., Curry, James A., Unterholzner, L., Jiang, Z., Horvath, G., Rathinam, Vijay A., Johnstone, Ricky W., Hornung, V., Latz, E., Bowie, Andrew G., Fitzgerald, Katherine A., & Xiao, T. S. (2012). Structures of the HIN Domain:DNA Complexes Reveal Ligand Binding and Activation Mechanisms of the AIM2 Inflammasome and IFI16 Receptor. *Immunity, 36*(4), 561-571.

Johnston, J. B., Barrett, J. W., Nazarian, S. H., Goodwin, M., Ricuttio, D., Wang, G., & McFadden, G. (2005). A Poxvirus-Encoded Pyrin Domain Protein Interacts with ASC-1 to Inhibit Host Inflammatory and Apoptotic Responses to Infection. *Immunity, 23*(6), 587-598.

Johnston, J. B., & McFadden, G. (2005). Immunomodulation by Poxviruses. In J.-P. Changeux, Palese, Peter (Ed.), *Modulation of Host Gene Expression and Innate Immunity by Viruses* (Vol. 1, pp. 163-195): Springer.

Joklik, W. K. (1962). The purification of four strains of poxvirus. *Virology, 18*(1), 9-18. doi:https://doi.org/10.1016/0042-6822(62)90172-1

Jønsson, K. L., Laustsen, A., Krapp, C., Skipper, K. A., Thavachelvam, K., Hotter, D., Egedal, J. H., Kjolby, M., Mohammadi, P., Prabakaran, T., Sørensen, L. K., Sun, C., Jensen, S. B., Holm, C. K., Lebbink, R. J., Johannsen, M., Nyegaard, M., Mikkelsen, J. G., Kirchhoff, F., Paludan, S. R., & Jakobsen, M. R. (2017). IFI16 is required for DNA sensing in human macrophages by promoting production and function of cGAMP. *Nature Communications, 8*, 14391.

Juang, Y.-T., Lowther, W., Kellum, M., Au, W.-C., Lin, R., Hiscott, J., & Pitha, P. M. (1998). Primary activation of interferon A and interferon B gene transcription by interferon regulatory factor 3. *Proceedings of the National Academy of Sciences, 95*(17), 9837-9842.

Jurk, M., Heil, F., Vollmer, J., Schetter, C., Krieg, A. M., Wagner, H., Lipford, G., & Bauer, S. (2002). Human TLR7 or TLR8 independently confer responsiveness to the antiviral compound R-848. *Nature Immunology, 3*(6), 499-499.

Kaczkowski, B., Rossing, M., Andersen, D. K., Dreher, A., Morevati, M., Visser, M. A., Winther, O., Nielsen, F. C., & Norrild, B. (2012). Integrative analyses reveal novel strategies in HPV11,-16 and -45 early infection. *Scientific reports, 2*, 515-515.

Kadowaki, N., Ho, S., Antonenko, S., de Waal Malefyt, R., Kastelein, R. A., Bazan, F., & Liu, Y.-J. (2001). Subsets of Human Dendritic Cell Precursors Express Different Toll-like Receptors and Respond to Different Microbial Antigens. *The Journal of Experimental Medicine, 194*(6), 863-870.

Kalamvoki, M., & Roizman, B. (2014). HSV-1 degrades, stabilizes, requires, or is stung by STING depending on ICP0, the US3 protein kinase, and cell derivation. *Proceedings of the National Academy of Sciences, 111*(5), E611-E617.

Kalvakolanu, D. V. (1999). Virus interception of cytokine-regulated pathways. *Trends in Microbiology, 7*(4), 166-171.

Kang, D., Gopalkrishnan, R. V., Lin, L., Randolph, A., Valerie, K., Pestka, S., & Fisher, P. B. (2004). Expression analysis and genomic characterization of human melanoma differentiation associated gene-5, mda-5: a novel type I interferon-responsive apoptosis-inducing gene. *Oncogene, 23*(9), 1789-1800.

Kaplan, C. (1958). The Heat Inactivation of Vaccinia Virus. *Microbiology, 18*(1), 58-63.

Karpova, A. Y., Trost, M., Murray, J. M., Cantley, L. C., & Howley, P. M. (2002). Interferon regulatory factor-3 is an in vivo target of DNA-PK. *Proceedings of the National Academy of Sciences, 99*(5), 2818-2823.

Kato, H., Sato, S., Yoneyama, M., Yamamoto, M., Uematsu, S., Matsui, K., Tsujimura, T., Takeda, K., Fujita, T., Takeuchi, O., & Akira, S. (2005). Cell Type-Specific Involvement of RIG-I in Antiviral Response. *Immunity, 23*(1), 19-28.

Kato, H., Takeuchi, O., Mikamo-Satoh, E., Hirai, R., Kawai, T., Matsushita, K., Hiiragi, A., Dermody, T. S., Fujita, T., & Akira, S. (2008). Length-dependent recognition of double-stranded ribonucleic acids by retinoic acid–inducible gene-I and melanoma differentiation–associated gene 5. *The Journal of Experimental Medicine, 205*(7), 1601-1610.

Kato, H., Takeuchi, O., Sato, S., Yoneyama, M., Yamamoto, M., Matsui, K., Uematsu, S., Jung, A., Kawai, T., Ishii, K. J., Yamaguchi, O., Otsu, K., Tsujimura, T., Koh, C.-S., Reis e Sousa, C., Matsuura, Y., Fujita, T., & Akira, S. (2006). Differential roles of MDA5 and RIG-I helicases in the recognition of RNA viruses. *Nature, 441*(7089), 101-105.

Katze, M. G., He, Y., & Gale, M. (2002). Viruses and interferon: a fight for supremacy. *Nature Reviews Immunology, 2*(9), 675-687.

Kawagoe, T., Sato, S., Matsushita, K., Kato, H., Matsui, K., Kumagai, Y., Saitoh, T., Kawai, T., Takeuchi, O., & Akira, S. (2008). Sequential control of Toll-like receptor–dependent responses by IRAK1 and IRAK2. *Nature Immunology, 9*(6), 684-691.

Kawai, T., & Akira, S. (2006). Innate immune recognition of viral infection. *Nature Immunology, 7*(2), 131-137.

Kawai, T., & Akira, S. (2008). Toll-like Receptor and RIG-1-like Receptor Signaling. *Annals of the New York Academy of Sciences, 1143*(1), 1-20.

Kawai, T., & Akira, S. (2010). The role of pattern-recognition receptors in innate immunity: update on Toll-like receptors. *Nature Immunology, 11*(5), 373-384.

Kawai, T., Sato, S., Ishii, K. J., Coban, C., Hemmi, H., Yamamoto, M., Terai, K., Matsuda, M., Inoue, J.-i., Uematsu, S., Takeuchi, O., & Akira, S. (2004). Interferon-α induction through Toll-like receptors involves a direct interaction of IRF7 with MyD88 and TRAF6. *Nature Immunology, 5*(10), 1061-1068.

Kawai, T., Takahashi, K., Sato, S., Coban, C., Kumar, H., Kato, H., Ishii, K. J., Takeuchi, O., & Akira, S. (2005). IPS-1, an adaptor triggering RIG-I- and Mda5-mediated type I interferon induction. *Nature Immunology, 6*(10), 981-988.

Keating, S. E., Baran, M., & Bowie, A. G. (2011). Cytosolic DNA sensors regulating type I interferon induction. *Trends in immunology, 32*(12), 574-581.

Kerur, N., Veettil, Mohanan V., Sharma-Walia, N., Bottero, V., Sadagopan, S., Otageri, P., & Chandran, B. (2011). IFI16 Acts as a Nuclear Pathogen Sensor to Induce the Inflammasome in Response to Kaposi Sarcoma-Associated Herpesvirus Infection. *Cell Host & Microbe, 9*(5), 363-375.

Khatiwada, S., Delhon, G., Nagendraprabhu, P., Chaulagain, S., Luo, S., Diel, D. G., Flores, E. F., & Rock, D. L. (2017). A parapoxviral virion protein inhibits NF-κB signaling early in infection. *PLOS Pathogens, 13*(8), e1006561.

Kim, T., Kim, T. Y., Song, Y.-H., Min, I. M., Yim, J., & Kim, T. K. (1999). Activation of Interferon Regulatory Factor 3 in Response to DNA-damaging Agents. *Journal of Biological Chemistry, 274*(43), 30686-30689.

Kim, T., Pazhoor, S., Bao, M., Zhang, Z., Hanabuchi, S., Facchinetti, V., Bover, L., Plumas, J., Chaperot, L., Qin, J., & Liu, Y.-J. (2010). Aspartate-glutamate-alanine-histidine box motif (DEAH)/RNA helicase A helicases sense microbial DNA in human plasmacytoid dendritic cells. *Proceedings of the National Academy of Sciences, 107*(34), 15181-15186.

Kim, Y.-M., Brinkmann, M. M., Paquet, M.-E., & Ploegh, H. L. (2008). UNC93B1 delivers nucleotide-sensing toll-like receptors to endolysosomes. *Nature, 452*(7184), 234-238.

Kitamura, A., Takahashi, K., Okajima, A., & Kitamura, N. (1994). Induction of the Human Gene for p44, a Hepatitis-C-associated Microtubular Aggregate Protein, by Interferon-α/β. *European Journal of Biochemistry, 224*(3), 877-883.

Kobayashi, S., Koujin, T., Kojidani, T., Osakada, H., Mori, C., Hiraoka, Y., & Haraguchi, T. (2015). BAF is a cytosolic DNA sensor that leads to exogenous DNA avoiding autophagy. *Proceedings of the National Academy of Sciences, 112*(22), 7027-7032.

Kok, K.-H., Lui, P.-Y., Ng, M.-Him J., Siu, K.-L., Au, Shannon Wing N., & Jin, D.-Y. (2011). The Double-Stranded RNA-Binding Protein PACT Functions as a Cellular Activator of RIG-I to Facilitate Innate Antiviral Response. *Cell Host & Microbe, 9*(4), 299-309.

Kolakofsky, D., Kowalinski, E., & Cusack, S. (2012). A structure-based model of RIG-I activation. *RNA, 18*(12), 2118-2127.

Kondo, T., Kobayashi, J., Saitoh, T., Maruyama, K., Ishii, K. J., Barber, G. N., Komatsu, K., Akira, S., & Kawai, T. (2013). DNA damage sensor MRE11 recognizes cytosolic double-stranded DNA and induces type I interferon by regulating STING trafficking. *Proceedings of the National Academy of Sciences, 110*(8), 2969-2974.

Konno, H., Konno, K., & Barber, Glen N. (2013). Cyclic Dinucleotides Trigger ULK1 (ATG1) Phosphorylation of STING to Prevent Sustained Innate Immune Signaling. *Cell, 155*(3), 688-698.

Kopfnagel, V., Wittmann, M., & Werfel, T. (2011). Human keratinocytes express AIM2 and respond to dsDNA with IL-1β secretion. *Exp Dermatol, 20*(12), 1027-1029. doi:10.1111/j.1600-0625.2011.01382.x

Kotenko, S. V., Gallagher, G., Baurin, V. V., Lewis-Antes, A., Shen, M., Shah, N. K., Langer, J. A., Sheikh, F., Dickensheets, H., & Donnelly, R. P. (2003). IFN-λs mediate antiviral protection through a distinct class II cytokine receptor complex. *Nature Immunology, 4*(1), 69-77.

Kowalinski, E., Lunardi, T., McCarthy, Andrew A., Louber, J., Brunel, J., Grigorov, B., Gerlier, D., & Cusack, S. (2011). Structural Basis for the Activation of Innate Immune Pattern-Recognition Receptor RIG-I by Viral RNA. *Cell, 147*(2), 423-435.

Koyama, S., Ishii, K. J., Coban, C., & Akira, S. (2008). Innate immune response to viral infection. *Cytokine, 43*(3), 336-341.

Kranzusch, Philip J., Lee, Amy S.-Y., Berger, James M., & Doudna, Jennifer A. (2013). Structure of Human cGAS Reveals a Conserved Family of Second-Messenger Enzymes in Innate Immunity. *Cell Reports, 3*(5), 1362-1368.

Kristiansen, H., Gad, H. H., Eskildsen-Larsen, S., Despres, P., & Hartmann, R. (2011). The oligoadenylate synthetase family: an ancient protein family with multiple antiviral activities. *Journal of Interferon & Cytokine Research, 31*, 41+.

Krug, A., French, A. R., Barchet, W., Fischer, J. A. A., Dzionek, A., Pingel, J. T., Orihuela, M. M., Akira, S., Yokoyama, W. M., & Colonna, M. (2004). TLR9-Dependent Recognition of MCMV by IPC and DC Generates Coordinated Cytokine Responses that Activate Antiviral NK Cell Function. *Immunity, 21*(1), 107-119.

Kuriakose, T., Man, S. M., Malireddi, R. K. S., Karki, R., Kesavardhana, S., Place, D. E., Neale, G., Vogel, P., & Kanneganti, T.-D. (2016). ZBP1/DAI is an innate sensor of influenza virus triggering the NLRP3 inflammasome and programmed cell death pathways. *Science Immunology, 1*(2), aag2045.

Kurt-Jones, E. A., Popova, L., Kwinn, L., Haynes, L. M., Jones, L. P., Tripp, R. A., Walsh, E. E., Freeman, M. W., Golenbock, D. T., Anderson, L. J., & Finberg, R. W. (2000). Pattern recognition receptors TLR4 and CD14 mediate response to respiratory syncytial virus. *Nature Immunology, 1*(5), 398-401.

Langland, J. O., & Jacobs, B. L. (2002). The Role of the PKR-Inhibitory Genes, E3L and K3L, in Determining Vaccinia Virus Host Range. *Virology, 299*(1), 133-141.

Lau, L., Gray, E. E., Brunette, R. L., & Stetson, D. B. (2015). DNA tumor virus oncogenes antagonize the cGAS-STING DNA-sensing pathway. *Science, 350*(6260), 568-571.

Lazear, H. M., Schoggins, J. W., & Diamond, M. S. (2019). Shared and Distinct Functions of Type I and Type III Interferons. *Immunity, 50*(4), 907-923.

Le, V. T. K., Trilling, M., Zimmermann, A., & Hengel, H. (2008). Mouse cytomegalovirus inhibits beta interferon (IFN-β) gene expression and controls activation pathways of the IFN-β enhanceosome. *Journal of General Virology, 89*(5), 1131-1141. doi:https://doi.org/10.1099/vir.0.83538-0

Lebre, M. C., van der Aar, A. M., van Baarsen, L., van Capel, T. M., Schuitemaker, J. H., Kapsenberg, M. L., & de Jong, E. C. (2007). Human keratinocytes express functional Toll-like receptor 3, 4, 5, and 9. *J Invest Dermatol, 127*(2), 331-341. doi:10.1038/sj.jid.5700530

Li, K., Foy, E., Ferreon, J. C., Nakamura, M., Ferreon, A. C. M., Ikeda, M., Ray, S. C., Gale, M., & Lemon, S. M. (2005). Immune evasion by hepatitis C virus NS3/4A protease-

mediated cleavage of the Toll-like receptor 3 adaptor protein TRIF. *Proceedings of the National Academy of Sciences of the United States of America, 102*(8), 2992-2997.

Li, T., Chen, J., & Cristea, Ileana M. (2013). Human Cytomegalovirus Tegument Protein pUL83 Inhibits IFI16-Mediated DNA Sensing for Immune Evasion. *Cell Host & Microbe, 14*(5), 591-599.

Li, W., Chen, H., Deng, H., Kuang, Z., Long, M., Chen, D., Liao, X., Li, M., Rock, D. L., Luo, S., & Hao, W. (2018). Orf Virus Encoded Protein ORFV119 Induces Cell Apoptosis Through the Extrinsic and Intrinsic Pathways. *Frontiers in Microbiology, 9*(1056).

Li, X.-D., Sun, L., Seth, R. B., Pineda, G., & Chen, Z. J. (2005). Hepatitis C virus protease NS3/4A cleaves mitochondrial antiviral signaling protein off the mitochondria to evade innate immunity. *Proceedings of the National Academy of Sciences of the United States of America, 102*(49), 17717-17722.

Li, X.-D., Wu, J., Gao, D., Wang, H., Sun, L., & Chen, Z. J. (2013). Pivotal Roles of cGAS-cGAMP Signaling in Antiviral Defense and Immune Adjuvant Effects. *Science, 341*(6152), 1390-1394.

Li, Y., Chen, R., Zhou, Q., Xu, Z., Li, C., Wang, S., Mao, A., Zhang, X., He, W., & Shu, H.-B. (2012). LSm14A is a processing body-associated sensor of viral nucleic acids that initiates cellular antiviral response in the early phase of viral infection. *Proceedings of the National Academy of Sciences, 109*(29), 11770-11775.

Lin, R., Genin, P., Mamane, Y., Sgarbanti, M., Battistini, A., Harrington, W. J., Barber, G. N., & Hiscott, J. (2001). HHV-8 encoded vIRF-1 represses the interferon antiviral response by blocking IRF-3 recruitment of the CBP/p300 coactivators. *Oncogene, 20*(7), 800-811.

Lippmann, J., Rothenburg, S., Deigendesch, N., Eitel, J., Meixenberger, K., Van Laak, V., Slevogt, H., N'Guessan, P. D., Hippenstiel, S., Chakraborty, T., Flieger, A., Suttorp, N., & Opitz, B. (2008). IFNβ responses induced by intracellular bacteria or cytosolic DNA in different human cells do not require ZBP1 (DLM-1/DAI). *Cellular Microbiology, 10*(12), 2579-2588.

Liu, D., Wu, H., Wang, C., Li, Y., Tian, H., Siraj, S., Sehgal, S. A., Wang, X., Wang, J., Shang, Y., Jiang, Z., Liu, L., & Chen, Q. (2019). STING directly activates autophagy to tune the innate immune response. *Cell Death & Differentiation, 26*(9), 1735-1749.

Liu, R., & Moss, B. (2018). Vaccinia Virus C9 Ankyrin Repeat/F-Box Protein Is a Newly Identified Antagonist of the Type I Interferon-Induced Antiviral State. *J Virol, 92*(9).

Liu, R., Olano, L. R., Mirzakhanyan, Y., Gershon, P. D., & Moss, B. (2019). Vaccinia Virus Ankyrin-Repeat/F-Box Protein Targets Interferon-Induced IFITs for Proteasomal Degradation. *Cell Reports, 29*(4), 816-828.

Liu, S., Cai, X., Wu, J., Cong, Q., Chen, X., Li, T., Du, F., Ren, J., Wu, Y.-T., Grishin, N. V., & Chen, Z. J. (2015). Phosphorylation of innate immune adaptor proteins MAVS, STING, and TRIF induces IRF3 activation. *Science, 347*(6227), aaa2630.

Liu, Y.-J. (2005). IPC: Professional Type 1 Interferon-Producing Cells and Plasmacytoid Dendritic Cell Precursors. *Annual Review of Immunology, 23*(1), 275-306.

Liu, Y., Goulet, M.-L., Sze, A., Hadj, S. B., Belgnaoui, S. M., Lababidi, R. R., Zheng, C., Fritz, J. H., Olagnier, D., & Lin, R. (2016). RIG-I-Mediated STING Upregulation Restricts Herpes Simplex Virus 1 Infection. *Journal of Virology, 90*(20), 9406-9419.

Liu, Y., Li, J., Chen, J., Li, Y., Wang, W., Du, X., Song, W., Zhang, W., Lin, L., & Yuan, Z. (2015). Hepatitis B Virus Polymerase Disrupts K63-Linked Ubiquitination of STING To Block Innate Cytosolic DNA-Sensing Pathways. *Journal of Virology, 89*(4), 2287-2300.

Liu, Y., Lu, N., Yuan, B., Weng, L., Wang, F., Liu, Y.-J., & Zhang, Z. (2014). The interaction between the helicase DHX33 and IPS-1 as a novel pathway to sense double-stranded RNA and RNA viruses in myeloid dendritic cells. *Cellular & Molecular Immunology, 11*(1), 49-57.

Loo, Y.-M., Fornek, J., Crochet, N., Bajwa, G., Perwitasari, O., Martinez-Sobrido, L., Akira, S., Gill, M. A., García-Sastre, A., Katze, M. G., & Gale, M. (2008). Distinct RIG-I and MDA5 Signaling by RNA Viruses in Innate Immunity. *Journal of Virology, 82*(1), 335-345.

Lorenzo, M. M., Galindo, I., & Blasco, R. (2004). Construction and isolation of recombinant vaccinia virus using genetic markers. *Methods Mol Biol, 269*, 15-30.

Lu, H., Lu, N., Weng, L., Yuan, B., Liu, Y.-j., & Zhang, Z. (2014). DHX15 Senses Double-Stranded RNA in Myeloid Dendritic Cells. *The Journal of Immunology, 193*(3), 1364-1372.

Lu, L. L., Puri, M., Horvath, C. M., & Sen, G. C. (2008). Select Paramyxoviral V Proteins Inhibit IRF3 Activation by Acting as Alternative Substrates for Inhibitor of κB Kinase ϵ (IKKe)/TBK1. *Journal of Biological Chemistry, 283*(21), 14269-14276.

Lu, Y., Wambach, M., Katze, M. G., & Krug, R. M. (1995). Binding of the Influenza Virus NS1 Protein to Double-Stranded RNA Inhibits the Activation of the Protein Kinase

That Phosphorylates the eIF-2 Translation Initiation Factor. *Virology, 214*(1), 222-228.

Lund, J. M., Alexopoulou, L., Sato, A., Karow, M., Adams, N. C., Gale, N. W., Iwasaki, A., & Flavell, R. A. (2004). Recognition of single-stranded RNA viruses by Toll-like receptor 7. *Proceedings of the National Academy of Sciences of the United States of America, 101*(15), 5598-5603.

Luo, R., Xiao, S., Jiang, Y., Jin, H., Wang, D., Liu, M., Chen, H., & Fang, L. (2008). Porcine reproductive and respiratory syndrome virus (PRRSV) suppresses interferon-β production by interfering with the RIG-I signaling pathway. *Molecular Immunology, 45*(10), 2839-2846.

Luthra, P., Sun, D., Silverman, R. H., & He, B. (2011). Activation of IFN-β expression by a viral mRNA through RNase L and MDA5. *Proceedings of the National Academy of Sciences, 108*(5), 2118-2123.

Lyttle, D. J., Fraser, K. M., Fleming, S. B., Mercer, A. A., & Robinson, A. J. (1994). Homologs of vascular endothelial growth factor are encoded by the poxvirus orf virus. *Journal of Virology, 68*(1), 84-92.

Ma, Z., & Damania, B. (2016). The cGAS-STING Defense Pathway and Its Counteraction by Viruses. *Cell Host & Microbe, 19*(2), 150-158.

Ma, Z., Jacobs, S. R., West, J. A., Stopford, C., Zhang, Z., Davis, Z., Barber, G. N., Glaunsinger, B. A., Dittmer, D. P., & Damania, B. (2015). Modulation of the cGAS-STING DNA sensing pathway by gammaherpesviruses. *Proceedings of the National Academy of Sciences, 112*(31), E4306-E4315.

Ma, Z., Ni, G., & Damania, B. (2018). Innate Sensing of DNA Virus Genomes. *Annual Review of Virology, 5*(1), 341-362.

Mackett, M., Smith, G. L., & Moss, B. (1984). General method for production and selection of infectious vaccinia virus recombinants expressing foreign genes. *Journal of Virology, 49*(3), 857-864.

MacMicking, J. D. (2012). Interferon-inducible effector mechanisms in cell-autonomous immunity. *Nature Reviews Immunology, 12*(5), 367-382.

Malaspina, A., Moir, S., DiPoto, A. C., Ho, J., Wang, W., Roby, G., O'Shea, M. A., & Fauci, A. S. (2008). CpG Oligonucleotides Enhance Proliferative and Effector Responses of B Cells in HIV-Infected Individuals. *The Journal of Immunology, 181*(2), 1199-1206.

Malathi, K., Dong, B., Gale, M., & Silverman, R. H. (2007). Small self-RNA generated by RNase L amplifies antiviral innate immunity. *Nature, 448*(7155), 816-819.

Malathi, K., Saito, T., Crochet, N., Barton, D. J., Gale, M., & Silverman, R. H. (2010). RNase L releases a small RNA from HCV RNA that refolds into a potent PAMP. *RNA, 16*(11), 2108-2119.

Maniatis, T., Falvo, J. V., Kim, T. H., Kim, T. K., Lin, C. H., Parekh, B. S., & Wathelet, M. G. (1998). Structure and Function of the Interferon-β Enhanceosome. *Cold Spring Harbor Symposia on Quantitative Biology, 63*, 609-620.

Mankan, A. K., Schmidt, T., Chauhan, D., Goldeck, M., Höning, K., Gaidt, M., Kubarenko, A. V., Andreeva, L., Hopfner, K.-P., & Hornung, V. (2014). Cytosolic RNA:DNA hybrids activate the cGAS–STING axis. *The EMBO Journal, 33*(24), 2937-2946.

Mansur, D. S., Maluquer de Motes, C., Unterholzner, L., Sumner, R. P., Ferguson, B. J., Ren, H., Strnadova, P., Bowie, A. G., & Smith, G. L. (2013). Poxvirus Targeting of E3 Ligase β-TrCP by Molecular Mimicry: A Mechanism to Inhibit NF-κB Activation and Promote Immune Evasion and Virulence. *PLOS Pathogens, 9*(2), e1003183.

Marié, I., Durbin, J. E., & Levy, D. E. (1998). Differential viral induction of distinct interferon-α genes by positive feedback through interferon regulatory factor-7. *The EMBO Journal, 17*(22), 6660-6669.

Marq, J.-B., Hausmann, S., Luban, J., Kolakofsky, D., & Garcin, D. (2009). The double-stranded RNA binding domain of the vaccinia virus E3L protein inhibits both RNA- and DNA-induced activation of interferon beta. *The Journal of biological chemistry, 284*(38), 25471-25478.

Marq, J.-B., Hausmann, S., Veillard, N., Kolakofsky, D., & Garcin, D. (2011). Short Double-stranded RNAs with an Overhanging 5′ ppp-Nucleotide, as Found in Arenavirus Genomes, Act as RIG-I Decoys. *Journal of Biological Chemistry, 286*(8), 6108-6116.

Marq, J.-B., Kolakofsky, D., & Garcin, D. (2010). Unpaired 5′ ppp-Nucleotides, as Found in Arenavirus Double-stranded RNA Panhandles, Are Not Recognized by RIG-I. *Journal of Biological Chemistry, 285*(24), 18208-18216.

Marques, J., Anwar, J., Eskildsen-Larsen, S., Rebouillat, D., Paludan, S. R., Sen, G., Williams, B. R. G., & Hartmann, R. (2008). The p59 oligoadenylate synthetase-like protein possesses antiviral activity that requires the C-terminal ubiquitin-like domain. *Journal of General Virology, 89*(11), 2767-2772.

Marques, J. T., Devosse, T., Wang, D., Zamanian-Daryoush, M., Serbinowski, P., Hartmann, R., Fujita, T., Behlke, M. A., & Williams, B. R. G. (2006). A structural basis for discriminating between self and nonself double-stranded RNAs in mammalian cells. *Nature Biotechnology, 24*(5), 559-565.

Martinelli, E., Cicala, C., Van Ryk, D., Goode, D. J., Macleod, K., Arthos, J., & Fauci, A. S. (2007). HIV-1 gp120 inhibits TLR9-mediated activation and IFN-α secretion in plasmacytoid dendritic cells. *Proceedings of the National Academy of Sciences, 104*(9), 3396-3401.

Martinez, J., Huang, X., & Yang, Y. (2010). Toll-like receptor 8-mediated activation of murine plasmacytoid dendritic cells by vaccinia viral DNA. *Proceedings of the National Academy of Sciences, 107*(14), 6442-6447.

Matsumoto, M., Kikkawa, S., Kohase, M., Miyake, K., & Seya, T. (2002). Establishment of a monoclonal antibody against human Toll-like receptor 3 that blocks double-stranded RNA-mediated signaling. *Biochemical and Biophysical Research Communications, 293*(5), 1364-1369.

Matta, H., Mazzacurati, L., Schamus, S., Yang, T., Sun, Q., & Chaudhary, P. M. (2007). Kaposi's Sarcoma-associated Herpesvirus (KSHV) Oncoprotein K13 Bypasses TRAFs and Directly Interacts with the IκB Kinase Complex to Selectively Activate NF-κB without JNK Activation. *Journal of Biological Chemistry, 282*(34), 24858-24865.

McCartney, S. A., Thackray, L. B., Gitlin, L., Gilfillan, S., Virgin Iv, H. W., & Colonna, M. (2008). MDA-5 Recognition of a Murine Norovirus. *PLOS Pathogens, 4*(7), e1000108.

McGuire, M. J., Johnston, S. A., & Sykes, K. F. (2012). Novel immune-modulator identified by a rapid, functional screen of the parapoxvirus ovis (Orf virus) genome. *Proteome science, 10*(1), 4-4.

McInnes, C. J., Wood, A. R., & Mercer, A. A. (1998). Orf Virus Encodes a Homolog of the Vaccinia Virus Interferon-Resistance Gene E3L. *Virus Genes, 17*(2), 107-115.

McWhirter, S. M., Barbalat, R., Monroe, K. M., Fontana, M. F., Hyodo, M., Joncker, N. T., Ishii, K. J., Akira, S., Colonna, M., Chen, Z. J., Fitzgerald, K. A., Hayakawa, Y., & Vance, R. E. (2009). A host type I interferon response is induced by cytosolic sensing of the bacterial second messenger cyclic-di-GMP. *The Journal of Experimental Medicine, 206*(9), 1899-1911.

Meade, N., King, M., Munger, J., & Walsh, D. (2019). mTOR Dysregulation by Vaccinia Virus F17 Controls Multiple Processes with Varying Roles in Infection. *Journal of Virology, 93*(15), e00784-00719.

Medzhitov, R. (2001). Toll-like receptors and innate immunity. *Nat Rev Immunol, 1*(2), 135-145.

Meier, A., Chang, J. J., Chan, E. S., Pollard, R. B., Sidhu, H. K., Kulkarni, S., Wen, T. F., Lindsay, R. J., Orellana, L., Mildvan, D., Bazner, S., Streeck, H., Alter, G., Lifson, J. D., Carrington, M., Bosch, R. J., Robbins, G. K., & Altfeld, M. (2009). Sex differences in the Toll-like receptor–mediated response of plasmacytoid dendritic cells to HIV-1. *Nature Medicine, 15*(8), 955-959.

Melchjorsen, J., Kristiansen, H., Christiansen, R., Rintahaka, J., Matikainen, S., Paludan, S. R., & Hartmann, R. (2009). Differential Regulation of the OASL and OAS1 Genes in Response to Viral Infections. *Journal of Interferon & Cytokine Research, 29*(4), 199-208.

Meng, X., Jiang, C., Arsenio, J., Dick, K., Cao, J., & Xiang, Y. (2009). Vaccinia Virus K1L and C7L Inhibit Antiviral Activities Induced by Type I Interferons. *Journal of Virology, 83*(20), 10627-10636.

Meng, X., Schoggins, J., Rose, L., Cao, J., Ploss, A., Rice, C. M., & Xiang, Y. (2012). C7L Family of Poxvirus Host Range Genes Inhibits Antiviral Activities Induced by Type I Interferons and Interferon Regulatory Factor 1. *Journal of Virology, 86*(8), 4538-4547.

Mercer, A., & Fleming, S. (2011). Parapoxvirus. In C. Tidona & G. Darai (Eds.), *The Springer Index of Viruses* (pp. 1495-1504). New York, NY: Springer New York.

Mercer, A. A., Fleming, S. B., & Ueda, N. (2005). F-Box-Like Domains are Present in Most Poxvirus Ankyrin Repeat Proteins. *Virus Genes, 31*(2), 127-133.

Mercer, A. A., Fraser, K., Barns, G., & Robinson, A. J. (1987). The structure and cloning of orf virus DNA. *Virology, 157*(1), 1-12.

Mercer, A. A., Ueda, N., Friederichs, S.-M., Hofmann, K., Fraser, K. M., Bateman, T., & Fleming, S. B. (2006). Comparative analysis of genome sequences of three isolates of Orf virus reveals unexpected sequence variation. *Virus Research, 116*(1), 146-158.

Meylan, E., Curran, J., Hofmann, K., Moradpour, D., Binder, M., Bartenschlager, R., & Tschopp, J. (2005). Cardif is an adaptor protein in the RIG-I antiviral pathway and is targeted by hepatitis C virus. *Nature, 437*(7062), 1167-1172.

Mibayashi, M., Martínez-Sobrido, L., Loo, Y.-M., Cárdenas, W. B., Gale, M., & García-Sastre, A. (2007). Inhibition of Retinoic Acid-Inducible Gene I-Mediated Induction of Beta Interferon by the NS1 Protein of Influenza A Virus. *Journal of Virology, 81*(2), 514-524.

Mitchiner, M. B. (1969). The Envelope of Vaccinia and Orf Viruses: an Electron-cytochemical Investigation. *Journal of General Virology, 5*(2), 211-220.

Mitoma, H., Hanabuchi, S., Kim, T., Bao, M., Zhang, Z., Sugimoto, N., & Liu, Y.-J. (2013). The DHX33 RNA Helicase Senses Cytosolic RNA and Activates the NLRP3 Inflammasome. *Immunity*, *39*(1), 123-135.

Miyahira, A. K., Shahangian, A., Hwang, S., Sun, R., & Cheng, G. (2009). TANK-Binding Kinase-1 Plays an Important Role during In Vitro and In Vivo Type I IFN Responses to DNA Virus Infections. *The Journal of Immunology*, *182*(4), 2248-2257.

Miyashita, M., Oshiumi, H., Matsumoto, M., & Seya, T. (2011). DDX60, a DEXD/H Box Helicase, Is a Novel Antiviral Factor Promoting RIG-I-Like Receptor-Mediated Signaling. *Molecular and Cellular Biology*, *31*(18), 3802-3819.

Mizushima, S., & Nagata, S. (1990). pEF-BOS, a powerful mammalian expression vector. *Nucleic Acids Research*, *18*(17), 5322-5322.

Moens, B., Pannecouque, C., López, G., Talledo, M., Gotuzzo, E., Khouri, R., Bittencourt, A., Farré, L., Galvão-Castro, B., Vandamme, A.-M., & Van Weyenbergh, J. (2012). Simultaneous RNA quantification of human and retroviral genomes reveals intact interferon signaling in HTLV-1-infected CD4+ T cell lines. *Virology Journal*, *9*(1), 171.

Mori, M., Yoneyama, M., Ito, T., Takahashi, K., Inagaki, F., & Fujita, T. (2004). Identification of Ser-386 of Interferon Regulatory Factor 3 as Critical Target for Inducible Phosphorylation That Determines Activation. *Journal of Biological Chemistry*, *279*(11), 9698-9702.

Mosallanejad, K., Sekine, Y., Ishikura-Kinoshita, S., Kumagai, K., Nagano, T., Matsuzawa, A., Takeda, K., Naguro, I., & Ichijo, H. (2014). The DEAH-Box RNA Helicase DHX15 Activates NF-κB and MAPK Signaling Downstream of MAVS During Antiviral Responses. *Science Signaling*, *7*(323), ra40.

Moss, B. (1991). Vaccinia virus: a tool for research and vaccine development. *Science*, *252*(5013), 1662-1667.

Moss, B. (2007). Poxviridae: The Viruses and Their Replication. In D. E. G. David M. Knipe, Robert A. Lamb, Stephen E. Straus, Peter M. Howley, Malcolm A. Martin, Bernard Roizman (Ed.), *Fields Virology* (5 ed., Vol. 2, pp. 2905-2946). Philadelphia Wolters Kluwer-Lippincott Williams & Wilkins.

Moss, B., & Senkevich, T. G. (2011). Orthopoxvirus. In C. Tidona & G. Darai (Eds.), *The Springer Index of Viruses* (pp. 1485-1494). New York, NY: Springer New York.

Mounce, B. C., Mboko, W. P., Bigley, T. M., Terhune, S. S., & Tarakanova, V. L. (2013). A Conserved Gammaherpesvirus Protein Kinase Targets Histone Deacetylases 1 and 2

To Facilitate Viral Replication in Primary Macrophages. *Journal of Virology, 87*(13), 7314-7325.

Nagendraprabhu, P., Khatiwada, S., Chaulagain, S., Delhon, G., & Rock, D. L. (2017). A parapoxviral virion protein targets the retinoblastoma protein to inhibit NF-κB signaling. *PLOS Pathogens, 13*(12), e1006779.

Nagesh, P. T., & Husain, M. (2016). Influenza A Virus Dysregulates Host Histone Deacetylase 1 That Inhibits Viral Infection in Lung Epithelial Cells. *Journal of Virology, 90*(9), 4614-4625.

Nagington, J., & Horne, R. W. (1962). Morphological studies of orf and vaccinia viruses. *Virology, 16*(3), 248-260.

Nagington, J., Newton, A. A., & Horne, R. W. (1964). The structure of orf virus. *Virology, 23*(4), 461-472.

Najarro, P., Traktman, P., & Lewis, J. A. (2001). Vaccinia Virus Blocks Gamma Interferon Signal Transduction: Viral VH1 Phosphatase Reverses Stat1 Activation. *Journal of Virology, 75*(7), 3185-3196.

Nájera, J. L., Gómez, C. E., Domingo-Gil, E., Gherardi, M. M., & Esteban, M. (2006). Cellular and biochemical differences between two attenuated poxvirus vaccine candidates (MVA and NYVAC) and role of the C7L gene. *Journal of Virology, 80*(12), 6033-6047.

Nestle, F. O., Di Meglio, P., Qin, J.-Z., & Nickoloff, B. J. (2009). Skin immune sentinels in health and disease. *Nature Reviews Immunology, 9*(10), 679-691.

Ni, G., Konno, H., & Barber, G. N. (2017). Ubiquitination of STING at lysine 224 controls IRF3 activation. *Science Immunology, 2*(11), eaah7119.

Nie, Y., & Wang, Y.-Y. (2013). Innate immune responses to DNA viruses. *Protein & Cell, 4*(1), 1-7.

O'Neill, L. A. J., & Bowie, A. G. (2007). The family of five: TIR-domain-containing adaptors in Toll-like receptor signalling. *Nature Reviews Immunology, 7*(5), 353-364.

Oda, S., Schröder, M., & Khan, A. R. (2009). Structural Basis for Targeting of Human RNA Helicase DDX3 by Poxvirus Protein K7. *Structure, 17*(11), 1528-1537.

Oh, D., Baumann, K., Hamouda, O., Eckert, J. K., Neumann, K., Kücherer, C., Bartmeyer, B., Poggensee, G., Oh, N., Pruss, A., Jessen, H., & Schumann, R. R. (2009). A frequent functional toll-like receptor 7 polymorphism is associated with accelerated HIV-1 disease progression. *AIDS, 23*(3), 297-307.

Onoguchi, K., Yoneyama, M., Takemura, A., Akira, S., Taniguchi, T., Namiki, H., & Fujita, T. (2007). Viral Infections Activate Types I and III Interferon Genes through a Common Mechanism. *Journal of Biological Chemistry, 282*(10), 7576-7581.

Orzalli, M. H., DeLuca, N. A., & Knipe, D. M. (2012). Nuclear IFI16 induction of IRF-3 signaling during herpesviral infection and degradation of IFI16 by the viral ICP0 protein. *Proceedings of the National Academy of Sciences, 109*(44), E3008-E3017.

Oshiumi, H., Matsumoto, M., Funami, K., Akazawa, T., & Seya, T. (2003). TICAM-1, an adaptor molecule that participates in Toll-like receptor 3–mediated interferon-β induction. *Nature Immunology, 4*(2), 161-167.

Oshiumi, H., Miyashita, M., Matsumoto, M., & Seya, T. (2013). A Distinct Role of Riplet-Mediated K63-Linked Polyubiquitination of the RIG-I Repressor Domain in Human Antiviral Innate Immune Responses. *PLOS Pathogens, 9*(8), e1003533.

Oshiumi, H., Miyashita, M., Okamoto, M., Morioka, Y., Okabe, M., Matsumoto, M., & Seya, T. (2015). DDX60 Is Involved in RIG-I-Dependent and Independent Antiviral Responses, and Its Function Is Attenuated by Virus-Induced EGFR Activation. *Cell Reports, 11*(8), 1193-1207.

Oshiumi, H., Sakai, K., Matsumoto, M., & Seya, T. (2010). DEAD/H BOX 3 (DDX3) helicase binds the RIG-I adaptor IPS-1 to up-regulate IFN-β-inducing potential. *European Journal of Immunology, 40*(4), 940-948.

Otsuka, M., Kato, N., Moriyama, M., Taniguchi, H., Wang, Y., Dharel, N., Kawabe, T., & Omata, M. (2005). Interaction between the HCV NS3 protein and the host TBK1 protein leads to inhibition of cellular antiviral responses. *Hepatology, 41*(5), 1004-1012.

Paludan, Søren R., & Bowie, Andrew G. (2013). Immune Sensing of DNA. *Immunity, 38*(5), 870-880.

Panda, D., Dinh, P. X., Beura, L. K., & Pattnaik, A. K. (2010). Induction of Interferon and Interferon Signaling Pathways by Replication of Defective Interfering Particle RNA in Cells Constitutively Expressing Vesicular Stomatitis Virus Replication Proteins. *Journal of Virology, 84*(9), 4826-4831.

Paoletti, E., & Grady, L. J. (1977). Transcriptional complexity of vaccinia virus in vivo and in vitro. *Journal of Virology, 23*(3), 608-615.

Parekh, N. J., Krouse, T. E., Reider, I. E., Hobbs, R. P., Ward, B. M., & Norbury, C. C. (2019). Type I interferon-dependent CCL4 is induced by a cGAS/STING pathway

that bypasses viral inhibition and protects infected tissue, independent of viral burden. *PLOS Pathogens, 15*(10), e1007778.

Parker, D., Martin, F. J., Soong, G., Harfenist, B. S., Aguilar, J. L., Ratner, A. J., Fitzgerald, K. A., Schindler, C., & Prince, A. (2011). Streptococcus pneumoniae DNA Initiates Type I Interferon Signaling in the Respiratory Tract. *mBio, 2*(3), e00016-00011.

Parvatiyar, K., Zhang, Z., Teles, R. M., Ouyang, S., Jiang, Y., Iyer, S. S., Zaver, S. A., Schenk, M., Zeng, S., Zhong, W., Liu, Z.-J., Modlin, R. L., Liu, Y.-j., & Cheng, G. (2012). The helicase DDX41 recognizes the bacterial secondary messengers cyclic di-GMP and cyclic di-AMP to activate a type I interferon immune response. *Nature Immunology, 13*(12), 1155-1161.

Pasieka, T. J., Baas, T., Carter, V. S., Proll, S. C., Katze, M. G., & Leib, D. A. (2006). Functional Genomic Analysis of Herpes Simplex Virus Type 1 Counteraction of the Host Innate Response. *Journal of Virology, 80*(15), 7600-7612.

Patel, J. R., Jain, A., Chou, Y.-y., Baum, A., Ha, T., & García-Sastre, A. (2013). ATPase-driven oligomerization of RIG-I on RNA allows optimal activation of type-I interferon. *EMBO reports, 14*(9), 780-787.

Pelham, H. R. B. (1977). Use of coupled transcription and translation to study mRNA production by vaccinia cores. *Nature, 269*(5628), 532-534.

Perdiguero B, E. M. (2009). The Interferon System and Vaccinia Virus Evasion Mechanisms. *Journal of Interferon & Cytokine Research, 29*(9), 581-598.

Perkus, M. E., Goebel, S. J., Davis, S. W., Johnson, G. P., Limbach, K., Norton, E. K., & Paoletti, E. (1990). Vaccinia virus host range genes. *Virology, 179*(1), 276-286.

Perkus, M. E., Goebel, S. J., Davis, S. W., Johnson, G. P., Norton, E. K., & Paoletti, E. (1991). Deletion of 55 open reading frames from the termini of vaccinia virus. *Virology, 180*(1), 406-410.

Perry, A. K., Chow, E. K., Goodnough, J. B., Yeh, W.-C., & Cheng, G. (2004). Differential Requirement for TANK-binding Kinase-1 in Type I Interferon Responses to Toll-like Receptor Activation and Viral Infection. *The Journal of Experimental Medicine, 199*(12), 1651-1658.

Peters, D., Müller, G., & Büttner, D. (1964). The fine structure of paravaccinia viruses. *Virology, 23*(4), 609-611.

Peters, N. E., Ferguson, B. J., Mazzon, M., Fahy, A. S., Krysztofinska, E., Arribas-Bosacoma, R., Pearl, L. H., Ren, H., & Smith, G. L. (2013). A Mechanism for the Inhibition of DNA-PK-Mediated DNA Sensing by a Virus. *PLOS Pathogens, 9*(10), e1003649.

Pfaffl, M. W. (2001). A new mathematical model for relative quantification in real-time RT–PCR. *Nucleic Acids Research, 29*(9), e45.

Pham, A. M., Santa Maria, F. G., Lahiri, T., Friedman, E., Marié, I. J., & Levy, D. E. (2016). PKR Transduces MDA5-Dependent Signals for Type I IFN Induction. *PLOS Pathogens, 12*(3), e1005489.

Pichlmair, A., Schulz, O., Tan, C.-P., Rehwinkel, J., Kato, H., Takeuchi, O., Akira, S., Way, M., Schiavo, G., & Reis e Sousa, C. (2009). Activation of MDA5 Requires Higher-Order RNA Structures Generated during Virus Infection. *Journal of Virology, 83*(20), 10761-10769.

Pichlmair, A., Schulz, O., Tan, C. P., Näslund, T. I., Liljeström, P., Weber, F., & Reis e Sousa, C. (2006). RIG-I-Mediated Antiviral Responses to Single-Stranded RNA Bearing 5'-Phosphates. *Science, 314*(5801), 997-1001.

Plotch, S. J., Bouloy, M., Ulmanen, I., & Krug, R. M. (1981). A unique cap(m7GpppXm)-dependent influenza virion endonuclease cleaves capped RNAs to generate the primers that initiate viral RNA transcription. *Cell, 23*(3), 847-858.

Poppers, J., Mulvey, M., Khoo, D., & Mohr, I. (2000). Inhibition of PKR Activation by the Proline-Rich RNA Binding Domain of the Herpes Simplex Virus Type 1 Us11 Protein. *Journal of Virology, 74*(23), 11215-11221.

Powell, P. P., Dixon, L. K., & Parkhouse, R. M. (1996). An IkappaB homolog encoded by African swine fever virus provides a novel mechanism for downregulation of proinflammatory cytokine responses in host macrophages. *Journal of Virology, 70*(12), 8527-8533.

Randall, R. E., & Goodbourn, S. (2008). Interferons and viruses: an interplay between induction, signalling, antiviral responses and virus countermeasures. *Journal of General Virology, 89*(1), 1-47.

Rasmussen, S. B., Jensen, S. B., Nielsen, C., Quartin, E., Kato, H., Chen, Z. J., Silverman, R. H., Akira, S., & Paludan, S. R. (2009). Herpes simplex virus infection is sensed by both Toll-like receptors and retinoic acid-inducible gene- like receptors, which synergize to induce type I interferon production. *Journal of General Virology, 90*(1), 74-78.

Rathinam, V. A. K., & Fitzgerald, K. A. (2011). Innate immune sensing of DNA viruses. *Virology, 411*(2), 153-162.

Rathinam, V. A. K., Jiang, Z., Waggoner, S. N., Sharma, S., Cole, L. E., Waggoner, L., Vanaja, S. K., Monks, B. G., Ganesan, S., Latz, E., Hornung, V., Vogel, S. N.,

Szomolanyi-Tsuda, E., & Fitzgerald, K. A. (2010). The AIM2 inflammasome is essential for host defense against cytosolic bacteria and DNA viruses. *Nature Immunology, 11*(5), 395-402.

Rehwinkel, J., Tan, C. P., Goubau, D., Schulz, O., Pichlmair, A., Bier, K., Robb, N., Vreede, F., Barclay, W., Fodor, E., & Reis e Sousa, C. (2010). RIG-I Detects Viral Genomic RNA during Negative-Strand RNA Virus Infection. *Cell, 140*(3), 397-408.

Riad, S., Xiang, Y., AlDaif, B., Mercer, A. A., & Fleming, S. B. (2020). Rescue of a Vaccinia Virus Mutant Lacking IFN Resistance Genes K1L and C7L by the Parapoxvirus Orf Virus. *Frontiers in Microbiology, 11*(1797). doi:10.3389/fmicb.2020.01797

Roberts, T. L., Idris, A., Dunn, J. A., Kelly, G. M., Burnton, C. M., Hodgson, S., Hardy, L. L., Garceau, V., Sweet, M. J., Ross, I. L., Hume, D. A., & Stacey, K. J. (2009). HIN-200 Proteins Regulate Caspase Activation in Response to Foreign Cytoplasmic DNA. *Science, 323*(5917), 1057-1060.

Robinson, A. J., Ellis, G., & Balassu, T. (1982). The genome of orf virus: Restriction endonuclease analysis of viral DNA isolated from lesions of orf in sheep. *Archives of Virology, 71*(1), 43-55.

Rodriguez-Madoz, J. R., Bernal-Rubio, D., Kaminski, D., Boyd, K., & Fernandez-Sesma, A. (2010). Dengue Virus Inhibits the Production of Type I Interferon in Primary Human Dendritic Cells. *Journal of Virology, 84*(9), 4845-4850. doi:10.1128/jvi.02514-09

Ronco, L. V., Karpova, A. Y., Vidal, M., & Howley, P. M. (1998). Human papillomavirus 16 E6 oncoprotein binds to interferon regulatory factor-3 and inhibits its transcriptional activity. *Genes & Development, 12*(13), 2061-2072.

Roth, S., Rottach, A., Lotz-Havla, A. S., Laux, V., Muschaweckh, A., Gersting, S. W., Muntau, A. C., Hopfner, K.-P., Jin, L., Vanness, K., Petrini, J. H. J., Drexler, I., Leonhardt, H., & Ruland, J. (2014). Rad50-CARD9 interactions link cytosolic DNA sensing to IL-1β production. *Nature Immunology, 15*(6), 538-545.

Rothenfusser, S., Goutagny, N., DiPerna, G., Gong, M., Monks, B. G., Schoenemeyer, A., Yamamoto, M., Akira, S., & Fitzgerald, K. A. (2005). The RNA Helicase Lgp2 Inhibits TLR-Independent Sensing of Viral Replication by Retinoic Acid-Inducible Gene-I. *The Journal of Immunology, 175*(8), 5260-5268.

Rudd, B. D., Smit, J. J., Flavell, R. A., Alexopoulou, L., Schaller, M. A., Gruber, A., Berlin, A. A., & Lukacs, N. W. (2006). Deletion of TLR3 Alters the Pulmonary Immune Environment and Mucus Production during Respiratory Syncytial Virus Infection. *The Journal of Immunology, 176*(3), 1937-1942.

Runge, S., Sparrer, K. M. J., Lässig, C., Hembach, K., Baum, A., García-Sastre, A., Söding, J., Conzelmann, K.-K., & Hopfner, K.-P. (2014). In Vivo Ligands of MDA5 and RIG-I in Measles Virus-Infected Cells. *PLOS Pathogens, 10*(4), e1004081.

Rziha, H., Rohde, J., & Amann, R. (2016). Generation and Selection of Orf Virus (ORFV) Recombinants. In A. Brun (Ed.), *Vaccine Technologies for Veterinary Viral Diseases: Methods and Protocols* (pp. 177-200). New York, NY: Springer New York.

Sadler, A. J., & Williams, B. R. G. (2008). Interferon-inducible antiviral effectors. *Nature Reviews Immunology, 8*(7), 559-568.

Saira, K., Zhou, Y., & Jones, C. (2007). The Infected Cell Protein 0 Encoded by Bovine Herpesvirus 1 (bICP0) Induces Degradation of Interferon Response Factor 3 and, Consequently, Inhibits Beta Interferon Promoter Activity. *Journal of Virology, 81*(7), 3077-3086.

Saito, T., Hirai, R., Loo, Y.-M., Owen, D., Johnson, C. L., Sinha, S. C., Akira, S., Fujita, T., & Gale, M. (2007). Regulation of innate antiviral defenses through a shared repressor domain in RIG-I and LGP2. *Proceedings of the National Academy of Sciences, 104*(2), 582-587.

Saito, T., Owen, D. M., Jiang, F., Marcotrigiano, J., & Gale Jr, M. (2008). Innate immunity induced by composition-dependent RIG-I recognition of hepatitis C virus RNA. *Nature, 454*(7203), 523-527.

Samanta, M., Iwakiri, D., & Takada, K. (2008). Epstein–Barr virus-encoded small RNA induces IL-10 through RIG-I-mediated IRF-3 signaling. *Oncogene, 27*(30), 4150-4160.

Sambrook, J., & Green, M. (2012). *Molecular Cloning: A Laboratory Manual* (4th ed. Vol. 1): Cold Springs Harbour Press.

Samuel, C. E. (1991). Antiviral actions of interferon. Interferon-regulated cellular proteins and their surprisingly selective antiviral activities. *Virology, 183*(1), 1-11.

Samuel, C. E. (2001). Antiviral Actions of Interferons. *Clinical Microbiology Reviews, 14*(4), 778-809.

Samuelsson, C., Hausmann, J., Lauterbach, H., Schmidt, M., Akira, S., Wagner, H., Chaplin, P., Suter, M., O'Keeffe, M., & Hochrein, H. (2008). Survival of lethal poxvirus infection in mice depends on TLR9, and therapeutic vaccination provides protection. *The Journal of clinical investigation, 118*(5), 1776-1784.

Sanchez, D. J., Miranda, D., Arumugaswami, V., Hwang, S., Singer, A. E., Senaati, A., Shahangian, A., Song, M. J., Sun, R., & Cheng, G. (2008). A Repetitive Region of

Gammaherpesvirus Genomic DNA Is a Ligand for Induction of Type I Interferon. *Journal of Virology, 82*(5), 2208-2217.

Santos, C. N. S., & Yoshikuni, Y. (2014). Engineering complex biological systems in bacteria through recombinase-assisted genome engineering. *Nature Protocols, 9*(6), 1320-1336.

Sato, M., Suemori, H., Hata, N., Asagiri, M., Ogasawara, K., Nakao, K., Nakaya, T., Katsuki, M., Noguchi, S., Tanaka, N., & Taniguchi, T. (2000). Distinct and Essential Roles of Transcription Factors IRF-3 and IRF-7 in Response to Viruses for IFN-α/β Gene Induction. *Immunity, 13*(4), 539-548.

Satoh, T., Kato, H., Kumagai, Y., Yoneyama, M., Sato, S., Matsushita, K., Tsujimura, T., Fujita, T., Akira, S., & Takeuchi, O. (2010). LGP2 is a positive regulator of RIG-I– and MDA5-mediated antiviral responses. *Proceedings of the National Academy of Sciences, 107*(4), 1512-1517.

Sauer, J.-D., Sotelo-Troha, K., von Moltke, J., Monroe, K. M., Rae, C. S., Brubaker, S. W., Hyodo, M., Hayakawa, Y., Woodward, J. J., Portnoy, D. A., & Vance, R. E. (2011). The N-Ethyl-N-Nitrosourea-Induced Goldenticket Mouse Mutant Reveals an Essential Function of Sting in the In Vivo Interferon Response to Listeria monocytogenes and Cyclic Dinucleotides. *Infection and Immunity, 79*(2), 688-694.

Savory, L. J., Stacker, S. A., Fleming, S. B., Niven, B. E., & Mercer, A. A. (2000). Viral Vascular Endothelial Growth Factor Plays a Critical Role in Orf Virus Infection. *Journal of Virology, 74*(22), 10699-10706.

Schlee, M., Roth, A., Hornung, V., Hagmann, C. A., Wimmenauer, V., Barchet, W., Coch, C., Janke, M., Mihailovic, A., Wardle, G., Juranek, S., Kato, H., Kawai, T., Poeck, H., Fitzgerald, K. A., Takeuchi, O., Akira, S., Tuschl, T., Latz, E., Ludwig, J., & Hartmann, G. (2009). Recognition of 5′ Triphosphate by RIG-I Helicase Requires Short Blunt Double-Stranded RNA as Contained in Panhandle of Negative-Strand Virus. *Immunity, 31*(1), 25-34.

Schmidt, A., Schwerd, T., Hamm, W., Hellmuth, J. C., Cui, S., Wenzel, M., Hoffmann, F. S., Michallet, M.-C., Besch, R., Hopfner, K.-P., Endres, S., & Rothenfusser, S. (2009). 5′-triphosphate RNA requires base-paired structures to activate antiviral signaling via RIG-I. *Proceedings of the National Academy of Sciences, 106*(29), 12067-12072.

Schnipper, L. E., Levin, M., Crumpacker, C. S., & Gilchrest, B. A. (1984). Virus Replication and Induction of Interferon in Human Epidermal Keratinocytes Following Infection

with Herpes Simplex Virus. *Journal of Investigative Dermatology, 82*(1), 94-96. doi:https://doi.org/10.1111/1523-1747.ep12259193

Schoggins, J. W. (2019). Interferon-Stimulated Genes: What Do They All Do? *Annual Review of Virology, 6*(1), 567-584.

Schoggins, J. W., MacDuff, D. A., Imanaka, N., Gainey, M. D., Shrestha, B., Eitson, J. L., Mar, K. B., Richardson, R. B., Ratushny, A. V., Litvak, V., Dabelic, R., Manicassamy, B., Aitchison, J. D., Aderem, A., Elliott, R. M., García-Sastre, A., Racaniello, V., Snijder, E. J., Yokoyama, W. M., Diamond, M. S., Virgin, H. W., & Rice, C. M. (2014). Pan-viral specificity of IFN-induced genes reveals new roles for cGAS in innate immunity. *Nature, 505*(7485), 691-695.

Schoggins, J. W., & Rice, C. M. (2011). Interferon-stimulated genes and their antiviral effector functions. *Current Opinion in Virology, 1*(6), 519-525.

Schoggins, J. W., Wilson, S. J., Panis, M., Murphy, M. Y., Jones, C. T., Bieniasz, P., & Rice, C. M. (2011). A diverse range of gene products are effectors of the type I interferon antiviral response. *Nature, 472*(7344), 481-485.

Schröder, M., Baran, M., & Bowie, A. G. (2008). Viral targeting of DEAD box protein 3 reveals its role in TBK1/IKKε-mediated IRF activation. *The EMBO Journal, 27*(15), 2147-2157.

Schröder, M., & Bowie, A. G. (2005). TLR3 in antiviral immunity: key player or bystander? *Trends in immunology, 26*(9), 462-468.

Schulz, O., Pichlmair, A., Rehwinkel, J., Rogers, N. C., Scheuner, D., Kato, H., Takeuchi, O., Akira, S., Kaufman, R. J., & Reis e Sousa, C. (2010). Protein Kinase R Contributes to Immunity against Specific Viruses by Regulating Interferon mRNA Integrity. *Cell Host & Microbe, 7*(5), 354-361.

Scutts, S. R., Ember, S. W., Ren, H., Ye, C., Lovejoy, C. A., Mazzon, M., Veyer, D. L., Sumner, R. P., & Smith, G. L. (2018). DNA-PK Is Targeted by Multiple Vaccinia Virus Proteins to Inhibit DNA Sensing. *Cell Reports, 25*(7), 1953-1965.

Seet, B. T., McCaughan, C. A., Handel, T. M., Mercer, A., Brunetti, C., McFadden, G., & Fleming, S. B. (2003). Analysis of an orf virus chemokine-binding protein: Shifting ligand specificities among a family of poxvirus viroceptors. *Proceedings of the National Academy of Sciences of the United States of America, 100*(25), 15137-15142.

Sen, G. C., & Peters, G. A. (2007). Viral stress-inducible genes. *Adv Virus Res, 70*, 233-263.

Servant, M. J., Grandvaux, N., tenOever, B. R., Duguay, D., Lin, R., & Hiscott, J. (2003). Identification of the Minimal Phosphoacceptor Site Required for in Vivo Activation of Interferon Regulatory Factor 3 in Response to Virus and Double-stranded RNA. *Journal of Biological Chemistry, 278*(11), 9441-9447.

Shahzad, N., Shuda, M., Gheit, T., Kwun, H. J., Cornet, I., Saidj, D., Zannetti, C., Hasan, U., Chang, Y., Moore, P. S., Accardi, R., & Tommasino, M. (2013). The T Antigen Locus of Merkel Cell Polyomavirus Downregulates Human Toll-Like Receptor 9 Expression. *Journal of Virology, 87*(23), 13009-13019.

Sharma, S., tenOever, B. R., Grandvaux, N., Zhou, G.-P., Lin, R., & Hiscott, J. (2003). Triggering the Interferon Antiviral Response Through an IKK-Related Pathway. *Science, 300*(5622), 1148-1151.

Sheppard, P., Kindsvogel, W., Xu, W., Henderson, K., Schlutsmeyer, S., Whitmore, T. E., Kuestner, R., Garrigues, U., Birks, C., Roraback, J., Ostrander, C., Dong, D., Shin, J., Presnell, S., Fox, B., Haldeman, B., Cooper, E., Taft, D., Gilbert, T., Grant, F. J., Tackett, M., Krivan, W., McKnight, G., Clegg, C., Foster, D., & Klucher, K. M. (2003). IL-28, IL-29 and their class II cytokine receptor IL-28R. *Nature Immunology, 4*(1), 63-68.

Shisler, J. L., & Jin, X.-L. (2004). The Vaccinia Virus K1L Gene Product Inhibits Host NF-κB Activation by Preventing IκBα Degradation. *Journal of Virology, 78*(7), 3553-3560.

Siegemund, S., Hartl, A., von Buttlar, H., Dautel, F., Raue, R., Freudenberg, M. A., Fejer, G., Büttner, M., Köhler, G., Kirschning, C. J., Sparwasser, T., & Alber, G. (2009). Conventional Bone Marrow-Derived Dendritic Cells Contribute to Toll-Like Receptor-Independent Production of Alpha/Beta Interferon in Response to Inactivated Parapoxvirus Ovis. *Journal of Virology, 83*(18), 9411-9422.

Sims, J. E., & Smith, D. E. (2010). The IL-1 family: regulators of immunity. *Nature Reviews Immunology, 10*(2), 89-102.

Singer, G. A. C., & Hickey, D. A. (2000). Nucleotide Bias Causes a Genomewide Bias in the Amino Acid Composition of Proteins. *Molecular Biology and Evolution, 17*(11), 1581-1588. doi:10.1093/oxfordjournals.molbev.a026257

Sioud, M. (2006). RNA interference below the immune radar. *Nature Biotechnology, 24*(5), 521-522.

Smith, C. A., Smith, T. D., Smolak, P. J., Friend, D., Hagen, H., Gerhart, M., Park, L., Pickup, D. J., Torrance, D., Mohler, K., Schooley, K., & Goodwin, R. G. (1997). Poxvirus

Genomes Encode a Secreted, Soluble Protein That Preferentially Inhibits β Chemokine Activity yet Lacks Sequence Homology to Known Chemokine Receptors. *Virology, 236*(2), 316-327.

Smith, E. J., Marié, I., Prakash, A., García-Sastre, A., & Levy, D. E. (2001). IRF3 and IRF7 Phosphorylation in Virus-infected Cells Does Not Require Double-stranded RNA-dependent Protein Kinase R or IκB Kinase but Is Blocked by Vaccinia Virus E3L Protein. *Journal of Biological Chemistry, 276*(12), 8951-8957.

Smith, G. L. (2007). Genus Orthopoxvirus: Vaccinia virus. In A. A. Mercer, A. Schmidt, & O. Weber (Eds.), *Poxviruses* (pp. 1-45). Basel: Birkhäuser Basel.

Smith, G. L., Benfield, C. T. O., Maluquer de Motes, C., Mazzon, M., Ember, S. W. J., Ferguson, B. J., & Sumner, R. P. (2013). Vaccinia virus immune evasion: mechanisms, virulence and immunogenicity. *Journal of General Virology, 94*(11), 2367-2392.

Smith, G. L., & Chan, Y. S. (1991). Two vaccinia virus proteins structurally related to the interleukin-1 receptor and the immunoglobulin superfamily. *Journal of General Virology, 72*(3), 511-518.

Smith, G. L., Symons, J. A., & Alcamí, A. (1998). Poxviruses: Interfering with Interferon. *Seminars in Virology, 8*(5), 409-418.

Smith, G. L., Talbot-Cooper, C., & Lu, Y. (2018). Chapter Fourteen - How Does Vaccinia Virus Interfere With Interferon? In M. Kielian, T. C. Mettenleiter, & M. J. Roossinck (Eds.), *Adv Virus Res* (Vol. 100, pp. 355-378): Academic Press.

Soberon, X., Covarrubias, L., & Bolivar, F. (1980). Construction and characterization of new cloning vehicles. IV. Deletion derivatives of pBR322 and pBR325. *Gene, 9*(3-4), 287-305.

Søby, S., Laursen, R. R., Østergaard, L., & Melchjorsen, J. (2012). HSV-1-induced chemokine expression via IFI16-dependent and IFI16-independent pathways in human monocyte-derived macrophages. *Herpesviridae, 3*(1), 6.

Soulat, D., Bürckstümmer, T., Westermayer, S., Goncalves, A., Bauch, A., Stefanovic, A., Hantschel, O., Bennett, K. L., Decker, T., & Superti-Furga, G. (2008). The DEAD-box helicase DDX3X is a critical component of the TANK-binding kinase 1-dependent innate immune response. *The EMBO Journal, 27*(15), 2135-2146.

Sparrer, K. M. J., & Gack, M. U. (2015). Intracellular detection of viral nucleic acids. *Current Opinion in Microbiology, 26*, 1-9.

Speer, S. D., Li, Z., Buta, S., Payelle-Brogard, B., Qian, L., Vigant, F., Rubino, E., Gardner, T. J., Wedeking, T., Hermann, M., Duehr, J., Sanal, O., Tezcan, I., Mansouri, N., Tabarsi, P., Mansouri, D., Francois-Newton, V., Daussy, C. F., Rodriguez, M. R., Lenschow, D. J., Freiberg, A. N., Tortorella, D., Piehler, J., Lee, B., García-Sastre, A., Pellegrini, S., & Bogunovic, D. (2016). ISG15 deficiency and increased viral resistance in humans but not mice. *Nature Communications, 7*(1), 11496.

Spengler, J. R., Patel, J. R., Chakrabarti, A. K., Zivcec, M., García-Sastre, A., Spiropoulou, C. F., & Bergeron, É. (2015). RIG-I Mediates an Antiviral Response to Crimean-Congo Hemorrhagic Fever Virus. *Journal of Virology, 89*(20), 10219-10229.

Spiropoulou, C. F., Ranjan, P., Pearce, M. B., Sealy, T. K., Albariño, C. G., Gangappa, S., Fujita, T., Rollin, P. E., Nichol, S. T., Ksiazek, T. G., & Sambhara, S. (2009). RIG-I activation inhibits ebolavirus replication. *Virology, 392*(1), 11-15.

Stack, J., Haga, I. R., Schröder, M., Bartlett, N. W., Maloney, G., Reading, P. C., Fitzgerald, K. A., Smith, G. L., & Bowie, A. G. (2005). Vaccinia virus protein A46R targets multiple Toll-like–interleukin-1 receptor adaptors and contributes to virulence. *The Journal of Experimental Medicine, 201*(6), 1007-1018.

Starr, T., Bauler, T. J., Malik-Kale, P., & Steele-Mortimer, O. (2018). The phorbol 12-myristate-13-acetate differentiation protocol is critical to the interaction of THP-1 macrophages with Salmonella Typhimurium. *PLoS ONE, 13*(3), e0193601.

Stetson, D. B., & Medzhitov, R. (2006). Recognition of Cytosolic DNA Activates an IRF3-Dependent Innate Immune Response. *Immunity, 24*(1), 93-103.

Strahle, L., Garcin, D., & Kolakofsky, D. (2006). Sendai virus defective-interfering genomes and the activation of interferon-beta. *Virology, 351*(1), 101-111.

Sueoka, N. (1988). Directional mutation pressure and neutral molecular evolution. *Proceedings of the National Academy of Sciences, 85*(8), 2653-2657. doi:10.1073/pnas.85.8.2653

Sugimoto, N., Mitoma, H., Kim, T., Hanabuchi, S., & Liu, Y.-J. (2014). Helicase proteins DHX29 and RIG-I cosense cytosolic nucleic acids in the human airway system. *Proceedings of the National Academy of Sciences, 111*(21), 7747-7752.

Sumner, R. P., Maluquer de Motes, C., Veyer, D. L., & Smith, G. L. (2014). Vaccinia Virus Inhibits NF-κB-Dependent Gene Expression Downstream of p65 Translocation. *Journal of Virology, 88*(6), 3092-3102.

Sun, L., Wu, J., Du, F., Chen, X., & Chen, Z. J. (2013). Cyclic GMP-AMP Synthase Is a Cytosolic DNA Sensor That Activates the Type I Interferon Pathway. *Science, 339*(6121), 786-791.

Sun, W., Li, Y., Chen, L., Chen, H., You, F., Zhou, X., Zhou, Y., Zhai, Z., Chen, D., & Jiang, Z. (2009). ERIS, an endoplasmic reticulum IFN stimulator, activates innate immune signaling through dimerization. *Proceedings of the National Academy of Sciences, 106*(21), 8653-8658.

Symons, J. A., Alcamí, A., & Smith, G. L. (1995). Vaccinia virus encodes a soluble type I interferon receptor of novel structure and broad species soecificity. *Cell, 81*(4), 551-560.

Tabeta, K., Hoebe, K., Janssen, E. M., Du, X., Georgel, P., Crozat, K., Mudd, S., Mann, N., Sovath, S., Goode, J., Shamel, L., Herskovits, A. A., Portnoy, D. A., Cooke, M., Tarantino, L. M., Wiltshire, T., Steinberg, B. E., Grinstein, S., & Beutler, B. (2006). The Unc93b1 mutation 3d disrupts exogenous antigen presentation and signaling via Toll-like receptors 3, 7 and 9. *Nature Immunology, 7*(2), 156-164.

Tait, S. W. G., Reid, E. B., Greaves, D. R., Wileman, T. E., & Powell, P. P. (2000). Mechanism of Inactivation of NF-κB by a Viral Homologue of IκBα: Signal-Induced Release of IκBα Results in Binding of the Viral Homologue to NF-κB. *Journal of Biological Chemistry, 275*(44), 34656-34664.

Takahasi, K., Yoneyama, M., Nishihori, T., Hirai, R., Kumeta, H., Narita, R., Gale, M., Inagaki, F., & Fujita, T. (2008). Nonself RNA-Sensing Mechanism of RIG-I Helicase and Activation of Antiviral Immune Responses. *Molecular Cell, 29*(4), 428-440.

Takaoka, A., Wang, Z., Choi, M. K., Yanai, H., Negishi, H., Ban, T., Lu, Y., Miyagishi, M., Kodama, T., Honda, K., Ohba, Y., & Taniguchi, T. (2007). DAI (DLM-1/ZBP1) is a cytosolic DNA sensor and an activator of innate immune response. *Nature, 448*(7152), 501-505.

Takaoka, A., & Yanai, H. (2006). Interferon signalling network in innate defence. *Cellular Microbiology, 8*(6), 907-922.

Takeda, K., & Akira, S. (2005). Toll-like receptors in innate immunity. *International Immunology, 17*(1), 1-14.

Takeuchi, O., & Akira, S. (2008). MDA5/RIG-I and virus recognition. *Curr Opin Immunol, 20*(1), 17-22.

Takeuchi, O., & Akira, S. (2009). Innate immunity to virus infection. *Immunological Reviews, 227*(1), 75-86.

Tamassia, N., Bazzoni, F., Le Moigne, V., Calzetti, F., Masala, C., Grisendi, G., Bussmeyer, U., Scutera, S., De Gironcoli, M., Costantini, C., Musso, T., & Cassatella, M. A. (2012). IFN-β Expression Is Directly Activated in Human Neutrophils Transfected with Plasmid DNA and Is Further Increased via TLR-4–Mediated Signaling. *The Journal of Immunology, 189*(3), 1500-1509.

Tanaka, N., Kawakami, T., & Taniguchi, T. (1993). Recognition DNA sequences of interferon regulatory factor 1 (IRF-1) and IRF-2, regulators of cell growth and the interferon system. *Molecular and Cellular Biology, 13*(8), 4531-4538.

Tanaka, Y., & Chen, Z. J. (2012). STING Specifies IRF3 Phosphorylation by TBK1 in the Cytosolic DNA Signaling Pathway. *Science Signaling, 5*(214), ra20.

Thanos, D., & Maniatis, T. (1995). Virus induction of human IFNβ gene expression requires the assembly of an enhanceosome. *Cell, 83*(7), 1091-1100.

Thapa, R. J., Ingram, J. P., Ragan, K. B., Nogusa, S., Boyd, D. F., Benitez, A. A., Sridharan, H., Kosoff, R., Shubina, M., Landsteiner, V. J., Andrake, M., Vogel, P., Sigal, L. J., tenOever, B. R., Thomas, P. G., Upton, J. W., & Balachandran, S. (2016). DAI Senses Influenza A Virus Genomic RNA and Activates RIPK3-Dependent Cell Death. *Cell Host & Microbe, 20*(5), 674-681.

Torseth, J. W., Nickoloff, B. J., Basham, T. Y., & Merigan, T. C. (1987). β Interferon Produced by Keratinocytes in Human Cutaneous Infection with Herpes Simplex Virus. *The Journal of infectious diseases, 155*(4), 641-648. doi:10.1093/infdis/155.4.641

Tremblay, N., Baril, M., Chatel-Chaix, L., Es-Saad, S., Park, A. Y., Koenekoop, R. K., & Lamarre, D. (2016). Spliceosome SNRNP200 Promotes Viral RNA Sensing and IRF3 Activation of Antiviral Response. *PLOS Pathogens, 12*(7), e1005772.

Tsuchida, T., Zou, J., Saitoh, T., Kumar, H., Abe, T., Matsuura, Y., Kawai, T., & Akira, S. (2010). The Ubiquitin Ligase TRIM56 Regulates Innate Immune Responses to Intracellular Double-Stranded DNA. *Immunity, 33*(5), 765-776.

Tsung, K., Yim, J. H., Marti, W., Buller, R. M., & Norton, J. A. (1996). Gene expression and cytopathic effect of vaccinia virus inactivated by psoralen and long-wave UV light. *Journal of Virology, 70*(1), 165-171.

Twu, J. S., & Schloemer, R. H. (1989). Transcription of the human beta interferon gene is inhibited by hepatitis B virus. *Journal of Virology, 63*(7), 3065-3071.

Uematsu, S., Sato, S., Yamamoto, M., Hirotani, T., Kato, H., Takeshita, F., Matsuda, M., Coban, C., Ishii, K. J., Kawai, T., Takeuchi, O., & Akira, S. (2005). Interleukin-1

receptor-associated kinase-1 plays an essential role for Toll-like receptor (TLR)7- and TLR9-mediated interferon-α induction. *The Journal of Experimental Medicine, 201*(6), 915-923.

Ugrinova, I., & Pasheva, E. (2017). Chapter Two - HMGB1 Protein: A Therapeutic Target Inside and Outside the Cell. In R. Donev (Ed.), *Advances in Protein Chemistry and Structural Biology* (Vol. 107, pp. 37-76): Academic Press.

Unterholzner, L. (2013). The interferon response to intracellular DNA: Why so many receptors? *Immunobiology, 218*(11), 1312-1321.

Unterholzner, L., Keating, S. E., Baran, M., Horan, K. A., Jensen, S. B., Sharma, S., Sirois, C. M., Jin, T., Latz, E., Xiao, T. S., Fitzgerald, K. A., Paludan, S. R., & Bowie, A. G. (2010). IFI16 is an innate immune sensor for intracellular DNA. *Nature Immunology, 11*(11), 997-1004.

Unterholzner, L., Sumner, R. P., Baran, M., Ren, H., Mansur, D. S., Bourke, N. M., Randow, F., Smith, G. L., & Bowie, A. G. (2011). Vaccinia Virus Protein C6 Is a Virulence Factor that Binds TBK-1 Adaptor Proteins and Inhibits Activation of IRF3 and IRF7. *PLOS Pathogens, 7*(9), e1002247.

Upton, Jason W., Kaiser, William J., & Mocarski, Edward S. (2012). DAI/ZBP1/DLM-1 Complexes with RIP3 to Mediate Virus-Induced Programmed Necrosis that Is Targeted by Murine Cytomegalovirus vIRA. *Cell Host & Microbe, 11*(3), 290-297.

Uzé, G., & Monneron, D. (2007). IL-28 and IL-29: Newcomers to the interferon family. *Biochimie, 89*(6), 729-734.

Vaidya, S. A., & Cheng, G. (2003). Toll-like receptors and innate antiviral responses. *Current Opinion in Immunology, 15*(4), 402-407.

Valentine, R., & Smith, G. L. (2010). Inhibition of the RNA polymerase III-mediated dsDNA-sensing pathway of innate immunity by vaccinia virus protein E3. *Journal of General Virology, 91*(9), 2221-2229.

van Kasteren, P. B., Beugeling, C., Ninaber, D. K., Frias-Staheli, N., van Boheemen, S., García-Sastre, A., Snijder, E. J., & Kikkert, M. (2012). Arterivirus and nairovirus ovarian tumor domain-containing Deubiquitinases target activated RIG-I to control innate immune signaling. *Journal of Virology, 86*(2), 773-785.

Varga, Z. T., Grant, A., Manicassamy, B., & Palese, P. (2012). Influenza Virus Protein PB1-F2 Inhibits the Induction of Type I Interferon by Binding to MAVS and Decreasing Mitochondrial Membrane Potential. *Journal of Virology, 86*(16), 8359-8366.

Veeranki, S., & Choubey, D. (2012). Interferon-inducible p200-family protein IFI16, an innate immune sensor for cytosolic and nuclear double-stranded DNA: Regulation of subcellular localization. *Molecular Immunology, 49*(4), 567-571.

Venkataraman, T., Valdes, M., Elsby, R., Kakuta, S., Caceres, G., Saijo, S., Iwakura, Y., & Barber, G. N. (2007). Loss of DExD/H Box RNA Helicase LGP2 Manifests Disparate Antiviral Responses. *The Journal of Immunology, 178*(10), 6444-6455.

Vercammen, E., Staal, J., & Beyaert, R. (2008). Sensing of Viral Infection and Activation of Innate Immunity by Toll-Like Receptor 3. *Clinical Microbiology Reviews, 21*(1), 13-25.

Vignuzzi, M., & López, C. B. (2019). Defective viral genomes are key drivers of the virus–host interaction. *Nature Microbiology, 4*(7), 1075-1087.

von Buttlar, H., Siegemund, S., Büttner, M., & Alber, G. (2014). Identification of Toll-Like Receptor 9 as Parapoxvirus Ovis-Sensing Receptor in Plasmacytoid Dendritic Cells. *PLoS ONE, 9*(8), e106188.

Waibler, Z., Anzaghe, M., Frenz, T., Schwantes, A., Pöhlmann, C., Ludwig, H., Palomo-Otero, M., Alcamí, A., Sutter, G., & Kalinke, U. (2009). Vaccinia Virus-Mediated Inhibition of Type I Interferon Responses Is a Multifactorial Process Involving the Soluble Type I Interferon Receptor B18 and Intracellular Components. *Journal of Virology, 83*(4), 1563-1571. doi:10.1128/jvi.01617-08

Wang, F., Gao, X., Barrett, J. W., Shao, Q., Bartee, E., Mohamed, M. R., Rahman, M., Werden, S., Irvine, T., Cao, J., Dekaban, G. A., & McFadden, G. (2008). RIG-I Mediates the Co-Induction of Tumor Necrosis Factor and Type I Interferon Elicited by Myxoma Virus in Primary Human Macrophages. *PLOS Pathogens, 4*(7), e1000099.

Wang, P., Zhu, S., Yang, L., Cui, S., Pan, W., Jackson, R., Zheng, Y., Rongvaux, A., Sun, Q., Yang, G., Gao, S., Lin, R., You, F., Flavell, R., & Fikrig, E. (2015). Nlrp6 regulates intestinal antiviral innate immunity. *Science, 350*(6262), 826-830.

Wang, S., Chi, X., Wei, H., Chen, Y., Chen, Z., Huang, S., & Chen, J.-L. (2014). Influenza A Virus-Induced Degradation of Eukaryotic Translation Initiation Factor 4B Contributes to Viral Replication by Suppressing IFITM3 Protein Expression. *Journal of Virology, 88*(15), 8375-8385.

Wang, T., Town, T., Alexopoulou, L., Anderson, J. F., Fikrig, E., & Flavell, R. A. (2004). Toll-like receptor 3 mediates West Nile virus entry into the brain causing lethal encephalitis. *Nature Medicine, 10*(12), 1366-1373.

Wang, Z., Choi, M. K., Ban, T., Yanai, H., Negishi, H., Lu, Y., Tamura, T., Takaoka, A., Nishikura, K., & Taniguchi, T. (2008). Regulation of innate immune responses by DAI (DLM-1/ZBP1) and other DNA-sensing molecules. *Proceedings of the National Academy of Sciences, 105*(14), 5477-5482.

Wathelet, M. G., Berr, P. M., & Huez, G. A. (1992). Regulation of gene expression by cytokines and virus in human cells lacking the type-I interferon locus. *European Journal of Biochemistry, 206*(3), 901-910.

Watson, R. O., Manzanillo, P. S., & Cox, J. S. (2012). Extracellular M. tuberculosis DNA targets bacteria for autophagy by activating the host DNA-sensing pathway. *Cell, 150*(4), 803-815.

Weber-Gerlach, M., & Weber, F. (2016). Standing on three legs: antiviral activities of RIG-I against influenza viruses. *Current Opinion in Immunology, 42*, 71-75.

Weber, F., Wagner, V., Rasmussen, S. B., Hartmann, R., & Paludan, S. R. (2006). Double-Stranded RNA Is Produced by Positive-Strand RNA Viruses and DNA Viruses but Not in Detectable Amounts by Negative-Strand RNA Viruses. *Journal of Virology, 80*(10), 5059-5064.

Weber, M., Gawanbacht, A., Habjan, M., Rang, A., Borner, C., Schmidt, Anna M., Veitinger, S., Jacob, R., Devignot, S., Kochs, G., García-Sastre, A., & Weber, F. (2013). Incoming RNA Virus Nucleocapsids Containing a 5′-Triphosphorylated Genome Activate RIG-I and Antiviral Signaling. *Cell Host & Microbe, 13*(3), 336-346.

Weber, O., Siegling, A., Friebe, A., Limmer, A., Schlapp, T., Knolle, P., Mercer, A., Schaller, H., & Volk, H.-D. (2003). Inactivated parapoxvirus ovis (Orf virus) has antiviral activity against hepatitis B virus and herpes simplex virus. *Journal of General Virology, 84*(7), 1843-1852.

Weiss, C. M., Trobaugh, D. W., Sun, C., Lucas, T. M., Diamond, M. S., Ryman, K. D., & Klimstra, W. B. (2018). The Interferon-Induced Exonuclease ISG20 Exerts Antiviral Activity through Upregulation of Type I Interferon Response Proteins. *mSphere, 3*(5), e00209-00218.

Weitzman, M. D., Lilley, C. E., & Chaurushiya, M. S. (2010). Genomes in Conflict: Maintaining Genome Integrity During Virus Infection. *Annual Review of Microbiology, 64*(1), 61-81.

Welte, T., Reagan, K., Fang, H., Machain-Williams, C., Zheng, X., Mendell, N., Chang, G.-J. J., Wu, P., Blair, C. D., & Wang, T. (2009). Toll-like receptor 7-induced immune

response to cutaneous West Nile virus infection. *Journal of General Virology, 90*(11), 2660-2668.

West, A. P., Khoury-Hanold, W., Staron, M., Tal, M. C., Pineda, C. M., Lang, S. M., Bestwick, M., Duguay, B. A., Raimundo, N., MacDuff, D. A., Kaech, S. M., Smiley, J. R., Means, R. E., Iwasaki, A., & Shadel, G. S. (2015). Mitochondrial DNA stress primes the antiviral innate immune response. *Nature, 520*(7548), 553-557.

West, J. A., Gregory, S. M., Sivaraman, V., Su, L., & Damania, B. (2011). Activation of Plasmacytoid Dendritic Cells by Kaposi's Sarcoma-Associated Herpesvirus. *Journal of Virology, 85*(2), 895-904.

West, J. A., Wicks, M., Gregory, S. M., Chugh, P., Jacobs, S. R., Zhang, Z., Host, K. M., Dittmer, D. P., & Damania, B. (2014). An Important Role for Mitochondrial Antiviral Signaling Protein in the Kaposi's Sarcoma-Associated Herpesvirus Life Cycle. *Journal of Virology, 88*(10), 5778-5787.

Westphal, D., Ledgerwood, E. C., Hibma, M. H., Fleming, S. B., Whelan, E. M., & Mercer, A. A. (2007). A novel Bcl-2-like inhibitor of apoptosis is encoded by the parapoxvirus ORF virus. *Journal of Virology, 81*(13), 7178-7188.

Westphal, D., Ledgerwood, E. C., Tyndall, J. D. A., Hibma, M. H., Ueda, N., Fleming, S. B., & Mercer, A. A. (2009). The orf virus inhibitor of apoptosis functions in a Bcl-2-like manner, binding and neutralizing a set of BH3-only proteins and active Bax. *Apoptosis, 14*(11), 1317.

Whitten, T. M., Quets, A. T., & Schloemer, R. H. (1991). Identification of the hepatitis B virus factor that inhibits expression of the beta interferon gene. *Journal of Virology, 65*(9), 4699-4704.

Wilson, J. R., de Sessions, P. F., Leon, M. A., & Scholle, F. (2008). West Nile Virus Nonstructural Protein 1 Inhibits TLR3 Signal Transduction. *Journal of Virology, 82*(17), 8262-8271.

Wise, L., McCaughan, C., Tan, C. K., Mercer, A. A., & Fleming, S. B. (2007). Orf virus interleukin-10 inhibits cytokine synthesis in activated human THP-1 monocytes, but only partially impairs their proliferation. *Journal of General Virology, 88*(6), 1677-1682.

Wu, J.-j., Li, W., Shao, Y., Avey, D., Fu, B., Gillen, J., Hand, T., Ma, S., Liu, X., Miley, W., Konrad, A., Neipel, F., Stürzl, M., Whitby, D., Li, H., & Zhu, F. (2015). Inhibition of cGAS DNA Sensing by a Herpesvirus Virion Protein. *Cell Host & Microbe, 18*(3), 333-344.

Wu, J., Sun, L., Chen, X., Du, F., Shi, H., Chen, C., & Chen, Z. J. (2013). Cyclic GMP-AMP Is an Endogenous Second Messenger in Innate Immune Signaling by Cytosolic DNA. *Science, 339*(6121), 826-830.

Wyatt, L. S., Earl, P. L., & Moss, B. (2017). Generation of Recombinant Vaccinia Viruses. *Current Protocols in Protein Science, 89*(1), 5.13.11-15.13.18.

Xia, P., Wang, S., Ye, B., Du, Y., Huang, G., Zhu, P., & Fan, Z. (2015). Sox2 functions as a sequence-specific DNA sensor in neutrophils to initiate innate immunity against microbial infection. *Nature Immunology, 16*(4), 366-375.

Xiang, Y., Condit, R. C., Vijaysri, S., Jacobs, B., Williams, B. R. G., & Silverman, R. H. (2002). Blockade of Interferon Induction and Action by the E3L Double-Stranded RNA Binding Proteins of Vaccinia Virus. *Journal of Virology, 76*(10), 5251-5259.

Xiao, T. S., & Fitzgerald, Katherine A. (2013). The cGAS-STING Pathway for DNA Sensing. *Molecular Cell, 51*(2), 135-139.

Xie, Q., Shen, H.-C., Jia, N.-N., Wang, H., Lin, L.-Y., An, B.-Y., Gui, H.-L., Guo, S.-M., Cai, W., Yu, H., Guo, Q., & Bao, S. (2009). Patients with chronic hepatitis B infection display deficiency of plasmacytoid dendritic cells with reduced expression of TLR9. *Microbes and Infection, 11*(4), 515-523.

Yamada, S., Shimojima, M., Narita, R., Tsukamoto, Y., Kato, H., Saijo, M., & Fujita, T. (2018). RIG-I-Like Receptor and Toll-Like Receptor Signaling Pathways Cause Aberrant Production of Inflammatory Cytokines/Chemokines in a Severe Fever with Thrombocytopenia Syndrome Virus Infection Mouse Model. *Journal of Virology, 92*(13), e02246-02217.

Yamamoto, M., Sato, S., Hemmi, H., Hoshino, K., Kaisho, T., Sanjo, H., Takeuchi, O., Sugiyama, M., Okabe, M., Takeda, K., & Akira, S. (2003). Role of Adaptor TRIF in the MyD88-Independent Toll-Like Receptor Signaling Pathway. *Science, 301*(5633), 640-643.

Yamamoto, M., Sato, S., Mori, K., Hoshino, K., Takeuchi, O., Takeda, K., & Akira, S. (2002). Cutting Edge: A Novel Toll/IL-1 Receptor Domain-Containing Adapter That Preferentially Activates the IFN-β Promoter in the Toll-Like Receptor Signaling. *The Journal of Immunology, 169*(12), 6668-6672.

Yanai, H., Ban, T., Wang, Z., Choi, M. K., Kawamura, T., Negishi, H., Nakasato, M., Lu, Y., Hangai, S., Koshiba, R., Savitsky, D., Ronfani, L., Akira, S., Bianchi, M. E., Honda, K., Tamura, T., Kodama, T., & Taniguchi, T. (2009). HMGB proteins function as

universal sentinels for nucleic-acid-mediated innate immune responses. *Nature, 462*(7269), 99-103.

Yang, K., Wang, J., Wu, M., Li, M., Wang, Y., & Huang, X. (2015). Mesenchymal stem cells detect and defend against gammaherpesvirus infection via the cGAS-STING pathway. *Scientific reports, 5*(1), 7820.

Yang, P., An, H., Liu, X., Wen, M., Zheng, Y., Rui, Y., & Cao, X. (2010). The cytosolic nucleic acid sensor LRRFIP1 mediates the production of type I interferon via a β-catenin-dependent pathway. *Nature Immunology, 11*(6), 487-494.

Yang, Y., Liang, Y., Qu, L., Chen, Z., Yi, M., Li, K., & Lemon, S. M. (2007). Disruption of innate immunity due to mitochondrial targeting of a picornaviral protease precursor. *Proceedings of the National Academy of Sciences, 104*(17), 7253-7258.

Yang, Y. L., Reis, L. F., Pavlovic, J., Aguzzi, A., Schäfer, R., Kumar, A., Williams, B. R., Aguet, M., & Weissmann, C. (1995). Deficient signaling in mice devoid of double-stranded RNA-dependent protein kinase. *The EMBO Journal, 14*(24), 6095-6106.

Yoneyama, M., & Fujita, T. (2007). Function of RIG-I-like receptors in antiviral innate immunity. *The Journal of biological chemistry, 282*(21), 15315-15318.

Yoneyama, M., & Fujita, T. (2008). Structural Mechanism of RNA Recognition by the RIG-I-like Receptors. *Immunity, 29*(2), 178-181.

Yoneyama, M., & Fujita, T. (2010). Recognition of viral nucleic acids in innate immunity. *Reviews in Medical Virology, 20*(1), 4-22.

Yoneyama, M., Kikuchi, M., Matsumoto, K., Imaizumi, T., Miyagishi, M., Taira, K., Foy, E., Loo, Y.-M., Gale, M., Akira, S., Yonehara, S., Kato, A., & Fujita, T. (2005). Shared and Unique Functions of the DExD/H-Box Helicases RIG-I, MDA5, and LGP2 in Antiviral Innate Immunity. *The Journal of Immunology, 175*(5), 2851-2858.

Yoneyama, M., Kikuchi, M., Natsukawa, T., Shinobu, N., Imaizumi, T., Miyagishi, M., Taira, K., Akira, S., & Fujita, T. (2004). The RNA helicase RIG-I has an essential function in double-stranded RNA-induced innate antiviral responses. *Nature Immunology, 5*(7), 730-737.

Yoo, J.-S., Kato, H., & Fujita, T. (2014). Sensing viral invasion by RIG-I like receptors. *Current Opinion in Microbiology, 20*, 131-138.

Yoshizumi, T., Ichinohe, T., Sasaki, O., Otera, H., Kawabata, S.-i., Mihara, K., & Koshiba, T. (2014). Influenza A virus protein PB1-F2 translocates into mitochondria via Tom40 channels and impairs innate immunity. *Nature Communications, 5*(1), 4713.

Zhang, G., Chan, B., Samarina, N., Abere, B., Weidner-Glunde, M., Buch, A., Pich, A., Brinkmann, M. M., & Schulz, T. F. (2016). Cytoplasmic isoforms of Kaposi sarcoma herpesvirus LANA recruit and antagonize the innate immune DNA sensor cGAS. *Proceedings of the National Academy of Sciences, 113*(8), E1034-E1043.

Zhang, J., Hu, M.-M., Wang, Y.-Y., & Shu, H.-B. (2012). TRIM32 Protein Modulates Type I Interferon Induction and Cellular Antiviral Response by Targeting MITA/STING Protein for K63-linked Ubiquitination. *Journal of Biological Chemistry, 287*(34), 28646-28655.

Zhang, P., & Samuel, C. E. (2008). Induction of Protein Kinase PKR-dependent Activation of Interferon Regulatory Factor 3 by Vaccinia Virus Occurs through Adapter IPS-1 Signaling. *Journal of Biological Chemistry, 283*(50), 34580-34587.

Zhang, S.-Y., Jouanguy, E., Ugolini, S., Smahi, A., Elain, G., Romero, P., Segal, D., Sancho-Shimizu, V., Lorenzo, L., Puel, A., Picard, C., Chapgier, A., Plancoulaine, S., Titeux, M., Cognet, C., von Bernuth, H., Ku, C.-L., Casrouge, A., Zhang, X.-X., Barreiro, L., Leonard, J., Hamilton, C., Lebon, P., Héron, B., Vallée, L., Quintana-Murci, L., Hovnanian, A., Rozenberg, F., Vivier, E., Geissmann, F., Tardieu, M., Abel, L., & Casanova, J.-L. (2007). TLR3 Deficiency in Patients with Herpes Simplex Encephalitis. *Science, 317*(5844), 1522-1527.

Zhang, X., Brann, T. W., Zhou, M., Yang, J., Oguariri, R. M., Lidie, K. B., Imamichi, H., Huang, D.-W., Lempicki, R. A., Baseler, M. W., Veenstra, T. D., Young, H. A., Lane, H. C., & Imamichi, T. (2011). Cutting Edge: Ku70 Is a Novel Cytosolic DNA Sensor That Induces Type III Rather Than Type I IFN. *The Journal of Immunology, 186*(8), 4541-4545.

Zhang, X., Shi, H., Wu, J., Zhang, X., Sun, L., Chen, C., & Chen, Zhijian J. (2013). Cyclic GMP-AMP Containing Mixed Phosphodiester Linkages Is An Endogenous High-Affinity Ligand for STING. *Molecular Cell, 51*(2), 226-235.

Zhang, X., Wang, C., Schook, L. B., Hawken, R. J., & Rutherford, M. S. (2000). An RNA helicase, RHIV -1, induced by porcine reproductive and respiratory syndrome virus (PRRSV) is mapped on porcine chromosome 10q13. *Microbial Pathogenesis, 28*(5), 267-278.

Zhang, Y., Yeruva, L., Marinov, A., Prantner, D., Wyrick, P. B., Lupashin, V., & Nagarajan, U. M. (2014). The DNA Sensor, Cyclic GMP–AMP Synthase, Is Essential for Induction of IFN-β during Chlamydia trachomatis Infection. *The Journal of Immunology, 193*(5), 2394-2404.

Zhang, Z., Filzmayer, C., Ni, Y., Sültmann, H., Mutz, P., Hiet, M.-S., Vondran, F. W. R., Bartenschlager, R., & Urban, S. (2018). Hepatitis D virus replication is sensed by MDA5 and induces IFN-β/λ responses in hepatocytes. *Journal of Hepatology, 69*(1), 25-35.

Zhang, Z., Yuan, B., Bao, M., Lu, N., Kim, T., & Liu, Y.-J. (2011). The helicase DDX41 senses intracellular DNA mediated by the adaptor STING in dendritic cells. *Nature Immunology, 12*(10), 959-965.

Zhang, Z., Yuan, B., Lu, N., Facchinetti, V., & Liu, Y.-J. (2011). DHX9 Pairs with IPS-1 To Sense Double-Stranded RNA in Myeloid Dendritic Cells. *The Journal of Immunology, 187*(9), 4501-4508.

Zhao, K., Song, D., He, W., Lu, H., Zhang, B., Li, C., Chen, K., & Gao, F. (2010). Identification and phylogenetic analysis of an Orf virus isolated from an outbreak in sheep in the Jilin province of China. *Veterinary Microbiology, 142*(3), 408-415.

Zhao, Y., Ye, X., Dunker, W., Song, Y., & Karijolich, J. (2018). RIG-I like receptor sensing of host RNAs facilitates the cell-intrinsic immune response to KSHV infection. *Nature Communications, 9*(1), 4841.

Zhong, B., Yang, Y., Li, S., Wang, Y.-Y., Li, Y., Diao, F., Lei, C., He, X., Zhang, L., Tien, P., & Shu, H.-B. (2008). The Adaptor Protein MITA Links Virus-Sensing Receptors to IRF3 Transcription Factor Activation. *Immunity, 29*(4), 538-550.

Zhou, J., Wang, Y., Chang, Q., Ma, P., Hu, Y., & Cao, X. (2018). Type III Interferons in Viral Infection and Antiviral Immunity. *Cellular Physiology and Biochemistry, 51*(1), 173-185.

Zhu, J., Huang, X., & Yang, Y. (2007). Innate Immune Response to Adenoviral Vectors Is Mediated by both Toll-Like Receptor-Dependent and -Independent Pathways. *Journal of Virology, 81*(7), 3170-3180.

Zhu, J., Zhang, Y., Ghosh, A., Cuevas, Rolando A., Forero, A., Dhar, J., Ibsen, Mikkel S., Schmid-Burgk, Jonathan L., Schmidt, T., Ganapathiraju, Madhavi K., Fujita, T., Hartmann, R., Barik, S., Hornung, V., Coyne, Carolyn B., & Sarkar, Saumendra N. (2014). Antiviral Activity of Human OASL Protein Is Mediated by Enhancing Signaling of the RIG-I RNA Sensor. *Immunity, 40*(6), 936-948.

Zimring, J. C., Goodbourn, S., & Offermann, M. K. (1998). Human Herpesvirus 8 Encodes an Interferon Regulatory Factor (IRF) Homolog That Represses IRF-1-Mediated Transcription. *Journal of Virology, 72*(1), 701-707.

Zupkovitz, G., Tischler, J., Posch, M., Sadzak, I., Ramsauer, K., Egger, G., Grausenburger, R., Schweifer, N., Chiocca, S., Decker, T., & Seiser, C. (2006). Negative and Positive Regulation of Gene Expression by Mouse Histone Deacetylase1. *Molecular and Cellular Biology*, *26*(21), 7913-7928.

Zwartouw, H. T., Westwood, J. C. N., & Appleyard, G. (1962). Purification of Pox Viruses by Density Gradient Centrifugation. *Microbiology*, *29*(3), 523-529. doi:https://doi.org/10.1099/00221287-29-3-523

9 APPENDICES

9.1 Solutions for Preparation and Transformation of *E*. coli Competent Cells

a. 2-YT Broth in 1 Litre

Reagent	Amount required/Litre	Final Concentration
Tryptone	16 g	-
Yeast Extract	10 g	-
Sodium Chloride (NaCl)	5 g	-

The medium was dissolved in 1 L of Milli-Q H2O and pH adjusted to 7.5 then autoclaved

b. 2-YT Agar in 1 Litre

Reagent	Amount required/Litre	Final Concentration
Tryptone	16 g	-
Yeast Extract	10 g	-
Sodium Chloride (NaCl)	5 g	-
Agar	15 g	-

The medium was dissolved in 1 L of Milli-Q H2O and pH adjusted to 7.5, then agar added and autoclaved.

c. SOB medium in 1 litre

Reagent	Amount Required/Litre	Final Concentration
Yeast Extract	5 g	0.5% (w/v)
Tryptone	20 g	2% (w/v)
Sodium Chloride (NaCl)	0.584 g	10 mM
Potassium Chloride (KCl)	0.186 g	2.5 mM
Magnesium Sulfate ($MgSO_4$)	2.4 g	20 mM

All contents were dissolved in Milli-Q H_2O and then autoclaved.

d. Transformation Buffer

Reagent	Amount Required/Litre	Final Concentration
Potassium Acetate (KOAc) pH 7.5	-	10 mM
Calcium Chloride (CaCl. 2H2O)	-	80 mM
Manganese Chloride ($MnCl_2$. $4H_2O$)	-	20 mM
Magnesium Chloride ($MgCl_2$. $6H_2O$)	-	10 mM
Glycerol	-	10%

The pH of solution was adjusted to 6.4 with 0.1 N HCl. The solution was filtered and stored at 4 °C.

9.2 Solutions for Alkaline Lysis Preparation of Plasmid DNA

a. Glucose/Tris/EDTA Solution in 100 ml

Reagent	Amount required	Final Concentration
Glucose	-	50 mM
Tris-HCl, pH 8	-	25 mM
EDTA	-	10 mM

The solution was made up to 100 ml with Milli-Q H_2O then autoclaved.

b. NaOH/SDS Solution in 100 ml

Reagent	Amount required	Final Concentration
Sodium Hydroxide (NaOH) 1 M	20 ml	0.2 M
Sodium Dodecyl Sulfate (SDS) 10%	10 ml	1%

The solution was made up to 100 with Milli-Q H_2O. The solution was made freshly.

c. Potassium Acetate Solution (pH 5) in 40 ml

Reagent	Amount Required	Final Concentration
Potassium Acetate, 5 M	25 ml	-
Absolute Glacial Acetic Acid	4.8 ml	12%

The solution was made up to 40 ml with Milli-Q H_2O.

9.3 Solutions for DNA Gel Electrophoresis

a. Agarose Gel

Reagent	Amount required	Final Concentration
Agarose Gel	1 g	1 % (w/v)

The solution was made up to 100 ml with TAE buffer and heated to dissolve, cooled at about 60 °C and ethidium bromide added to final concentration of 0.5 µg/ml before casting.

b. DNA Loading Dye

Reagent	Amount required	Final Concentration
Bromophenol blue	25 mg	0.25 % (w/v)
Xylene	25 mg	0.25 % (w/v)
Glycerol	5 ml	50 %
EDTA		0.05 M

The solution was made up to 10 ml with MilliQ H_2O and stored at room temperature.

c. 50X Tris-Acetate (TAE) buffer

Reagent	Amount Required	Final Concentration
Tris-base	242 g	-
Glacial acetic acid	57.1 ml	-
EDTA pH 8.0, 0.5 M	100 ml	-

The solution was made up to 1L with MilliQ H_2O and stored at room temperature. For working solution, the buffer was diluted 50X with MilliQ H_2O.

d. Ethidium Bromide 10 mg/ml

Reagent	Amount Required	Final Concentration
Ethidium Bromide	50 mg	10 mg/ml

The solution was made up to 5 ml with MilliQ H_2O and stored in light-tight container at room temperature.

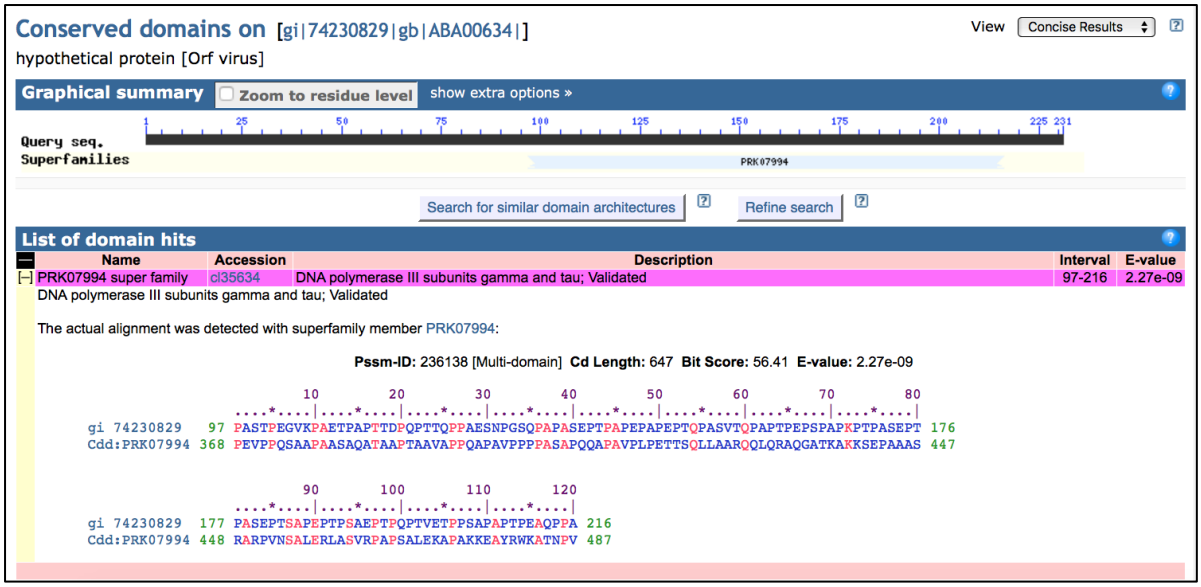

Figure 9.1. Conserved domain on ORF116 found from NCBI search.

Table 9.1. Reagents used in this study.

Reagents	Source	Catalog No.	Solvent
LyoVec Cationic lipid	InvivoGen	lyec-12, lyec-22	Milli-Q H_2O
Poly(dA:dT) naked Double-stranded B-DNA deoxyadenylic-deoxythymidlic acid	InvivoGen	tlrl-patn-1, tlrl-patn-1	Sterile endotoxin-free physiological H_2O provided
Poly(I:C) Double-stranded RNA polyinosinic-polycytidylic acid	Sigma-Aldrich	P9582	Milli-Q H_2O
Phorbol 12-Myristate 13-Acetate (PMA)	Sigma Aldrich	P8139-1MG	DMSO
RNA Polymerase III inhibitor (ML60218)	Calbiochem	557403-10MG	DMSO
EZview Red Protein G Affinity Gel	Sigma-Aldrich	E3403	-
Adenosine N'-Oxide (ANO)	Sigma-Aldrich	A-8540	Milli-Q H_2O
Escherichia coli O55:B5 lipopolysaccharide (LPS)	Sigma-Aldrich	L2880	Milli-Q H_2O
Lipofectamine 2000	ThermoFisher	11668019	-
Phosphosafe Extraction reagent	Merck Millipore	71296	-

Table 9.2. Accession numbers of virus strains used in ORF116 sequence analysis.

Species	Strain	GenBank Accession Number		References
		DNA Sequence ID	Amino Acid ID	
Orf Virus (ORFV)	NZ2	DQ184476	ABA00634.1	(Mercer, A. A. *et al.*, 2006)
	IA82	AY386263	AAR98211.1	(Delhon, G. *et al.*, 2004)
	D1701	HM133903.1	ADY76829.1	(McGuire, M. J. *et al.*, 2012)
	SY17	MG712417	AYN61062.1	-
	B029	KF837136	AHH34301.1	(Friederichs, S. *et al.*, 2014)
	HN3/12	KY053526.1	ASY92413.1	-
	NA1/11	KF234407.1	AHZ33814.1	-
	SA00	AY386264.1	AAR98341.1	(Delhon, G. *et al.*, 2004)
	NA17	MG674916.2	AYM26057.1	-
	SJ1	KP010356.1	AKU76994.1	(Chi, X. *et al.*, 2015)
	YX	KP010353.1	AKU76606.1	(Chi, X. *et al.*, 2015)
	GO	KP010354.1	AKU76738.1	(Chi, X. *et al.*, 2015)
Pseudocowpoxvirus (PC)	VR634	GQ329670.1	ADC54019.1	(Hautaniemi, M. *et al.*, 2010)
	IT1303/05	JF800906.1	AEO18266.1	(Hautaniemi, M. *et al.*, 2011)

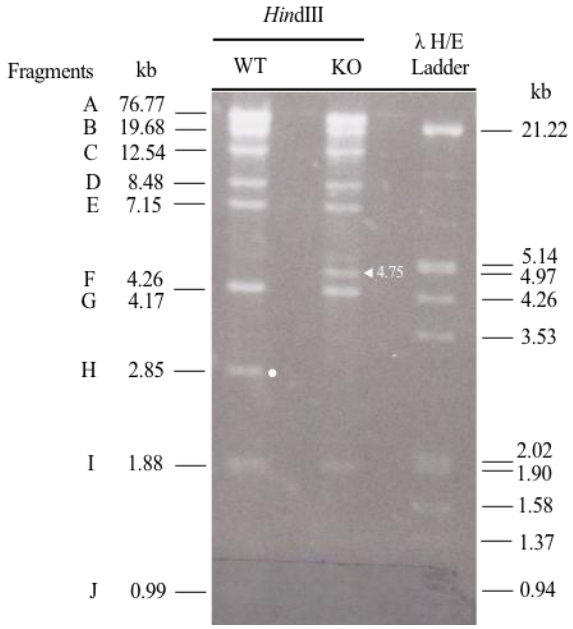

Figure 9.2. *Hin*dIII restriction analysis of wild type and knockout-116 virus DNA. Genomic DNA of wild type and knockout-116 virus was digested with the restriction endonucleases *Hin*dIII and the fragments were separated by gel electrophoresis. Size marker bacteriophage lambda λ DNA was digested with *Eco*RI and *Hin*dIII. Genomic restriction endonuclease fragments of wild type are indicated with their sizes in kb. The *Hin*dIII-H fragments in the wild type virus is indicated by white dot with size shown in kb and the *Hin*dIII 4.75 kb fragment produced in the ORF116 knockout virus is indicated by white arrow with size shown in kb. This data was produced by Virus Research Unit, University of Otago.

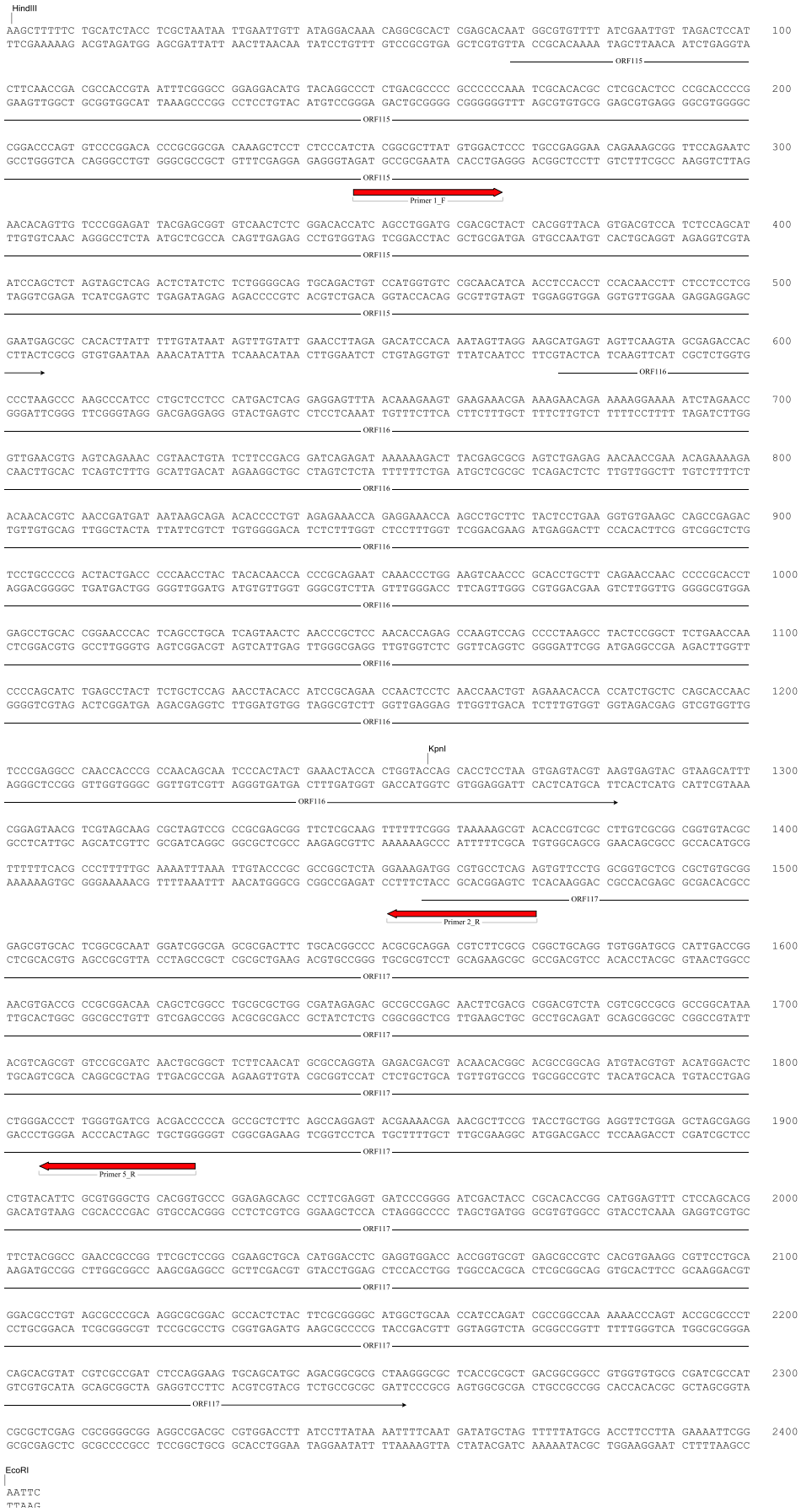

Figure 9.3. Sequence of *Hin*dIII/*Eco*RI fragment in wild type OV-NZ2.

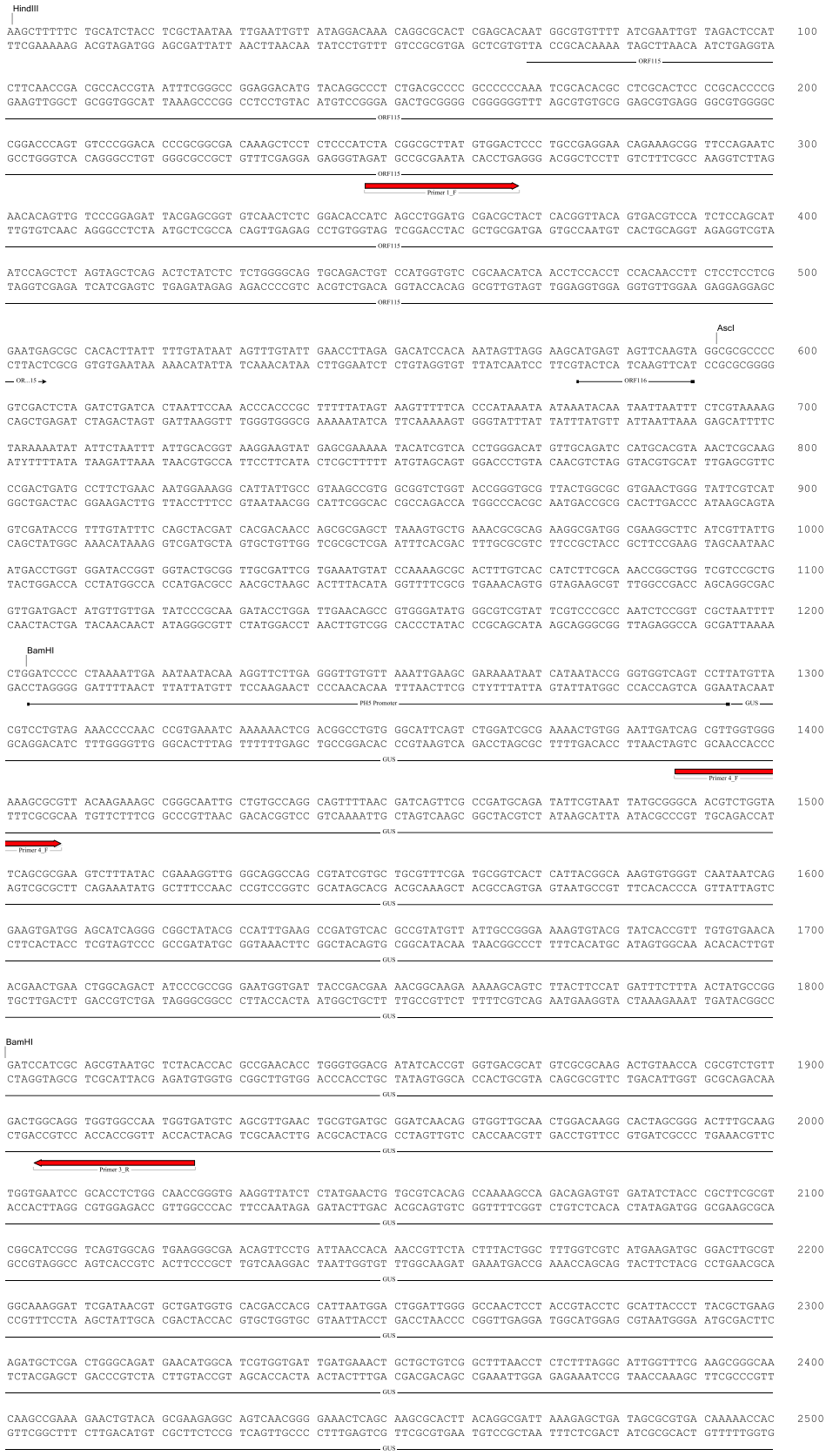

Continued next page

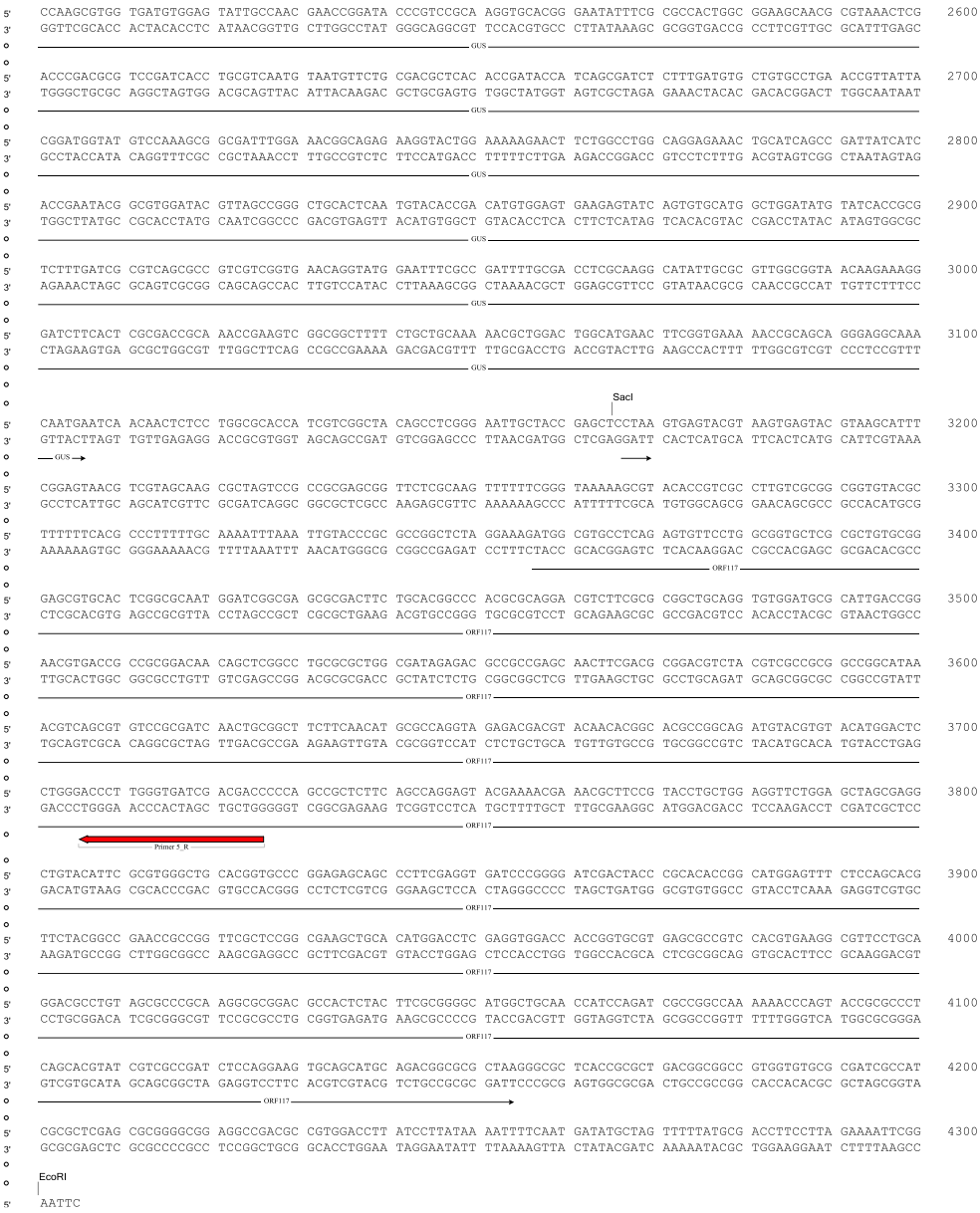

Figure 9.4. Sequence of *Hin*dIII/*Eco*RI fragment in knockout OV-NZ2Δ116.

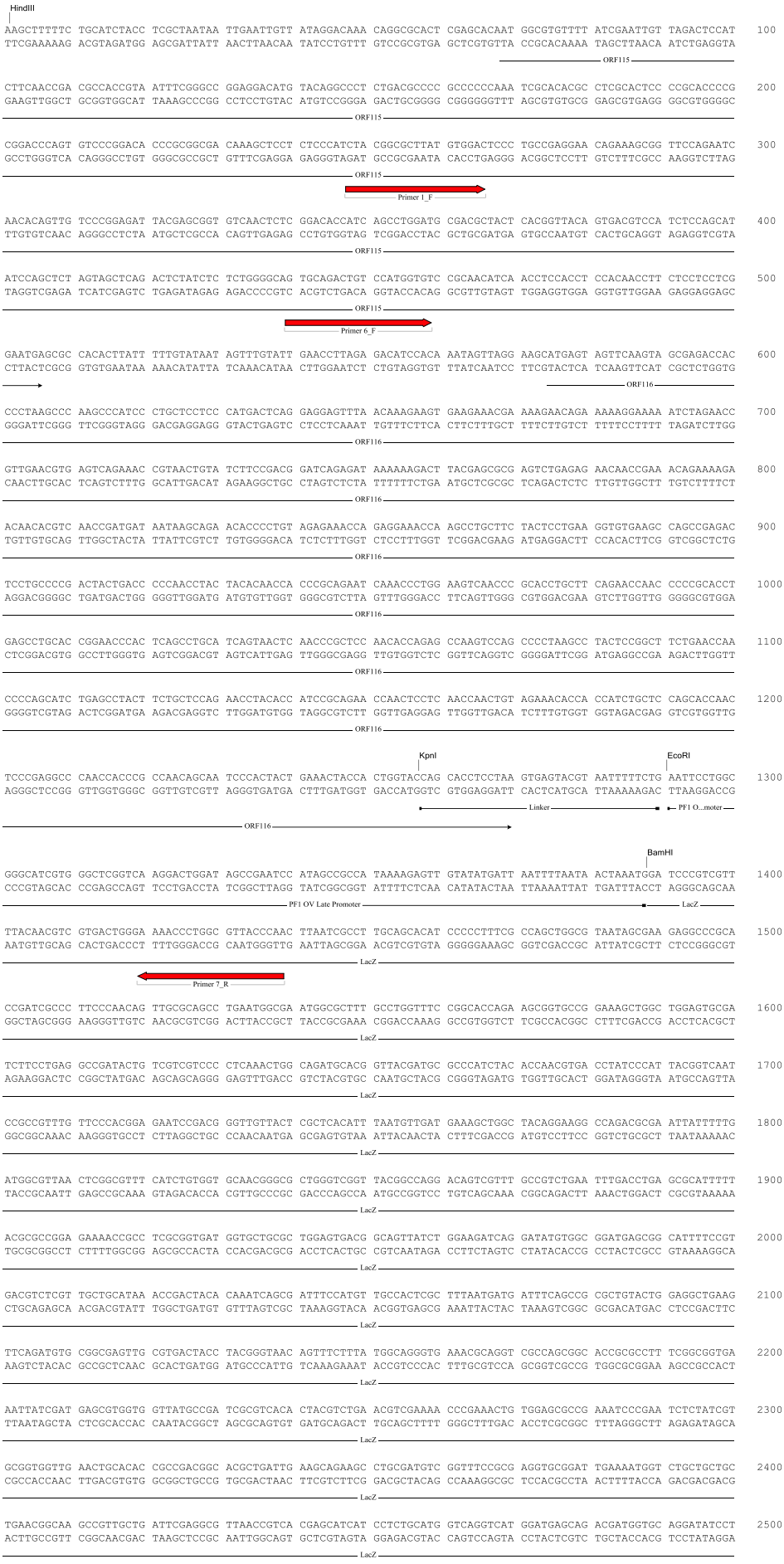

Continued next page

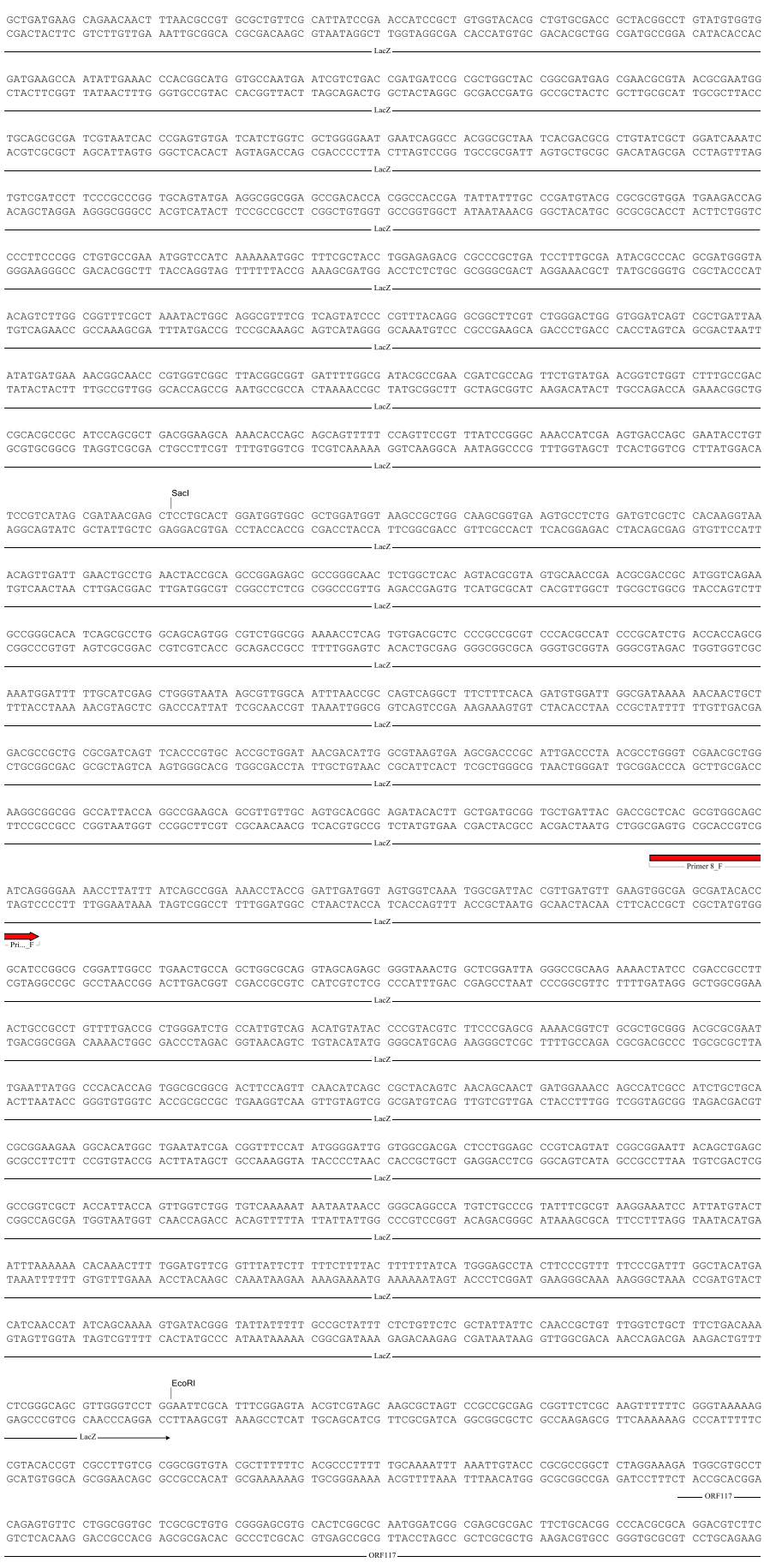

Continued next page

Figure 9.5. Sequence of *Hin*dIII/*Eco*RI fragment in Revertant OV-NZ2-Rev116.

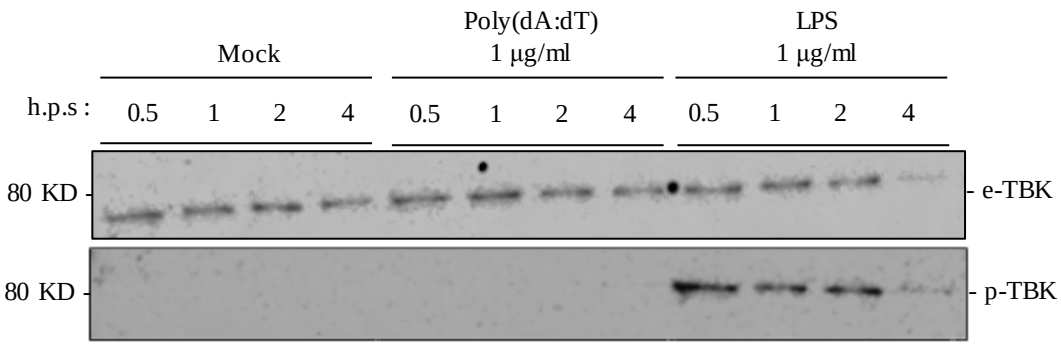

Figure 9.6. Detection of p-TBK1 molecules in THP-1 cells by western blotting. The cells were mock or stimulated with either 1 µg/ml of poly(dA:dT) or with LPS for indicated times. Cells were harvested and lyzed in phophosafe reagent buffer then equal amount of cell lysate was resolved on a 10 % SDS-polyacrylamide gel and proteins transferred onto nitrocellulose membrane. Proteins were detected with antibodies against e-TBK1 or p-TBK1. Proteins were visualized by chemiluminescence on the odyssey Fc imaging system.

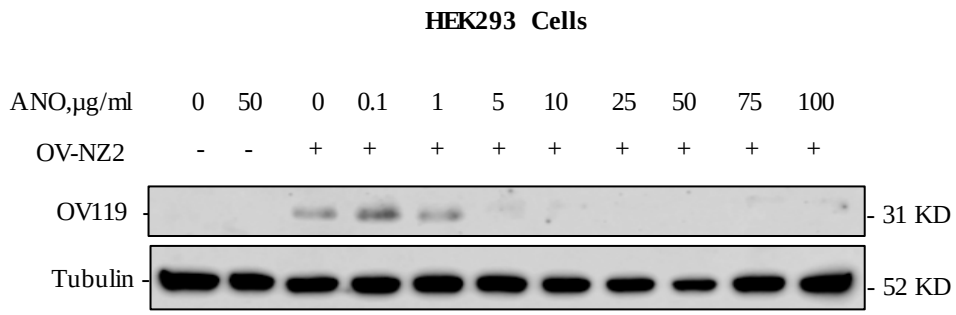

Figure 9.7. Inhibitory Effect of ANO on OV-NZ2 early protein synthesis in HEK293 cells. The cells were pre-treated with either ANO for 6 hours at indicated concentration. Then the cells were infected with Orf virus at MOI of 5 for HEK293 4 hrs. Cells were harvested and lyzed for OV119 protein detection. Equal amount of cell lysate was resolved on a 10 % SDS-polyacrylamide gel and proteins transferred onto nitrocellulose membrane. The membrane was incubated with rabbit anti-OV119 Ab (Harfoot, R. T., 2015) and anti-tubulin antibody as loading control for overnight. Protein was detected by chemiluminescence.

A.

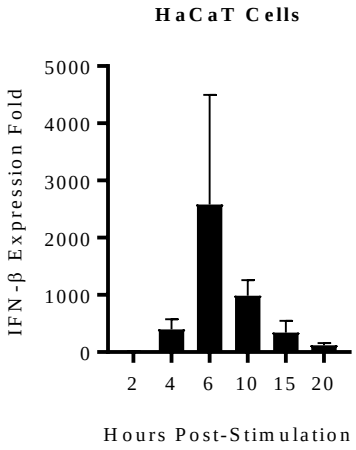

B.

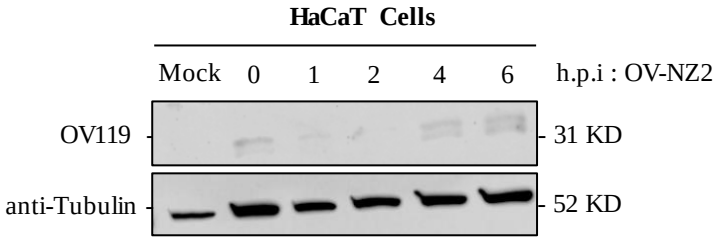

C.

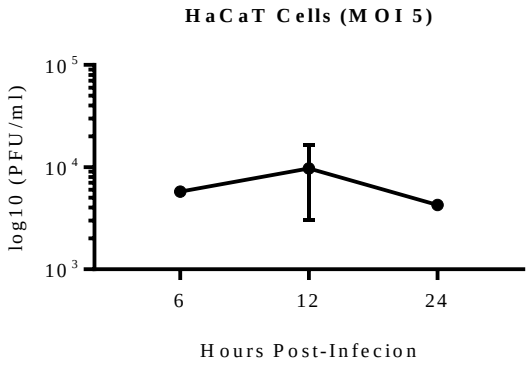

Figure 9.8. Characterization of OV-NZ2 growth in HaCaT cells. (A) Cells were stimulated with 0.5 µg/ml of poly(dA:dT) in 6-well plate and incubated for indicated times. Cells were harvested by trypsinization and total RNA isolated. IFN-β induction was quantified by qPCR. qPCR was conducted in duplicate and data represent one experiment of two independent experiments. Error bars represent mean ±SD. (B) Cells were infected with OV-NZ2 at an MOI of 5 pfu per cell in 6-well plate and incubated until harvesting time indicated. Cells were lyzed and 10 µl of cell lysate was resolved on SDS-PAGE gel and proteins transferred onto nitrocellulose membrane. The membrane was incubated with anti-OV119 Ab or anti-tubulin as loading control and proteins detected by chemiluminescence. This data represent two experiments. (C) Cells were infected at an MOI of 5 with OV-NZ2. After 1hr adsorption, cells were washed with PBS then 2 ml of DMEM 2 % FCS then cells incubated for indicated times. Medium and infected cells were harvested and subjected to three cycles of freezing and thawing, the virus was sonicated and viral titres determined on LT cells. Data represent one experiment and Error bars represent mean ±SD.

9.4 Tissue Culture Media

a. Minimal Essential Medium (MEM), (GIBCO, Invitrogen)

Reagent	Amount required/Litre	Final Concentration
Sigma MEM	1 packet	-
MilliQ H2O	950 ml	-
NaHCO3	2.2 g	-

The medium was made up to 1 L then filtered into sterile bottles with positive pressure. Store at 37 °C for overnight to check sterility, then store at 4 °C until used.

b. Dulbecco's Modified Eagle Medium (DMEM), (GIBCO, Invitrogen)

Reagent	Amount required/Litre	Final Concentration
Sigma DMEM	1 packet	-
$NaHCO_3$	3.7 g	-
Hepes.	4.77 g	-
MilliQ H_2O	950 ml	-
2-mercaptoethanol	1.5 µl	-

The pH was adjusted to 7.4 and made up to 1 L, then medium filtered into sterile bottles with positive pressure. Store at 37 °C for overnight to check sterility, then store at 4 °C until used.

c. RPMI 1670 Medium (GIBCO, Invitrogen)

Reagent	Amount Required/Litre	Final Concentration
RPMI	1 packet	-
$NaHCO_3$	2 g	-
MilliQ H_2O	950 ml	-

The pH was adjusted to 7.0-7.4 and made up to 1 L, then medium filtered into sterile bottles with positive pressure. Store at 37 °C for overnight to check sterility, then store at 4 °C until used.

d. Supplement/additives

Reagent	Amount Required/Litre	Final Concentration
Fetal Calf Serum (FCS)	-	2 or 10 %
Penicillin	-	500 U/ml
Streptomycin	-	0.5 mg/ml
Kanamycin	-	0.1 mg/ml

9.5 Maintenance of Tissue Culture

a. Phosphate Buffered Saline (PBS)

Reagent	Amount required/Litre	Final Concentration
PBS	1 tablet	-
MilliQ H_2O	100 ml	-

One tablet of PBS was dissolved in 100 ml MilliQ H_2O, then autoclaved and stored at 4 °C.

b. Trypsin 0.25%

Reagent	Amount required/Litre	Final Concentration
Phosphate Buffered Saline (PBS)	100 ml	-
Trypsin	0.25 g	-
0.5M EDTA	80 µl	-
0.4% Phenol Red	0.5 ml	-

The solution was dissolved and filtered then aliquated. The solution was stored at -20 °C until used and once opened stored at 4 °C.

c. Trypan Blue (0.2 %)

Reagent	Amount Required/Litre	Final Concentration
Trypan blue powder	0.2 g	-
PBS	100 ml	-

The trypan blue powder was dissolved in 100 ml PBS and store at room temperature.

d. Splitting and setting up plates or flasks with cells

When cell monolayer was confluent, using aseptic technique, the medium aspirated and cell monolayer washed with PBS twice. Appropriate amount of Trypsin was added then discarded. Another same amount of trypsin was added and the flask was incubated at 37 °C to trypsinize until detach from the surface of the flask for about 10 min and let this on the cell until they can be seen to be leaving the side of the flask. Appropriate amount of complete medium was added 9 ml and the cell suspension was pipetted up and down to break up the clumps of cells. The cell suspension was divided into the required ratio and make up with appropriate volume of complete medium then incubate at 37 °C, 5 % CO_2.

9.6 Solutions for Preparation of Gel for SDS-PAGE

a. 1.5 M Tris-HCl, pH 8.8

Reagent	Amount required	Final Concentration
Tris	27.23 g	1.5 M
MilliQ H_2O	80 ml	-

The pH of the solution was adjusted to 8.8 with 6N HCl then volume made up to 150 ml with MilliQ H2O.

b. 1 M Tris-HCl, pH 6.8

Reagent	Amount required	Final Concentration
Tris	7.26 g	1 M
MilliQ H_2O	60 ml	-

The pH of the solution was adjusted to 6.8 with 6N HCl then volume made up to 100 ml with H_2O.

c. 10 % Sodium Dodecyl Sulfate (SDS)

Reagent	Amount Required	Final Concentration
SDS	10 g	10 %
MilliQ H_2O	100 ml	-

d. 10 % Ammonium Persulfate (APS)

Reagent	Amount Required	Final Concentration
APS	0.5 g	10 %
MilliQ H_2O	5 ml	-

The solution was made and aliquoted then stored at -20 °C until used.

e. 30 % Acrylamide

f. TEMED

g. Resolving Gel, 10 %

Reagents	Amount Required	Final Concentration
MilliQ H_2O	5.9 ml	-
SDS, 10 %	150 µl	-
1.5 M Tris (pH 8.8)	3.8 ml	-
Acrylamide, 30 %	5 ml	10 %
APS	150 µl	-
TEMED	6 µl	-

The components were mixed to cast the gel.

h. Stacking gel, 5 %

Reagent	Amount Required	Final Concentration
MilliQ H_2O	6.8 ml	-
SDS, 10 %	100 µl	-
1 M Tris (pH 6.8)	1.25 ml	-
Acrylamide, 30 %	1.7 ml	5 %
APS, 10 %	100 µl	-

TEMED	10 µl	-

The components were mixed to cast the gel.

i. Casting the gel

The gel was set by siding two plates into the casting frame and then placed on the casting stand. Firstly the resolving gel was poured up to 1 cm below the comb, then the gel was covered with water. After 30 min of polymerization, the water was discarded and stacking gel was poured immediately on top of the polymerized resolving gel up to the top. The comb was inserted and allowed for 30 min to polymerize.

9.7 Solutions for Western Blotting

a. 10 X Running Buffer

Reagents	Amount Required	Final Concentration
Tris-base	30 g	-
Glycine	144 g	-
SDS	10 g	-

The volume made up to 1 L with MilliQ H_2O. The buffer was diluted at 1 X for electrophoresis.

b. Transfer Buffer

Reagent	Amount Required	Final Concentration
Tris-base	12.12 g	-
Glycine	57.63 g	-
Methanol	700 ml	-
Distilled H_2O	3.2 L	-

The solution was kept at 4 °C.

c. Tris, 1 M, pH 7.4

Reagent	Amount Required	Final Concentration
Tris base	60.57 g	1 M
MilliQ H_2O	500 ml	-

pH was adjusted to 7.4 with HCl.

d. NaCl, 5 M

Reagent	Amount Required	Final Concentration
NaCl	146.1 g	5 M
MilliQ H_2O	500 ml	-

e. Tris-Buffered Saline (TBS), pH 7.4

Reagent	Amount Required	Final Concentration
1M Tris, pH 7.4	25 ml	-
5M NaCl	15 ml	-
MilliQ H_2O	460 ml	-

The components were mixed and stored at room temperature.

f. TBS-T

Reagent	Amount Required	Final Concentration
TBS	500 ml	-
Tween20	1 ml	-

The components were mixed and stored at room temperature.

g. Blocking Buffer using skimmed milk

Reagent	Amount Required	Final Concentration
TBS-T	20 ml	-
Skimmed milk powder	1 g	5 %

The buffer was freshly prepared.

h. Blocking Buffer using bovine serum albumin (BSA)

Reagent	Amount Required	Final Concentration
TBS-T	20 ml	
BSA	1 g	5 %

The buffer was freshly prepared.